GREENHOUSE GAS EMISSIONS AND TERRESTRIAL ECOSYSTEMS

EDITED BY: Amit Kumar, Amit Kumar, Jahangeer A. Bhat and Munesh Kumar
PUBLISHED IN: Frontiers in Environmental Science

frontiers Research Topics

frontiers

ISSN 1664-8714
ISBN 978-2-88974-656-9
DOI 10.3389/978-2-88974-656-9

About Frontiers

Frontiers is more than just an open-access publisher of scholarly articles: it is a pioneering approach to the world of academia, radically improving the way scholarly research is managed. The grand vision of Frontiers is a world where all people have an equal opportunity to seek, share and generate knowledge. Frontiers provides immediate and permanent online open access to all its publications, but this alone is not enough to realize our grand goals.

Frontiers Journal Series

The Frontiers Journal Series is a multi-tier and interdisciplinary set of open-access, online journals, promising a paradigm shift from the current review, selection and dissemination processes in academic publishing. All Frontiers journals are driven by researchers for researchers; therefore, they constitute a service to the scholarly community. At the same time, the Frontiers Journal Series operates on a revolutionary invention, the tiered publishing system, initially addressing specific communities of scholars, and gradually climbing up to broader public understanding, thus serving the interests of the lay society, too.

Dedication to Quality

Each Frontiers article is a landmark of the highest quality, thanks to genuinely collaborative interactions between authors and review editors, who include some of the world's best academicians. Research must be certified by peers before entering a stream of knowledge that may eventually reach the public - and shape society; therefore, Frontiers only applies the most rigorous and unbiased reviews.
Frontiers revolutionizes research publishing by freely delivering the most outstanding research, evaluated with no bias from both the academic and social point of view. By applying the most advanced information technologies, Frontiers is catapulting scholarly publishing into a new generation.

What are Frontiers Research Topics?

Frontiers Research Topics are very popular trademarks of the Frontiers Journals Series: they are collections of at least ten articles, all centered on a particular subject. With their unique mix of varied contributions from Original Research to Review Articles, Frontiers Research Topics unify the most influential researchers, the latest key findings and historical advances in a hot research area! Find out more on how to host your own Frontiers Research Topic or contribute to one as an author by contacting the Frontiers Editorial Office: frontiersin.org/about/contact

GREENHOUSE GAS EMISSIONS AND TERRESTRIAL ECOSYSTEMS

Topic Editors:
Amit Kumar, Nanjing University of Information Science and Technology, China
Amit Kumar, Central Muga Eri Research and Training Institute (CMERTI), India
Jahangeer A. Bhat, Fiji National University, Fiji
Munesh Kumar, Hemwati Nandan Bahuguna Garhwal University, India

Citation: Kumar, A., Kumar, A., Bhat, J. A., Kumar, M., eds. (2022). Greenhouse Gas Emissions and Terrestrial Ecosystems. Lausanne: Frontiers Media SA.
doi: 10.3389/978-2-88974-656-9

Table of Contents

04 ***Editorial: Greenhouse Gas Emissions and Terrestrial Ecosystems***
Amit Kumar, Amit Kumar, Munesh Kumar and Jahangeer A. Bhat

07 ***Appraisal of Carbon Capture, Storage, and Utilization Through Fruit Crops***
Sunny Sharma, Vishal Singh Rana, Heerendra Prasad, Johnson Lakra and Umesh Sharma

17 ***Greenhouse Gas Emissions and Carbon Sinks of an Italian Natural Park***
Giampiero Grossi, Andrea Vitali, Umberto Bernabucci, Nicola Lacetera and Alessandro Nardone

29 ***Greenhouse Gas Emissions and Crop Yields From Winter Oilseed Rape Cropping Systems are Unaffected by Management Practices***
M. O'Neill, G. J. Lanigan, P. D. Forristal and B. A. Osborne

44 ***Assessment of Greenhouse Gases Emission in Maize-Wheat Cropping System Under Varied N Fertilizer Application Using Cool Farm Tool***
Rakesh Kumar, S. Karmakar, Asisan Minz, Jitendra Singh, Abhay Kumar and Arvind Kumar

53 ***Achieving Chinese Carbon Neutrality Based on Water–Temperature–Radiation–Land Coupling Use***
Yinglin Tian, Di Xie, Tiejian Li, Jiaye Li, Yu Zhang, Huan Jing, Deyu Zhong and Guangqian Wang

60 ***COVID-19 and Greenhouse Gas Emission Mitigation: Modeling the Impact on Environmental Sustainability and Policies***
Muhammad Mohsin, Sobia Naseem, Muddassar Sarfraz, Larisa Ivascu and Gadah Albasher

69 ***Quantifying Tree Diversity, Carbon Stocks, and Sequestration Potential for Diverse Land Uses in Northeast India***
Uttam Kumar Sahoo, Om Prakash Tripathi, Arun Jyoti Nath, Sourabh Deb, Dhruba Jyoti Das, Asha Gupta, N. Bijayalaxmi Devi, Shiva Shankar Charturvedi, Soibam Lanabir Singh, Amit Kumar and Brajesh Kumar Tiwari

83 ***Biomass Production Assessment in a Protected Area of Dry Tropical forest Ecosystem of India: A Field to Satellite Observation Approach***
Tarun K. Thakur, Digvesh K. Patel, Anita Thakur, Anirudh Kumar, Arvind Bijalwan, Jahangeer A. Bhat, Amit Kumar, M. J. Dobriyal, Munesh Kumar and Amit Kumar

100 ***Root-To-Shoot Ratios of Flood-Tolerant Perennial Grasses Depend on Harvest and Fertilization Management: Implications for Quantification of Soil Carbon Input***
Claudia Kalla Nielsen, Uffe Jørgensen and Poul Erik Lærke

frontiers in Environmental Science

EDITORIAL
published: 16 February 2022
doi: 10.3389/fenvs.2022.834444

Editorial: Greenhouse Gas Emissions and Terrestrial Ecosystems

Amit Kumar[1]*, *Amit Kumar*[2]*, *Munesh Kumar*[3] and *Jahangeer A. Bhat*[4]

[1]Nanjing University of Information Science and Technology, Nanjing, China, [2]Central Muga Eri Research and Training Institute (CMERTI), Jorhat, India, [3]Hemwati Nandan Bahuguna Garhwal University, Srinagar, India, [4]Fiji National University, Suva, Fiji

Keywords: GHGs, terrestrial ecosystem, carbon stock, mitigation, carbon dynamics

Editorial on the Research Topic

Greenhouse Gas Emissions and Terrestrial Ecosystems

In recent decades, greenhouse gas (GHG, particularly CO_2 and CH_4) emissions are mainly responsible for the increase in global mean temperature due to natural and anthropogenic activities (Hui et al., 2021; Kumar et al., 2021). Grossi et al. (2021) proposed a holistic methodological approach to estimate (quantitatively and qualitatively) the annual GHG emissions and removals occurring in the natural parks and suggest their significance in mitigation of climate change and respective adaptation. In general, the alarming rate of climate change and global warming is critically governed by the rapid increase in urbanization, industrialization, fossil fuel burning, forest fire, change in land use and land cover (LULC; responsible for 10–12% of anthropogenic GHG emissions), agricultural activities in the catchment, slash and burn activities, etc. (Kumar et al., 2021a). LULC change is estimated to emit 1.3 ± 0.5 peta-grams C y^{-1} (~8% of annual emission). Sahoo et al. (2021) worked in the northeastern region of Indian forest and estimated biomass and carbon (C) storage potential under diverse land uses. He found a strong relationship between the biomass C storage and tree basal area. The mean vegetation C stock followed a pattern of temperate forests > subtropical plantations > subtropical forests > tropical forests > tropical plantations > temperate plantations and is useful for the C reduction strategies. Furthermore, accurate quantification of total C stock (forest biomass and soil) is a decisive commission in decision support related to climate and land use management. Nielsen et al. (2021) highlighted the importance of root: shoot (R/S) ratios in imprecise modeling evaluations of the soil C input. An increase in the number of annual cuts was found to lower the R/S (Nielsen et al., 2021). Thakur et al. (2021) worked on a protected area of dry tropical forest and estimated the mean value of net primary productivity (NPP) as 8.74 Mg ha^{-1} yr^{-1} (varied from 7.61 to 9.94 Mg ha^{-1} yr^{-1}) where above-ground biomass contributes 1/3rd of total NPP and further plays an important role in carbon (C) mitigation in central India. In general, tropical ecosystems are hot spots of GHG emissions compared to temperate ones because of higher temperatures and low humidity.

The change in soil C stock under conservation agriculture practices in the Indo-Gangetic Plains and sub-Saharan Africa compared to conventional practice ranged from 0.16 to 0.49 Mg C ha^{-1} yr^{-1} and 0.28 to 0.96 Mg C ha^{-1} yr^{-1}, respectively. These wide ranges energized the young scientists to explore in detail their ecological footprint, energy, and economic effectiveness. Moreover, the significant amount of methane (CH_4) from rice fields, peat lands, bogs, etc.; nitrous oxide (N_2O) from agricultural crops and forest floor; and CO_2 from plants and animals through respiration; soil respiration (efflux of CO_2) and sinks into the terrestrial ecosystems and in the form of crop production, the transportation and production of forest biomass, and agricultural activities also contributes to atmospheric GHG emissions (**Figure 1**). Kumar et al. (2021b) concluded that extensive inter-culture operations (i.e., sowing, irrigation, tillage, fertilizer application, and pest control management) extensively influence the GHG emissions (CO_2 and N_2O) from wheat–maize agricultural soil. However, O'Neill et al. (2021) concluded that management practices, especially row spacing width (125 and 750 mm) and variety of crops, have no consistent effect on

Edited and reviewed by:
Hayley Jane Fowler, Newcastle University, United Kingdom

***Correspondence:**
Amit Kumar
amit_bio80@yahoo.com
Amit Kumar
amitkdah@nuist.edu.cn

Specialty section:
This article was submitted to Interdisciplinary Climate Studies, a section of the journal Frontiers in Environmental Science

Received: *13 December 2021*
Accepted: *26 January 2022*
Published: *16 February 2022*

Citation:
Kumar A, Kumar A, Kumar M and Bhat JA (2022) Editorial: Greenhouse Gas Emissions and Terrestrial Ecosystems. Front. Environ. Sci. 10:834444. doi: 10.3389/fenvs.2022.834444

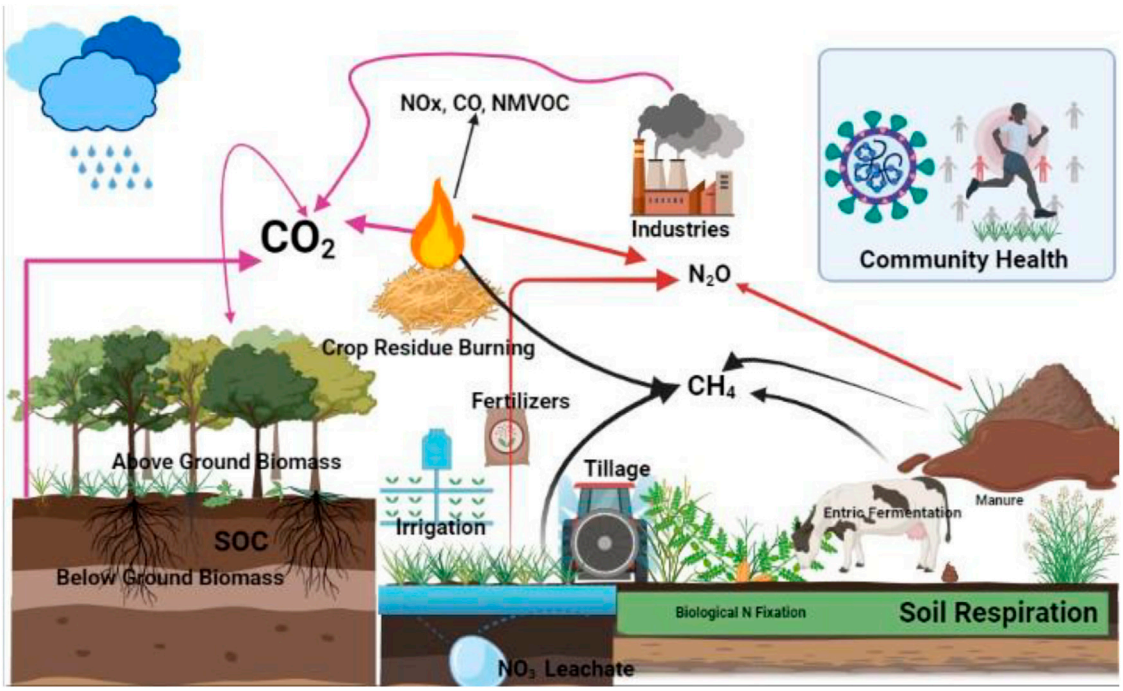

FIGURE 1 | Process, mechanism, and factors affecting carbon dynamics in terrestrial ecosystem.

soil emissions, and modifications in seed yield per plant countered differences in planting density in winter oilseed rape crop grown in Ireland.

The rapid climate change results in loss of terrestrial biodiversity and affects the C dynamics (source and/or sink) both directly and indirectly (Heimann and Reichstein, 2008; Liu et al., 2018). Mohsin et al. (2021) emphasize that a catchment area treatment planning in advance can be helpful in carbon reduction and further enhance the quality of the environment. Nowadays, sector-specific mitigation strategies play an important role in terrestrial GHG trade-offs. In recent decades, management practices, such as catchment area treatment plan, afforestation of plants having high carbon sequestration potential, forest protection (e.g., forest fire), agriculture conservation, zero tillage practices, and incorporation of waste residue could help in increasing C sink or mitigation of the C emission significantly from the terrestrial ecosystems. The rate of C sequestration and forest protection ranges from 0.04 to 7.52 t C·hm^{-2}·a^{-1} and 0.33 to 5.20 t C·hm^{-2}·a^{-1}, respectively. Based on the comprehensive use of natural resources, Tian et al. (2021) suggested that the necessity and possibility of C trading and redistribution of the natural resources are highly recommended ways to ensure carbon reduction by 2060.

Forest vegetation and perennial crops have high C density (above- and below-ground biomass; ABG and BGB) and tree species richness to support ecosystem resilience to future climate change, besides a strong potential to support forest biodiversity and agricultural productivity (Sharma et al., 2021). Missing the Paris agreement target to achieve global mean temperature (i.e., 2°C) could destabilize Earth's climate, terrestrial ecosystems with terrible consequences for ecosystem services, biodiversity, and humans. Therefore, a strategic management plan is urgently needed to reduce the potential of C by implementing climate change mitigation and adaptation measures in terrestrial ecosystems.

All the guest editors hope that the article (review/research) published in this special issue will help the policy makers, environmentalists, foresters, and young researchers to understand the carbon dynamics in the terrestrial ecosystem at the regional and/or global scale. Furthermore, the mitigation strategies suggested by the different authors will help in C reduction in the terrestrial ecosystem.

AUTHOR CONTRIBUTIONS

All authors listed have made a substantial, direct, and intellectual contribution to the work and approved it for publication.

REFERENCES

Heimann, M., and Reichstein, M. (2008). Terrestrial Ecosystem Carbon Dynamics and Climate Feedbacks. *Nature* 451, 289–292. doi:10.1038/nature06591

Hui, D., Deng, Q., Tian, H., and Luo, Y. (2021). "Global Climate Change and Greenhouse Gases Emissions in Terrestrial Ecosystems," in *Handbook of Climate Change Mitigation and Adaptation*. Editors M. Lackner, B. Sajjadi, and W. Y. Chen (New York, NY: Springer). doi:10.1007/978-1-4614-6431-0_13-3

Kumar, A., Bhatia, A., Sehgal, V. K., Tomer, R., Jain, N., and Pathak, H. (2021b). Net Ecosystem Exchange of Carbon Dioxide in Rice-Spring Wheat System of Northwestern Indo-Gangetic Plains. *Land* 10 (7), 701. doi:10.3390/land10070701

Kumar, A., Kumar, M., Pandey, R., ZhiGuo, Y., and Cabral-Pinto, M. (2021a). Forest Soil Nutrient Stocks along Altitudinal Range of Uttarakhand Himalayas: An Aid to Nature Based Climate Solutions. *CATENA* 207, 105667. doi:10.1016/j.catena.2021.105667

Liu, S., Ji, C., Wang, C., Chen, J., Jin, Y., Zou, Z., et al. (2018). Climatic Role of Terrestrial Ecosystem under Elevated CO2: A Bottom-Up Greenhouse Gases Budget. *Ecol. Lett.* 21 (7), 1108–1118. doi:10.1111/ele.13078

Conflict of Interest: The authors declare that the research was conducted in the absence of any commercial or financial relationships that could be construed as a potential conflict of interest.

Publisher's Note: All claims expressed in this article are solely those of the authors and do not necessarily represent those of their affiliated organizations, or those of the publisher, the editors and the reviewers. Any product that may be evaluated in this article, or claim that may be made by its manufacturer, is not guaranteed or endorsed by the publisher.

frontiers in Environmental Science

REVIEW
published: 29 July 2021
doi: 10.3389/fenvs.2021.700768

Appraisal of Carbon Capture, Storage, and Utilization Through Fruit Crops

Sunny Sharma[1], *Vishal Singh Rana*[1], *Heerendra Prasad*[1]*, *Johnson Lakra*[1] and *Umesh Sharma*[2]

[1]Department of Fruit Science, Dr. Yashwant Singh Parmar University of Horticulture and Forestry, Nauni, India, [2]Department of Tree Improvement and Genetic Resources, Dr. Yashwant Singh Parmar University of Horticulture and Forestry, Nauni, India

Nowadays, rapid increases in anthropogenic activities have resulted in increased greenhouse gases (GHGs; CO_2, CH_4, N_2O) release in the atmosphere, resulting in increased global mean temperature, aberrant precipitation patterns, and several other climate changes that affect ecological and human lives on this planet. This article reviews the adaptation and mitigation of climate change by assessing carbon capture, storage, and utilization by fruit crops. Perennial plants in forests, fruit orchards, and grasslands are efficient sinks of atmospheric carbon, whereas field crops are a great source of GHG due to soil disturbance, emission of CH_4 and/or N_2O from burning straw, and field management involving direct (fuel) or indirect (chemicals) emissions from fossil fuels. Thus, there is a need to establish sustainable agricultural systems that can minimize emissions and are capable of sequestering carbon within the atmosphere. Fruit orchards and vineyards have great structural characteristics, such as long life cycle; permanent organs such as trunk, branches, and roots; null soil tillage (preserving soil organic matter); high quality and yield, which allow them to accumulate a significant amount of carbon. Hence, the fruit plants have significant potential to sequester carbon in the atmosphere. However, the efficiency of carbon sequestration by different fruit crops and their management systems may vary due to their growth and development patterns, physiological behavior, biomass accumulation, and environmental factors.

Keywords: carbon emission, climate changes, fruit trees, production, storage

OPEN ACCESS

Edited by:
Amit Kumar,
Nanjing University of Information Science and Technology, China

Reviewed by:
Tarun Kumar Thakur,
Indira Gandhi National Tribal University, India
Marina Cabral Pinto,
University of Aveiro, Portugal
Vinod Kumar Kairon,
Forest Research Institute (FRI), India

***Correspondence:**
Heerendra Prasad
heerendrasagar@gmail.com

Specialty section:
This article was submitted to Interdisciplinary Climate Studies, a section of the journal Frontiers in Environmental Science

Received: *26 April 2021*
Accepted: *25 June 2021*
Published: *29 July 2021*

Citation:
Sharma S, Rana VS, Prasad H, Lakra J and Sharma U (2021) Appraisal of Carbon Capture, Storage, and Utilization Through Fruit Crops. Front. Environ. Sci. 9:700768. doi: 10.3389/fenvs.2021.700768

INTRODUCTION

The worldwide population is expected to be around 9.1 billion by 2050, which would be 34% higher than the existing population (UN, 2019). This will enhance the food demand to match the needs of the rising population. Horticultural commodities, in general, and fruits, in particular, have been designated as the sources of nutraceuticals (Sharma et al., 2021). The global mean surface temperature increment of pre-industrial values has reached up to 0.87 ± 0.10°C during the 2006–2015 decade (Hoegh-Guldberg et al., 2018). According to the Fifth Assessment Report (AR_5) of the Intergovernmental Panel on Climate Change (IPCC), 2013–2014, the mean global temperature of the land and the ocean showed a warming of 0.85°C, i.e., range b/w 0.65–1.06°C during 1880–2012 (Wolf et al., 2017). The main reason behind this increase is anthropogenic interference (Hartmann et al., 2013; Stocker et al., 2013). An IPCC Special Report has confirmed that the rise in the mean temperature globally affected peoples, different ecosystems, and livelihoods worldwide. Moreover, climate change might obstruct progress toward a world without hunger for all people. A robust change in global pattern is noticeable in the effects of the inclination of temperature

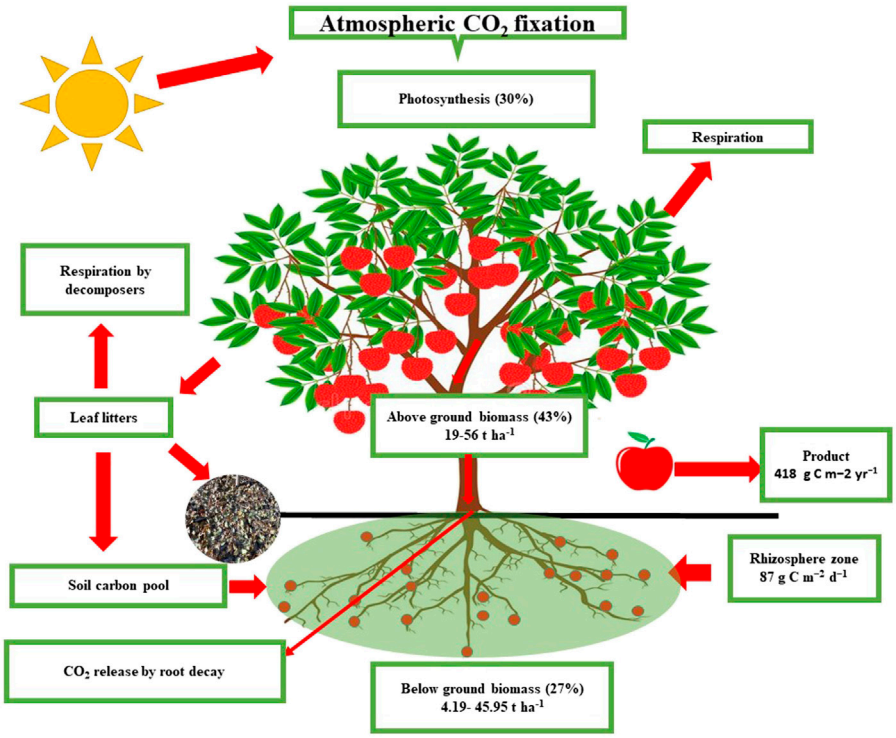

FIGURE 1 | Schematic diagram of carbon pools in an apple tree (redrawn from Buchmann and Schulze, 1999). The yearly NEP, GPP, and NPP are 403 g Cm^{-2}, 1,346, and 906 g Cm^{-2} year^{-1}, respectively. The average NECB indicates significant potential for CO_2 sequestration. OM/OA: organic manures/organic amendment; GPP: gross primary production; NPP: net primary production; NEP: net ecosystem production; NECB: net ecosystem carbon balance; NBP: net biome productivity; RA: autotropic respiration; RH: heterotrophic respiration; Harvest: fruit production; R_{ECO}: ecosystem respiration.

on sustainable crop production. Due to climate change, the steadiness of food systems might be at risk because of the short-term variability in the supply chain (Wheeler and Von Braun, 2013). However, the prospective consequences are less clear at provincial scales, but climate change will directly impact food security in areas that are susceptible to hunger and malnutrition (IPCC, 2018). Similarly, it indirectly influences the household and individual earning and causes loss of access to drinking water and damage to health. The emissions of greenhouse gas (GHG) is inclining globally day by day, but many practices are available to maintain the emission of these gases, the most prevalent one being the cultivation and conservation of trees like fruit orchards or agroforestry (Boonen, 2015; Kumar and Sharma, 2015; Kumar et al., 2020; Sarkar et al., 2021; Thakur et al., 2021). This practice might be a vital solution to reduce the emission of harmful gases and has many positive effects on the environment, also known as "climate-smart cultivation" (Brown et al., 1995; Canadell and Raupach, 2008; Nair et al., 2010; Shaffer, 2010; Zanotelli et al., 2013; Chakrabarti, 2017). Fruit cultivation is considered a potential tool of good agricultural practices that might be reduced by the impact of climate change (Rana and Rana, 2003; Jhalegar et al., 2012). Hence, the combination of trees, usually in different systems, increases productivity, improves the nutrient cycle, and helps maintain the ecological balance because of the "biological carbon sequestration potential" (Ospina, 2017; Rana et al. 2020; Kumar et al. 2021; Rai et al., 2021; Sheikh et al., 2021; Tamang et al., 2021). Given the above-mentioned fact, this review article showed the complete effect of fruit crops on carbon sequestration, that is, the process by which carbon source is taken from the atmosphere and stored in another place. The present article mainly focuses on assessing the above-ground biomass (AGB) and below-ground biomass (BGB) of fruit orchards and their corresponding carbon stocks so that net contributors of GHG to the atmosphere could be estimated. Besides, mitigation measures are also suggested to reduce the C-stock and GHG emissions from fruit orchards in the future under CO_2 enrichment and global warming.

RELATIONSHIP BETWEEN FRUITS TREE AND CARBON SEQUESTRATION

Carbon sequestration in terrestrial ecosystems is the process of net exclusion of carbon sources like CO_2 from the environment or reducing its emissions from terrestrial ecosystems and storing them into another form in a productive manner (IPCC, 2018). The process of removal of carbon through photosynthesis process in green plant (vegetation) in which inclined CO_2 uptake from atmosphere takes place and CO_2 is stored in different photosynthetic or non-photosynthetic parts such as trunks, branches, leaves, and roots of the plants (IPCC, 2018). Carbon

sequestration of soil induction of the possible amount of organic carbon (OC) into the soil also reduced the amount of atmospheric C (De Moraes Sá and Lal, 2009). CO_2 gas is a chief source of the atmospheric greenhouse effect depiction (**Figure 1**). From 1951, the rapid changes in the level of CO_2 took place, hence influencing global climate changes. According to NASA, the concentration of CO_2 globally was 416.14 ppm up to March 2021 (NOAA, 2021). However, many other gases such as methane (CH_4), water vapor (H_2O), ozone (O_3), and nitrous oxide (N_2O) also play a vital role in climate change because of their higher global warming potential compared to the CO_2 (Barbera et al., 2018). Land management practices are one of the important factors affecting carbon sequestration (Lal, 2018). The alteration in the global carbon balance occurs through anthropogenic activities such as burning of fuel, production of cement (67%), and agriculture and land use changes (33%) (Friedlingstein et al., 2020). Perennial crops, such as citrus, apple (orchards), kiwifruit, and grapes (vineyards), are significantly important for converting more atmospheric carbon compared to annual crops like flowers and field crops (Robertson et al., 2000; Xiao et al., 2003; Kalcsits et al., 2020).

In general, crops have some structural characteristics that allow them to capture more carbon sources because of their life cycle and large photosynthetic activity (Bationo et al., 2007; Xu et al., 2019). In addition, fruit growers not only depend on the quantity they produce but also on quality to enhance income (grape berry color and shape). Some fruit crops show less potential in terms of yield because of less distribution of carbon to the fruits than that of high-yielding crops (Kumari et al., 2020). Hence, the net primary production (NPP) is prevalent in the accumulation C cycle or distributed into the permanent structures of the tree. NPP is the distinction between total photosynthesis and respiration in flora and fauna and is assessed through estimating the quantity of the new organic matter (OM) formed, i.e., in living plants under a specific time given time (Clark et al., 2001; Levesque et al., 2019). There is limited literature available on the potential of fruit crops to sequestering carbon and environmental service. However, fruit orchards greatly influence sustainable development under changing climate scenarios (FAO, 2010). However, the benefit to the fruit growers is restricted or limited as compared to forest and plantation crops (Xiaoetal., 2003; Liu et al., 2018), but with the emergence of Kyoto protocol fruit, orchardists can derive their remuneration via carbon trading and gaining creditability (Page et al., 2011).

Fruits farming is a sustainable system of production where solar energy can be utilized at different levels, soil resources can be used efficiently and cropping intensity can also be altered (Nimbolkar et al., 2016). The system consists of three main components: main crop, filler crop, and intercrops, which occupy three different tiers in the production system (Nimbolkar et al., 2016). Orchards are recognized for carbon storage because they can capture a large quantity of C in their vegetative organs for a longer period of time (Nardino et al., 2013). Like orchards, soil is the primary terrestrial carbon sink globally (Hammad et al., 2020). However, its sequestering potential depends on several factors, such as climate, type of soil, crop and vegetation, and management practices (Meena et al., 2020). The carbon stored in soil organic matter (SOM) is affected by the addition of dead plant materials and loss of carbon through respiration, the microbial status process, and soil disturbance (natural and human disturbance) (Koné and Yao, 2021). The carbon capture process can be done by different plant organs: trunks, branches, leaves, flowers, fruits, and roots (Henry et al., 2020). There are various fruit trees, namely, avocado, banana, citrus, mangosteen, and mango, which significantly increase the rate of photosynthesis, thereby increasing the tree biomass. By applying CO_2 at 800 ppm for one year, Schaffer (2009) has ameliorated the photosynthesis rate by 40–60% compared to ambient CO_2 concentration in mangosteen. The heavy bearing ability of fruit trees has a great tendency to increase carbon capturing from the atmosphere and store it in the form of cellulose (Patil and Kumar, 2017; Zade et al., 2020). Fruit orchards can significantly contribute to sustainable fruit production under changing climate scenarios in tropical and sub-tropical areas (FAO, 2010; Nath et al., 2019).

CARBON SEQUESTERING IN TREES AND SOILS

Fruit orchards might play an important role in climate change via the sequestration of carbon, biological growth (increasing biomass), and deforestation (increasing carbon emissions) (Hammad et al., 2020; Khan et al., 2021). The process of photosynthesis is that a tree can capture the little amount of carbon stored in the form of carbohydrates and return some of the amount to the atmosphere through the respiration (**Figure 1**) process (Nunes et al., 2020). Carbon is stored not only in tree biomass but also in soils (Sedjo and Sohngen, 2012). Therefore, carbon present in the plant tissue is either consumed by humans (fruits) or added to the soil in the form of litter when the plant dies and decomposes (Patil and Kumar, 2017). Carbon is stored in the soil in the form of soil organic matter (SOM) (Cotrufo et al., 2019). It is a combination of carbon compounds formed after the decomposition of plant and animal tissues (Khatoon et al., 2017). These materials can be developed with the help of soil biotas such as protozoa, nematodes, fungi, and bacteria and then are associated with soil minerals (Zhang et al., 2021). Thereafter, carbon can remain stored in soils for a long time or can rapidly return back to the atmosphere *via* the respiration process by soil microbes (Sharma et al., 2018; Zhang et al., 2021). Various factors like climatic conditions, natural vegetation, soil physicochemical properties, drainage, and human land use affect the amount of carbon and the length of time carbon is stored in soil (Wiesmeier et al., 2019).

FACTOR AFFECTING CARBON SEQUESTRATION IN FRUIT CROPS

Numerous factors influence the carbon sequestration in fruit crops. Out of these factors, latitude, water availability, plant age and species, nutrients, temperature, and atmospheric gases highly influence the carbon sequestration rate.

Solar Radiation

Solar radiation is one of the important factors by which the photosynthesis process is directed (Pawar and Rana, 2019). The photosynthesis process depends on light duration intensity and the duration (Hüve et al., 2019) and further regulates the metabolic process of carbon in fruit trees. The rapid increase in carbon sequestration rate was found to increase significantly with incoming solar radiation (Gough et al., 2012; Rao et al., 2021). Moreover, the intensity of light increases or decreases the pattern of the carbon storage (Shaver et al., 1992).

Water Availability

Like light, water availability to the plants is also part of the photosynthesis process (Pawar and Rana, 2019). The availability of water affects NPP because the moisture content helps increase leaf area index (LAI) (Li et al., 2020). The density of foliage is directly proportional to the productivity of the tree because of the more capturing tendency for carbohydrates molecules (DeMattos et al., 2020). However, water scarcity will cause wilting of plants due to reduced photosynthetic activity, falling C uptake, and less carbon capture (Gower, 2001).

Nutrients Requirement

Nutrients are a vital component for several internal biological processes because crops species cannot complete their life cycle events in the absence of this element (Jones, 1997). There are 17 essential nutrient elements required for the tree species and the role of each nutrient element is specific to a specific plant species (Das and Avasthe, 2018). The tree foliages consist of variable numbers and amounts of nutrients (Gough et al., 2012). Trees species are able to proliferate themselves with an optimum supply of nutrients; therefore, a greater amount of carbon is sequestered (Pawar and Rana, 2019; Sharma et al., 2021).

Temperature

Temperature is an important ecophysiological factor that affects the ratio of plant growth and development (Restrepo-Díaz et al., 2010). The metabolic activities are also influenced by the rate of temperature. If the rate of temperature increases, then metabolic activities (photosynthesis and respiration) also increase significantly up to optimum temperature and then decline rapidly (Pawar and Rana, 2019). For this reason, temperate fruit crops capture the least amount of carbon in the winter because the canopy is leafless (winter dormancy). In contrast, more carbon is captured in the summer when the temperature is increased and carbon is gained via the photosynthesis process (Gough et al., 2012).

Atmospheric Gases

The concentration of atmospheric gases (particularly CO_2 and O_3) affects the rate of carbon sequestration. The rate of atmospheric CO_2 levels affects carbon availability to the plants. Karberg et al. (2005) have revealed an increase in NPP (20%) with an increase in the rate of CO_2. Unfortunately, some harmful compositions like ground-level ozone might be increased with the increment of carbon values in the atmosphere; therefore, NPP rate has decreased (Pregitzer et al., 2008).

CARBON CAPTURE OF LONG RESIDENCE WOODY, LEAF, FRUIT, AND ROOTS

The atmospheric CO_2 is absorbed during the photosynthesis process; the carbohydrates and their accumulation follow anabolic pathways (Farquhar and Sharkey, 1982; Kumar et al., 2017). Similarly, the loss occurs through green and non-green organs *via* the process of respiration (Haslam and Treagust, 1987; Yu et al., 2018; Chen and Chen, 2019). The accumulated portion is conglomerated with organic compounds; later on, it is distributed into different plant parts, leading to the formation of new biomass, represented as the net primary production (NPP) (Clark et al., 2001). Gross primary product (GPP) and NPP are the prime phases of the carbon cycle under ecosystems where GPP is the aggregate CO_2 level adjusted by photosynthesis, i.e., signifying the ability of crops to collect carbon and energy (Badawy, 2011). C losses occur at the ecosystem level because of the respiration of heterotrophic organisms under the soil (Rh) (Wang et al., 2019). The main difference between NPP and Rh is denoted as net ecosystem production (NEP). NEP is a vital ecological factor that signals out of the photosynthesis or respiration, which is a dominant factor used in assessing the ecosystem potential (Rodda et al., 2021). Moreover, net ecosystem carbon balance (NECB), particularly in agricultural systems, increases or decreases the carbon level by cultivation over a passage of time (Antar et al., 2021), as depicted in **Figure 2**. It is also dependent on the value of carbon that comes in *via* organic amendments and moves out *via* end-products like fruits or timber (Oviedo-Ocaña et al., 2021).

Literature available on carbon fluxes under fruit crop and NPP and GPP for horticultural crops, especially fruit crops (Ceschia et al., 2010; Marín et al., 2016; Shi et al., 2017; Khalsa et al., 2020), is summarized in **Table 1**. Fruit trees (woody, leaf, fruit, and roots) represent a valuable portion of land use in various areas and have an important role in capturing net carbon dioxide sink and storing carbon compounds in the permanent woody parts of the fruit tree (Scandellari et al., 2016; Chamizo et al., 2017; Tezza et al., 2019). Moreover, the prospect of using organic manures or soil amenders may ameliorate the capability of fruit orchards systems as CO_2 sink. In horticultural systems, in terms of the addition or removal of carbon over time, for example, during cultivation (NECB), the volume of carbon entry depends on the amount of manure applied to the crop, and produce like fruits is an example of carbon removal. Furthermore, planting orchards is a valuable land use form worldwide.

Scandellari et al. (2016) have analyzed the biomass, NPP and NECB, and net carbon balance by either direct or eddy covariance methodology. They showed that above-ground NPP ranged between 10 and 20 t ha^{-1} with direct methodology, whereas the below-ground NPP was reduced by 20 percent from the total NPP. The carbon removal through the fruit system ranged between 2 and 3 t ha^{-1}. Fruit orchard ecosystems had shown significant results on the net ecosystem productivity, ranging from 4.30 to 7.5 t C ha^{-1} yr^{-1}in Apple-2 and Grape-1, respectively. Moreover, NECB, ranging 0.6–5.9 t C $ha^{-1}$$year^{-1}$, indicates potential carbon capturing through long residence woody, leaf, fruit, and roots and storage of the carbon

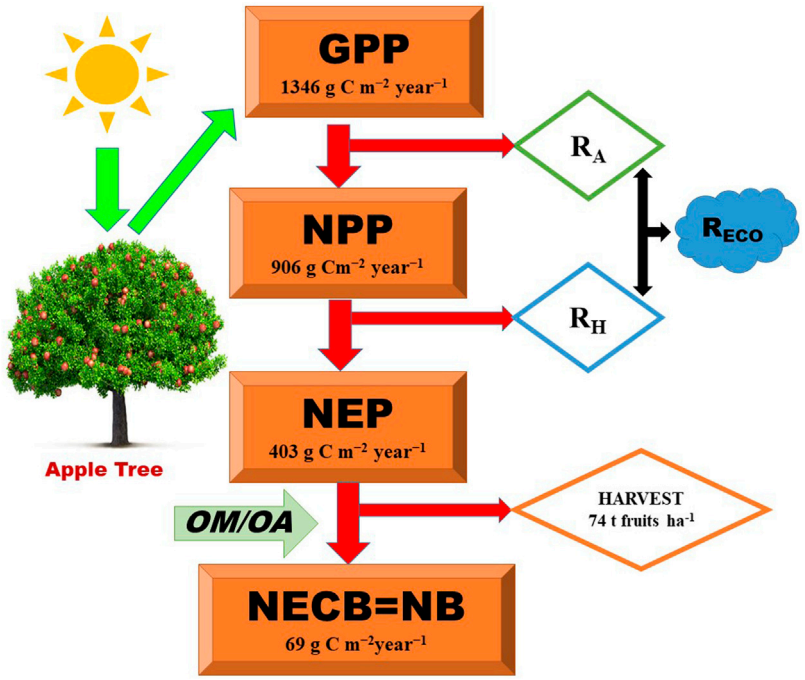

FIGURE 2 | Relationship between fruit trees and carbon sequestration.

TABLE 1 | Carbon fixation (NPP, NEP, and NECB) by different fruit tree orchards.

Tree/vine/tree ecosystem	NPP (g C ha^{-1}yr^{-1})	NEP	NECB	References
Agroforestry system and citrus	17.7			Marín et al. (2016)
Tropical palm plantation	16.1			Navarro et al. (2008)
Tropical forests	12.5			Grace 2004
Citrus trees	11.4			Quiñones et al., 2013
Kiwi fruits	8.0			Facini et al., 2007
Apple	5.2–13.3			Wu et al. (2012)
Apple				
"Gala"	11.81	4.30 to 7.5 t C ha^{-1} y^{-1}	0.6 to 5.9 t C ha^{-1} y^{-1}	Scandellari et al. (2016)
Apple				
"Fuji"	17.44			
Peach				
"Supercrimson"	9.94			
Citrus				
"Tarocco"	11.88			
Grape	9.96			
Cocoa	18.8			Morel et al. (2019)
Peach		11.7–17.5 t C ha^{-1} year^{-1} 3^{1}	90 g Cm^{-2} yr^{-1}–730 g Cm^{-2} yr^{-1}	Montanaro et al. (2021)
Oil palm plantation	121.7			Melenya et al. (2015)

(Scandellari et al., 2016). Bhatnagar et al. (2016) have reported that carbon accumulation values in fruits ranged 32–41%, whereas the other structural organs like twigs, branches, and stems stored ~25% of the total carbon. Hence, Nagpur mandarin is regarded as another vital sink for carbon partitioning of around 6 kg C^{-1} tree^{-1}yr^{-1} (2.5 Mg C^{-1}ha^{-1}yr^{-1}). Khalsa et al. (2020) have shown that the application of nitrogen (N) supplement an orchard enhanced the capturing of more C, thus lowering the net global warming potential (GWP) in a California almond orchard. In this intensive system, 309 kg N ha^{-1} yr^{-1} fertilizer N rates also increased the net primary productivity (Mg C ha^{-1}), N productivity (kg N ha^{-1}), and net nitrogen mineralization (mg N kg^{-1} soil d^{-1}). Wu et al. (2012) have analyzed the carbon sequestration capability in apple orchards and stated that the capability of trees for carbon sequestration is enhanced when they reach 18 years of age and declines with age. The net carbon sink and C storage (biomass) in Chinese apple orchards are between 14 and 32 Tg C and 230 and 475 Tg C, respectively, from 1990 to

TABLE 2 | Effect of different fruit tree species on biomass and carbon sequestration with special reference to age and spacing.

Crop	Botanical name	Biomass kg/tree or vine	Age Year old	Spacing	Country	Carbon sequestration	References
Apple	*Malus domestica Borkh.*	224.08	18	3 × 5 m	China	6,871.8 C^{-1} $m2^{-1}$ yr^{-1}	Wu et al. (2012)
Litchi	*Litchi chinensis*	8.42	7	10 × 10 m	India	30.81 Mg ha^{-1}	Kanime et al., 2013
Mango	*Mangifera indica*	27.02	15	10 × 10 m		98.90 Mg ha^{-1}	
Chinese plum	*Prunus saliciana*	8.05	5	5 × 5 m		29.40 Mg ha^{-1}	
Apple	*Malus domestica Borkh.*				India	0.01–35.00 MT ha^{-1}	Attar et al. (2016)
Apricot	*Prunus americana*					0.04–61.22 MT ha^{-1}	
Walnut	*Juglans regi*					0.35–62.50 MT ha^{-1}	
Citrus	*Citrus reticulata*				India	217 g $C^{-1}m2^{-1}yr^{-1}$	Bhatnagar et al. (2016)
Nagpur Mandarin	*C. reticulata*	5.94	6		India	1.65 t ha^{-1}	Mehta et al. (2016)
Mango	*Mangifera indica*	733.025			India	73.59 t ha^{-1}	Ganeshamurthy et al. (2019a)
Mango	*Mangifera indica*	269.07			Konkan, India	26.91 t ha^{-1}	Ganeshamurthy et al. (2019b)
Hazelnut	*Corylus avellana*		17	5 × 5 m	Italy	58.8 Mg ha^{-1} $year^{-1}$	Granata et al. (2020)

2010. The calculated net carbon sequestration in the apple from 1990 to 2010 was approx. 4.5% of the total net carbon sink in the terrestrial ecosystems in China. Therefore, apple production systems can be considered an important carbon sink in fruit culture (Wu et al., 2012). Similarly, many reports on carbon emission in various crops have been confirmed by other researchers globally (Piao et al., 2009; Bhatnagar et al., 2016; Marín et al., 2016; Shi et al., 2017; Khalsa et al., 2020).

Kumar et al. (2019) have used various models for estimating biomass of plants, i.e., 225 mg ha^{-1} with biomass accumulation and carbon storage reduced by roots followed by twigs and leaves and branches. Mehta et al. (2016) have reported a similar result in fruit orchards, i.e., fixation by the fruit crop is higher than that of annual and herbaceous crops. The mean AGB and BGB was 13.21 kg $tree^{-1}$, where the above-ground contribution maximum share was 76% and the below-ground contribution was 24%. The maximum carbon was stored by the fruit biomass (2.10 Kg $tree^{-1}$), followed by roots and branches in a six-year-old citrus plant in a plantation orchard. Many reports have studied the potential of carbon sequestration in many fruit orchards, mainly perennials species, which is the key point in mitigating climate change scenario (Marín et al., 2016). Navarro et al. (2008) have assessed carbon accumulation in vegetative organs of palm trees, which was approximately 16.1 Mg C^{-1} ha^{-1} yr^{-1}. Likewise, Janiola and Marin (2016) have suggested that tropical fruit trees, like mango, are more capable of accumulating more carbon in fifteen-year-old orchards, i.e., 45 Mg C^{-1} ha^{-1} yr^{-1}. Similarly, the carbon (1750 g $C^{-1}m^2$ yr^{-1}) accumulation rates were found in citrus Pernice et al. (2006). Further, Rossi et al. (2007) have assayed the carbon storage (1,160 g C m^{-2}) in kiwifruit cv. Hayward within seven months. Various researchers have confirmed that orchards like citrus, wine grape, apple, olive, peach, hazelnut, and orange could be a substantial sink for atmospheric carbon (Liguori et al., 2009; Granata et al., 2020). Similarly, any agricultural practices, like the use of organic manures or AM fungi, may act as carbon sinks (Shi et al., 2017; Sharma et al., 2018; Verbruggen et al., 2021). Several studies have shown that the application of organic manures improves the physicochemical properties of soil (Evanylo et al., 2008; Bravo et al., 2012; Sharma et al., 2018; Sharma et al., 2021) and ameliorates root development (Baldi et al., 2010; Sarita et al., 2019). Granata et al. (2020) have quantified the CO_2 sequestered by *Corylus avellana* L. (hazelnut) orchards. They have reported that the total amount of CO_2 accumulated by hazelnut was 58.8 ± 9.1 Mg ha^{-1} $year^{-1}$, where the highest value of carbon capturing is in May (12.4 ± 2.0 Mg CO_2 ha^{-1} $month^{-1}$). Hence, not only is the cultivation of hazelnut is important from the nut production point of view, but it also has a greater role as a carbon sink. Ganeshamurthy et al. (2019a) have estimated the AGB and BGB carbon in the mango orchards in different states, ranging from 776.9 to 1,574 kg $tree^{-1}$ (**Table 2**). The above reports have suggested that fruit orchards may act as a great means for carbon accumulation in biomass. Hence, this pool of carbon fixation might help reduce atmospheric CO_2. Thus, fruit culture could play an efficient role in mitigating climate change scenarios.

CONCLUSION AND THE WAY FORWARD

After careful deliberations, it can be concluded that climate change due to different anthropogenic activities could potentially disturb improvement toward a world without hunger. A robust and coherent global pattern is discernible of the impacts of climate change on crop productivity that could have consequences for food availability. Various fruit crops like apple mango, citrus, and grapes have shown their potential roles in sequestrating carbon, thus enhancing biological yield. The carbon sources also improve the NPP, NEP, and NECB of various fruits compared to those of annual crops. The calculation of C biomass gives an idea about the quantity and quality of carbon available in the area and how it behaves in tree species compared to the annual crops, where the carbon is eventually degraded to GHGs to the environment causing global warming and climate change. The recommendation of suitable mitigation measures is also given in order to reduce GHG emissions. Hence, crop-fixing

carbon might help reduce atmospheric CO_2 and has a great capability of CO_2 capture, storage, and utilization of carbon sources.

Various crops have a tremendous potential toward sequestering the carbon; however, the potential of many fruit trees is still unexploited. Hence, there is an urgent need to know the carbon sequestration potential in fruit crop species. A smart approach is required to develop and identify suitable propagation methods, systems, and appropriate tree species to ameliorate carbon storage and enhance fruit production.

AUTHOR CONTRIBUTIONS

All authors listed have made a substantial, direct, and intellectual contribution to the work and approved it for publication. SS, VR: (Writing - original draft preparation); SS and HP, (Figures and Tables); VR and SS (Conceptualization and supervision); US and HP (Helped in data compilation and arrangement); SS, VR and HP (Reviewed the write up and Helped in finalizing the draft); SS and HP (Revised the Manuscript).

REFERENCES

Antar, M., Lyu, D., Nazari, M., Shah, A., Zhou, X., and Smith, D. L. (2021). Biomass for a Sustainable Bioeconomy: An Overview of World Biomass Production and Utilization. *Renew. Sustain. Energ. Rev.* 139, 110691. doi:10.1016/j.rser.2020.110691

Attar, S. K., Thakur, N. S., Kumar, N., and Solanki, P. D. (2016). "Potential of Sequestering Carbon through Fruit Orchards.(2016)," in Proceedings of the Forest and Tree Based Land Use Systems for Livelihood, Nutritional and Environmental Security, Navsari, India, January 21–23, 2016 (Navsari: COF), 209–216.

Badawy, B. A. A. M. (2011). Quantifying Carbon Processes of the Terrestrial Biosphere in a Global Atmospheric Inversion Based on Atmospheric Mixing Ratio, Remote Sensing and Meteorological Data. Doctoral dissertation. Jena (Germany): Universität Jena.

Baldi, E., Toselli, M., Eissenstat, D. M., Marangoni, B., and Peter, M. (2010). Organic Fertilization Leads to Increased Peach Root Production and Lifespan. *Tree Physiol.* 30, 1373–1382. doi:10.1093/treephys/tpq078

Barbera, A. C., Vymazal, J., and Maucieri, C. (2018). "Greenhouse Gases Formation and Emission." in *Encyclopedia of Ecology*, 2nd ed. Editor B. Fath (Elsevier), 329–333.

Bationo, A., Kihara, J., Vanlauwe, B., Waswa, B., and Kimetu, J. (2007). Soil Organic Carbon Dynamics, Functions and Management in West African Agro-Ecosystems. *Agric. Syst.* 94, 13–25. doi:10.1016/j.agsy.2005.08.011

Bhatnagar, P., Singh, J., Chauhan, P. S., Sharma, M. K., Meena, C. B., and Jain, M. C. (2016). Carbon Assimilation Potential of Nagpur Mandarin (Citrus Reticulata Blanco.). *Int. J. Sci. Env. Tech.* 5, 1402–1409.

Boonen, R. (2015). How to Feed and Not to Eat Our World? Available at: https://lirias.kuleuven.be/1717149?limo=0 1–179 (Accessed April 1, 2021). doi:10.1530/endoabs.37.s23.1

Bravo, K., Toselli, M., Baldi, E., Marcolini, G., Sorrenti, G., Quartieri, M., et al. (2012). Effect of Organic Fertilization on Carbon Assimilation and Partitioning in Bearing Nectarine Trees. *Scientia Horticulturae* 137, 100–106. doi:10.1016/j.scienta.2012.01.030

Brown, S., Sathaye, J., Cannell, M., and Kauppi, P. E. (1995). *Management of Forests for Mitigation of Greenhouse Gas Emissions*. United Kingdom: Cambridge University Press.

Canadell, J. G., and Raupach, M. R. (2008). Managing Forests for Climate Change Mitigation. *Science* 320 (5882), 1456–1457. doi:10.1126/science.1155458

Ceschia, E., Béziat, P., Dejoux, J. F., Aubinet, M., Bernhofer, C., Bodson, B., et al. (2010). Management Effects on Net Ecosystem Carbon and GHG Budgets at European Crop Sites. *Agric. Ecosyst. Environ.* 139, 363–383. doi:10.1016/j.agee.2010.09.020

Chakrabarti, S. (2017). "The Nutrition Advantage: Harnessing Nutrition Co-benefits of Climate-Resilient Agriculture," in IFAD Advantage Series, Rome, September 2017 (Rome: IFAD), 1–49. doi:10.2139/ssrn.3671605

Chamizo, S., Rodríguez-Caballero, E., Román, J. R., and Cantón, Y. (2017). Effects of Biocrust on Soil Erosion and Organic Carbon Losses under Natural Rainfall. *Catena* 148, 117–125. doi:10.1016/j.catena.2016.06.017

Chen, X., and Chen, H. Y. H. (2019). Plant Diversity Loss Reduces Soil Respiration across Terrestrial Ecosystems. *Glob. Change Biol.* 25, 1482–1492. doi:10.1111/gcb.14567

Clark, D. A., Brown, S., Kicklighter, D. W., Chambers, J. Q., Thomlinson, J. R., and Ni, J. (2001). Measuring Net Primary Production in Forests: Concepts and Field Methods. *Ecol. Appl.* 11, 356–370. doi:10.1890/1051-0761(2001)01110.1890/1051-0761(2001)011[0356:mnppif]2.0.co;2

Cotrufo, M. F., Ranalli, M. G., Haddix, M. L., Six, J., and Lugato, E. (2019). Soil Carbon Storage Informed by Particulate and mineral-associated Organic Matter. *Nat. Geosci.* 12, 989–994. doi:10.1038/s41561-019-0484-6

Das, S. K., and Avasthe, R. K. (2018). Plant Nutrition Management Strategy: A Policy for Optimum Yield. *Actascienti. Agric.* 2 (5), 65–70.

de Mattos, E. M., Binkley, D., Campoe, O. C., Alvares, C. A., and Stape, J. L. (2020). Variation in Canopy Structure, Leaf Area, Light Interception and Light Use Efficiency Among Eucalyptus Clones. *For. Ecol. Manage.* 463, 118038. doi:10.1016/j.foreco.2020.118038

De Moraes Sá, J. C., and Lal, R. (2009). Stratification Ratio of Soil Organic Matter Pools as an Indicator of Carbon Sequestration in a Tillage Chronosequence on a Brazilian Oxisol. *Soil Tillage Res.* 103, 46–56. doi:10.1016/j.still.2008.09.003

Evanylo, G., Sherony, C., Spargo, J., Starner, D., Brosius, M., and Haering, K. (2008). Soil and Water Environmental Effects of Fertilizer-, Manure-, and Compost-Based Fertility Practices in an Organic Vegetable Cropping System. *Agric. Ecosyst. Environ.* 127, 50–58. doi:10.1016/j.agee.2008.02.014

FAO (2010). The State of Food and Agriculture 2010: Food Aid for Food Security? 1–62. Available at http://www.fao.org/3/i1683e/i1683e.pdf (Accessed April 10, 2021).

Farquhar, G. D., and Sharkey, T. D. (1982). Stomatal Conductance and Photosynthesis. *Annu. Rev. Plant Physiol.* 33, 317–345. doi:10.1146/annurev.pp.33.060182.001533

Friedlingstein, P., O'Sullivan, M., Jones, M. W., Andrew, R. M., Hauck, J., Olsen, A., et al. (2020). Global Carbon Budget 2020. *Ear.Sys. Sci. Data* 12, 3269–3340.

Ganeshamurthy, A. N., Ravindra, V., and Rupa, T. R. (2019a). Carbon Sequestration Potential of Mango Orchards in India. *CurrSci.* 117, 2006–2013. doi:10.18520/cs/v117/i12/2006-2013

Ganeshamurthy, A. N., Ravindra, V., Rupa, T. R., and Bhatt, R. M. (2019b). Carbon Sequestration Potential of Mango Orchards in the Tropical Hot and Humid Climate of Konkan Region, India. *Curr. Sci.* 116, 1417–1423. doi:10.18520/cs/v116/i8/1417-1423

Gough, L., Gross, K. L., Cleland, E. E., Clark, C. M., Collins, S. L., Fargione, J. E., et al. (2012). Incorporating Clonal Growth Form Clarifies the Role of Plant Height in Response to Nitrogen Addition. *Oecologia* 169, 1053–1062. doi:10.1007/s00442-012-2264-5

Granata, M. U., Bracco, F., and Catoni, R. (2020). Carbon Dioxide Sequestration Capability of Hazelnut Orchards: Daily and Seasonal Trends. *Energ. Ecol. Environ.* 5, 153–160. doi:10.1007/s40974-020-00161-7

Hammad, H. M., Fasihuddin Nauman, H. M., Abbas, F., Ahmad, A., Bakhat, H. F., Saeed, S., et al. (2020). Carbon Sequestration Potential and Soil Characteristics of Various Land Use Systems in Arid Region. *J. Environ. Manage.* 264, 110254. doi:10.1016/j.jenvman.2020.110254

Hartmann, D. L., Tank, A. M. G. K., MatildeRusticucci, L. V. R., Brönnimann, S., Abdul RahmanCharabi, Y., Dentener, F. J., et al. (2013). "Observations: Atmosphere and Surface." in *Climate Change 2013 the Physical Science Basis: Working Group I Contribution to the Fifth Assessment Report of the Intergovernmental Panel on Climate Change*. United Kingdom: Cambridge Uni Press, 159–254.

Haslam, F., and Treagust, D. F. (1987). Diagnosing Secondary Students' Misconceptions of Photosynthesis and Respiration in Plants Using a Two-Tier Multiple Choice Instrument. *J. Biol. Educ.* 21, 203–211. doi:10.1080/00219266.1987.9654897

Henry, R. J., Furtado, A., and Rangan, P. (2020). Pathways of Photosynthesis in Non-leaf Tissues. *Biology* 9, 438. doi:10.3390/biology9120438

Hoegh-Guldberg, O., Jacob, D., Bindi, M., Brown, S., Camilloni, I., Diedhiou, A., et al. (2018). "Impacts of 1.5°C Global Warming on Natural and Human Systems," in *Global warming of 1.5°C. An IPCC Special Report on Impacts of Global Warming of 1.5°C Above Pre-Industrial Levels and Related Global Greenhouse Gas Emission Pathways, in the Context of Strengthening the Global Response to the Threat of Climate Change, Sustainable Development, and Efforts to Eradicate Poverty*. Editors V. Masson-Delmotte, P. Zhai, H. O. Pörtner, D. Roberts, J. Skea, P. R. Shukla, et al. Geneva: IPCC.

Hüve, K., Bichele, I., Kaldmäe, H., Rasulov, B., Valladares, F., and Niinemets, Ü. (2019). Responses of aspen Leaves to Heatflecks: Both Damaging and Non-damaging Rapid Temperature Excursions Reduce Photosynthesis. *Plants* 8, 145. doi:10.3390/plants8060145

IPCC (2018). *Global Warming of 1.5°C*. Available at: https://www.ipcc.ch/2018/10/08/summary-for-policymakers-of-ipcc-special-report-on-global-warming-of-1-5c-approved-bygovernments/#:~:text=The%20report%20was%20prepared%20under,all%20three%20IPCC%20working%20groups.&text=As%20part%20of%20the%20decision,global%20greenhouse%20gas%20emission%20pathways (Accessed April 1, 2021).

Janiola, M. D. C., and Marin, A. (2016). Carbon Sequestration Potential of Fruit Tree Plantations in Southern Philippines. *J. Biodivers. Environ. Sci.* 8, 164–174.

Jhalegar, M. J., Sharma, R. R., Pal, R. K., and Rana, V. (2012). Effect of Postharvest Treatments with Polyamines on Physiological and Biochemical Attributes of Kiwifruit (Actinidia Deliciosa) Cv. Allison. *Fruits* 67, 13–22. doi:10.1051/fruits/2011062

Kalcsits, L., Lotze, E., Tagliavini, M., Hannam, K. D., Mimmo, T., Neilsen, D., et al. (2020). Recent Achievements and New Research Opportunities for Optimizing Macronutrient Availability, Acquisition, and Distribution for Perennial Fruit Crops. *Agronomy* 10, 1738. doi:10.3390/agronomy10111738

Karberg, N. J., Pregitzer, K. S., King, J. S., Friend, A. L., and Wood, J. R. (2005). Soil Carbon Dioxide Partial Pressure and Dissolved Inorganic Carbonate Chemistry under Elevated Carbon Dioxide and Ozone. *Oecologia* 142, 296–306. doi:10.1007/s00442-004-1665-5

Khalsa, S. D. S., Smart, D. R., Muhammad, S., Armstrong, C. M., Sanden, B. L., Houlton, B. Z., et al. (2020). Intensive Fertilizer Use Increases Orchard N Cycling and Lowers Net Global Warming Potential. *Sci. Total Environ.* 722, 137889. doi:10.1016/j.scitotenv.2020.137889

Khan, N., Jhariya, M. K., Raj, A., Banerjee, A., and Meena, R. S. (2021). "Soil Carbon Stock and Sequestration: Implications for Climate Change Adaptation and Mitigation," in *Ecological Intensification of Natural Resources for Sustainable Agriculture*. Editors M. K. Jhariya, R. S. Meena, and A. Banerjee (Singapore: Springer), 461–489.

Khatoon, H., Solanki, P., Narayan, M., Tewari, L., Rai, J., and HinaKhatoon, C. (2017). Role of Microbes in Organic Carbon Decomposition and Maintenance of Soil Ecosystem. *Int. J. Chem. Stud.* 5, 1648–1656.

Koné, A. W., and Yao, M. K. (2021). Soil Microbial Functioning and Organic Carbon Storage: Can Complex Timber Tree Stands Mimic Natural Forests? *J. Environ. Manage.* 283, 112002. doi:10.1016/j.jenvman.2021.112002

Kumar, A., Cabral-Pinto, M., Kumar, A., Kumar, M., and Dinis, P. A. (2020). Estimation of Risk to the Eco-Environment and Human Health of Using Heavy Metals in the Uttarakhand Himalaya, India. *Appl. Sci.* 10, 7078. doi:10.3390/app10207078

Kumar, A., and Sharma, M. P. (2015). Assessment of Carbon Stocks in forest and its Implications on Global Climate Changes. *J. Mater. Environ. Sci.* 6, 3548–3564.

Kumar, M., Kumar, A., Kumar, R., Konsam, B., Pala, N. A., and Bhat., J. A. (2021). Carbon Stock Potential in Pinus Roxburghii Forests of Indian Himalayan Regions. *Environ. Dev. Sustain.* 23, 12463–12478. doi:10.1007/s10668-020-01178-y

Kumar, P. A., Mishra, A. K., Kumar, M., Chaudhari, S. K., Singh, R., Singh, K., et al. (2019). Biomass Production and Carbon Sequestration of Eucalyptus Tereticornis Plantation in Reclaimed Sodic Soils of north-west India. *Ind. J. Agr. Sci.* 89, 1091–1095.

Kumar, S., Sreeharsha, R. V., MudalkarS Sarashetti, S., Sarashetti, P. M., and Reddy, A. R. (2017). Molecular Insights into Photosynthesis and Carbohydrate Metabolism in Jatropha Curcas Grown under Elevated CO2 Using Transcriptome Sequencing and Assembly. *Sci. Rep.* 7, 11066. doi:10.1038/s41598-017-11312-y

Kumari, R., Kundu, M., Das, A., Rakshit, R., Sahay, S., Sengupta, S., et al. (2020). Long-Term Integrated Nutrient Management Improves Carbon Stock and Fruit Yield in a Subtropical Mango (Mangifera Indica L.) Orchard. *J. Soil Sci. Plant Nutr.* 20, 725–737. doi:10.1007/s42729-019-00160-6

Lal, R. (2018). Digging Deeper: A Holistic Perspective of Factors Affecting Soil Organic Carbon Sequestration in Agroecosystems. *Glob. Change Biol.* 24, 3285–3301. doi:10.1111/gcb.14054

Levesque, M., Andreu-Hayles, L., Smith, W. K., Williams, A. P., Hobi, M. L., Allred, B. W., et al. (2019). Tree-ring Isotopes Capture Interannual Vegetation Productivity Dynamics at the Biome Scale. *Nat. Commun.* 10, 1–10. doi:10.1038/s41467-019-08634-y

Li, C., Sun, H., Wu, X., and Han, H. (2020). An Approach for Improving Soil Water Content for Modeling Net Primary Production on the Qinghai-Tibetan Plateau Using Biome-BGC Model. *Catena* 184, 104253. doi:10.1016/j.catena.2019.104253

Liguori, G., Gugliuzza, G., and Inglese, P. (2009). Evaluating Carbon Fluxes in orange Orchards in Relation to Planting Density. *J. Agric. Sci.* 147, 637–645. doi:10.1017/S002185960900882X

Liu, C. L. C., Kuchma, O., and Krutovsky, K. V. (2018). Mixed-species versus Monocultures in Plantation Forestry: Development, Benefits, Ecosystem Services and Perspectives for the Future. *Glob. Ecol. Conservation* 15, e00419. doi:10.1016/j.gecco.2018.e00419

Marín, Q. M. P., Andrade, H. J., and Sandoval, A. P. (2016). Fijación de carbonoatmosferico en la biomasa total de sistemas de producción de cacao en el departamento del Tolima, Colombia. *Rev. U.D.C.A Act. Div. Cient.* 19, 351–360. (in Spanish). doi:10.31910/rudca.v19.n2.2016.89

Meena, R. S., Kumar, S., and Yadav, G. S. (2020). "Soil Carbon Sequestration in Crop Production," in *Nutrient Dynamics for Sustainable Crop Production*. Editor R. Meena (Singapore: Springer), 1–39. doi:10.1007/978-981-13-8660-2_1

Mehta, L. C., Singh, J., Chauhan, P. S., Singh, B., and Manhas, R. K. (2016). Biomass Accumulation and Carbon Storage in Six-Year-Old Citrus Reticulata Blanco. *Plantation. Ind. For.* 142, 563–568 .

Melenya, C., Bonsu, M., Logah, V., Quansah, C., Adjei-Gyapong, T., Yeboah, I. B., et al. (2015). Carbon Sequestration in Soils under Different Land Use Systems and it Impact on Climate Change. *Appl. Res. J.* 1, 164–168.

Montanaro, G., Dichio, B., Mininni, A. N., Berloco, T., Capogrossi, A., and Xiloyannis, C. (2021). Managing Carbon Fluxes in a Peach Orchard. *Acta Hortic.* 1304, 201–206. doi:10.17660/ActaHortic.2021.1304.28

Morel, A. C., Adu Sasu, M., Adu-Bredu, S., Quaye, M., Moore, C., Ashley Asare, R., et al. (2019). Carbon Dynamics, Net Primary Productivity and Human-Appropriated Net Primary Productivity across a forest-cocoa Farm Landscape in West Africa. *Glob. Change Biol.* 25, 2661–2677. doi:10.1111/gcb.14661

Nair, P. R., Nair, V. D., Kumar, B. M., and Showalter, J. M. (2010). Carbon Sequestration in Agroforestry Systems. *Adv. in.Agron.* 108, 237–307. doi:10.1016/S0065-2113(10)08005-3

Nardino, M., Pernice, F., Rossi, F., Georgiadis, T., Facini, O., Motisi, A., et al. (2013). Annual and Monthly Carbon Balance in an Intensively Managed Mediterranean Olive Orchard. *Photosynt.* 51, 63–74. doi:10.1007/s11099-012-0079-6

Nath, V., Kumar, G., Pandey, S. D., and Pandey, S. (2019). "Impact of Climate Change on Tropical Fruit Production Systems and its Mitigation Strategies," in *Climate Change and Agriculture in India: Impact and Adaptation*. Editors S. Sheraz Mahdi (Cham: Springer), 129–146. doi:10.1007/978-3-319-90086-5_11

Navarro, M. N. V., Jourdan, C., Sileye, T., Braconnier, S., Mialet-Serra, I., Saint-Andre, L., et al. (2008). Fruit Development, Not GPP, Drives Seasonal Variation in NPP in a Tropical palm Plantation. *Tree Physiol.* 28, 1661–1674. doi:10.1093/treephys/28.11.1661

Nimbolkar, P. K., Awachare, C., Chander, S., and Husain, F. (2016). Multi Storied Cropping System in Horticulture-A Sustainable Land Use Approach. *Int. J. Agr. Sci.* 8, 3016–3019.

NOAA (2021). Despite Pandemic Shutdowns, Carbon Dioxide and Methane Surged in 2020. Available at: https://research.noaa.gov/article/ArtMID/587/ArticleID/2742/Despite-pandemic-shutdowns-carbon-dioxide-and-methane-surged-in-2020 (Accessed April 12, 2021).

Nunes, L. J. R., Meireles, C. I. R., Pinto Gomes, C. J., and Almeida Ribeiro, N. M. C. (2020). Forest Contribution to Climate Change Mitigation: Management Oriented to Carbon Capture and Storage. *Climate* 8, 21. doi:10.3390/cli8020021

Ospina, C. (2017). *Climate and Economic Benefits of Agroforestry Systems*. Washington: The Climate Institute. Available at: http://climate.org/wp-content/uploads/2017/03/Agroforestry-Article-3.6.17.pdf.

Oviedo-Ocaña, E. R., Hernández-Gómez, A. M., Ríos, M., Portela, A., Sánchez-Torres, V., Domínguez, I., et al. (2021). A Comparison of Two-Stage and Traditional Co-composting of Green Waste and Food Waste Amended with Phosphate Rock and Sawdust. *Sustainability* 13, 1109. doi:10.3390/su13031109

Page, G., Kelly, T., Minor, M., and Cameron, E. (2011). Modeling Carbon Footprints of Organic Orchard Production Systems to Address Carbon Trading: an Approach Based on Life Cycle Assessment. *Horts* 46, 324–327. doi:10.21273/hortsci46.2.324

Patil, P., and Kumar, A. K. (2017). Biological Carbon Sequestration through Fruit Crops (Perennial Crops-Natural "Sponges" for Absorbing Carbon Dioxide from Atmosphere). *Pl Arch.* 17, 1041–1046 .

Pawar, R., and Rana, V. S. (2019). Manipulation of Source-Sink Relationship in Pertinence to Better Fruit Quality and Yield in Fruit Crops: A Review. *Agric. Rev.* 40, 200–207. doi:10.18805/ag.r-1934

Piao, S., Fang, J., Ciais, P., Peylin, P., Huang, Y., Sitch, S., et al. (2009). The Carbon Balance of Terrestrial Ecosystems in China. *Nature* 458, 1009–1013. doi:10.1038/nature07944

Pregitzer, K. S., Burton, A. J., King, J. S., and Zak, D. R. (2008). Soil Respiration, Root Biomass, and Root Turnover Following Long-Term Exposure of Northern Forests to Elevated Atmospheric CO 2 and Tropospheric O 3. *New Phytol.* 180, 153–161. doi:10.1111/j.1469-8137.2008.02564.x

Rai, P., Vineeta, G., Shukla, G., Manohar K, A., Bhat, J. A., Kumar, A., et al. (2021). Carbon Storage of Single Tree and Mixed Tree Dominant Species Stands in a Reserve Forest-Case Study of the Eastern Sub-himalayan Region of India. *Land* 10, 435. doi:10.3390/land10040435

Rana, K., Kumar, M., and Kumar, A. (2020). Assessment of Annual Shoot Biomass and Carbon Storage Potential of Grewia Optiva: an Approach to Combat Climate Change in Garhwal Himalaya. *Water Air Soil Pollut.* 231, 450. doi:10.1007/s11270-020-04825-2

Rana, V. S., and Rana, N. S. (2003). Studies on Fruit Growth and Organic Metabolites in Developing Kiwifruit. *Ind. J. Pl. Physio* 8, 138–140.

Rao, Z., Bao, S., Liu, X., Taylor, R. A., and Liao, S. (2021). Estimating Allowable Energy Flux Density for the Supercritical Carbon Dioxide Solar Receiver: A Service Life Approach. *Appl. Therm. Eng.* 182, 116024. doi:10.1016/j.applthermaleng.2020.116024

Restrepo-Díaz, H., Melgar, J. C., and Lombardini, L. (2010). Ecophysiology of Horticultural Crops: an Overview. *Agron.Colomb.* 28, 71–79. doi:10.1590/S1677-04202007000400014

Rita, S., Bakshi, P., Kour, K., Mehla, U., wana, B., Sharma, S., et al. (2019). Effect of Different Potting Media on Nutrient Composition of Soil and Leaves of Litchi Air Layers. *Int. J. Curr. Microbiol. App. Sci.* 8, 928–933. doi:10.20546/ijcmas.2019.810.108

Robertson, G. P., Paul, E. A., and Harwood, R. R. (2000). Greenhouse Gases in Intensive Agriculture: Contributions of Individual Gases to the Radiative Forcing of the Atmosphere. *Science* 289 (5486), 1922–1925. doi:10.1126/science.289.5486.1922

Rodda, S. R., Thumaty, K. C., Praveen, M., Jha, C. S., and Dadhwal, V. K. (2021). Multi-year Eddy Covariance Measurements of Net Ecosystem Exchange in Tropical Dry Deciduous forest of India. *Agric. For. Meteorology* 301-302, 108351. doi:10.1016/j.agrformet.2021.108351

Rossi, F., Facini, O., Georgiadis, T., and Nardino, M. (2007). Seasonal CO2 Fluxes and Energy Balance in a Kiwifruit Orchard. *Rivis.Ital di.Agromet.* 1, 44–56.

Sarkar, P. K., Sarkar, P., Kumar, A., Pala, N. A., and Kumar, M. (2021). Carbon Storage Potential of a Waterlogged Agroforestry System of Tripura, India. *Water Air Soil Pollut.* 232, 151. doi:10.1007/s11270-021-05098-z

Scandellari, F., Liguori, G., Caruso, G., Meggio, F., Inglese, P., Gucci, R., et al. (2017). Carbon Sequestration Potential of Italian Orchards and Vineyards. *Acta Hortic.* 1177, 145–150. doi:10.17660/ActaHortic.2017.1177.19

Sedjo, R., and Sohngen, B. (2012). Carbon Sequestration in Forests and Soils. *Annu. Rev. Resour. Econ.* 4, 127–144. doi:10.1146/annurev-resource-083110-115941

Shaffer, G. (2010). Long-term Effectiveness and Consequences of Carbon Dioxide Sequestration. *Nat. Geosci* 3, 464–467. doi:10.1038/ngeo896

Sharma, S., Rana, V. S., Kumari, M., and Mishra, P. (2018). Biofertilizers: Boon for Fruit Production. *J. Pharmacogn. Phytochem.* 7, 3244–3247 .

Sharma, S., Rana, V. S., Pawar, R., Lakra, J., and Racchapannavar, V. (2021). Nanofertilizers for Sustainable Fruit Production: a Review. *Environ. Chem. Lett.* 19, 1693–1714. doi:10.1007/s10311-020-01125-3

Sheikh, M. A., Kumar, M., Todaria, N. P., Bhat, J. A., Kumar, A., and Pandey, R. (2021). Contribution of Cedrus Deodara Forests for Climate Mitigation along Altitudinal Gradient in Garhwal Himalaya, India. *Mitig Adapt Strateg. Glob. Change* 26, 5. doi:10.1007/s11027-021-09941-w

Shi, L., Wang, J., Liu, B., Nara, K., Lian, C., Shen, Z., et al. (2017). Ectomycorrhizal Fungi Reduce the Light Compensation point and Promote Carbon Fixation of Pinus Thunbergii Seedlings to Adapt to Shade Environments. *Mycorrhiza* 27, 823–830. doi:10.1007/s00572-017-0795-7

Stocker, T. F., Qin, D., Plattner, G. K., Alexander, L. V., Allen, S. K., Bindoff, N. L., et al. (2013). "Technical Summary," in *Climate Change 2013: The Physical Science Basis. Contribution of Working Group I to the Fifth Assessment Report of the Intergovernmental Panel on Climate Change*. United Kingdom: Cambridge University Press, 33–115.

Tamang, M., Chettri, R., Vineeta, G., Shukla, G., Bhat, J. A., Kumar, A., et al. (2021). Stand Structure, Biomass and Carbon Storage in Gmelina Arborea Plantation at Agricultural Landscape in Foothills of Eastern Himalayas. *Land* 10, 387. doi:10.3390/land10040387

Tezza, L., Vendrame, N., and Pitacco, A. (2019). Disentangling the Carbon Budget of a Vineyard: The Role of Soil Management. *Agric. Ecosyst. Environ.* 272, 52–62. doi:10.1016/j.agee.2018.11.002

Thakur, U., Bisht, N. S., Kumar, M., and Kumar, A. (2021). Influence of Altitude on Diversity and Distribution Pattern of Trees in Himalayan Temperate Forests of Churdhar Wildlife Sanctuary, India. *Water Air Soil Pollut.* 232, 205. doi:10.1007/s11270-021-05162-8

UN (2019). World Population Projected to Reach 9.8 Billion in 2050, and 11.2 Billion in 2100. Available at: https://www.un.org/development/desa/en/news/population/world-population-prospects-2017.html (Accessed April 14, 2021).

Verbruggen, E., Struyf, E., and Vicca, S. (2021). Can Arbuscularmycorrhizal Fungi Speed up Carbon Sequestration by Enhanced Weathering? *Plants, People Planet.* 1–9. doi:10.1002/ppp3.1017

Wang, J., Song, B., Ma, F., Tian, D., Li, Y., Yan, T., et al. (2019). Nitrogen Addition Reduces Soil Respiration but Increases the Relative Contribution of Heterotrophic Component in an alpine Meadow. *Funct. Ecol.* 33, 2239–2253. doi:10.1111/1365-2435.13433

Wheeler, T., and Von Braun, J. (2013). Climate Change Impacts on Global Food Security. *Science* 341, 508–513. doi:10.1126/science.1239402

Wiesmeier, M., Urbanski, L., Hobley, E., Lang, B., von Lützow, M., Marin-Spiotta, E., et al. (2019). Soil Organic Carbon Storage as a Key Function of Soils - A Review of Drivers and Indicators at Various Scales. *Geoderma.* 333, 149–162. doi:10.1016/j.geoderma.2018.07.026

Wolf, E., Arnell, N., Friedlingstein, P., Gregory, J., Haigh, J., Haines, A., et al. (2017). *Climate Updates: What Have We Learnt since the IPCC 5th Assessment Report?*, 1–36.

Wu, T., Wang, Y., Yu, C., Chiarawipa, R., Zhang, X., Han, Z., et al. (2012). Carbon Sequestration by Fruit Trees - Chinese Apple Orchards as an Example. *PLoS One* 7, e38883. doi:10.1371/journal.pone.0038883

Xiao, C.-W., Yuste, J. C., Janssens, I. A., Roskams, P., Nachtergale, L., Carrara, A., et al. (2003). Above- and Belowground Biomass and Net Primary Production in a 73-Year-Old Scots pine forest. *Tree Physiol.* 23, 505–516. doi:10.1093/treephys/23.8.505

Xu, X., Gu, X., Wang, Z., Shatner, W., and Wang, Z. (2019). Progress, Challenges and Solutions of Research on Photosynthetic Carbon Sequestration Efficiency

of Microalgae. *Renew. Sustain. Energ. Rev.* 110, 65–82. doi:10.1016/j.rser.2019.04.050

Yu, Y., Tao, H., Yao, H., and Zhao, C. (2018). Assessment of the Effect of Plastic Mulching on Soil Respiration in the Arid Agricultural Region of China under Future Climate Scenarios. *Agric. For. Meteorol.* 256-257, 1–9. doi:10.1016/j.agrformet.2018.02.025

Zade, S. P., Bhosale, S. L., and Gourkhede, P. H. (2020). Carbon Status in Major Fruit Orchard Soils of Parbhani District of Maharashtra. *Int. J. Curr. Microbiol. App. Sci.* 9, 1969–1979. doi:10.20546/ijcmas.2020.903.229

Zanotelli, D., Montagnani, L., Manca, G., and Tagliavini, M. (2013). Net Primary Productivity, Allocation Pattern and Carbon Use Efficiency in an Apple Orchard Assessed by Integrating Eddy Covariance, Biometric and Continuous Soil Chamber Measurements. *Biogeosciences* 10, 3089–3108. doi:10.5194/bg-10-3089-2013

Zhang, K., Maltais-Landry, G., and Liao, H.-L. (2021). How Soil Biota Regulate C Cycling and Soil C Pools in Diversified Crop Rotations. *Soil Biol. Biochem.* 156, 108219. doi:10.1016/j.soilbio.2021.108219

Conflict of Interest: The authors declare that the research was conducted in the absence of any commercial or financial relationships that could be construed as a potential conflict of interest.

frontiers in Environmental Science

ORIGINAL RESEARCH
published: 09 August 2021
doi: 10.3389/fenvs.2021.706880

Greenhouse Gas Emissions and Carbon Sinks of an Italian Natural Park

Giampiero Grossi, Andrea Vitali, Umberto Bernabucci, Nicola Lacetera* and Alessandro Nardone*

Department of Agriculture and Forest Sciences (DAFNE), University of Tuscia, Viterbo, Italy

Natural parks (NPs) have a primary role in supporting people's welfare by maintaining natural and cultural resources. Various activities, such as those related to conservation of flora and fauna, forestry, agriculture and livestock, residential, and tourism, coexist within the boundaries of NPs. All these activities may contribute as a source or sink of carbon dioxide and, despite some NPs having started to promote their environmental services, there is currently a lack of information on their carbon footprint (CF). Although various international standards have provided guidelines to assess the CF of organizations, a lack of explicit formulation and procedure in these standards makes them difficult to apply, especially when the organizations to be evaluated embed a wide range of biological and anthropogenic activities. The framework proposed in this paper provides for the first time a holistic methodological approach to quantitatively and qualitatively estimate the annual greenhouse gas (GHG) emissions and removals occurring in NPs. The main data needed for the NP's GHG inventory were directly collected on-site. The activity data and emissions factors as well as the methodologies involved were all referenced to their data sources, including the use of a biogeochemical model, IPCC equations, Ecoinvent database, and a literature review. This method highlighted that, by emitting 0.55 Mg CO_{2e} ha^{-1} $year^{-1}$, the NP generates an annual CF of about 3,300 Mg of CO_{2e}. The agricultural activities with 43.4% of share showed the largest incidence, followed by wild fauna (17.8%), tourism (15.1%), and, to a lesser extent, all the other sectors considered in the assessment. On the other hand, when the annual soil and forest C sequestration rates were included in the balance, the NP contributes to sequester about 3.7 Mg CO_{2e} ha^{-1} $year^{-1}$, thus resulting in it being an important C-sink site (i.e., about 22,000 Mg CO_{2e} $year^{-1}$). By providing granular information on GHG emissions and carbon removals trend, the methodological approach involved in this study could help NPs in both planning effective mitigation strategies and supporting environmental certification processes. CF of NPs could increase tourists' awareness of the important role that these protected natural areas have in climate change mitigation and adaptation.

Keywords: national parks, LCA, carbon footprint, carbon sequestration, mitigation

OPEN ACCESS

Edited by:
Amit Kumar,
Central Muga Eri Research and Training Institute (CMERTI), India

Reviewed by:
Sandeep K. Malyan,
Agricultural Research Organization (ARO), Israel
Ashish K. Chaturvedi,
Centre for Water Resources Development and Management, India

****Correspondence:***
Andrea Vitali
vitali@unitus.it
Nicola Lacetera
nicgio@unitus.it

Specialty section:
This article was submitted to Interdisciplinary Climate Studies, a section of the journal Frontiers in Environmental Science

Received: *08 May 2021*
Accepted: *21 June 2021*
Published: *09 August 2021*

Citation:
Grossi G, Vitali A, Bernabucci U, Lacetera N and Nardone A (2021) Greenhouse Gas Emissions and Carbon Sinks of an Italian Natural Park. Front. Environ. Sci. 9:706880. doi: 10.3389/fenvs.2021.706880

INTRODUCTION

Human activities such as those related to industries, transport, energy, and agriculture have led to the release of anthropogenic greenhouse gases (GHGs) into the atmosphere (Malyan et al., 2016; IPCC, 2019). Fortunately, as society prospers, there is an increasing awareness of the environmental impact of these activities. The Carbon Footprint (CF) is a term used to describe the measurement of GHG emissions generated by a product or an organization. Wiedmann and Minx (2008) define the CF as a measure of the total amount of CO_2 emissions that are directly and indirectly caused over the life stages of a product or activity. However, as most of the anthropogenic activities emit other GHGs than CO_2 (e.g., CH_4, N_2O, HFCs, etc.), the term carbon dioxide equivalent (CO_{2e}) is commonly used in CF assessments. Specifically, the term equivalent means that the global warming factor of every GHG is calculated using CO_2 as means of comparison (Tjandra et al., 2016). CF assessment may have a wide range of applications in the development of products, environmental policies, and marketing. The applications that, among others, can be highlighted are decision making, research and development, identification of areas of improvement, environmental labeling, and ecological product statement (Calderón et al., 2010).

The ISO 14064–1 is an international standard for quantifying and reporting GHG emissions and removals at the organization level (ISO, 2019). The ISO broadly classified GHG emissions as direct and indirect. The direct GHG emissions are the ones resulting from sources that are owned and controlled by the organization, while the indirect are those that are a consequence of the company' activities but occur from sources owned or controlled by a different entity. A further classification is represented by the GHG removals. The ISO 14064–1 defines the C stocks as the quantity of C stored in soil organic matter (SOC), above and below-ground biomass, dead organic matter, and harvested wood products. Due to the reversibility of these C stock reservoirs (i.e., these could be re-emitted into the atmosphere), the ISO standards recommends reporting the GHG removals separately from the other GHG emissions, and, in doing so, it suggests expressing the net annual GHG flux as the net sum of CO_{2e} emissions and C-sink from the atmosphere. This reporting aspect became particularly important when assessing CFs of NPs. Indeed, these protected areas, by both increasing C stock reservoirs and preventing the loss of C that is already present in forest biomass and soil organic matter, play an important role in regulating GHG concentrations in the atmosphere and became perfect candidates for mitigation strategies aimed at enhancing forest and land C-sinks.

To the best of our knowledge, there is not a specific methodological approach to assess CF of NPs. Although a study (Villalba et al., 2013) aimed to evaluate the CF of an NP was found in literature, the GHG emissions generated from soil and animals (i.e., wild and domestic) biological processes, as well soil and forest C-sinks dynamics, were outside the scope of that study. The present work aimed (i) to develop a methodological approach based on ISO 14064–1 to assess the CFs of NPs and (ii) to test its applicability on a practical case study.

MATERIAL AND METHODS

Greenhouse Gas Inventory Boundaries of National Park

The system boundary (SB) is the basis used to delimitate the processes included within the assessment of CF based on ISO 14064–1. Within the SB of an NP there are several sectors/activities that could take place, such as (i) nature-based tourism activities (e.g., camping, hiking, fishing, birdwatching, etc.), (ii) tourist facilities (e.g., restaurant, gift shops, hotel, etc.), (iii) construction and maintenance of infrastructure (e.g., buildings, roads, etc.), (iv) residential sector, (v) fauna and flora preservation and, (vi) agricultural and farming activities. The case study was conducted on Castelporziano Nature Reserve (Reserve hereinafter), a residence of the President of the Italian Republic[1] that extends from the south-southwest of Rome towards the Tyrrhenian Sea and covers 5,980 ha of land (**Figure 1**).

The largest part of the Reserve is covered with natural or semi-natural vegetation, and the area classified as woodland reaches 4,511 ha (i.e., 75.7% of the total). The Reserve can be considered a unique environment in the Mediterranean area since it includes uncontaminated beaches, recent and old stabilized sand dunes, ample back dune wetlands, Mediterranean scrubland, and thickets featuring typical evergreen and aromatic species. Recent investigations show that, within the Reserve, about 90% of the forest areas have maintained their destination use without changes since 1950 (Pignatti et al., 2015). Besides the great range of vegetation, the Reserve hosts native wild boars, fallow deer (*Dama*), and deer (*Cervus elaphus*). Small fauna (e.g., foxes, badgers, porcupines, etc.) is also present. Large predators are absent, and no sport hunting is allowed. Within the Reserve, native Maremmana beef cattle and Maremmano horses are bred in pureness, and about 620 ha of the Reserve are dedicated to the pasture and related cropping activities. As regards the touristic attractions, in addition to the several natural routes that can be enjoyed, the Reserve includes buildings from the 14th century, such as the castle and the historical residence. A naturalistic museum, an archaeological museum, and a carriages hall can also be visited. A canteen is open during lunchtime to tourists and Reserve employees/workers. Unless invited to the events organized during the year, tourists visiting the Reserve are not allowed to go inside using their own transportation, and a shuttle bus service is provided during the opening season (from March 14 to June 21). A small residential hamlet (i.e., 24 households) is present within the Reserve, and it is mainly composed of people who are in different ways involved in the activities taking place within the NP. Mechanical and carpentry workshops are also present. Within the Reserve, there are firefighters who patrol the area during the summer season, and security forces, which guarantees the safety of the Presidential Estate all year round. Finally, the Reserve promotes the implementation of scientific research programs aimed at enhancing its environmental and agroforestry-pastoral

[1]https://palazzo.quirinale.it/residenze/c_porziano_en.html

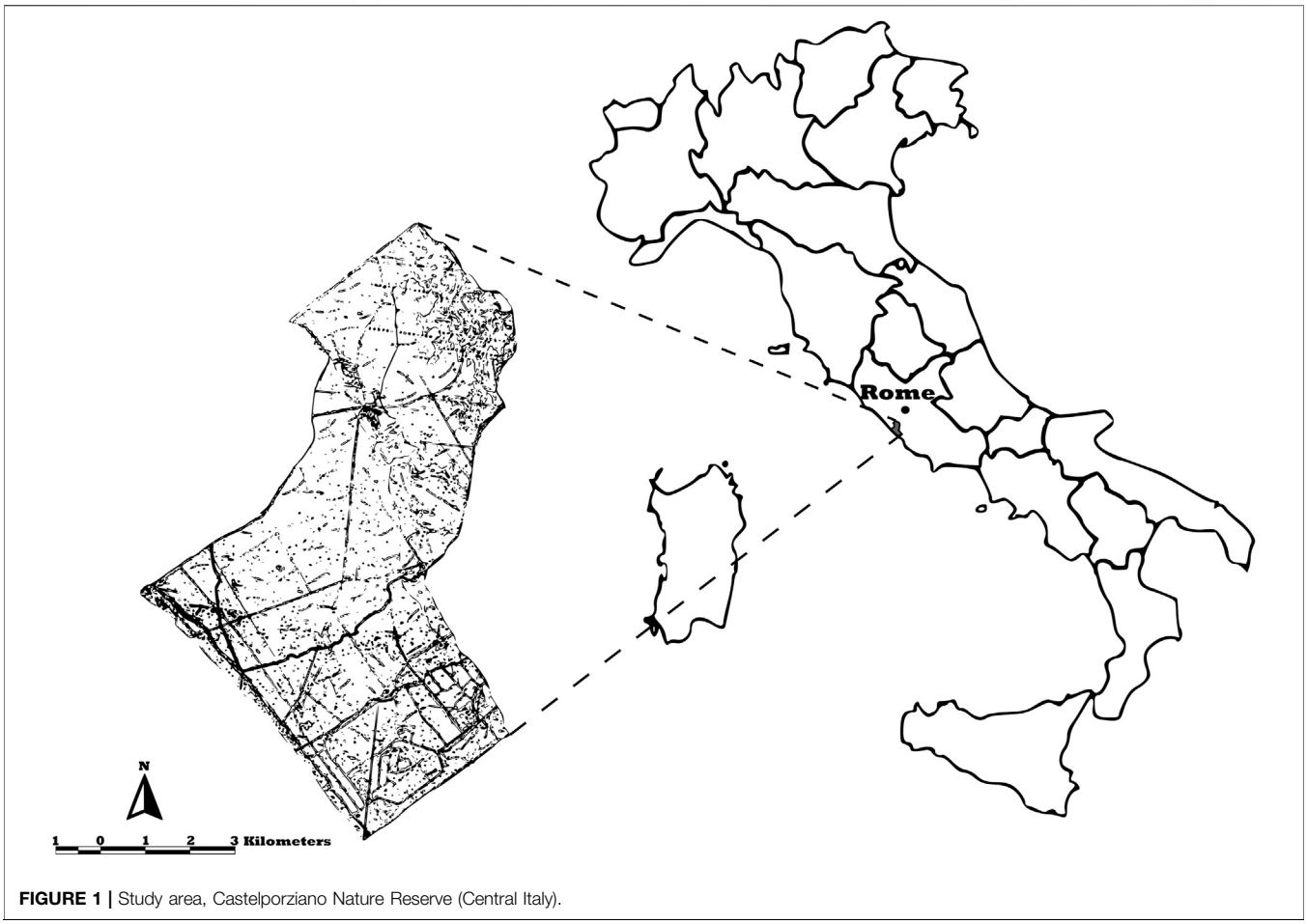

FIGURE 1 | Study area, Castelporziano Nature Reserve (Central Italy).

heritage. In fact, numerous researchers are involved in projects concerning sustainable development, conservation of biodiversity, climate change (CC), and desertification.

Quantification of the Greenhouse Gas Emissions

The boundary system setting involves the categorization of direct and indirect GHG emissions and removals (ISO, 2019). Specifically, direct GHG emissions and removals occur from GHG sources or sinks which are placed inside the boundaries that are owned or controlled by the Reserve. The indirect GHG emissions are those related to the Reserve's activities but that are generated outside the boundaries of NP's direct control. The boundary system of the Reserve with the direct, indirect, and GHG removals is shown in **Figure 2**. A comprehensive inventory of the primary and secondary data involved within each sector can be consulted in the supplementary material (**Supplementary Table S1–S8**).

Direct Greenhouse Gas Emissions and Removals

The direct GHG emissions within the Reserve's boundary have included those arising from (i) agricultural soils and animal's (i.e., wild and domestic) biological processes (ii) energy combustion (i.e., fuel and gas); for farming, forestry, residential, offices, museum, and canteen and transport activity; and (iii) refrigerant gas leaks. Within the direct GHG removals were included the C-sinks related to the agricultural soil and the above-ground forest biomass growth. Below are indicated the methods adopted for accounting for the emissions sources. Further details were reported in the supplementary materials: emission factors (EFs) in **Supplementary Table S9**, and numbered [1–10] equations in **Supplementary Table S10**.

Different methods were involved for the estimations of the enteric methane emitted annually by cattle, horses, and wild fauna living within the Reserve. Specifically, the Tier 2 equation (**Supplementary Table S10** [1]) proposed by IPCC (IPCC, 2019) was adopted for cattle. The IPCC Tier 1 EF (**Supplementary Table S1**) was involved for horses, while the equation (**Supplementary Table S10** [2]) proposed by Smith et al. (2015) was used for wild animals (i.e., wild boars, fallow deer, and deer).

A Tier 3 approach involving the use of a process-based model named the Denitrification-Decomposition (DNDC) model (Li et al., 2000) was used for the assessment of GHG emissions (i.e., CH_4, direct and indirect N_2O) coming from the manure deposited on pasture by cattle (Grossi et al., 2020). A Tier 1 (Velthof, 2014; IPCC, 2019) approach was used for the

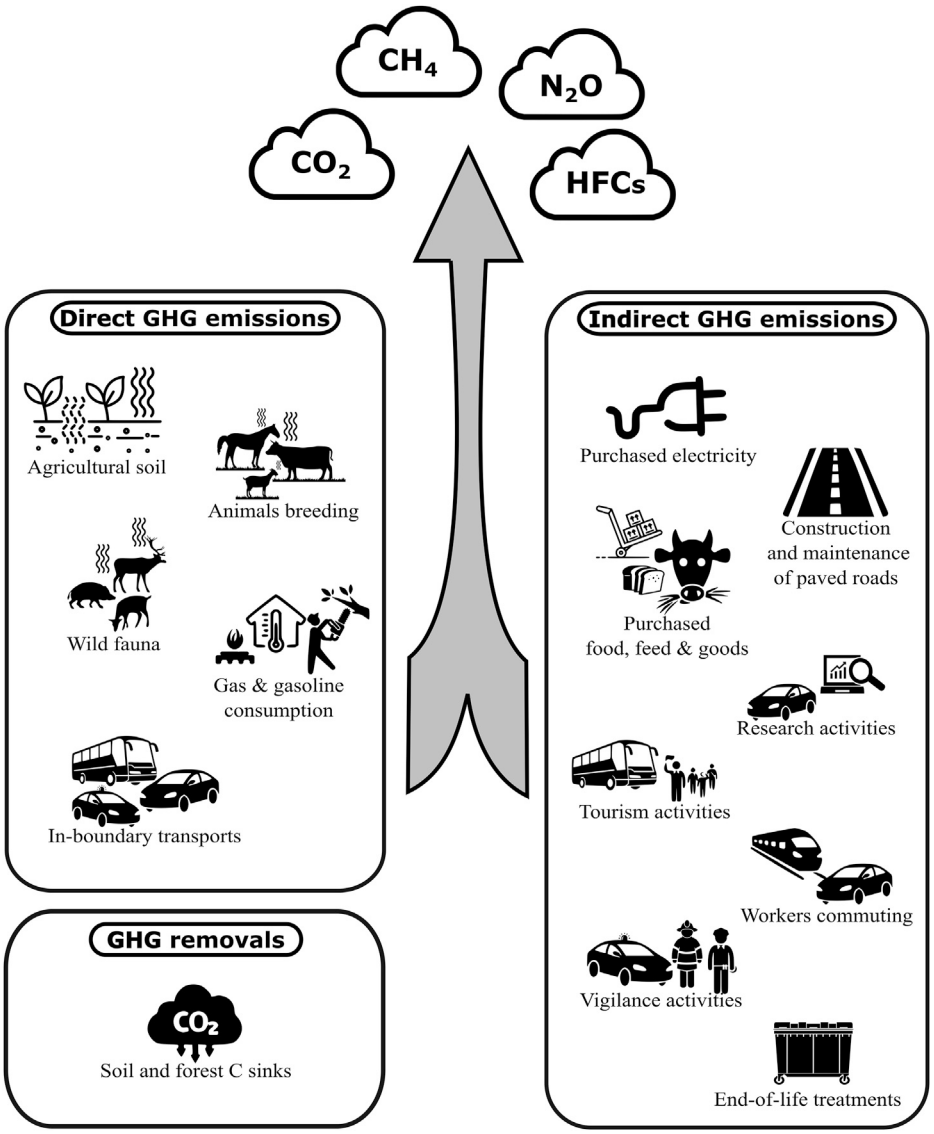

FIGURE 2 | System boundaries of the direct, indirect, and GHG removals considered within the Reserve carbon footprint assessment.

estimations of the GHG from both horses and wild fauna' manure (**Supplementary Table S10** [3–4]).

The GHG emissions generated from the use of fuels (i.e., tillage and motor pumps) and natural gas (i.e., cooking in the canteen and heating office), were accounted for based on the annual consumptions provided by the Reserve and the EFs (**Supplementary Table S9**) provided by the Ecoinvent database (Wernet et al., 2016) and Bradbury et al. (2015), respectively. The estimation of the natural gas consumption of the several offices and museums placed inside the Reserve was estimated by a combination of primary data, equation (**Supplementary Table S10** [5]) proposed by Moreci et al. (2016), and parameters indicated in De Rosa et al. (2015).

The GHG generated during the construction and maintenance of the paved road networks was accounted based on the area occupied by the Reserve's roads and the EFs (**Supplementary Table S9**) proposed by Araújo et al. (2014).

The in-boundary transports have considered the use of vehicles inside the Reserve for (i) wild fauna monitoring and census (i.e., by cars), (ii) tourists (i.e., by shuttlebus and cars), (iii) food for canteens (i.e., lorries), (iv) commuting of employees and workers (i.e., by cars and buses), (v) policemen and firefighters' patrols (i.e., by cars and lorries), and (vi) residents' and other vehicles' recorded activity (i.e., by cars). Annual distances traveled inside the Reserve were estimated for all types of in-boundary transports and different EFs (**Supplementary Table S9**) from the Ecoinvent database, and a bibliography was adopted in relation to the vehicle declared (Wernet et al., 2016; To et al., 2019).

The annual GHG emissions resulting from the refrigerant gas leaked from the fridges (i.e., canteen) and air conditioners (e.g., offices, museums, workshops, etc.) were accounted for based on the total number of devices, and the specific equipment' gas leaks rates (Cowan et al., 2010; EPA, 2014) (**Supplementary Table S10** [9]).

The annual GHG removals attributable to the agricultural soil C-sinks were quantified by using the DNDC model (Grossi et al., 2020). Differently, by assuming an equilibrium state (Demertzi et al., 2016; Peñaloza et al., 2019), the forest soil C-dynamics were not included in the CF. Ultimately, the annual C-sinks related to the annual above-ground forest biomass growth were estimated starting from the Reserve's forest inventory data provided by Scrinzi et al. (2019).

Indirect Greenhouse Gas Emissions of Reserve

This category includes the GHG for the production, transportation, and end-of-life of goods (durable, and non-durable) functional to the Reserve activities but emitted outside its boundary. As for the direct ones, further details regarding EFs and equations involved in the assessment were reported in the **Supplementary Tables S9, S10**, respectively.

The GHG emissions generated by the electricity consumption from the Reserve activities (e.g., touristic attractions, offices, workshops, etc.) were calculated using the EF (**Supplementary Table S9**) referring to the Italian electricity mix provided by the Italian National Inventory of emissions (ISPRA, 2020).

The annual amount of electricity (kWh) was provided directly by the Reserve when available or estimated starting from the inventory of the electronic devices inside the building (e.g., lighting bulbs, air conditioners, PC, etc.) by following the approach (**Supplementary Table S10** [6-7-8]) proposed by Tjandra et al. (2016). The annual amount of electricity (kWh) consumed by the residential sector (**Supplementary Table S5**) was extrapolated from average National statistics data (ISTAT, 2019).

The GHG emissions arising from the life cycle of the durable goods such: agricultural buildings and machinery (Wernet et al., 2016), paved roads (Araújo et al., 2014.), electronic devices (Wernet et al., 2016), and air conditioners (De Kleine, 2009) were accounted considering their potential lifespans. Regarding the non-durable goods, were included the GHG arising from the production of fossil fuel (Wernet et al., 2016), feed for livestock, seeds, and organic fertilizers for cropping (Adom et al., 2013; Wernet et al., 2016; Havukainen, 2018), meals (Wernet et al., 2016; Hanssen et al., 2017; Espinoza-Orias and Azapagic, 2018), kraft paper, and Low-Density Polyethylene (LDPE) used for the packaging (Wernet et al., 2016), printer paper (Wernet et al., 2016), and toners (Kara, 2010) (**Supplementary Table S9**).

All the GHG emissions generated by the out-boundary transports related to non-durable goods (including their disposal) were estimated considering the type of transports used, the weight carried, the distance driven, and the EFs (**Supplementary Table S9**) provided by Wernet et al. (2016). Furthermore, working with assumptions, it was possible to estimate the annual GHG emissions generated by the out-boundary transports related to the bus, minibus (Shorter, 2011), and cars involved in tourist activities (**Supplementary Table S10** [10]). Particularly, because of the large involvement of organized excursions (e.g., school groups, elderly centers, etc.), it was assumed that all the visiting tourists reach the entrance of the Reserve by tour buses, which have a transporting capacity of 30 people transported for an average distance of 500 km (roundtrip). Regarding the out-boundary transport' emissions associated with the cars, it was instead assumed that each car arriving at the park carries 2.5 people and drives for 300 km (roundtrip). The GHG emissions associated with the workers and employees commuting were accounted for as well. It was assumed an average commuting distance of 30 km, and that 75% of the employees/workers use their own car, and the remaining use public transport (i.e., bus). Finally, since the distance separating the security and firefighters' headquarters from the Reserve was already accounted for within the annual kilometers provided by the related representatives, it was assumed that 85% of that distance was driven within the Reserve and the remaining 25% outside the boundary.

The GHG emissions arising from the end-of-life of durable goods, such as air conditioners (De Kleine, 2009), agricultural buildings and tractors (Wernet et al., 2016), and paved roads (Araújo et al., 2014), were assessed considering the associated lifespans. The end-of-life GHG contribution of non-durable goods like toners (Kara, 2010), Kraft papers and LDPE (Turner et al., 2015) to pack meals, and meal waste (Hanssen et al., 2017; Moult et al., 2018) were also accounted for.

Inventory Analysis and Impact Assessment

The annual emissions of CO_2, CH_4, and N_2O were converted according to CO_{2e} (equivalent) using the IPCC 100 years global warming characterization factors (IPCC, 2013), while characterization factors (100 years) provided by Tian et al. (2015) and EPA (2014) were used to convert in terms of CO_{2e} gas leaks of the hydrofluorocarbons (HFCs).

The GHG sinks generated by the Reserve (reported separately from the active emissions) were quantified from the annual C-sinks related to both agricultural soils, and above-ground forest biomass growth. Specifically, the annual C-sinks were converted in CO_{2e} considering the atomic weight of C and the molecular weight of CO_2, therefore multiplying the amount of C by 3.67. The use of a DNDC model allowed us to account for soil GHG emissions and annual SOC dynamics (Grossi et al., 2020). Due to lack of data, the forest soil C stock changes were not accounted for and were assumed, according to the Tier 1 IPCC (2019) approach, to currently be in equilibrium (Demertzi et al., 2016; Peñaloza et al., 2019).

Nevertheless, the annual C stored by the growth of the aboveground woody biomass was included. Specifically, from the findings of Project ELITE/SIFTeC, which involved the use of Laser Imaging Detection and Ranging (LIDAR) and Geographical Information System (GIS), it was possible to obtain a detailed inventory of the whole forest area of the Reserve. Particularly, the live epigean biomass of the Reserve' forest (given by the weight of the significant wood volume and the weight of the twig and foliage) exceeds 800,000 tons (in dry weight), and one million tons in fresh weight (Scrinzi et al., 2019). Therefore, by considering an average amount of 50% C content on wood dry biomass (Thomas and Martin, 2012), and an annual overall forest growth rate of 1.7% (value based on expert opinion), it was possible to account for the annual C sequestered by the aboveground forest biomass growth.

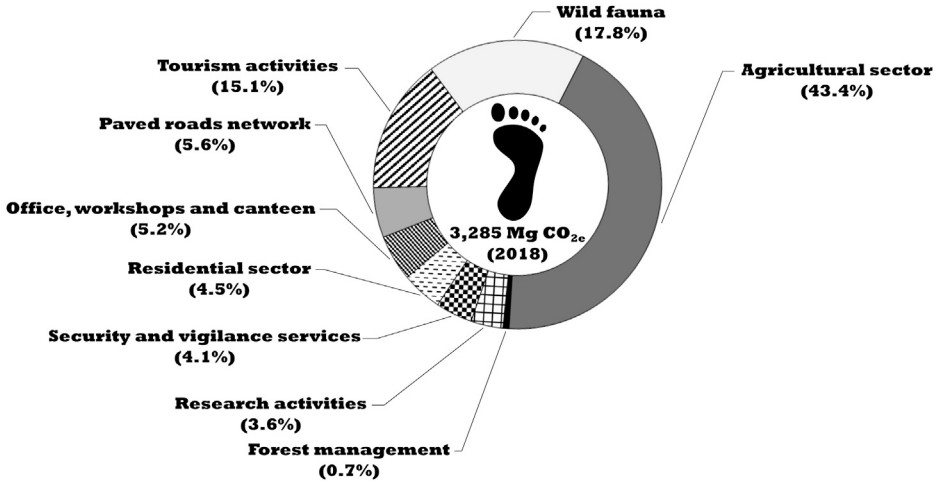

FIGURE 3 | Carbon footprint of the whole Reserve area including the incidence (%) of all sectors considered during the reporting year (2018).

Uncertainty Assessment

According to the GHG protocol and Frischknecht et al. (2007), in all cases where measured single parameter uncertainties are unknown, a pedigree matrix (Weidema and Wesnaes, 1996) can be used to calculate uncertainties. Specifically, the data sources are assessed according to five Data Quality Indicators (DQIs): precision, completeness, temporal representativeness, geographic representativeness, and technological representativeness. Subsequently, each DQI is assigned a data quality rate (i.e., very good, good, fair, and poor), which is then used to estimate quantitatively the overall level of uncertainty.

The approach used in this case study has included a pedigree matrix for quantifying single parameter uncertainty, while a Taylor series expansion (Hong et al., 2010) has been adopted to propagate individual parameter uncertainties and to determine the overall system uncertainty (Bravo et al., 2017). The Taylor series expansion method requires the assumption that the uncertainty distribution for each input parameter is log-normally distributed.

An open-source tool[2] developed by the WRI has been used for the quantitative uncertainty assessment of the annual GHG emission arising from the Reserve. Differently, the uncertainty range provided for the annual C-sinks rates coming from the agricultural soil (Grossi et al., 2020) and the aboveground forest growth (Scrinzi et al., 2019) were those reported by the authors of the estimations.

RESULTS

The Natural Reserve of Castelporziano generated a total CF of about 3,300 Mg of CO_{2e} in 2018. The agricultural sector, with a 43.4% share, showed the largest incidence of overall CF (**Figure 3**). The GHG emissions generated from wild fauna (17.8%) and tourism activities (15.1%) were the second and third sources of GHG, respectively. Lower contributions accounted for paved road networks (5.6%); office, workshops and canteen activities (5.2%); residential sector (4.5%); security/vigilance services (4.1%); research activities (3.6%); and forest management (i.e., pruning) (0.7%).

Figure 4 shows the shares, both within the total and within each sector, of the direct and indirect GHG emissions, while **Table 1** provides detailed information regarding the framework of the overall Reserve's annual GHG emissions and removals.

Greenhouse Gas Emissions From Direct Sources

The annual GHG emissions directly connected to the activities controlled by the Reserve accounted for 63% of the total CF. Specifically, wild fauna (99%), agricultural and livestock activities (92%), and forest management (59%) were the sectors where the direct GHG emissions contribute to the largest share (**Figure 4**).

Emissions generated by the agricultural sector were about 1,500 Mg CO_{2e}, and, within it, enteric methane (44.6%) from cattle and N_2O from soil (36.9%) were the main GHG contributors. Those arising from the wild fauna sector amounted to about 600 Mg CO_{2e} $year^{-1}$ and were almost totally (99%) attributable to the CH_4 and N_2O generated by the biological processes involving manure decomposition, and wild ruminant' enteric methane (**Table 1**). Lastly, the forest sector generated about 22 Mg CO_{2e} $year^{-1}$, the combustion of the fossil fuel used for the pruning activities resulted as the main GHG source of the sector.

Greenhouse Gas Emissions From Indirect Sources

The annual GHG emissions indirectly connected to the Reserve's activities accounted for 37% of the total CF. Individually, research activities (96%), paved roads network (96%), tourism activities (86%), residential sector (67%), and office, workshops, and

[2]https://ghgprotocol.org/calculation-tools

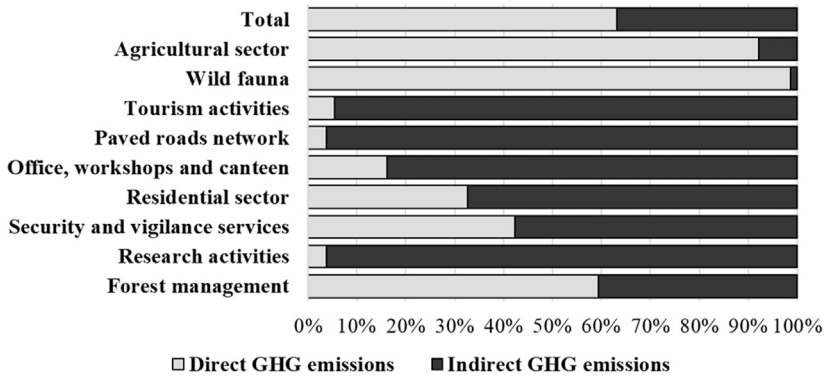

FIGURE 4 | Breakdown of the direct and indirect GHG emissions on the total Reserve' carbon footprint and within each sector considered.

canteens (63%) were the sectors where the indirect GHG emissions showed the largest incidence (**Figure 4**).

The GHG (i.e., about 500 Mg CO_{2e}) from the touristic activities came mainly (about 82%) from the out-boundary transports. The raw materials extraction and mixtures production were the main (about 80%) hotspots of the total GHG emissions (180 Mg CO_{2e}) arising from the life cycle of the paved roads (i.e., pre-construction, construction, maintenance, and end-of-life).

The overall activities related to the office, workshops, and canteen accounted for about 170 Mg CO_{2e}. More than 50% of these emissions came from the out-boundary transports associated with the commuting of employees and business trips.

The GHG emissions arising annually from the residential sector were about 150 Mg CO_{2e}, with the domestic' electricity consumption being responsible for about 67% of this amount.

The whole annual activities associated with the security and vigilance services accounted for about 140 Mg CO_{2e}. The in-boundary transports accounted for 40% of the sector, followed by the homemade meals consumed by the policemen (about 36%).

The out-boundary transports were the main GHG contributor (about 94% of 120 Mg CO_{2e}) of the sector related to the research activities taking place within the Reserve.

Carbon Sinks

The C-sinks resulting from the annual forest above-ground biomass growth accounted for 6,840 Mg of C $year^{-1}$, corresponding to about 25,000 Mg CO_{2e} $year^{-1}$. The oak wood (2,353 ha) and pinewoods (1,008 ha), due to the wide area taken within the Reserve, were the tree species showing the largest C-sinks contributions (**Supplementary Table S8**). The soil organic carbon (SOC) sequestered annually within the Reserve's agricultural area (620 ha) due to the current soil management and grazing pasture was about 220 Mg of CO_{2e} (**Table 1**).

DISCUSSION

The GHG emissions generated in 2018 from the whole Castelporziano Reserve sectors were about 0.55 Mg CO_{2e} $hectare^{-1}$. When including the agricultural soil and forest C-sinks in the CF assessment, the Reserve could be considered as an important CO_2 sink that, in terms of net GHG emissions, in 2018 has stored about 3.7 Mg CO_{2e} $hectare^{-1}$, corresponding to a total of about 22,000 Mg CO_{2e} removed from the atmosphere.

To successfully implement a green marketing strategy that engages the final consumers (tourists in this case) and makes it easier to understand the Reserve' progress towards the environmental targets, the organizations need to effectively communicate and report their current achievements and future GHG reduction commitments. In this context, the GHG reporting standards defined by the ISO 14064–1, which propose to relate the GHG emissions and removals at organization levels (i.e., occurring within the system boundaries), are an effective way to communicate the progress achieved toward the sustainability. Nevertheless, this type of reporting becomes less suitable when comparing GHG emissions and removals generated by NPs characterized by different sizes. For this reason, in this paper, the GHG results were presented referring also to one representative hectare of the Reserve, a reference unit that lends itself well to cases where GHG comparations between parks different in size are needed.

According to Villalba et al. (2013), a different referring unit (i.e., GHG emissions/visitor-day) could potentially reflect better the annual CF, and the efficiency of the NPs in servicing the tourists. However, it is also true that, because of its potential large year-to-year variability, the application of this unit could fail in representing the effectiveness of specific mitigation strategies implemented during the year. Therefore, although other referring units can be developed and integrated to the one proposed by the ISO 14064–1, the authors agreed that the organization-level and the representative-hectare are the most effective in communicating the environmental goals and in comparing GHG results, respectively.

By providing both a general and a detailed picture of the GHG annually emitted by a system embedding a wide range of physical, chemical, and biological activities, the methodological approach proposed in this study has proved to be suitable in evaluating the CFs of such complex environments. Although characterized by different sizes and incidence, the sectors (e.g., residential,

TABLE 1 | Overall GHG emissions and sink of the Reserve and incidence of the main emitting sources within each sector.

Sector	*Category*	*Sub-sector*	*Mg CO_{2e}/year*	*% on sector*	*Total Mg CO_{2e}/year*
Agricultural sector	Direct	Enteric methane	636.84	44.6%	1,427 (1,084; 1877)
		Soil emissions	525.81	36.9%	
		Fuel combustion	152.75	10.7%	
	Indirect	Extra-farm feed [(p;t;e)]	55.48	3.9%	
		Fuel [(p;t)]	21.85	1.5%	
		Auxiliary products [(p;t;e)]	19.02	1.3%	
		Others	14.82	1%	
Wild fauna	Direct	Manure emissions	387.8	66.5%	583 (379; 897)
		Enteric methane	187.2	32.1%	
		In-boundary transport	0.45	0.1%	
	Indirect	Corn grains [(p;t;e)]	7.2	1.2%	
		Out-boundary transport	0.7	0.1%	
Tourism activities	Direct	Heating and cooking	17.0	3.4%	496 (207; 1,184)
		In-boundary transport	5.7	1.1%	
		Refrigerant gas leaks	4.3	0.9%	
	Indirect	Electricity	42.1	8.5%	
		Out-boundary transport	411.3	82.9%	
		Meals [(p;t;e)]	15.0	3%	
		Air conditioners [(p;e)]	0.9	0.2%	
Paved roads network	Direct	*In-situ* operations	6.8	3.7%	184 (131; 257)
	Indirect	Transport	30.7	16.7%	
		Raw materials extraction	69.3	37.7%	
		Mixture production	76.9	41.9%	
Office workshops and canteen	Direct	In-boundary transport	10.9	6.4%	169 (83; 346)
		Heating and cooking	13.4	7.9%	
		Refrigerant gas leaks	3.0	1.8%	
	Indirect	Electricity	35.0	20.6%	
		Out-boundary transport	88.1	52%	
		Meals [(p;t;e)]	16.5	9.7%	
		Others	2.6	1.5%	
Residential sector	Direct	In-boundary transport	48.8	32.6%	150 (100; 223)
	Indirect	Electricity	100.8	67.4%	
Security and vigilance	Direct	In-boundary transport	54.2	40%	136 (68; 271)
		Refrigerant gas leaks	2.6	1.9%	
		Heating system	0.6	0.4%	
	Indirect	Electricity	10.4	7.7%	
		Meals [(p;t;e)]	49.5	36.5%	
		Out-boundary transport	15.9	11.8%	
		Others	2.4	1.8%	
Research activities	Direct	In-boundary transport	4.5	3.8%	118 (43; 325)
	Indirect	Out-boundary transport	111.4	94.2%	
		Meals [(p;e)]	2.4	2%	
Forest management	Direct	Fuel combustion	13.2	59.3%	22 (18; 28)
	Indirect	Fuel [(p;t)]	2.2	9.9%	
		Tractors [(p;m;e)]	6.9	30.8%	
	Total annual GHG emissions generate annually by the Reserve				3,285 (2,679; 4,027)
C -sinks		Agricultural soil			−216 ± 30[b]
		Forest biomass growth			−25,103 ± 6,275[c]

[a]*p = Production; t = Transport; m = Maintenance; e = End-of-life. The values in the brackets are the lower and upper limits respectively of the 95% confidence interval (CI).*
[b]*Uncertainty range reported by the authors of the paper (Grossi et al., 2020).*
[c]*Uncertainty range reported by the authors of the paper (Scrinzi et al., 2019).*

agriculture, public transportations, offices, etc.) included in the CF of the Reserve can be treated similarly to other systems different from NPs. Indeed, due to their analogies, the methodological approaches and the guideline proposed in this study could be suitable also for an estimation of the GHG sources/sinks, which are normally associated with cities and/or productive districts.

Greenhouse Gas Emissions From Direct Sources

When looking at the possible mitigation strategies that could be implemented, the direct GHG emissions are the ones where organizations should focus more considering the larger control exercised on them. However, in the specific case of the Reserve,

where the main direct GHG emissions sources have biological origins (i.e., enteric and soil emissions), the reduction strategies need to consider complex interactions between climate, soil, and livestock in order to be really effective.

The losses in gross energy intake associated with the enteric methane of cattle resulted in a consistent contribution (19.4%) to the overall Reserve GHG emissions (Vitali et al., 2018). In pasture-based cattle farming like that investigated in this study, the adoption of adequate pasture management combined with the provision of high-quality hay (when grazing is not feasible) could potentially reduce the enteric CH_4 emissions. The lignin content of the forage, which increases during plant maturity, is an aspect that severely affects enteric methane production by reducing plant digestibility and altering nutrient density (Thompson and Rowntree, 2020). Therefore, harvesting forage at an earlier stage of maturity is a practice that could effectively contribute to the reduction of this GHG emission source.

As concern the pasture management instead, the adoption of continuous grazing systems could potentially lead to overgrazing issues, which in turn could reduce plant diversity and increase undesirable or low-quality forages (Thompson and Rowntree, 2020). On the contrary, low-to-moderate grazing density prolonged for a limited time (i.e., rotational grazing) can directly stimulate biomass regrowth, carbon sequestration, and better land utilization (Byrnes et al., 2018). Indeed, the more uniform nitrogen excreta distribution resulting from greater control of the stocking density and grazing duration has been demonstrated to reduce soil N_2O emissions (Eckard et al., 2010).

Greenhouse Gas Emissions From Indirect Sources

The out-boundary transports represented about 19% of the overall annual Reserve CF and more than 50% of the total indirect GHG emissions. Generally, within the sectors where transports are the biggest source of GHG emission, exploring a flexible way of working, and engaging people (e.g., tourists, workers, and employees) in reducing travel and commuting, could represent a good mitigation opportunity (McKinnon and Piecyk, 2012). This source of emission is a complex task to reduce and can only be accomplished with the agreement and participation of the stakeholders. For example, the organizations can encourage the use of public transport by offering free shuttle bus from nearby stations to their offices, or a discount on the entrance ticket to the tourists that reach the park using sustainable transports (e.g., public transport, electric vehicle, bicycle, etc.).

The Reserve's electricity consumption accounted for 16% of the Reserve's indirect GHG emissions. In this regard, a greater use of energy-saving light bulbs (e.g., in the office, museums, etc.), an optimal thermostat temperature setting of the air-conditioning in the office rooms (Mardookhy et al., 2014), or the switch to a totally renewable energy supply (Amponsah et al., 2014), are just some examples that could be effective in reducing the overall contribution of this scope. However, to reliably quantify the effectiveness of these sector-specific GHG mitigation strategies, attention shall be given to the inventory data collection.

In this context, an effective data lifecycle management based on the digitalization of the key input and output data could help NPs in both keeping track of the information that might make a significant difference in terms of environmental performance and in evaluating the effect of minor sector-specific mitigation strategies that otherwise could remain undetected. In presence of detailed and granular data (e.g., out-boundary distance driven, type of meals, number and type of lighting bulbs, etc.) it becomes then possible to quantify the benefits of equally detailed and granular mitigation strategies (e.g., a more efficient commuting, pattern diet shifts, greater use of energy-saving light bulbs, etc.). This is especially important when assessing those activities resulting in a significant contribution within each sector.

Carbon Sinks

The incidence of the forest sector on the overall Reserve's CF becomes extremely significant when considering the related GHG sinks dynamics. Indeed, the forest plays a strategic role in carbon balance (Nunes et al., 2019), and protected natural areas can be effective in both preventing conversion of land uses and implementing mitigation strategies. For instance, providing sufficient time for forests to recover, reducing the intensity of each cut (Zhou et al., 2013), replacing dying or low productivity stands, protecting young sprouts from damage after harvest, and planting tree mixes that are more resilient (Bellassen and Luyssaert, 2014) are just some examples of managements that could help enhancing forest C storages.

Wildlife is integral to the life of the forest, and it is therefore normal for animals to feed there and leave signs of their presence. However, animals can cause damage to their environment, ranging from few minor depredations to severe ecological damage that reflects an overall imbalance. Wild boars are effective soil disturbers since, if soil conditions are favorable, they can root to a depth of 1 m (Tyler and Long, 2009). This bioturbation, by breaking up aggregates and aerating the soil, may have negative consequences for forest SOC stocks and can thus cause side effects for the global C cycle and climate change (Liu et al., 2020). Browsing (removal and consumption of young shoots) by *cervidae* (e.g., deer and fallow deer) is another problem that may affect forest regeneration (Moore et al., 2000), and then the aboveground C-sinks potential of trees. In this context, using a fencing system to prevent wild animals from reaching vulnerable areas is an effective way to prevent damage. Fencing can be permanent or temporary depending on the severity of the damage and seasonal patterns. Furthermore, a reliable census is crucial for any effective resource management or wild animal population control (Franzetti et al., 2012).

In terms of agricultural soil management instead, the adoption of less soil-invasive tillage practices could increase the current annual agricultural soil C-sink rates, which in turn could decrease the overall incidence of this sector on the total. In fact, a switch from the current Reserve' soil tillage practices (i.e., 30 cm plowing) to no-tillage ones, showed a significant potential reduction (26%) of the GHG emissions arising from the beef cattle rearing (Grossi et al., 2020), which in turn has the potential to reduce the overall Reserve CF by about 8.5%.

CONCLUSION

To the best of our knowledge, the present study could be considered the first cradle-to-grave Carbon Footprint of a National Park. The proposed methodology is both feasible and suitable in terms of providing a granular picture of the main GHG emission sources and sinks of the Castelporziano Natural Reserve. Although anthropogenic activities such as agriculture and tourism are the main GHG sources within National Parks, mitigating solutions are possible to improve their sustainability. Moreover, the contribution to the C-sink of the protected natural areas may be considered strategic in planning adaptation and mitigation strategies at the country level.

The National Parks, by providing annual Carbon Footprint reports, may both effectively inform public opinion of their contribution to Climate Change and monitor the impact of the adoption of new specific mitigation policies. Finally, the guideline proposed in this paper could be the starting point for developing a widely accepted standard procedure to be followed to obtain environmental declarations (i.e., eco-labeling) for National parks.

DATA AVAILABILITY STATEMENT

The original contributions presented in the study are included in the article/**Supplementary Material**, further inquiries can be directed to the corresponding authors.

AUTHOR CONTRIBUTIONS

GG: acquisition, analysis, and interpretation of the data and drafting of the manuscript. AV: Study conception and design, interpretation of the data, and drafting manuscript. UB, NL, and AN: Study conception and design, critical revision.

ACKNOWLEDGMENTS

The research was carried out in the frame of the MIUR (MInistry for education, University and Research) initiative "Department of excellence" (Law 232/2016). The authors would like to express their gratitude to the General Secretariat of the Presidency of the Republic, to the Accademia Nazionale delle Scienze "detta dei XL", to the management of the Estate of Castelporziano, and to the Scientific-Technical Commission of Castelporziano that enabled this study and the publication of the data.

SUPPLEMENTARY MATERIAL

The Supplementary Material for this article can be found online at: https://www.frontiersin.org/articles/10.3389/fenvs.2021.706880/full#supplementary-material

REFERENCES

Adom, F., Workman, C., Thoma, G., and Shonnard, D. (2013). Carbon Footprint Analysis of Dairy Feed from a Mill in Michigan, USA. *Int. Dairy J.* 31, S21–S28. doi:10.1016/j.idairyj.2012.09.008

Amponsah, N. Y., Troldborg, M., Kington, B., Aalders, I., and Hough, R. L. (2014). Greenhouse Gas Emissions from Renewable Energy Sources: A Review of Lifecycle Considerations. *Renew. Sustainable Energ. Rev.* 39, 461–475. doi:10.1016/j.rser.2014.07.087

Araújo, J. P. C., Oliveira, J. R. M., and Silva, H. M. R. D. (2014). The Importance of the Use Phase on the LCA of Environmentally Friendly Solutions for Asphalt Road Pavements. *Transp. Res. D: Transport Environ.* 32, 97–110. doi:10.1016/j.trd.2014.07.006

Bellassen, V., and Luyssaert, S. (2014). Carbon Sequestration: Managing Forests in Uncertain Times. *Nature* 506, 153–155. doi:10.1038/506153a

Bradbury, J., Clement, Z., and Down, A. (2015). *Greenhouse Gas Emissions and Fuel Use within the Natural Gas Supply Chain - Sankey Diagram Methodology*. off. Energy Policy Syst. Anal. 1–22. Available at: https://www.energy.gov/sites/prod/files/2015/07/f24/QER%20Analysis%20-%20Fuel%20Use%20and%20GHG%20Emissions%20from%20the%20Natural%20Gas%20System,%20Sankey%20Diagram%20Methodology_0.pdf (last access April 30, 2020).

Bravo, G., López, D., Vásquez, M., and Iriarte, A. (2017). Carbon Footprint Assessment of Sweet Cherry Production: Hotspots and Improvement Options. *Pol. J. Environ. Stud.* 26 (2), 559–566. doi:10.15244/pjoes/65361

Byrnes, R. C., Eastburn, D. J., Tate, K. W., and Roche, L. M. (2018). A Global Meta-Analysis of Grazing Impacts on Soil Health Indicators. *J. Environ. Qual.* 47, 758–765. doi:10.2134/jeq2017.08.0313

Calderón, L. A., Iglesias, L., Laca, A., Herrero, M., and Díaz, M. (2010). The Utility of Life Cycle Assessment in the Ready Meal Food Industry. *Resour. Conserv. Recycl.* 54 (12), 1196–1207. doi:10.1016/j.resconrec.2010.03.015

Cowan, D., Gartshore, J., Chaer, I., Francis, C., and Maidment, G. (2010). "REAL Zero - Reducing Refrigerant Emissions & Leakage - Feedback from the IOR Project," in Proc. Inst. Refrig, 1–16. Available at: https://openresearch.lsbu.ac.uk/item/879xq (last access January 17, 2021). doi:10.1093/oxfordhb/9780199542475.013.0015

De Kleine, R. (2009). *Life Cycle Optimization of Residential Air Conditioner Replacement. A Report of the Centre for Sustainable Systems*. Report no. CSS09-12. Ann Arbor, Michigan. Available at: http://css.umich.edu/sites/default/files/css_doc/CSS09-12.pdf (last access, April 30, 2020).

De Rosa, M., Bianco, V., Scarpa, F., and Tagliafico, L. A. (2015). Historical Trends and Current State of Heating and Cooling Degree Days in Italy. *Energ. Convers. Manage.* 90, 323–335. doi:10.1016/j.enconman.2014.11.022

Demertzi, M., Paulo, J. A., Arroja, L., and Dias, A. C. (2016). A Carbon Footprint Simulation Model for the Cork Oak Sector. *Sci. Total Environ.* 566-567, 499–511. doi:10.1016/j.scitotenv.2016.05.135

Eckard, R. J., Grainger, C., and de Klein, C. A. M. (2010). Options for the Abatement of Methane and Nitrous Oxide from Ruminant Production: a Review. *Livestock Sci.* 130, 47–56. doi:10.1016/j.livsci.2010.02.010

EPA (2014). *Direct Fugitive Emissions from Refrigeration, Air Conditioning, Fire Suppression, and Industrial Gases*. Washington. Available at: https://www.epa.gov/sites/production/files/2015-07/documents/fugitiveemissions.pdf (last access, April 30, 2020).

Espinoza-Orias, N., and Azapagic, A. (2018). Understanding the Impact on Climate Change of Convenience Food: Carbon Footprint of Sandwiches. *Sustainable Prod. Consumption* 15, 1–15. doi:10.1016/j.spc.2017.12.002

Franzetti, B., Ronchi, F., Marini, F., Scacco, M., Calmanti, R., Calabrese, A., et al. (2012). Nocturnal Line Transect Sampling of Wild Boar (*Sus scrofa*) in a Mediterranean forest: Long-Term Comparison with Capture-Mark-Resight Population Estimates. *Eur. J. Wildl. Res.* 58, 385–402. doi:10.1007/s10344-011-0587-x

Frischknecht, R., Jungbluth, N., Althaus, H. J., Doka, G., Heck, T., Hellweg, S., et al. (2007). *Overview and Methodology*. Ecoinvent Report No. 1. (Dübendorf: Swiss Centre for Life Cycle Inventories). Available at: https://www.ecoinvent.org/files/200712_frischknecht_jungbluth_overview_methodology_ecoinvent2.pdf (last access, June 21, 2020).

Grossi, G., Vitali, A., Lacetera, N., Danieli, P. P., Bernabucci, U., and Nardone, A. (2020). Carbon Footprint of Mediterranean Pasture-Based Native Beef: Effects

of Agronomic Practices and Pasture Management under Different Climate Change Scenarios. *Animals* 10, 415–417. doi:10.3390/ani10030415

Hanssen, O. J., Vold, M., Schakenda, V., Tufte, P.-A., Møller, H., Olsen, N. V., et al. (2017). Environmental Profile, Packaging Intensity and Food Waste Generation for Three Types of Dinner Meals. *J. Clean. Prod.* 142, 395–402. doi:10.1016/j.jclepro.2015.12.012

Havukainen, J., Uusitalo, V., Koistinen, K., Liikanen, M., and Horttanainen, M. (2018). Carbon Footprint Evaluation of Biofertilizers. *Int. J. SDP* 13, 1050–1060. doi:10.2495/SDP-V13-N8-1050-1060

Hong, J., Shaked, S., Rosenbaum, R. K., and Jolliet, O. (2010). Analytical Uncertainty Propagation in Life Cycle Inventory and Impact Assessment: Application to an Automobile Front Panel. *Int. J. Life Cycle Assess.* 15, 499–510. doi:10.1007/s11367-010-0175-4

IPCC (2013). *Climate Change 2013: The Physical Science Basis. Contribution of Working Group I to the Fifth Assessment Report of the Intergovernmental Panel on Climate Change*. Editors T.F. Stocker, D. Qin, G.-K. Plattner, M. Tignor, S.K. Allen, J. Boschung, et al. (Cambridge, United Kingdom and New York, NY, USA: Cambridge University Press), 1–1535. doi:10.1017/CBO9781107415324

IPCC (2019). *Refinement to the 2006 IPCC Guidelines for National Greenhouse Gas Inventories*. Editors E. Calvo Buendia, K. Tanabe, A. Kranjc, J. Baasansuren, M. Fukuda, S. Ngarize, et al. (Switzerland: Published: IPCC). Available at: https://www.ipcc.ch/report/2019-refinement-to-the-2006-ipcc-guidelines-for-national-greenhouse-gas-inventories/ (last access January 9, 2021).

ISO (2019). Greenhouse Gases - Part 1: Specification with Guidance at the Organization Level for Quantification and Reporting of Greenhouse Gas Emissions and Removals. Available at: https://www.iso.org/standard/66453.html (last access January 7, 2021).

ISPRA (2020). *Italian Greenhouse Gas Inventory 1990-2018. Institute for Environmental Protection and Research Environmental Assessment.* ISBN 978-88-448-0993-5. Available at: http://www.isprambiente.gov.it/ (last access April 30, 2020).

ISTAT (2019). Italian National Institute of Statistics. Available at: https://www.istat.it/ (last access, April 30, 2020).

Kara, H. (2010). *Comparative Carbon Footprint Analysis of New and Remanufactured Inkjet Cartridges*. London: Centre for Remanufacturing and Reuse. Available online at: http://www.ebpgroup.eu/wp-content/uploads/pdf/CCFreport.pdf (last access April 30, 2020).

Li, C., Aber, J., Stange, F., Butterbach-Bahl, K., and Papen, H. (2000). A Process-Oriented Model of N2O and NO Emissions from forest Soils: 1. Model Development. *J. Geophys. Res.* 105, 4369–4384. doi:10.1029/1999JD900949

Liu, Y., Liu, X., Yang, Z., Li, G., and Liu, S. (2020). Wild Boar Grubbing Causes Organic Carbon Loss from Both Top- and Sub-soil in an oak forest in central China. *For. Ecol. Manage.* 464, 118059. doi:10.1016/j.foreco.2020.118059

Malyan, S. K., Bhatia, A., Kumar, A., Gupta, D. K., Singh, R., Kumar, S. S., et al. (2016). Methane Production, Oxidation and Mitigation: A Mechanistic Understanding and Comprehensive Evaluation of Influencing Factors. *Sci. Total Environ.* 572, 874–896. doi:10.1016/j.scitotenv.2016.07.182

Mardookhy, M., Sawhney, R., Ji, S., Zhu, X., and Zhou, W. (2014). A Study of Energy Efficiency in Residential Buildings in Knoxville, Tennessee. *J. Clean. Prod.* 85, 241–249. doi:10.1016/j.jclepro.2013.09.025

McKinnon, A., and Piecyk, M. (2012). Setting Targets for Reducing Carbon Emissions from Logistics: Current Practice and Guiding Principles. *Carbon Manage.* 3 (6), 629–639. doi:10.4155/cmt.12.62

Moore, N. P., Hart, J. D., Kelly, P. F., and Langton, S. D. (2000). Browsing by Fallow Deer (Dama Dama) in Young Broadleaved Plantations: Seasonality, and the Effects of Previous Browsing and Bud Eruption. *Forestry* 73 (5), 437–445. doi:10.1093/forestry/73.5.437

Moreci, E., Ciulla, G., and Lo Brano, V. (2016). Annual Heating Energy Requirements of Office Buildings in a European Climate. *Sustainable Cities Soc.* 20, 81–95. doi:10.1016/j.scs.2015.10.005

Moult, J. A., Allan, S. R., Hewitt, C. N., and Berners-Lee, M. (2018). Greenhouse Gas Emissions of Food Waste Disposal Options for UK Retailers. *Food Policy* 77, 50–58. doi:10.1016/j.foodpol.2018.04.003

Nunes, L. J. R., Meireles, C. I. R., Pinto Gomes, C. J., and Almeida Ribeiro, N. M. C. (2019). Forest Management and Climate Change Mitigation: A Review on Carbon Cycle Flow Models for the Sustainability of Resources. *Sustainability* 11, 5276–5285. doi:10.3390/su11195276

Peñaloza, D., Røyne, F., Sandin, G., Svanström, M., and Erlandsson, M. (2019). The Influence of System Boundaries and Baseline in Climate Impact Assessment of forest Products. *Int. J. Life Cycle Assess.* 24, 160–176. doi:10.1007/s11367-018-1495-z

Pignatti, S., Capanna, E., and Porceddu, E. (2015). Castelporziano, Research and Conservation in a Mediterranean Forest Ecosystem: Presentation of the Volume. *Rend. Fis. Acc. Lincei* 26, 265–266. doi:10.1007/s12210-015-0463-9

Scrinzi, G., Colle, G., Presutti Saba, E., Clementel, F., Maffei, L., Tinelli, A., et al. (2019). L'approccio LiDAR/GIS per la realizzazione dell'inventario forestale e del piano selvicolturale della Foresta Presidenziale di Castelporziano. *Ifm* 74, 341–356. Available at: http://ojs.aisf.it/index.php/ifm/article/view/1172 (last access June 30, 2020). doi:10.4129/ifm.2019.6.01

Shorter, B. (2011). *Guidelines on Greenhouse Gas Emissions for Various Transport Types. Winchester Action on Climate Change*. Hampshire. Available at: https://www.winacc.org.uk/downloads/STAP/Shorter_Transport%20Emissions%20Report_110328.pdf (last access, April 30, 2020).

Smith, F. A., Lyons, S. K., Wagner, P. J., and Elliott, S. M. (2015). The Importance of Considering Animal Body Mass in IPCC Greenhouse Inventories and the Underappreciated Role of Wild Herbivores. *Glob. Change Biol.* 21, 3880–3888. doi:10.1111/gcb.12973

Thomas, S. C., and Martin, A. R. (2012). Carbon Content of Tree Tissues: A Synthesis. *Forests* 3, 332–352. doi:10.3390/f3020332

Thompson, L. R., and Rowntree, J. E. (2020). Invited Review: Methane Sources, Quantification, and Mitigation in Grazing Beef Systems. *Appl. Anim. Sci.* 36, 556–573. doi:10.15232/aas.2019-01951

Tian, Q., Cai, D., Ren, L., Tang, W., Xie, Y., He, G., et al. (2015). An Experimental Investigation of Refrigerant Mixture R32/R290 as Drop-In Replacement for HFC410A in Household Air Conditioners. *Int. J. Refrig.* 57, 216–228. doi:10.1016/j.ijrefrig.2015.05.005

Tjandra, T. B., Ng, R., Yeo, Z., and Song, B. (2016). Framework and Methods to Quantify Carbon Footprint Based on an Office Environment in Singapore. *J. Clean. Prod.* 112, 4183–4195. doi:10.1016/j.jclepro.2015.06.067

To, S., Coughenour, C., and Pharr, J. (2019). The Environmental Impact and Formation of Meals from the Pilot Year of a Las Vegas Convention Food Rescue Program. *Ijerph* 16, 1718–1727. doi:10.3390/ijerph16101718

Turner, D. A., Williams, I. D., and Kemp, S. (2015). Greenhouse Gas Emission Factors for Recycling of Source-Segregated Waste Materials. *Resour. Conserv. Recycl.* 105, 186–197. doi:10.1016/j.resconrec.2015.10.026

Tyler, A., and Long, D. B. (2009). Feral Swine Damage and Damage Management in Forested Ecosystems. *For. Ecol. Manag.* 257, 2319–2326. doi:10.1016/j.foreco.2009.03.036

Velthof, G. L. (2014). *Report Task 1 of Methodological Studies in the Field of Agro-Environmental Indicators.* Lot 1 excretion factors. Final draft. Alterra, Part of Wageningen UR. Available at: https://ec.europa.eu/eurostat/documents/2393397/8259002/LiveDate_2014_Task1.pdf/e1ac8f30-3c76-4a61-b607-de99f98fc7cd (last access, April 30, 2020).

Villalba, G., Tarnay, L., Campbell, E., and Gabarrell, X. (2013). A Life-Cycle Carbon Footprint of Yosemite National Park. *Energy Policy* 62, 1336–1343. doi:10.1016/j.enpol.2013.07.024

Vitali, A., Grossi, G., Martino, G., Bernabucci, U., Nardone, A., and Lacetera, N. (2018). Carbon Footprint of Organic Beef Meat from Farm to fork: a Case Study of Short Supply Chain. *J. Sci. Food Agric.* 98, 5518–5524. doi:10.1002/jsfa.9098

Weidema, B. P., and Wesnæs, M. S. (1996). Data Quality Management for Life Cycle Inventories-An Example of Using Data Quality Indicators. *J. Clean. Prod.* 4, 167–174. doi:10.1016/S0959-6526(96)00043-1

Wernet, G., Bauer, C., Steubing, B., Reinhard, J., Moreno-ruiz, E., and Weidema, B. (2016). The Ecoinvent Database Version 3 (Part I): Overview and Methodology. *Int. J. Life Cycle Assess.* 21, 1218–1230. doi:10.1007/s11367-016-1087-8

Wiedmann, T., and Minx, J. (2008). "A Definition of "Carbon Footprint,"," in *Ecological Economics Research Trends*. Editor C. C. Pertsova (Hauppauge NY, USA: Nova Science Publishers), 1–11. Available at: http://citeseerx.ist.psu.edu/viewdoc/download?doi=10.1.1.467.6821&rep=rep1&type=pdf (last access, April 30, 2020).

Zhou, D., Zhao, S. Q., Liu, S., and Oeding, J. (2013). A Meta-Analysis on the Impacts of Partial Cutting on forest Structure and Carbon Storage. *Biogeosciences* 10, 3691–3703. doi:10.5194/bg-10-3691-2013

Conflict of Interest: The authors declare that the research was conducted in the absence of any commercial or financial relationships that could be construed as a potential conflict of interest.

Publisher's Note: All claims expressed in this article are solely those of the authors and do not necessarily represent those of their affiliated organizations, or those of the publisher, the editors and the reviewers. Any product that may be evaluated in this article, or claim that may be made by its manufacturer, is not guaranteed or endorsed by the publisher.

frontiers in Environmental Science

ORIGINAL RESEARCH
published: 15 September 2021
doi: 10.3389/fenvs.2021.716636

Greenhouse Gas Emissions and Crop Yields From Winter Oilseed Rape Cropping Systems are Unaffected by Management Practices

M. O'Neill[1]*, *G. J. Lanigan*[1], *P. D. Forristal*[2] and *B. A. Osborne*[3,4]

[1]Teagasc, Environmental Research Centre, Wexford, Ireland, [2]Teagasc, Crops Research Centre, Carlow, Ireland, [3]UCD Earth Institute, Dublin, Ireland, [4]UCD School of Biology of Environmental Science, Dublin, Ireland

Winter oilseed rape is traditionally established via plough-based soil cultivation and conventional sowing methods. Whilst there is potential to adopt lower cost, and less intensive establishment systems, the impact of these on greenhouse gas emissions have not been evaluated. To address this, field experiments were conducted in 2014/2015 and 2015/2016 to investigate the effects of 1) crop establishment method and 2) sowing method on soil greenhouse gas emissions from a winter oilseed rape crop grown in Ireland. Soil carbon dioxide, nitrous oxide and methane emission measurements were carried out using the static chamber method. Yield (t seed ha^{-1}) and the yield-scaled global warming potential (kg CO_2-eq. kg^{-1} seed) were also determined for each management practice. During crop establishment, conventional tillage induced an initially rapid loss of carbon dioxide (2.34 g C m^{-2} hr^{-1}) compared to strip tillage (0.94 g C m^{-2} hr^{-1}) or minimum tillage (0.16 g C m^{-2} hr^{-1}) ($p < 0.05$), although this decreased to background values within a few hours. In the crop establishment trial, the cumulative greenhouse gas emissions were, apart from methane, unaffected by tillage management when sown at a conventional (125 mm) or wide (600 mm) row spacing. In the sowing method trial, cumulative carbon dioxide emissions were also 21% higher when plants were sown at 10 seeds m^{-2} compared to 60 seeds m^{-2} ($p < 0.05$). Row spacing width (125 and 750 mm) and variety (conventional and semi-dwarf) were found to have little effect on greenhouse gas emissions and differences in seed yield between the sowing treatments were small. Overall, management practices had no consistent effect on soil greenhouse gas emissions and modifications in seed yield per plant countered differences in planting density.

Keywords: crop management, tillage, row spacing, seed rate, variety, GHG (greenhouse gases), oilseed rape

OPEN ACCESS

Edited by:
Amit Kumar,
Nanjing University of Information Science and Technology, China

Reviewed by:
Munesh Kumar,
Hemwati Nandan Bahuguna Garhwal University, India
Wanfa Wang,
Tianjin University, China

***Correspondence:**
M. O'Neill
macdara.oneill@teagasc.ie

Specialty section:
This article was submitted to Biogeochemical Dynamics, a section of the journal Frontiers in Environmental Science

Received: *02 June 2021*
Accepted: *19 August 2021*
Published: *15 September 2021*

Citation:
O'Neill M, Lanigan GJ, Forristal PD and Osborne BA (2021) Greenhouse Gas Emissions and Crop Yields From Winter Oilseed Rape Cropping Systems are Unaffected by Management Practices. Front. Environ. Sci. 9:716636. doi: 10.3389/fenvs.2021.716636

INTRODUCTION

Atmospheric concentrations of the greenhouse gases (GHG) carbon dioxide (CO_2), nitrous oxide (N_2O) and methane (CH_4) continue to rise globally due to anthropogenic activities. Agriculture is responsible for approximately 12% of global GHG emissions with livestock systems, soil cultivation, rice production and crop residue management making the more significant contributions (Ciais et al., 2014). In terms of land use impacts, croplands make one of the major contributions to agricultural GHG emissions through various farming and management activities. Field operations

such as soil tillage, sowing, fertilizer addition and chemical treatment that are normally required to maximize plant productivity and yield can have significant impacts on GHG emissions through perturbations in the carbon (C), nitrogen (N) and water dynamics of these ecosystem (Bondeau et al., 2007; Osborne et al., 2010). Mitigation of GHG emissions from agricultural sources involves measures that aim to increase soil organic carbon (SOC) sequestration, reduce GHG emission rates, or both, through improved management practices (Smith et al., 2007; Minasny et al., 2017; Ogle et al., 2019). Cropland management practices that involve the adoption of less intensive soil cultivation and agronomic interventions that improve agricultural productivity may can lead to reductions in GHG emissions and determine whether these ecosystems function as sinks or sources of C (Ceschia et al., 2010).

Soil CO_2 is produced by autotrophic and heterotrophic processes. Autotrophic respiration is derived from roots and/or the metabolism of photosynthetic substrates released by roots (Högberg and Read, 2006) whereas heterotrophic respiration is associated with the microbial decomposition of SOC or root exudates (Trumbore, 2000). Agriculture accounts for ~60% of the global anthropogenic N_2O emissions primarily due to increased N-fertilizer use (Smith, 2017), with croplands accounting for at least 80% these emissions (Tian et al., 2019). Nitrous oxide production in soils arise from nitrification; the conversion of ammonium (NH_4^+) to nitrite (NO_2^-) and subsequently nitrate (NO_3^-) in aerobic soils, and denitrification, the sequential reduction of NO_3^- to gaseous N_2O or N_2 in anaerobic soils (Butterbach-Bahl et al., 2013). The soil-atmosphere exchange of CH_4 is largely governed by the balance between net CH_4 production by methanogens and net CH_4 oxidation/uptake by methanotrophs (Serrano-Silva et al., 2014). Although upland arable soils are generally aerobic and considered CH_4 sinks, intensive soil management practices have reduced the capacity of many soils to oxidise CH_4 (Suwanwaree and Robertson, 2005). Land management practices thus often govern whether cropland soils are net sinks or sources of GHGs (Ceschia et al., 2010).

Tillage and sowing are management practices that influence crop establishment, plant growth, nutrient uptake, canopy/soil microclimate and yield (Sharratt and McWilliams, 2005; Malhi et al., 2006; Soane et al., 2012), and subsequently impact on C and N and the GHG balance in croplands (Ceschia et al., 2010; Moors et al., 2010). Conventional tillage (CT) encompasses soil inversion, and crop residue incorporation, facilitating seedbed preparation for the succeeding crop. However, CT practices result in the mechanical disruption of soil aggregates and the release of protected organic C from soil organic matter (SOM) resulting in enhanced CO_2 emissions. Altering the turnover rate of SOM can directly impact C sequestration and the emissions of CO_2, N_2O and CH_4 (Six et al., 2004; Abdalla et al., 2013; Abdalla et al., 2016; Shakoor et al., 2021). Agricultural practices that minimize or reduce tillage operations can increase soil aggregate formation potentially retaining ~30% of crop residues on the soil surface increasing nutrient availability and reducing soil erosion (CTIC, 2004). These practices include minimum tillage (MT), involving shallow cultivation to a depth of 5–10 cm, and strip tillage (ST), combining cultivated strips (25 cm depth) with direct drilling whilst leaving the inter-row spaces unaffected, have been promoted as alternative management practices to CT (Davies and Finney, 2002; Morris et al., 2010) that could reduce GHG emissions and increase C sequestration. In combination with these approaches crop residues may also be retained on the soil surface to protect the C in soil aggregates. The argument being that these non-inversion tillage systems will reduce the exposure and subsequent oxidation of SOC and lower GHG emissions.

In addition to CO_2, soil tillage can also affect the emissions of N_2O and CH_4. Both N_2O and CH_4 have global warming potentials (GWP) that are 265 and 28 times higher than CO_2, respectively (Myhre et al., 2013). In some cases, reductions in CO_2 emissions that have been attributed to a particular tillage management may be off-set by increases in the emissions of N_2O (Six et al., 2004). The rate of N_2O production is controlled by factors that are affected by tillage intensity, such as the soil water-filled pore space (WFPS), soil organic C availability and temperature (Butterbach-Bahl et al., 2013). The reported effects of RT operations on N_2O emissions are equivocal, showing either increases (Ball et al., 1999; Shakoor et al., 2021), decreases (Kessavalou et al., 1998; Chatskikh and Olesen, 2007; Ussiri et al., 2009) or similar N_2O emissions (Abdalla et al., 2010; O'Neill et al., 2020).

Methane fluxes are regulated by factors such as soil moisture, temperature, oxygen availability, SOM content and C and N availability (Jacinthe and Lal, 2005). Therefore, tillage practices, through their effects on soil physicochemical properties, can influence net CH_4 emissions (Hütsch, 1998). Well-aerated soils with higher oxygen availability that facilitate CH_4 diffusion to methanotrophic sites tend to have higher rates of CH_4 uptake than poorly drained soils that restrict CH_4 oxidation (Prajapati and Jacinthe, 2014). Soils may also differ in their capacity to oxidise methane, however, the mechanism(s) involved is not fully understood (Lang et al., 2020).

Oilseed rape (*Brassica napus* L.; OSR) is the third most important oil crop in the world after oil palm and soybean (FAOSTAT, 2021). The winter OSR variety is predominantly cultivated in temperate climatic regions of Europe, where the mean yield of winter and spring OSR varieties (2.7 t ha^{-1}) consistently exceed the global average (2.1 t ha^{-1}) (FAOSTAT, 2021). In Ireland, WOSR is cultivated as a break crop in cereal production systems on ~10,000 ha annually (Zahoor et al., 2015; CSO, 2020) and traditionally established via CT sowing operations (Forristal and Murphy, 2010). Compared to CT practices, the crop area under reduced tillage in Ireland is small at 40,000 ha (Meade and Mullins, 2005) although there is increasing interest by growers in the adoption of RT approaches for crop establishment for environmental and economic reasons.

Several studies have quantified GHG emissions from WOSR and/or canola systems. Management practices varied considerably between these experiments spanning 3 decades of research where the soil was cultivated by CT, RT or NT practices or the crops were established using a wide range of row

TABLE 1 | Management practices and GHG emission measurement methodologies as described in previous studies of OSR.

Study	Tillage	Row spacing (mm)	Seed rate (m^2)	Cultivar	Chamber methodology
Ball et al. (1999)	CT/NT	—	—	—	Inter-row spacing
Chatskikh et al. (2008)	CT/RT/DD	—	—	—	Plant + Soil
Dobbie et al. (1999)	—	—	—	—	Plant + Soil
Drewer et al. (2012)	DD	—	—	—	Inter-row spacing
Hénault et al. (1998)	—	—	—	—	Inter-row spacing
Jeuffroy et al. (2013)	CT	—	52	Mendel	Plant + Soil
Kaiser et al. (1998)	CT	—	—	—	Plant + Soil
Kavdir et al. (2008)	—	—	—	—	Inter-row spacing
Keane et al. (2018)	DD	—	—	—	Plant + Soil
Kern et al. (2012)	CT	—	—	—	Inter-row spacing
Li et al. (2016)	CT/NT	250	4 kg ha^{-1}	Hyola555 TT	Plant + Soil
Merino et al. (2012)	CT	300	—	Standing	Inter-row spacing
Ruser et al. (2017)	CT	360	40–45	Visby	Inter-row spacing
Schwenke et al. (2015)	NT	500	—	Hyola 50	Inter-row spacing
Thers et al. 2019; Thers et al. 2020	CT[a]	480–500	—	DK Exclusiv	Inter-row spacing
Vinzent et al. (2018)	—	125	40	Xenon and Avartar	Inter-row spacing
Wagner-Riddle and Thurtell (1998)	CT	—	—	—	Inter-row spacing

[a]*Winter barley straw was removed prior to ploughing.*
CT = Conventional tillage; RT = Reduced tillage; NT = No-tillage; DD = Direct drilling.

spacing's and seed rates (**Table 1**; Walter et al., 2015 and references therein). Another confounding factor in previous studies is that the chambers used for GHG emission measurements were either placed in the inter-row space between plant rows or enclosed both the plant row and inter-row areas. This could complicate an assessment of the impact of different management practices as the presence of plants could directly or indirectly have an impact on GHG emissions. Given the broad range of management practices used it is also difficult to generalize about the reason(s) for any observed differences in GHG emissions.

Other agronomic management practices, such as row spacing and seed rate, are often optimized by growers to encourage rapid plant emergence, canopy closure and development from sowing to harvest. Crop row spacing and plant density influence canopy architecture, which affects solar radiation interception, and the utilization of water and nutrients. Increasing row width and/or reducing the seed rate may expose surface soils to increases in solar radiation, precipitation and wind, resulting in microclimate-related modifications in soil temperature and moisture that influence GHG emissions.

Although there are some studies that have examined the link between WOSR yields, tillage practice, row spacing or seed rate (Christian and Bacon, 1990; Vann et al., 2016) the link between cultivation practices, GHG emissions and yield has not yet been examined. The objectives of this study were to examine the effects of: 1) non-inversion tillage and row spacing, 2) row spacing and seed rate, using two WOSR cultivars, on CO_2, N_2O and CH_4 emissions, compared to the conventional management practice typically used on Irish farms (CT; 125 mm row spacing, 60 seeds m^{-2}). Given the importance of agronomic practices that can contribute to GHG mitigation whilst having no yield penalty we also assess the effects on GWP per unit of yield (i.e., the yield-scaled GWP) in different WOSR cultivation systems.

MATERIALS AND METHODS

Experiment 1: Crop Cultivation

The different cultivation treatments ("Exp. 1") were established in the Hockey field at Knockbeg (52°51′42″N, 6°56′28″W) around 5 km from the Teagasc Crops Research Facility in 2014/2015 (**Figure 1B**). The soil at this site is a sandy loam-to-loam texture (Conry, 1987) and before cultivation had been under a permanent pasture for at least 10 years. Since the 1990s the site has been under CT with continuous crop cultivation (van Groenigen et al., 2011).

Winter oilseed rape (*Brassica napus* L. cv. Compass) was cultivated using CT, strip tillage (ST) and MT. The CT treatment consisted of a primary cultivation, soil inversion to a depth of 200–250 mm, with a 5-fin mouldboard plough followed by one pass of a roller to consolidate the soil after ploughing. Secondary cultivation (power harrowing) was performed immediately prior to sowing the seed. The ST treatment is a modified non-inversion tillage technique where strips of soil (200 mm) are cultivated to the conventional plough depth (200–250 mm) whilst the inter-row spacing between plants is left uncultivated with the previous crop residue retained on the soil surface (He-va Sub-Tiller, Denmark). The MT treatment consisted of non-inversion soil cultivation to a depth of 100–125 mm using a stubble cultivator with tines spaced 300 mm apart followed by leveling discs and a cage roller (Horsch, Terrano FX3, United States). A dynamic 3 m cultivator drill (Vaderstad, Rapid 300S, Sweden) capable of working in a range of seedbed types delivered seed through individual hydraulic metering units to a disc coulter.

Plants were sown at a rate of 60 seeds m^{-2} at two row spacing's, 125 and 600 mm, giving a total of five treatments as there was no 125 mm spacing for the ST treatment. The treatments (25 m × 5 m) were laid out in a randomised block design with four replications. Calcium ammonium nitrate (CAN) was applied

in two split applications of 76 kg N ha^{-1} (March 16, 2015) and 150 kg N ha^{-1} (April 1, 2015). Management details are listed in the **Supplementary Table S1** of the Supplementary Information. The crop was harvested on the August 8, 2015.

Experiment 2: Sowing Treatments

The sowing treatments ("Exp. 2") were established in a privately-owned field in Goresbridge, Co. Kilkenny (52°38′8″N, 7°0′43″W) in 2015/2016 (**Figure 1C**). The soil is a loam texture and has been under continuous wheat cultivation for >10 years. The field was cultivated by deep MT (200–250 mm) (Horsch, Terrano Simba, United States) on the August 22, 2015 and conventional (cv. Compass: C) and semi-dwarf (cv. Troy: T) varieties of WOSR were sown on the August 31, 2015. Plants were sown at four row spacing's (125, 250, 500 and 750 mm) and four seeding rates (10, 15, 30 and 60 seeds m^{-2}). The experiment was a laid out in a randomised split-plot design with four replications. The main plots (variety) were divided into sub-plots (30 m × 5 m) each containing a combination of different row spacings and seed rates. For logistical reasons, only eight treatments that considered the row spacing/seed rate "extremes" were examined in this study: 1) C125/10, 2) C125/60 (control), 3) C750/10, 4) C750/60, 5) T125/10, 6) T125/60, 7) T750/10 and 8) T750/60. Nitrogen fertiliser (188 kg N ha^{-1}) was supplied in three split applications: 53 kg ha^{-1} ammonium sulphate nitrate, 80 and 55 kg N ha^{-1} (both CAN). Fungicide, insecticide and herbicide were applied throughout the season and the crop was harvested on the July 29, 2016. Further management details are listed in **Supplementary Table S1** of the Supplementary Information. Soil chemical properties for each site are described in **Table 2**.

Soil CO_2, N_2O and CH_4 Emission Measurements

Circular stainless-steel collars (225 mm ∅, area = 0.03 m^2) with rubber gaskets were inserted into the inter-row spacing (100 mm depth) of all cultivation treatments. Soil CO_2 emission measurements were carried out using an infrared gas analyzer (EGM-4, PP Systems, United Kingdom) by slowly sealing an unvented chamber (0.0034 m^3) onto a rubber O-ring gasket lining the collar. The enclosure time was 120 s with readings taken every 20 s. After sampling, the chamber was removed, and the CO_2 concentration was allowed to equilibrate before placement on the next collar. Gas accumulation was linear within the headspace and measurements with $R^2 > 0.8$ were retained for analysis (Widén and Lindroth, 2003). Additionally, in Exp. 2, four PVC Collars (160 mm ∅) were inserted into bare soil which had plants removed adjacent to the main experimental plots to estimate soil basal/heterotrophic respiration (R_h).

Emissions of N_2O and CH_4 were measured using the manual closed chamber method (Chadwick et al., 2014). Accumulation of N_2O within the chamber headspace, measured at four time points over 1 hour (T_0, T_{20}, T_{40}, T_{60}), was determined to be linear on 84% of occasions (O'Neill et al., 2020). The unvented chambers (above) were sealed onto the collars for an enclosure period of 40 min (T_{40}) and sampling carried out between 9.00 and 13.00 h (Barton et al., 2015). The chambers were covered with aluminium foil to prevent solar radiation induced temperature changes inside the headspace during the enclosure period.

For gas sampling, headspace air was withdrawn through a stopcock fitted to the chamber vent using a 20 ml polypropylene syringe (BD Plastipak, Spain). The chamber headspace was mixed by flushing air slowly with the syringe plunger twice prior to the withdrawal of the gas sample. Using a hypodermic needle, samples were immediately transferred into pre-evacuated 7 ml glass exetainers (Sigma-Aldrich, United Kingdom) fitted with double wadded septa (Labco, High Wycombe, United Kingdom). The exetainers were injected with a 12 ml sample to create an overpressure and prevent back diffusion of ambient air during storage. Four ambient air samples were also taken near ground level before and after each sampling occasion to obtain a surrogate time zero (T_0) sample for each chamber (Chadwick et al., 2014; Charteris et al., 2020). Sampling frequency was increased during the period of fertilizer application: four times per week for 2 weeks, then twice a week for 2 weeks, then once a week until harvest. Additional samples were taken before or after precipitation events, which are known to stimulate denitrification (Butterbach-Bahl et al., 2013).

Analysis of N_2O and CH_4 concentrations were carried out with a Gas Chromatograph with a 63Ni electron capture detector (ECD) at 60°C with a flame ionization detector (FID) at 300°C (Bruker Scion 456, Germany). Samples were injected into the GC using a Combi-PAL auto-sampler (CTC Analytics AG, Switzerland). Results were expressed in parts per million by volume (ppmv).

Daily GHG emissions were calculated using the **Eq. 1**:

$$F(GHG) = (\Delta C/\Delta t) \times ((MW \times P)/(R \times T)) \times (V/A) \quad (1)$$

where $\Delta C/\Delta t$ is the rate of change of CO_2 (T_o to T_2; IRGA) N_2O and CH_4 concentration (T_0 to T_{40}; GC), where ΔC is the change in concentration of the gas in the headspace volume (ppmv or ppbv), Δt is the enclosure time period (minutes), MW is the molar mass of CO_2-C (12 g), N_2O-N (28 g) or CH_4-C (12 g), P is the atmospheric pressure at the time of sampling (Pa), R is the gas constant (8.314 J mol^{-1} K^{-1}), T is the air temperature at the time of sampling (K), V is the headspace volume within the chamber (m^3) and A is the area covered by the base (m^2). Cumulative GHG emissions (±SE) were calculated by trapezoidal integration of the daily means.

The global warming potential (GWP) was calculated for each management practice by converting N_2O and CH_4 emissions to CO_2 equivalent emissions (CO_2-eq.) for a 100 years time horizon. The radiative forcing potential used relative to CO_2 was 265 for N_2O and 28 for CH_4 (Myhre et al., 2013). Yield-scaled GWP was calculated by dividing the CO_2-equivalent emissions by the seed yield (harvested at 9% moisture) and expressed in units of kg CO_2-eq. kg^{-1}. The contribution of CO_2 to GWP was excluded based on: 1) the assumption that the soil CO_2-C efflux was largely off-set by high rates of net primary productivity (C input) and biomass removal at harvest (C export) (Smith et al., 2007) and 2) the absence of accurate crop residue (straw and root C) data to quantify the annual change in SOC (Mosier et al., 2006).

Soil and Climatic Measurements

Soil mineral N (NH_4^+ and NO_3^-) concentrations were determined during the spring-summer growth period. Soil cores (0–10 cm depth) were taken weekly after fertilization for 1 month and every 3–4 weeks thereafter until harvest. Soils were

initially stored at 4°C and extracted either on the same day of collection, or within 24 h, using 2 M KCL at a ratio of 5:1 (v:w) water: soil (Maynard et al., 1993). The NH_4^+ and NO_3^- concentrations of the extract were analyzed with an Aquakem 600 discrete analyzer (Thermo Fisher Scientific, United States).

Soil volumetric moisture content (%) (GS3, Decagon Devices, United States) and soil temperature (°C; Exp. 2 only) (ELE International, Bedfordshire, United Kingdom) were measured (50–100 mm depth) in the inter-row spacing adjacent to the collars. Water-filled pore space (WFPS) was calculated using **Eq. 2**:

$$WFPS(\%) = VWC/[1 - Bd/Pd] \times 100 \quad (2)$$

where Bd is the bulk density measured at the soil surface (70 mm depth) and Pd is particle density estimated at 2.65 g cm^{-3} (Linn and Doran, 1984).

Climatic measurements of mean air temperature (°C), atmospheric pressure (Pa), rainfall (mm) and soil temperature (°C) were taken from the Met Eireann automated weather station at Oakpark, Co. Carlow, Ireland, which was located 5 km from the Exp. 1 and 30 km from the Exp. 2 sites.

Statistical Analysis

Statistical analysis was conducted using SAS 9.4 (Cary, NY, United States) and R software (R 3.6.1, R Core Team, 2019). Normality and homogeneity of variance were checked using histograms and residual graphs. Where necessary, log or square root transformations (y or y + constant) were applied to data to achieve homogeneity of variance. For Exp. 1, the PROC GLIMMIX procedure in SAS was used to test for differences between the treatments. Tillage (CT, MT, and ST) and row spacing (125 and 600 mm) were the main effects. To account for the missing treatment (i.e., ST125) in the model, additional parameters were created, each with two levels: a "Nested Group" (Factors = CT + MT; Single = ST) and a "Variable Group" (1 = CT125, 2 = all others). The *_residual_* option was used in the RANDOM statement. Significant pairwise differences were determined according to the *simulate* post-hoc test ($p < 0.05$). For Exp. 2, a linear-mixed effects model (*lmer*) in the "lme4" (Bates et al., 2012) and "lmerTest" packages (Kuznetsova et al., 2017). Variety (cvs. Compass and Troy), row spacing (125 and 750 mm) and seed rate (10 m^{-2} and 60 m^{-2}) were set as the main effects with *block* and *block x variety* set as the random effects. Model effects were examined using the *emmeans* function (Lenth, 2019) where ANOVA and pairwise comparisons (normal and back-transformed data) were examined by the Tukey method at a significance level of $p < 0.05$. Plots were made using the "ggplot2" package in R (Wickham, 2016).

RESULTS

Crop Cultivation

Meteorological data was similar for both sites during the gas measurement periods (**Figure 2**). The mean air temperatures were 10.9°C (2.9–19.9°C) and 11.0°C (3.6–19.8°C) for Exp. 1 and Exp. 2, respectively. Cumulative rainfall was similar from the period of 27th February to 22nd July each year in Exp. 1 (261 mm) and Exp. 2 (265 mm), representing 28 and 37% of the annual rainfall, respectively. During the growing seasons, the wettest months for Exp. 1 and Exp. 2 were May (90 mm) and April (64 mm) whilst the driest months were April (26 mm) and July (24 mm), respectively.

A rapid loss of CO_2 was observed after the implementation of CT (maximum recorded value of 2.34 g C m^{-2} hr^{-1}) at a rate 2.5 times that of ST (maximum recorded value of 0.94 g C m^{-2} hr^{-1}) and 14.6 times that of MT (maximum recorded value of 0.16 g C m^{-2} hr^{-1}) (**Figure 3**). These decreased rapidly to 0.16 g C m^{-2} hr^{-1} (CT) and 0.07 g C m^{-2} hr^{-1} (ST) after the tillage events and then remained largely stable for the rest of the measurement period. Excluding the anomalously high value found in the MT treatment after 3 days, the daily soil CO_2 emissions ranged from 0.04 to 1.38 g C m^{-2} h^{-1} across all treatments during the 12 days period.

Daily soil CO_2 emissions where generally higher during the early part of the growing season and showed two peaks, each occurring around 7 days after the first and second N fertilizer applications, respectively (**Figure 4A**). Soil CO_2 emissions tended to be greater in the CT125 system with maximum daily emissions of 4.0 and 4.2 g C m^{-2} d^{-1}. The emissions of CO_2 converged towards similar values in all systems by mid-April until June, where the mean CO_2 loss was 1.16 ± 0.07 g C m^{-2} d^{-1}. Higher CO_2 emissions were generally observed between 32 and 70% WFPS, with a tendency for lower emissions under both drier (25% WFPS) and wetter (85% WFPS) conditions. Cumulative CO_2 emissions were not significantly affected by the crop cultivation treatment, with values ranging from 1,083 to 1,683 kg C ha^{-1}, although higher CO_2 emissions were generally found in the 125 mm row spacing treatment (**Table 3**).

Slight increases in N_2O were observed in the ST600 system (11.6–27.3 g N ha^{-1} d^{-1}) *ca.* 10 days after the first fertilization (**Figure 4B**). The highest N_2O emissions were observed in the MT125 (53.8 g N ha^{-1} d^{-1}), MT600 (62.8 g N ha^{-1} d^{-1}) and ST600 (70.0 g N ha^{-1} d^{-1}) treatments 4 days after the second N application and a second peak occurred in the ST600 (69.3 g N ha^{-1} d^{-1}) treatment 2 days later. These were observed at 72–79% WFPS when the soil temperature was >10°C (Supplementary Information, **Supplementary Figure S1**), however, the majority of the N_2O emissions occurred across a wide range of WFPS (25–90%) (**Figure 4B**). Maximum N_2O emissions were lower in the CT125 and CT600 treatments, with values of 30.5 and 18.5 g N ha^{-1} d^{-1}, respectively, occurring 58 days after fertilization. There was no significant effect of tillage or row spacing on the cumulative N_2O emissions, with values ranging from 0.81 to 2.05 kg N ha^{-1} (**Table 3**).

Daily CH_4 emissions displayed similar temporal patterns and ranged from −10.7 to 5.4 g C ha^{-1} d^{-1} (**Figure 4C**). Net CH_4 emissions preceded by significant uptake of CH_4 were observed after the second N application. With some exceptions, net CH_4 uptake was generally sustained until June. For the cumulative CH_4 uptake values, a significant tillage x nested effect ($p < 0.05$) was observed with a 55% increase in uptake in the CT (−0.34 ± 0.03 kg C ha^{-1}) compared to the MT systems (−0.22 ± 0.03 kg C ha^{-1}), with the total CH_4 uptake in the ST treatment midway between the CT and MT treatments (**Table 3**).

FIGURE 1 | Geographical overview of Ireland **(A)** and the locations of the study sites in **(B)** Knockbeg, Co. Laois and **(C)** Goresbridge, Co. Kilkenny, with the surrounding agricultural land uses (Google Earth; created on 31st July 2021). Orange lines indicate the location of the experimental trial plots.

Sowing Treatments

Daily GHG emissions for the two WOSR varieties are illustrated in **Figure 5**. Transient fluctuations in soil CO_2 emissions were found during the season, ranging from 0.11 to 3.20 g C m^{-2} d^{-1} (**Figure 5A**), with no clear seasonal trend. Nitrogen fertilizer application tended to initially suppress CO_2 emissions, which was followed by increases in CO_2 emissions 1–2 weeks later. Soil CO_2 emissions increased temporarily in the 125/10 and 750/10 plots in June, however, little variation existed between sowing treatments during the main growing season.

Daily soil N_2O emissions were clearly associated with N fertilizer applications (**Figure 5B**). Higher N_2O emissions were found from the cv. Troy plots particularly the 125/10 treatment, and were also observed for soil temperatures >10°C and WFPS values approaching 80% (Supplementary Information, **Supplementary Figure S1**). Nitrous oxide emissions fell to background rates around 1 month after the final N application.

Daily soil CH_4 emissions ranged from −38.2 to 26.3 g C ha^{-1} d^{-1} across all sowing treatments (**Figure 5C**). Low net CH_4 uptake rates occurred after mineral N was applied to the soils. The sharp increase in CH_4 uptake in April coincided with a decrease in soil NH_4^+ and NO_3^- concentrations in late-April (Supplementary Information, **Supplementary Figures S2, S3**). Several treatments associated with the Compass and Troy cultivars displayed transient net CH_4 emission peaks but, in general, there was a consistent trend of increasing net CH_4 uptake towards the summer months. The highest net CH_4 uptake rates occurred within a narrow temperature range of 13–15°C but a broader range (26–45%) of WFPS. Combining the data from Exp. 1 and Exp. 2, WFPS explained around one quarter of the variance (R^2 = 0.29) in the CH_4 emissions (Supplementary Information, **Supplementary Figure S4**). Neither the cumulative N_2O nor CH_4 emissions were affected by row spacing, seed rate or variety (**Table 4**).

Yield and Yield-Scaled GWP

Seed yields were unaffected by crop cultivation treatment, canopy management or sowing method (**Tables 3**, **4**). Yields averaged 4.98 t seed ha^{-1} in Exp. 1 and 4.56 t seed ha^{-1} in Exp. 2. Yield-scaled GWP values ranged from 0.06 to 0.16 kg CO_2-eq. kg^{-1} in Exp. 1 and 0.05–0.19 kg CO_2-eq. kg^{-1} in Exp. 2. In the latter experiment, the mean yield-scaled GWP of cv. Troy (0.12 kg CO_2-eq. kg^{-1}) was double that of the cv. Compass sown plots (0.06 kg CO_2-eq. kg^{-1}) ($p < 0.05$).

DISCUSSION

Crop Management and GHG Emissions

In this study, short-term CO_2 emissions after tillage operations were characterized by an initially rapid increase followed by a fast

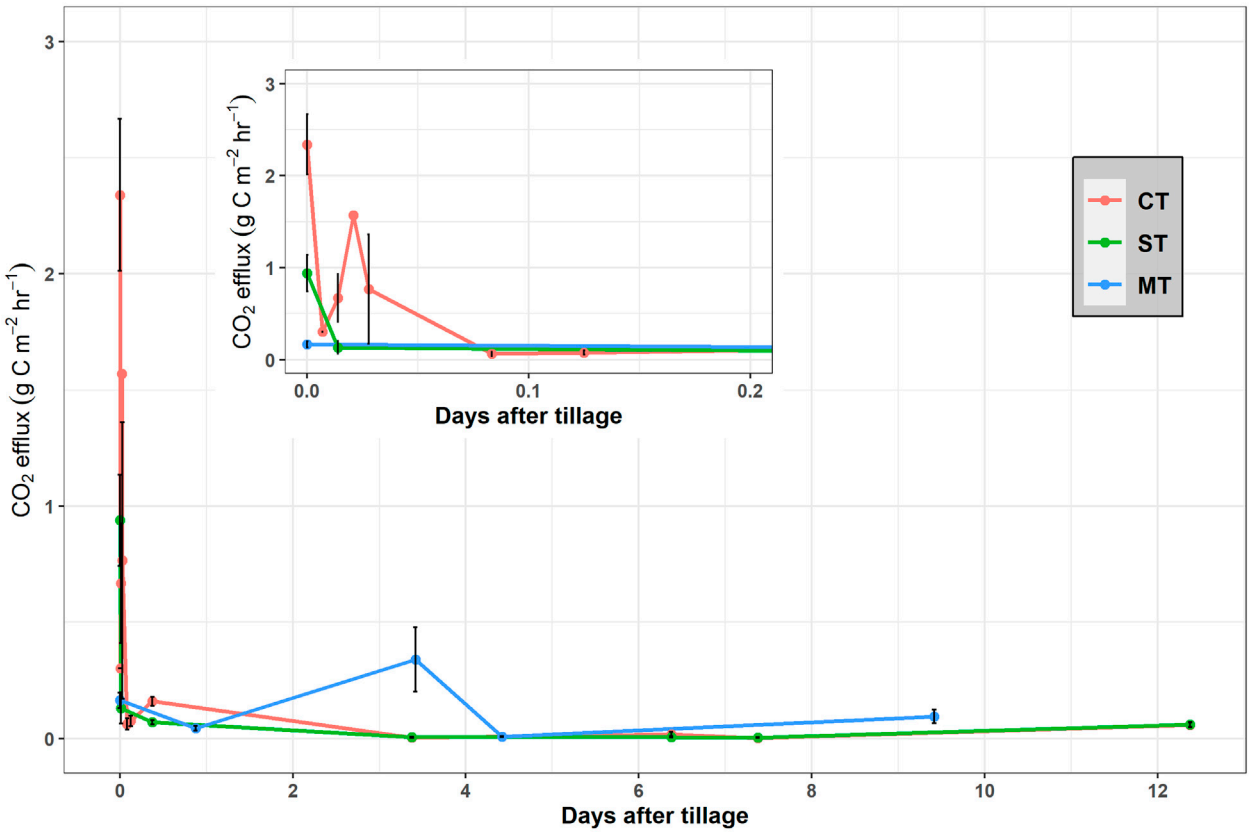

FIGURE 2 | Daily air temperature (blue line) and rainfall (grey bars) recorded from the automated weather station at Oakpark covering the 2-year period from sowing in Exp. 1 to harvest in Exp. 2 (August 2014–August 2016). The shaded red areas indicate the gas measurement periods in Exp. 1 (17/03/2015 – 21/07/2015) and Exp. 2 (27/02/2016 – 22/07/2021).

exponential decline (**Figure 3**). The CT treatment resulted in a maximum CO_2 efflux rate *ca.* 2.5 times that of ST and 14.6 times that of MT which is consistent with an effect of gaseous diffusion due to soil disturbance (Jackson et al., 2003; La Scala et al., 2006; Reicosky and Archer, 2007; Morell et al., 2010). The large loss of CO_2 from the MT plot (0.34 g C m^{-2} hr^{-1} or 8.15 g C m^{-2} d^{-1}) *ca.* 3.5 days after tillage coincided with a rainfall event, a phenomenon often called the "Birch Effect" (Gebremichael et al., 2019). Increased organic matter mineralization after MT in combination with favorable soil moisture and temperature may have led to the relatively larger efflux of CO_2 compared to CT and ST (Franzluebbers et al., 1995; Jabro et al., 2008). Overall, however tillage had very little impact on short-term CO_2 emissions.

Soil CO_2 emissions during spring-summer were unaffected by variations in tillage intensity (**Table 3** and **Table 4**) in line with earlier studies that reported no significant effects of RT systems on CO_2 emissions (Kessavalou et al., 1998; Chatskikh et al., 2008; Abdalla et al., 2014). Tillage management can affect soil CO_2 emissions through its influence on soil moisture, soil temperature and soil organic C accumulation (Buyanovsky et al., 1986; Hendrix et al., 1988; Franzluebbers et al., 1995; Fortin et al., 1996). In RT systems this is often associated with the retention of crop residues that lower soil temperatures and increase soil moisture content (Chen and McKyes, 1993). However, daily soil temperatures and WFPS values varied little between treatments indicating that the effect of contrasting tillage regimes on residue retention had little effect on CO_2 emissions. In this study, the highest soil CO_2 emissions occurred during the spring period of the growing season suggesting that phenology, through its effects on root respiration processes and/or the rhizodeposition of labile C, contributed to CO_2 production (Rood et al., 1984; Whipps, 1990; Franzluebbers et al., 1995; Rochette and Flanagan, 1997; Jans et al., 2010). In OSR, the highest values for leaf area index were reached close to flowering, which is consistent with the higher soil CO_2 emissions observed in March and April across all experiments (except cv. Troy in Exp. 2). Crops allocate, on average, 21% of their photosynthetically fixed C to their roots of which a smaller proportion of this C is released to the soil in root exudates (Pausch and Kuzykayov, 2018). The absence of variation between tillage management may reflect either a low

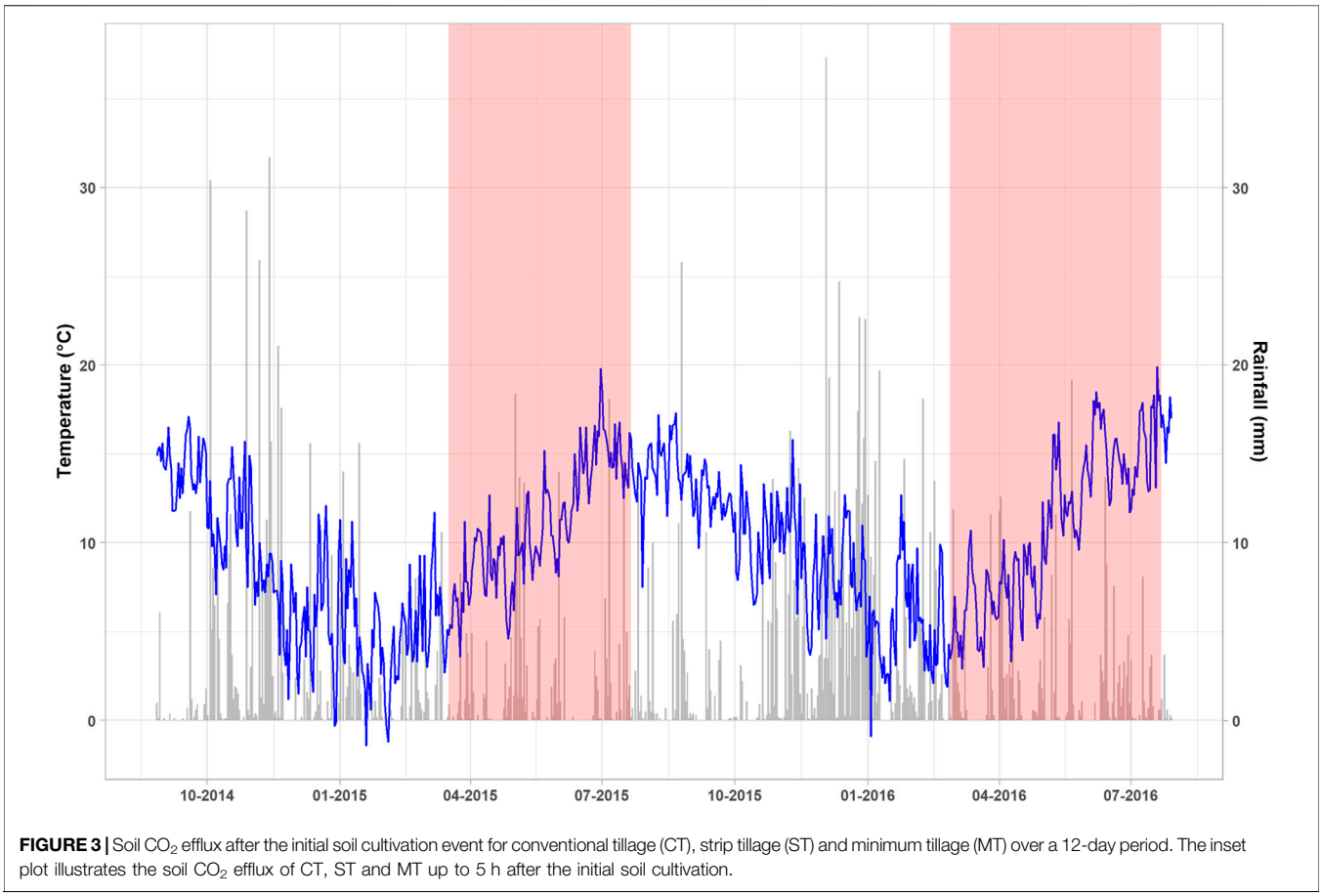

FIGURE 3 | Soil CO_2 efflux after the initial soil cultivation event for conventional tillage (CT), strip tillage (ST) and minimum tillage (MT) over a 12-day period. The inset plot illustrates the soil CO_2 efflux of CT, ST and MT up to 5 h after the initial soil cultivation.

supply of labile C belowground or labile C substrate was not limiting CO_2 production.

Tillage management had little impact on N_2O emissions in this study (**Table 2** and **Table 3**) in line with earlier work examining CT and RT systems (Abdalla et al., 2010; Liu et al., 2016). Peak N_2O emissions that were found in the MT and ST but not in the CT treatments coincided with a higher WFPS (>70%) and higher temperatures (>10°C) as noted in previous studies (Adviento-Borbe et al., 2007; Abdalla et al., 2010; Žurovec et al., 2017; O'Neill et al., 2020). This indicates that denitrification is the main source of N_2O production and the N_2O emissions are largely dependent on the extent of soil anaerobiosis. A lower WFPS and an associated increase in soil oxygenation may explain the absence of any impact of fertilization on N_2O emissions in the CT systems (**Figure 4B**).

Cumulative CH_4 uptake was *ca.* 55% greater in the CT compared to the MT treatments ($p < 0.05$, **Table 2**). Plaza-Bonilla et al. (2014) also reported a significantly higher cumulative uptake of CH_4 in CT (2.69 kg C ha^{-1}) compared to NT (1.16 kg C ha^{-1}) under Mediterranean dryland conditions ($p < 0.05$). The authors suggested that the greater CH_4 oxidation found under CT might be explained by the short duration of NT (3 years) and the possible lack of differences in soil pore structure and methanotrophic communities between CT/NT plots. Reduced tillage practices can however result in a more porous and stable soil structure that facilitates CH_4 diffusion (Ball et al., 1997; Hütsch, 1998; Ussiri et al., 2009) and the long-term implementation of RT (>40 years) has been shown to restore the CH_4 oxidation capacity of arable soil (Ussiri et al., 2009; Jacinthe et al., 2014). Although the reason(s) for the observed differences between tillage treatments in this study are not clear, it could be explained by both the enhanced diffusion of atmospheric CH_4 into the soil and the greater CH_4 oxidation rates under CT as the soils became drier in summer.

Soil WFPS had the largest effect on CH_4 emissions and explained approximately one quarter of the variability in the daily CH_4 emissions (Supplementary Information, **Supplementary Figure S4**). Higher soil water content inhibits the diffusive transport of CH_4 and oxygen to active microbial sites, consequently reducing CH_4 uptake in arable soils (Flessa et al., 1995; Drewer et al., 2012). The results of this study are consistent with the recent review by Cowan et al. (2020) who found soil volumetric water content as the strongest predictor of CH_4 emissions across agricultural soils in the United Kingdom and Ireland ($R^2 < 0.1$). This indicates that soil water content and its impact on diffusion processes may override the effect of tillage management in regulating CH_4 exchange in arable soils.

TABLE 2 | Soil chemical properties for each site.

	Depth (cm)	SOM (%)	SOC (%)[a]	TN (%)	Soil pH
Knockbeg-Hockey Field	0–30	4.80	2.40	0.157	7.21
	30–60	3.12	1.56	0.057	7.94
	60–90	2.58	1.29	0.041	8.13
Goresbridge	0–30	4.70	2.35	0.190	7.16
	30–60	2.20	1.10	0.048	7.87
	60–90	1.20	0.60	0.071	8.42

[a]*SOC = (SOM × 0.5) (Pribyl, 2010).*

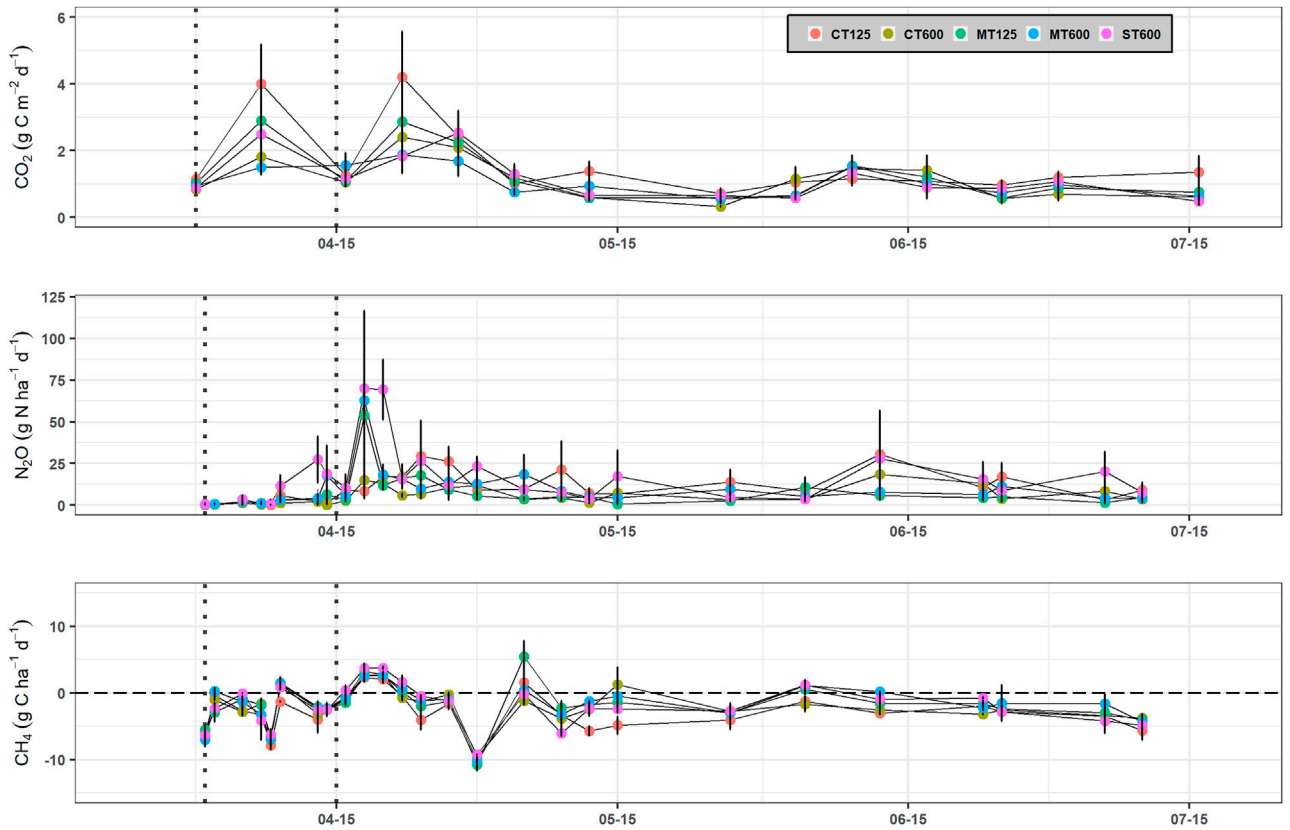

FIGURE 4 | Soil CO_2, N_2O and CH_4 emissions for each crop establishment system in Exp. 1: conventional tillage at 125 (CT125) and 600 mm (CT600) row spacing, minimum tillage at 125 (MT125) and 600 mm (MT600) row spacing, and strip tillage at 600 mm row spacing (ST600). Vertical dashed lines indicate fertilizer application and vertical lines on each data point represent the standard error of the means.

Row spacing was found to have no significant effect on GHG emissions. In OSR, row spacing influences plant height, branching, leaf area, pod number and the overall canopy architecture. Plants sown in narrow rows reach canopy closure quicker than wide row cropping systems and thus, it was hypothesised that row spacing would influence factors such as root distribution, root C input, water use, N uptake, light interception and soil temperature, and directly or indirectly influence GHG emissions (Sharratt and McWilliams, 2005). Zapata et al. (2021) reported higher CO_2 emissions from soybean compared to wheat (wide vs. narrow row spacing) due to prolonged exposure of surface soil to direct sunlight and high intensity rainfall. The absence of a row spacing effect in this study may be due to comparable above-ground vegetative growth rates and rapid canopy closure, irrespective of plant stand structure, thereby limiting the potential microclimatic effects of row spacing on GHG emissions.

Seed rate was a significant factor affecting GHG emissions in Exp. 2 (**Table 3**). Mean cumulative CO_2 emissions (Compass and Troy) were 21% higher in the 10 seeds m^{-2} compared to the 60 seeds m^{-2} treatments ($p < 0.05$). Seed rate determines the plant density and the canopy architecture and, like row spacing, will influence light interception, water and nutrient use and soil

TABLE 3 | Cumulative GHG emissions, seed yield and yield-scaled GWP for Exp. 1.

Tillage	Row spacing (mm)	CO_2 (kg C ha^{-1})	N_2O (kg N ha^{-1})	CH_4 (kg C ha^{-1})	Yield (t DM ha^{-1})	Yield-scaled GWP (kg CO_2-eq. kg^{-1} seed)
Conventional tillage	125	1,683 ± 277	1.45 ± 0.48	−0.39 ± 0.03a	4.82 ± 0.15	0.11 ± 0.04
Conventional tillage	600	1,108 ± 137	1.00 ± 0.50	−0.29 ± 0.04a	5.00 ± 0.06	0.09 ± 0.05
Minimum tillage	125	1,289 ± 89	0.81 ± 0.15	−0.24 ± 0.05b	5.14 ± 0.13	0.06 ± 0.01
Minimum tillage	600	1,083 ± 126	1.13 ± 0.18	−0.21 ± 0.03b	5.00 ± 0.10	0.09 ± 0.01
Strip tillage	600	1,218 ± 116	2.05 ± 0.86	−0.27 ± 0.03ab	4.98 ± 0.22	0.16 ± 0.07
ANOVA						
Nested		NS	NS	NS	NS	NS
Tillage*Nested		NS	NS	$p < 0.05$	NS	NS
Row*Nested		NS	NS	NS	NS	NS
Tillage*Row*Nested		NS	NS	NS	NS	NS

Different lowercase letters indicate significant variation between treatments.

TABLE 4 | Cumulative GHG emissions, seed yield and yield-scaled GWP for Exp. 2.

Variety	Row spacing (mm)	Seed rate (m^2)	CO_2 (kg C ha^{-1})	N_2O (kg N ha^{-1})	CH_4 (kg C ha^{-1})	Yield (t DM ha^{-1})	Yield-scaled GWP (kg CO_2-eq. kg^{-1} seed)
Compass	125	10	1,555 ± 215b	1.38 ± 0.29	−1.58 ± 0.24	4.64 ± 0.07	0.09 ± 0.03a
	125	60	1,110 ± 33a	1.01 ± 0.10	−1.81 ± 0.46	4.59 ± 0.18	0.05 ± 0.01a
	750	10	1,312 ± 118b	1.34 ± 0.36	−2.07 ± 0.68	4.80 ± 0.22	0.07 ± 0.02a
	750	60	1,166 ± 180a	1.14 ± 0.33	−3.15 ± 1.50	4.58 ± 0.13	0.03 ± 0.02a
Troy	125	10	1,280 ± 212b	2.28 ± 0.70	−1.29 ± 0.22	4.41 ± 0.14	0.19 ± 0.07b
	125	60	1,189 ± 113a	1.12 ± 0.26	−2.35 ± 0.60	4.37 ± 0.05	0.05 ± 0.03b
	750	10	1,304 ± 99b	1.66 ± 0.36	−1.61 ± 0.49	4.46 ± 0.07	0.12 ± 0.03b
	750	60	1,028 ± 40a	1.89 ± 0.48	−1.65 ± 0.65	4.64 ± 0.15	0.13 ± 0.04b
ANOVA							
Variety			NS	NS	NS	NS	$p < 0.05$
Row			NS	NS	NS	NS	NS
Seed			$p < 0.05$	NS	NS	NS	NS
Variety*Row			NS	NS	NS	NS	NS
Row*Seed			NS	NS	NS	NS	NS
Variety*Row*Seed			NS	NS	NS	NS	NS

Different lowercase letters indicate significant variation between treatments.

microclimate. For OSR crops, Roques and Berry (2016) found that high seed rate plots accelerated flowering and earlier maturation whereas plots with low seed rates remain greener for longer. The longer a plant retains its leaves, or delays leaf senescence, the greater the photosynthetic capacity of the stand and the amount of labile C that is released via root exudates to the rhizosphere. Soil CO_2 emissions in the bare soil plots (R_h) also tended to be higher during pod development in June (data not shown). This result points to a parallel increase in the rate of OM decomposition in the cropped soils caused by a reduction in shading and increases in soil temperature in the 10 seeds m^{-2} treatments. An increase in belowground OM inputs during vegetative growth and/or decomposition of native SOM at maturity may have both contributed to the greater soil CO_2 emissions.

Variation in Yield and GWP Across Different Management Practices

Despite the use of a wide range of a management practices (tillage intensity, row spacing, seed rate and variety), seed yield was unaffected (**Table 2** and **Table 3**). These results support earlier studies that found no effect of tillage, row spacing and seed rate on final seed yields (Degenhardt and Kondra, 1981; Christensen and Drabble, 1984; Christian and Bacon, 1990; Bonari et al., 1995; Vann et al., 2016; Wynne et al., 2020).

Although seed yield and yield components are determined by plant density (Leach et al., 1999; Diepenbrock, 2000; Rathke et al., 2006; Kuai et al., 2015), individual OSR plants can counter variations in plant density by increasing yield per plant (Diepenbrock, 2000), so that the seed yield is not compromised by sowing technique.

The two varieties also produced similar seed yields (**Table 3**). The shorter height of the cv. Troy plants had no detrimental impact on yield components and many of the commercially available semi-dwarf genotypes produce similar yields to conventional varieties (Sieling and Kage, 2008). Miersch et al. (2016) noted that semi-dwarf varieties yielded higher than the conventional types when N is the limiting resource. The non-limiting soil mineral N concentrations in this study (0–10 cm)

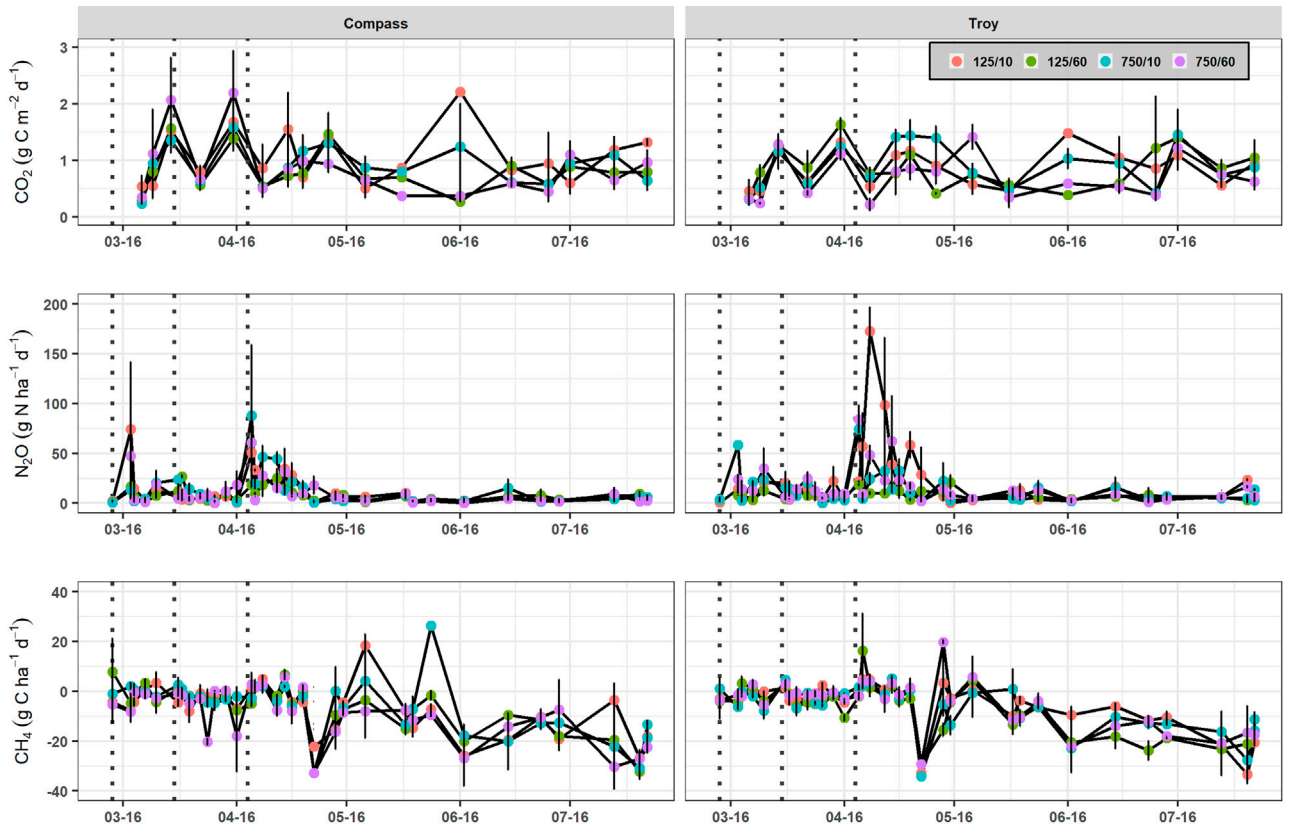

FIGURE 5 | Soil CO_2, N_2O and CH_4 emissions for each sowing method treatment in Exp. 2: the conventional ("cv. Compass") and semi-dwarf ("cv. Troy") biomass varieties sown at 125 mm or 750 mm row spacing with 10 or 60 seeds m^{-2}. Vertical dashed lines indicate fertilizer application and the vertical lines on each data point represent standard error of the means.

may have resulted in the similar yields, although semi-dwarf varieties, such as cv Troy, may also perform better in low N input systems compared to conventional varieties. Semi-dwarf varieties may also be favoured by farmers for their higher lodging resistance plus easier harvesting and pesticide applications (Sieling and Kage, 2008).

Yield-scaled GWP values were unaffected by crop management practice. In Exp. 2, cv. Troy had a yield scaled GWP that was double that of cv. Compass ($p < 0.05$). Cumulative N_2O emissions did not significantly differ between treatments, however, the greater GWP was attributed to N-fertilizer applied in excess in the 10 seeds m^{-2} cv. Troy plots, as indicated by the large N_2O emission peaks after the third N application (**Figure 5**). Sowing at a higher seed rate may circumvent the high GWP of cv. Troy but puts the variety at an inferior position to cv. Compass insofar as low seed rates can achieve similar yields to conventional sowing without adversely affecting GWP.

Our yield-scaled GWP values 0.05–0.16 kg CO_2-eq. kg^{-1} are within the range of those for crops reported in the literature. Linquist et al. (2012) calculated a yield-scaled GWP of 0.166 for wheat and 0.185 kg CO_2-eq. kg^{-1} for maize in their meta-analysis of 57 cropland sites which included rice 0.657 kg CO_2-eq. kg^{-1}. Rajaniemi et al. (2011) found slightly higher yield-scaled GWP values for barley, oats, wheat and rye (0.57, 0.57, 0.59 and 0.87 kg CO_2-eq. kg^{-1}). Gan et al. (2012) calculated a farm-scale carbon footprint of 0.281–0.317 kg CO_2-eq. kg^{-1} for barley succeeding oilseed rape. These studies, however, included the GWP of additional upstream sources such as fuel emissions, production and use of fertilizers and seed production.

The short measurement campaign (6-months) may pose some limitations for the longer-term interpretation of results. We did not take gas measurements after tillage in Exp. 2 meaning we may have missed any transient emissions of CO_2, N_2O or CH_4, whilst the low temporal frequency of measurements in the winter/spring of Exp. 1 could have introduced large errors in the estimation of the cumulative GHG emissions when determined by linear interpolation. To reduce any bias, only the higher temporal frequency measurements made during spring were considered as representative of yield scaled GWP. Annual GWP values are also required to cover the fallow and post-tillage periods as these can be a large source of GHG emissions from croplands (Linquist et al., 2012). Including all factors leading to CO_2 emissions on-farm (tillage, herbicide, pesticide, fertilization) as well as upstream activities (harvest, fertilizer manufacturing, other chemical inputs, transport) (Sainju, 2016) would provide a more complete assessment of the GHG balance of WOSR production systems.

CONCLUSION

Overall, management practice had a minimal effect on GHG emissions, crop yield and yield scaled GWP. Soil tillage and row spacing had no significant impact on CO_2 and N_2O emissions. Consequently, the management approach used for WOSR cropping systems can be tailored to the particular conditions and economic factors. The low seeding rate resulted in higher CO_2 emissions irrespective of WOSR variety, whilst the yield-scaled GWP of cv. Troy was, on average, higher than that of the cv. Compass. Sowing the semi-dwarf variety at low seeding rates may therefore increase the risk of higher C and/or N emissions from OSR systems. The overall findings indicate that considerable flexibility is possible in the way that OSR crops are established, grown and managed according to local/regional conditions and economics, without compromising yield or GHG emissions. Longer-term, high temporal resolution measurements are required to examine whether the observed GHG and GWP values can be attributed more to management or climatic effects.

DATA AVAILABILITY STATEMENT

The datasets presented in this article are not readily available because The data analyzed in this study is subject to the following licenses/restrictions: confidential. Requests to access the datasets should be directed to Macdara O'Neill, macdara.oneill@teagasc.ie.

AUTHOR CONTRIBUTIONS

MO'N, GL, PF, and BO conceived of and designed the experiments. MO performed the experimental work and gaseous emission measurements. MO'N, GL, PF, and BO wrote the manuscript.

FUNDING

This work was supported through the Teagasc Walsh Fellowship Scheme awarded to MO'N (RMIS 6363).

ACKNOWLEDGMENTS

The authors would like to thank the staff at Teagasc Oakpark and Johnstown Castle for their technical support and assistance with the experimental setup, fieldwork and laboratory analysis. We would also like to thank the reviewers for their valuable input to the manuscript.

SUPPLEMENTARY MATERIAL

The Supplementary Material for this article can be found online at: https://www.frontiersin.org/articles/10.3389/fenvs.2021.716636/full#supplementary-material

REFERENCES

Abdalla, K., Chivenge, P., Ciais, P., and Chaplot, V. (2016). No-tillage lessens soil CO2 emissions the most under arid and sandy soil conditions: results from a meta-analysis. *Biogeosciences* 13 (12), 3619–3633. doi:10.5194/bgd-12-15495-201510.5194/bg-13-3619-2016

Abdalla, M., Hastings, A., Helmy, M., Prescher, A., Osborne, B., Lanigan, G., et al. (2014). Assessing the combined use of reduced tillage and cover crops for mitigating greenhouse gas emissions from arable ecosystem. *Geoderma* 223-225, 9–20. doi:10.1016/j.geoderma.2014.01.030

Abdalla, M., Jones, M., Ambus, P., and Williams, M. (2010). Emissions of nitrous oxide from Irish arable soils: effects of tillage and reduced N input. *Nutr. Cycl. Agroecosyst.* 86 (1), 53–65. doi:10.1007/s10705-009-9273-8

Abdalla, M., Osborne, B., Lanigan, G., Forristal, D., Williams, M., Smith, P., et al. (2013). Conservation tillage systems: a review of its consequences for greenhouse gas emissions. *Soil Use Manage* 29 (2), 199–209. doi:10.1111/sum.12030

Adviento-borbe, M. A. A., Haddix, M. L., Binder, D. L., Walters, D. T., and Dobermann, A. (2007). Soil greenhouse gas fluxes and global warming potential in four high-yielding maize systems. *Glob. Change Biol.* 13 (9), 1972–1988. doi:10.1111/j.1365-2486.2007.01421.x

Ball, B. C., Dobbie, K. E., Parker, J. P., and Smith, K. A. (1997). The influence of gas transport and porosity on methane oxidation in soils. *J. Geophys. Res.* 102 (D19), 23301–23308. doi:10.1029/97JD00870

Ball, B. C., Parker, J. P., and Scott, A. (1999). Soil and residue management effects on cropping conditions and nitrous oxide fluxes under controlled traffic in Scotland. *Soil Tillage Res.* 52 (3-4), 191–201. doi:10.1016/S0167-1987(99)00081-1

Barton, L., Wolf, B., Rowlings, D., Scheer, C., Kiese, R., Grace, P., et al. (2015). Sampling frequency affects estimates of annual nitrous oxide fluxes. *Sci. Rep.* 5, 15912. doi:10.1038/srep15912

Bates, D., Maechler, M., Bolker, B., Walker, S., Christensen, R. H. B., Singmann, H., and Scheipl, F. (2012). *Package 'lme4'*. Vienna, Austria: CRAN. R Foundation for Statistical Computing.

Bonari, E., Mazzoncini, M., and Peruzzi, A. (1995). Effects of conventional and minimum tillage on winter oilseed rape (Brassica napus L.) in a sandy soil. *Soil Tillage Res.* 33 (2), 91–108. doi:10.1016/0167-1987(94)00440-P

Bondeau, A., Smith, P. C., Zaehle, S., Schaphoff, S., Lucht, W., Cramer, W., et al. (2007). Modelling the role of agriculture for the 20th century global terrestrial carbon balance. *Glob. Change Biol.* 13 (3), 679–706. doi:10.1111/j.1365-2486.2006.01305.x

Butterbach-Bahl, K., Baggs, E. M., Dannenmann, M., Kiese, R., and Zechmeister-Boltenstern, S. (2013). Nitrous oxide emissions from soils: how well do we understand the processes and their controls? *Phil. Trans. R. Soc. B* 368 (1621), 20130122. doi:10.1098/rstb.2013.0122

Buyanovsky, G. A., Wagner, G. H., and Gantzer, C. J. (1986). Soil respiration in a winter wheat ecosystem. *Soil Sci. Soc. America J.* 50 (2), 338–344. doi:10.2136/sssaj1986.03615995005000020017x

Central Statistics Office (CSO) (2020). *Area, yield and production of crops 2020*. Retrieved from https://www.cso.ie/en/statistics/agriculture/areayieldandproductionofcrops/.

Ceschia, E., Béziat, P., Dejoux, J. F., Aubinet, M., Bernhofer, C., Bodson, B., et al. (2010). Management effects on net ecosystem carbon and GHG budgets at European crop sites. *Agric. Ecosyst. Environ.* 139 (3), 363–383. doi:10.1016/j.agee.2010.09.020

Chadwick, D. R., Cardenas, L., Misselbrook, T. H., Smith, K. A., Rees, R. M., Watson, C. J., et al. (2014). Optimizing chamber methods for measuring nitrous oxide emissions from plot-based agricultural experiments. *Eur. J. Soil Sci.* 65 (2), 295–307. doi:10.1111/ejss.12117

Charteris, A. F., Chadwick, D. R., Thorman, R. E., Vallejo, A., Klein, C. A. M., Rochette, P., et al. (2020). Global Research Alliance N 2 O chamber methodology guidelines: Recommendations for deployment and accounting for sources of variability. *J. Environ. Qual.* 49 (5), 1092–1109. doi:10.1002/jeq2.20126

Chatskikh, D., and Olesen, J. E. (2007). Soil Tillage Enhanced CO_2 and N_2O Emissions from Loamy Sand Soil Under Spring Barley. *Soil Till. Res.* 97 (1), 5–18.

Chatskikh, D., Olesen, J. E., Hansen, E. M., Elsgaard, L., and Petersen, B. M. (2008). Effects of reduced tillage on net greenhouse gas fluxes from loamy sand soil

under winter crops in Denmark. *Agric. Ecosyst. Environ.* 128 (1-2), 117–126. doi:10.1016/j.agee.2008.05.010

Chen, Y., and McKyes, E. (1993). Reflectance of light from the soil surface in relation to tillage practices, crop residues and the growth of corn. *Soil Tillage Res.* 26 (2), 99–114. doi:10.1016/0167-1987(93)90037-p

Christensen, J. V., and Drabble, J. C. (1984). Effect of row spacing and seeding rate on rapeseed yield in northwest Alberta. *Can. J. Plant Sci.* 64 (4), 1011–1013. doi:10.4141/cjps84-137

Christian, D. G., and Bacon, E. T. G. (1990). A long-term comparison of ploughing, tine cultivation and direct drilling on the growth and yield of winter cereals and oilseed rape on clayey and silty soils. *Soil Tillage Res.* 18 (4), 311–331. doi:10.1016/0167-1987(90)90117-V

Ciais, P., Sabine, C., Bala, G., Bopp, L., Brovkin, V., Canadell, J., et al. (2014). "Carbon and other biogeochemical cycles," in *Climate change 2013: the physical science basis. Contribution of Working Group I to the Fifth Assessment Report of the Intergovernmental Panel on Climate Change*. Editors T. F. Stocker, D. Qin, G.- K. Plattner, M. Tignor, S. K. Allen, J. Boschung, A. Nauels, Y. Xia, V. Bex, and P. M. Midgley (Cambridge, UK: Cambridge University Press), 465–570.

Conry, M. J. (1987). *Soils of Co. Laois. National Soil Survey of Ireland, Soil Survey Bulletin No. 41*. Dublin, Ireland: An Foras Talúntais.

Cowan, N., Maire, J., Krol, D., Cloy, J. M., Hargreaves, P., Murphy, R., et al. (2020). Agricultural soils: A sink or source of methane across the British Isles? *Eur. J. Soil Sci.* 72, 1842–1862. doi:10.1111/ejss.13075

CTIC (2004). *National Survey of Conservation Tillage Practices*. West Lafayette: Conservation Technology Information Center., IN. http://www.ctic.purdue.edu/CTIC/CRM.html.

Davies, D. B., and Finney, J. B. (2002). "Reduced cultivations for cereals: research, development and advisory needs under changing economic circumstances," in *Home Grown Cereals Authority Review*, 48. Available from: http://cereals.adhb.org.uk/media/288079/rr48.

Degenhardt, D. F., and Kondra, Z. P. (1981). The influence of seeding date and seeding rate on seed yield and yield components of five genotypes of Brassica napus. *Can. J. Plant Sci.* 61 (2), 175–183. doi:10.4141/cjps81-027

Diepenbrock, W. (2000). Yield analysis of winter oilseed rape (Brassica napus L.): a review. *Field Crops Res.* 67 (1), 35–49. doi:10.1016/S0378-4290(00)00082-4

Dobbie, K. E., McTaggart, I. P., and Smith, K. A. (1999). Nitrous oxide emissions from intensive agricultural systems: variations between crops and seasons, key driving variables, and mean emission factors. *J. Geophys. Res.* 104 (D21), 26891–26899. doi:10.1029/1999JD900378

Drewer, J., Finch, J. W., Lloyd, C. R., Baggs, E. M., and Skiba, U. (2012). How do soil emissions of N2O, CH4 and CO2 from perennial bioenergy crops differ from arable annual crops? *Glob. Change Biol. Bioenergy* 4 (4), 408–419. doi:10.1111/j.1757-1707.2011.01136.x

Flessa, H., Dörsch, P., and Beese, F. (1995). Seasonal variation of N2O and CH4fluxes in differently managed arable soils in southern Germany. *J. Geophys. Res.* 100 (D11), 23115–23124. doi:10.1029/95JD02270

Food and Agricultural Organization of the United Nations Corporate Statistical Database (FAOSTAT) (2021). Crops. Retrieved from https://www.fao.org/faostat/en/#data/QC.

Forristal, P., and Murphy, K. (2010). Crop establishment systems for winter oilseed rape. *Adv. Anim. Biosciences* 1 (1), 9. doi:10.1017/s2040470010001524

Fortin, M.-C., Rochette, P., and Pattey, E. (1996). Soil Carbon Dioxide Fluxes from Conventional and No-Tillage Small-Grain Cropping Systems. *Soil Sci. Soc. America J.* 60 (5), 1541–1547. doi:10.2136/sssaj1996.03615995006000050036x

Franzluebbers, A. J., Hons, F. M., and Zuberer, D. A. (1995). Tillage-induced seasonal changes in soil physical properties affecting soil CO2 evolution under intensive cropping. *Soil Tillage Res.* 34 (1), 41–60. doi:10.1016/0167-1987(94)00450-S

Gan, Y., Liang, C., Huang, G., Malhi, S. S., Brandt, S. A., and Katepa-Mupondwa, F. (2012). Carbon footprint of canola and mustard is a function of the rate of N fertilizer. *Int. J. Life Cycle Assess.* 17 (1), 58–68. doi:10.1007/s11367-011-0337-z

Gebremichael, A., Orr, P. J., and Osborne, B. (2019). The impact of wetting intensity on soil CO2 emissions from a coastal grassland ecosystem. *Geoderma* 343, 86–96. doi:10.1016/j.geoderma.2019.02.016

Hénault, C., Devis, X., Lucas, J. L., and Germon, J. C. (1998). Influence of different agricultural practices (type of crop, form of N-fertilizer) on soil nitrous oxide emissions. *Biol. Fertil. Soils* 27 (3), 299–306. doi:10.1007/s003740050437

Hendrix, P., Han, C., and Groffman, P. (1988). Soil respiration in conventional and no-tillage agroecosystems under different winter cover crop rotations. *Soil Tillage Res.* 12 (2), 135–148. doi:10.1016/0167-1987(88)90037-2

Högberg, P., and Read, D. (2006). Towards a more plant physiological perspective on soil ecology. *Trends Ecol. Evol.* 21 (10), 548–554. doi:10.1016/j.tree.2006.06.004

Hütsch, B. W. (1998). Tillage and land use effects on methane oxidation rates and their vertical profiles in soil. *Biol. Fertil. Soils* 27 (3), 284–292. doi:10.1007/s003740050435

Jabro, J. D., Sainju, U., Stevens, W. B., and Evans, R. G. (2008). Carbon dioxide flux as affected by tillage and irrigation in soil converted from perennial forages to annual crops. *J. Environ. Manag.* 88 (4), 1478–1484. doi:10.1016/j.jenvman.2007.07.012

Jacinthe, P.-A., Dick, W. A., Lal, R., Shrestha, R. K., and Bilen, S. (2014). Effects of no-till duration on the methane oxidation capacity of Alfisols. *Biol. Fertil. Soils* 50 (3), 477–486. doi:10.1007/s00374-013-0866-7

Jacinthe, P.-A., and Lal, R. (2005). Labile carbon and methane uptake as affected by tillage intensity in a Mollisol. *Soil Tillage Res.* 80 (1-2), 35–45. doi:10.1016/j.still.2004.02.018

Jackson, L. E., Calderon, F. J., Steenwerth, K. L., Scow, K. M., and Rolston, D. E. (2003). Responses of soil microbial processes and community structure to tillage events and implications for soil quality. *Geoderma* 114 (3-4), 305–317. doi:10.1016/S0016-7061(03)00046-6

Jans, W. W. P., Jacobs, C. M. J., Kruijt, B., Elbers, J. A., Barendse, S., and Moors, E. J. (2010). Carbon exchange of a maize (Zea mays L.) crop: Influence of phenology. *Agric. Ecosyst. Environ.* 139 (3), 316–324. doi:10.1016/j.agee.2010.06.008

Jeuffroy, M. H., Baranger, E., Carrouée, B., de Chezelles, E., Gosme, M., Hénault, C., et al. (2013). Nitrous oxide emissions from crop rotations including wheat, oilseed rape and dry peas. *Biogeosciences* 10 (3), 1787–1797. doi:10.5194/bg-10-1787-2013

Kaiser, E.-A., Kohrs, K., Kücke, M., Schnug, E., Heinemeyer, O., and Munch, J. C. (1998). Nitrous oxide release from arable soil: importance of N-fertilization, crops and temporal variation. *Soil Biol. Biochem.* 30 (12), 1553–1563. doi:10.1016/S0038-0717(98)00036-4

Keane, B. J., Ineson, P., Vallack, H. W., Blei, E., Bentley, M., Howarth, S., et al. (2018). Greenhouse gas emissions from the energy crop oilseed rape (Brassica napus); the role of photosynthetically active radiation in diurnal N2 O flux variation. *GCB Bioenergy* 10 (5), 306–319. doi:10.1111/gcbb.12491

Kern, J., Hellebrand, H. J., Gömmel, M., Ammon, C., and Berg, W. (2012). Effects of climatic factors and soil management on the methane flux in soils from annual and perennial energy crops. *Biol. Fertil. Soils* 48 (1), 1–8. doi:10.1007/s00374-011-0603-z

Kessavalou, A., Mosier, A. R., Doran, J. W., Drijber, R. A., Lyon, D. J., and Heinemeyer, O. (1998). Fluxes of Carbon Dioxide, Nitrous Oxide, and Methane in Grass Sod and Winter Wheat-Fallow Tillage Management. *J. Environ. Qual.* 27 (5), 1094–1104. doi:10.2134/jeq1998.00472425002700050015x

Kuai, J., Sun, Y., Zuo, Q., Huang, H., Liao, Q., Wu, C., et al. (2015). The yield of mechanically harvested rapeseed (*Brassica napus* L.) can be increased by optimum plant density and row spacing. *Sci. Rep.* 5, 18835. doi:10.1038/srep18835

Kuznetsova, A., Brockhoff, P. B., and Christensen, R. H. (2017). lmerTest package: tests in linear mixed effects models. *J. Stat. Softw.* 82 (13), 1–26. doi:10.18637/jss.v082.i13

La Scala, N., Jr, Bolonhezi, D., and Pereira, G. T. (2006). Short-term soil CO2 emission after conventional and reduced tillage of a no-till sugar cane area in southern Brazil. *Soil Tillage Res.* 91 (1-2), 244–248. doi:10.1016/j.still.2005.11.012

Lang, R., Goldberg, S. D., Blagodatsky, S., Piepho, H.-P., Hoyt, A. M., Harrison, R. D., et al. (2020). Mechanism of methane uptake in profiles of tropical soils converted from forest to rubber plantations. *Soil Biol. Biochem.* 145, 107796. doi:10.1016/j.soilbio.2020.107796

Leach, J. E., Stevenson, H. J., Rainbow, A. J., and Mullen, L. A. (1999). Effects of high plant populations on the growth and yield of winter oilseed rape (Brassica napus). *J. Agric. Sci.* 132 (2), 173–180. doi:10.1017/S0021859698006091

Lenth, R. (2019). emmeans: Estimated Marginal Means, aka Least-Squares Means. R package version 1.3.2. Available online at: https://CRAN.R-project.org/package=emmeans.

Li, G. D., Conyers, M. K., Schwenke, G. D., Hayes, R. C., Liu, D. L., Lowrie, A. J., et al. (2016). Tillage does not increase nitrous oxide emissions under dryland

canola (Brassica napus L.) in a semiarid environment of south-eastern Australia. *Soil Res.* 54 (5), 512–522. doi:10.1071/SR15289

Linn, D. M., and Doran, J. W. (1984). Effect of Water-Filled Pore Space on Carbon Dioxide and Nitrous Oxide Production in Tilled and Nontilled Soils. *Soil Sci. Soc. America J.* 48 (6), 1267–1272. doi:10.2136/sssaj1984.03615995004800060013x

Linquist, B., Groenigen, K. J., Adviento-Borbe, M. A., Pittelkow, C., and Kessel, C. (2012). An agronomic assessment of greenhouse gas emissions from major cereal crops. *Glob. Change Biol.* 18 (1), 194–209. doi:10.1111/j.1365-2486.2011.02502.x

Malhi, S. S., Lemke, R., Wang, Z. H., and Chhabra, B. S. (2006). Tillage, nitrogen and crop residue effects on crop yield, nutrient uptake, soil quality, and greenhouse gas emissions. *Soil Tillage Res.* 90 (1-2), 171–183. doi:10.1016/j.still.2005.09.001

Maynard, D. G., Kalra, Y. P., and Crumbaugh, J. A. (1993). Nitrate and exchangeable ammonium nitrogen. *Soil Sampl. Methods Anal.* 1, 25–33. doi:10.1080/1065657x.1993.10757875

Meade, C. V., and Mullins, E. D. (2005). "Gm Crop Cultivation in Ireland: Ecological and Economic Considerations," in *Biology and Environment: Proceedings of the Royal Irish Academy* (Ireland: Royal Irish Academy), 105, 33–52. doi:10.3318/bioe.2005.105.1.33

Merino, P., Artetxe, A., Castellón, A., Menéndez, S., Aizpurua, A., and Estavillo, J. M. (2012). Warming potential of N2O emissions from rapeseed crop in Northern Spain. *Soil Tillage Res.* 123, 29–34. doi:10.1016/j.still.2012.03.005

Miersch, S., Gertz, A., Breuer, F., Schierholt, A., and Becker, H. C. (2016). Influence of the Semi-dwarf Growth Type on Seed Yield and Agronomic Parameters at Low and High Nitrogen Fertilization in Winter Oilseed Rape. *Crop Sci.* 56 (4), 1573–1585. doi:10.2135/cropsci2015.09.0554

Minasny, B., Malone, B. P., McBratney, A. B., Angers, D. A., Arrouays, D., Chambers, A., et al. (2017). Soil carbon 4 per mille. *Geoderma* 292, 59–86. doi:10.1016/j.geoderma.2017.01.002

Moors, E. J., Jacobs, C., Jans, W., Supit, I., Kutsch, W. L., Bernhofer, C., et al. (2010). Variability in carbon exchange of European croplands. *Agric. Ecosyst. Environ.* 139 (3), 325–335. doi:10.1016/j.agee.2010.04.013

Morell, F. J., Álvaro-Fuentes, J., Lampurlanés, J., and Cantero-Martínez, C. (2010). Soil CO2 fluxes following tillage and rainfall events in a semiarid Mediterranean agroecosystem: effects of tillage systems and nitrogen fertilization. *Agric. Ecosyst. Environ.* 139 (1-2), 167–173. doi:10.1016/j.agee.2010.07.015

Morris, N. L., Miller, P. C. H., J.H.Orson, J. H., and Froud-Williams, R. J. (2010). The adoption of non-inversion tillage systems in the United Kingdom and the agronomic impact on soil, crops and the environment-A review. *Soil Tillage Res.* 108 (1-2), 1–15. doi:10.1016/j.still.2010.03.004

Mosier, A. R., Halvorson, A. D., Reule, C. A., and Liu, X. J. (2006). Net global warming potential and greenhouse gas intensity in irrigated cropping systems in northeastern Colorado. *J. Environ. Qual.* 35 (4), 1584–1598. doi:10.2134/jeq2005.0232

Myhre, G., Shindell, D., Bréon, F. M., Collins, W., Fuglestvedt, J., Huang, J., and Zhang, H. (2013). "Climate change 2013: the physical science basis," in *Contribution of Working Group I to the Fifth Assessment Report of the Intergovernmental Panel on Climate Change*. Editors M. Tignor, S. K. Allen, J. Boschung, A. Nauels, Y. Xia, V. Bex, and P. M. Midgley (Cambridge, United Kingdom and New York, NY, USA: Cambridge University Press).

Ogle, S. M., Alsaker, C., BaldockBernoux, J. M., Bernoux, M., Breidt, F. J., McConkey, B., et al. (2019). Climate and Soil Characteristics Determine where No-Till Management Can Store Carbon in Soils and Mitigate Greenhouse Gas Emissions. *Sci. Rep.* 9, 11665. doi:10.1038/s41598-019-47861-7

O'Neill, M., Gallego-Lorenzo, L., Lanigan, G. J., Forristal, P. D., and Osborne, B. A. (2020). Assessment of nitrous oxide emission factors for arable and grassland ecosystems. *J. Integr. Environ. Sci.* 17, 165–185. doi:10.1080/1943815X.2020.1825227

Osborne, B., Saunders, M., Walmsley, D., Jones, M., and Smith, P. (2010). Key questions and uncertainties associated with the assessment of the cropland greenhouse gas balance. *Agric. Ecosyst. Environ.* 139 (3), 293–301. doi:10.1016/j.agee.2010.05.009

Pausch, J., and Kuzyakov, Y. (2018). Carbon input by roots into the soil: quantification of rhizodeposition from root to ecosystem scale. *Glob. Change Biol.* 24 (1), 1–12. doi:10.1111/gcb.13850

Plaza-Bonilla, D., Cantero-Martínez, C., Bareche, J., Arrúe, J. L., and Álvaro-Fuentes, J. (2014). Soil Carbon Dioxide and Methane Fluxes as Affected by Tillage and N Fertilization in Dryland Conditions. *Plant Soil* 381 (1), 111–130.

Prajapati, P., and Jacinthe, P. A. (2014). Methane oxidation kinetics and diffusivity in soils under conventional tillage and long-term no-till. *Geoderma* 230-231, 161–170. doi:10.1016/j.geoderma.2014.04.013

Pribyl, D. W. (2010). A critical review of the conventional SOC to SOM conversion factor. *Geoderma* 156 (3-4), 75–83. doi:10.1016/j.geoderma.2010.02.003

Rajaniemi, M., Mikkola, H., and Ahokas, J. (2011). Greenhouse gas emissions from oats, barley, wheat and rye production. *Agron. Res.* 9, 189–195.

Rathke, G., Behrens, T., and Diepenbrock, W. (2006). Integrated nitrogen management strategies to improve seed yield, oil content and nitrogen efficiency of winter oilseed rape (Brassica napus L.): a review. *Agric. Ecosyst. Environ.* 117 (2-3), 80–108. doi:10.1016/j.agee.2006.04.006

Reicosky, D. C., and Archer, D. W. (2007). Moldboard plow tillage depth and short-term carbon dioxide release. *Soil Tillage Res.* 94 (1), 109–121. doi:10.1016/j.still.2006.07.004

Rochette, P., and Flanagan, L. B. (1997). Quantifying Rhizosphere Respiration in a Corn Crop Under Field Conditions. *Soil Sci. Soc. Am. J.* 61 (2), 466–474.

Rood, S. B., Major, D. J., and Charnetski, W. A. (1984). Seasonal changes in 14CO2 assimilation and 14C translocation in oilseed rape. *Field Crops Res.* 8, 341–348. doi:10.1016/0378-4290(84)90081-9

Roques, S. E., and Berry, P. M. (2016). The yield response of oilseed rape to plant population density. *J. Agric. Sci.* 154 (2), 305–320. doi:10.1017/S0021859614001373

Ruser, R., Fuß, R., Andres, M., Hegewald, H., Kesenheimer, K., Köbke, S., et al. (2017). Nitrous oxide emissions from winter oilseed rape cultivation. *Agric. Ecosyst. Environ.* 249, 57–69. doi:10.1016/j.agee.2017.07.039

Sainju, U. M. (2016). A global meta-analysis on the impact of management practices on net global warming potential and greenhouse gas intensity from cropland soils. *PloS one* 11 (2), e0148527. doi:10.1371/journal.pone.0148527

Schwenke, G. D., Herridge, D. F., Scheer, C., Rowlings, D. W., Haigh, B. M., and McMullen, K. G. (2015). Soil N2O emissions under N2-fixing legumes and N-fertilised canola: a reappraisal of emissions factor calculations. *Agric. Ecosyst. Environ.* 202, 232–242. doi:10.1016/j.agee.2015.01.017

Serrano-Silva, N., Sarria-guzmán, Y., Dendooven, L., and Luna-Guido, M. (2014). Methanogenesis and methanotrophy in soil: a review. *Pedosphere* 24 (3), 291–307. doi:10.1016/S1002-0160(14)60016-3

Shakoor, A., Shahbaz, M., Farooq, T. H., Sahar, N. E., Shahzad, S. M., Altaf, M. M., et al. (2021). A global meta-analysis of greenhouse gases emission and crop yield under no-tillage as compared to conventional tillage. *Sci. Total Environ.* 750, 142299. doi:10.1016/j.scitotenv.2020.142299

Sharratt, B. S., and McWilliams, D. A. (2005). Microclimatic and Rooting Characteristics of Narrow-Row versus Conventional-Row Corn. *Agron. J.* 97 (4), 1129–1135. doi:10.2134/agronj2004.0292

Sieling, K., and Kage, H. (2008). The potential of semi-dwarf oilseed rape genotypes to reduce the risk of N leaching. *J. Agric. Sci.*, 146(1), 77–84. doi:10.1017/S0021859607007472

Six, J., Ogle, S. M., Jay Breidt, F., Conant, R. T., Mosier, A. R., and Paustian, K. (2004). The potential to mitigate global warming with no-tillage management is only realized when practised in the long term. *Glob. Change Biol.* 10 (2), 155–160. doi:10.1111/j.1529-8817.2003.00730.x

Smith, K. A. (2017). Changing views of nitrous oxide emissions from agricultural soil: key controlling processes and assessment at different spatial scales. *Eur. J. Soil Sci.* 68 (2), 137–155. doi:10.1111/ejss.12409

Smith, P., Martino, Z., and Cai, D. (2007). "Agriculture," in *Climate change 2007: Mitigation. Contribution of Working Group III to the Fourth Assessment Report of the Intergovernmental Panel on Climate Change*. Editors B. Netz, O. R. Davidson, P. R. Bosch, R. Dave, and L. A) Meyer (Cambridge, UK and New York, NY, USA: Cambridge University Press), 497–540.

Soane, B. D., Ball, B. C., Arvidsson, J., Basch, G., Moreno, F., and Roger-Estrade, J. (2012). No-till in northern, western and south-western Europe: A review of problems and opportunities for crop production and the environment. *Soil Tillage Res.* 118, 66–87. doi:10.1016/j.still.2011.10.015

Suwanwaree, P., and Robertson, G. P. (2005). Methane Oxidation in Forest, Successional, and No-till Agricultural Ecosystems. *Soil Sci. Soc. Am. J.* 69 (6), 1722–1729. doi:10.2136/sssaj2004.0223

Thers, H., Abalos, D., Dörsch, P., and Elsgaard, L. (2020). Nitrous oxide emissions from oilseed rape cultivation were unaffected by flash pyrolysis biochar of different type, rate and field ageing. *Sci. Total Environ.* 724, 138140. doi:10.1016/j.scitotenv.2020.138140

Thers, H., Petersen, S. O., and Elsgaard, L. (2019). DMPP reduced nitrification, but not annual N2O emissions from mineral fertilizer applied to oilseed rape on a sandy loam soil. *GCB Bioenergy* 11 (12), 1396–1407. doi:10.1111/gcbb.12642

Tian, H., Yang, J., Xu, R., Lu, C., Canadell, J. G., Davidson, E. A., et al. (2019). Global soil nitrous oxide emissions since the preindustrial era estimated by an ensemble of terrestrial biosphere models: Magnitude, attribution, and uncertainty. *Glob. Change Biol.* 25 (2), 640–659. doi:10.1111/gcb.14514

Trumbore, S. (2000). Age of soil organic matter and soil respiration: radiocarbon constraints on belowground C dynamics. *Ecol. Appl.* 10 (2), 399–411. doi:10.1890/1051-0761(2000)010[0399:AOSOMA]2.0.CO;2

Ussiri, D. A. N., Lal, R., and Jarecki, M. K. (2009). Nitrous oxide and methane emissions from long-term tillage under a continuous corn cropping system in Ohio. *Soil Tillage Res.* 104 (2), 247–255. doi:10.1016/j.still.2009.03.001

van Groenigen, K. J., Hastings, A., Forristal, D., Roth, B., Jones, M., and Smith, P. (2011). Soil C storage as affected by tillage and straw management: An assessment using field measurements and model predictions. *Agric. Ecosyst. Environ.* 140 (1-2), 218–225. doi:10.1016/j.agee.2010.12.008

Vann, R. A., Reberg-Horton, S. C., and Brinton, C. M. (2016). Row spacing and seeding rate effects on canola population, weed competition, and yield in winter organic canola production. *Agron. J.* 108 (6), 2425–2432. doi:10.2134/agronj2016.02.0097

Vinzent, B., Fuss, R., Maidl, F.-X., and Hülsbergen, K.-J. (2018). N 2 O emissions and nitrogen dynamics of winter rapeseed fertilized with different N forms and a nitrification inhibitor. *Agric. Ecosyst. Environ.* 259, 86–97. doi:10.1016/j.agee.2018.02.028

Wagner-Riddle, C., and Thurtell, G. W. (1998). Nitrous oxide emissions from agricultural fields during winter and spring thaw as affected by management practices. *Nutrient Cycling in Agroecosystems* 52 (2), 151–163. doi:10.1023/A:1009788411566

Walter, K., Don, A., Fuß, R., Kern, J., Drewer, J., and Flessa, H. (2015). Direct Nitrous Oxide Emissions from Oilseed Rape Cropping–A Meta-Analysis. *Gcb Bioener.* 7 (6), 1260–1271.

Whipps, J. M. (1990). "Carbon economy," in *The Rhizosphere*. Editor J. M. Lynch (Chichester: Wiley), 59–97.

Widén, B., and Lindroth, A. (2003). A Calibration System for Soil Carbon Dioxide-Efflux Measurement Chambers. *Soil Sci. Soc. Am. J.* 67 (1), 327–334. doi:10.2136/sssaj2003.3270

Wynne, K., Neely, C. B., Adams, C., Kimura, E., DeLaune, P. B., Hathcoat, D., et al. (2020). Testing row spacing and planting rate for fall-planted spring canola in the southern United States. *Agron.j.* 112 (3), 1952–1962. doi:10.1002/agj2.20201

Zahoor, F., Forristal, D., and Gillespie, G. (2015). CropQuest: Minor Crops Report. *Teagasc.*

Zapata, D., Rajan, N., Mowrer, J., Casey, K., Schnell, R., and Hons, F. (2021). Long-term tillage effect on with-in season variations in soil conditions and respiration from dryland winter wheat and soybean cropping systems. *Sci. Rep.* 11 (1), 1–10. doi:10.1038/s41598-021-80979-1

Žurovec, O., Sitaula, B. K., Čustović, H., Žurovec, J., and Dörsch, P. (2017). Effects of tillage practice on soil structure, N2O emissions and economics in cereal production under current socio-economic conditions in central Bosnia and Herzegovina. *PloS one* 12 (11), e0187681. doi:10.1371/journal.pone.0187681

Conflict of Interest: The authors declare that the research was conducted in the absence of any commercial or financial relationships that could be construed as a potential conflict of interest.

Publisher's Note: All claims expressed in this article are solely those of the authors and do not necessarily represent those of their affiliated organizations, or those of the publisher, the editors and the reviewers. Any product that may be evaluated in this article, or claim that may be made by its manufacturer, is not guaranteed or endorsed by the publisher.

frontiers in Environmental Science

ORIGINAL RESEARCH
published: 16 September 2021
doi: 10.3389/fenvs.2021.710108

Assessment of Greenhouse Gases Emission in Maize-Wheat Cropping System Under Varied N Fertilizer Application Using Cool Farm Tool

Rakesh Kumar[1], S. Karmakar[2], Asisan Minz[1], Jitendra Singh[3], Abhay Kumar[2] and Arvind Kumar[1]*

[1]Department of Soil Science and Agricultural Chemistry, Birsa Agricultural University, Ranchi, India, [2]Department of Agronomy, Birsa Agricultural University, Ranchi, India, [3]Central Tasar Research and Training Institute, Ranchi, India

In recent decades, climate change induced by enhanced global warming is one of the biggest challenges at the global level. Agriculture sectors significantly contribute to total anthropogenic greenhouse gas emission to the atmosphere. Wheat and maize, cultivated globally, and consumed in different forms, are considered as crucial staple cereal for ensuring food security to global population. The management practices involving land preparation, sowing, fertilizer application, irrigation, pest management, etc. significantly influence the emission of carbon dioxide (CO_2) and nitrous oxide (N_2O) from agricultural soil. In this study, CO_2 and N_2O emission were assessed from maize and wheat crops at four different levels of N fertilizer using cool farm tool model. Emissions of CO_2 per hectare varied from 331.4 to 1,088.3 kgCO_2 in maize and ranged from 292.3 to 765.3 kgCO_2 in wheat on application of different doses of N. The total GHG emission in maize crops ranged from 859.5 to 3,003.4 kgCO_2 eq per hectare with the application of nitrogen at varying levels (0–240 kg N per hectare). The highest N_2O efflux (0.368 kg per ton) was observed at 240 kg N per hectare under wheat crop. The total on-farm emissions, through fertilizer production, account for about 33.7%, and emission of N_2O contributes only 65.9%, whereas pesticides account merely 0.4% under maize-wheat cropping. This study confirms that the direct emission of N_2O was totally dependent on N fertilizers application rate; however, the indirect emission was controlled by the fuels and energy consumption.

Keywords: maize, wheat, carbon dioxide, greenhouse gases, nitrous oxide, nitrogen fertilizer

OPEN ACCESS

Edited by:
Jahangeer A. Bhat,
Fiji National University, Fiji

Reviewed by:
Sandeep K. Malyan,
National Institute of Hydrology, India
Gopal Shukla,
Uttar Banga Krishi Viswavidyalaya, India

****Correspondence:***
Rakesh Kumar
rkssacbau@rediffmail.com

Specialty section:
This article was submitted to Interdisciplinary Climate Studies, a section of the journal Frontiers in Environmental Science

Received: *15 May 2021*
Accepted: *10 August 2021*
Published: *16 September 2021*

Citation:
Kumar R, Karmakar S, Minz A, Singh J, Kumar A and Kumar A (2021) Assessment of Greenhouse Gases Emission in Maize-Wheat Cropping System Under Varied N Fertilizer Application Using Cool Farm Tool. Front. Environ. Sci. 9:710108. doi: 10.3389/fenvs.2021.710108

INTRODUCTION

The production of food grains (maize, rice, wheat, etc.) is being adversely affected by climate change, and agricultural activities leading to emission of methane (CH_4), carbon di-oxide (CO_2), and nitrous oxide (N_2O) (Malyan et al., 2021) serve as a major contributing factor to future climate change. The main anthropogenic source of CH_4 (77%) and N_2O (60%) emissions contributes in Indian Agriculture (Sharma et al., 2021). Methane emissions are confined to rice and enteric fermentation (Kumar et al., 2020b), while CO_2 and N_2O are uniformly released from all agricultural crops as consequences of crop raising activities such as soil manipulation and fertilizer applications (Kumar et al., 2016a; Kumar et al., 2016b; Bhattacharyya et al., 2018; Sapkota et al., 2021). The addition of nitrogen to agricultural soil changes GHG fluxes. Since

1960, consumption of nitrogen fertilizer has increased 66 times (Fagodiya et al., 2020a). In India, the use of irrational nutrient applications has resulted in low input use efficiency, lower income, and enhanced pollution (Pampolino et al., 2012). In India, fertilizer recommendation is based on response of a crop over a broad geographical area which could not concede the spatial variation in soil nutrient supplying ability (Majumdar et al., 2013). It is a well known fact that aeration, soil temperature, soil moisture, organic carbon (OC) supplies, fertilization, pH, and other environmental factors like production and transport influence N_2O and CO_2 emission in soil (Kumar and Sharma, 2017a; Kumar et al., 2020a; Fagodiya et al., 2020a).

In general, nitrogen is the most critical and limiting nutrient in agricultural production. The global consumption of nitrogen fertilizer has increased from 12 Tg (1960) to 113 Tg (2010) (Fagodiya et al., 2017). Moreover, the main components of nitrogen cycle are nitrification, assimilation, ammonification, and denitrification (Kumar et al., 2016b; Kumar and Sharma, 2017a; Kumar and Sharma, 2017b). Several compounds like NH_3, NOx, NO, N_2O, NO_3 etc. could be released into the atmosphere during the nitrogen cycle, influencing the climate system. The reactive nitrogen (Nr) plays direct and indirect roles on N_2O emissions in soil. N_2O emissions are of major concern because of their extensive atmospheric lifespan (approx. 116 years), maximum potential of global warming (310 times that of CO_2), and high global climate change potential (290 on a100–year basis) (Fagodiya et al., 2020a). N_2O emissions can occur both directly and indirectly from fertilizer N input to the soil. Additional fertilizer N application to the same soil is referred as direct emissions (Holka and Bienkowski, 2020). Indirect N_2O emissions are those that occur from the different sources except soil that should not be limited, like N_2O generated through waters and leaching of NO3 to the soil (IPCC, 2006). Farms and horticultural enterprises account for just about 8% CO_2 emission. N_2O and CH_4 are important GHG which contribute 57% and 35%, respectively, to global warming (FAS, 2014). N_2O is a potent GHG that contributes directly to global warming. For a period of 100 years, N_2O emissions were more sensitive than other GHG because of its long atmospheric habitation (114 years), global climate change potential (290 times higher than CO_2), and global warming potential (265 times higher than CO_2). All these gases contribute as the third most abundant GHG after CO_2 and CH_4. Approx. 18.09% of total GHG and 73.29% of total N_2O were emitted from the agricultural sector in India during 2014. The use of nitrogen fertilizer fulfills the demand of food production considering the growing population, resulting in higher N_2O emissions from the country's agriculture.

Maize is an aerobic crop and unlike rice, puddling or submergence is not required for its cultivation. As a result, less energy is needed for tillage operation as well as less water is required for maize, resulting in fewer CH_4 emissions in comparison to rice fields. Hence, maize is a better option for minimizing ground water depletion, soil degradation, and CH_4 emissions from the Eastern plateau region of India. Maize, the third most important cereal crop, contributes 78.2 million tons to world total food grain production with an area of about 150 million hectares (McCann, 2007; Parihar et al., 2011). India is producing 30.41 million tons from 9.1 million hectares (mha) area with a productivity of 2,771 $kgha^{-1}$ (USDA, 2019). Maize-wheat cropping system ranked third after rice-wheat and rice-rice cropping systems (Jat et al., 2014). Consequently, wheat can be grown in a variety of climates around the world, covering more than 200 mha. The estimated production of the world crossed 750 million metric tons in 2016–17. India contributed 87 million metric tons from 30.22 mha area in 2016–17, core production of wheat (98.5 million ton) was registered from 30.72 mha in 2017–18, and a forecast of reduction in production in 2018–19 was estimated to 94 million metric ton (USDA, 2018) suggesting a degree of uncertainty in production level. Being less CH_4 gas emitter, maize-wheat is appealing as an alternative cropping system compared to rice-wheat system. Most of the studies conducted on mitigation of GHG emission in eastern plateau region of India are mainly based on rice-wheat cropping system. The N_2O emissions from MWR have rarely been reported. The GHG emissions associated with the manufacture of synthetic N fertilizers were estimated to be 41.44 and 59.71 Mt CO_2-eq $year^{-1}$ for wheat and maize in China, respectively. And the direct N_2O emissions derived from synthetic N fertilization were estimated to be 35.82 and 69.44 Gg N_2O $year^{-1}$ for wheat and maize, respectively (Chai et al., 2019). The carbon sequestration under maize-wheat cropping system provides promising prospects for reducing GHG emission. GHG emission can be measured with the help of Cool Farm Tool (Hillier et al., 2011) which has been defined as an empirical GHG quantification model into a single tool. Cool farm tool (CFT) enables the user to make choices appropriate to existing practices. The CFT is open-source software integrating several globally determined empirical models into a GHG emission calculator. At farm level, the tool identifies context-specific factors like pedo-climatic characteristics, output inputs, and other management activities that affect GHG emission. The Cool Farm Tool (CFT) calculates the total emission of GHG in terms of "per unit area" as well as "per unit product." The key objective of this study is to estimate the CO_2 and N_2O emission under maize-wheat cropping system at four different levels of N fertilizer application and three modes of application, by using the CFT model as the direct measurement to GHG emission.

MATERIALS AND METHODS

Description of Research Site

The research programme was carried out during 2015–16 and 2016–17 at the research farm of Ranchi Agriculture College under Birsa Agricultural University, Ranchi, under Maize-Wheat cropping system (**Figure 1**). The research field was located at 23°19' N and 83°17' E, at altitude of 625 m above mean sea level (MASL) in the Chhotanagpur Plateau, which comes under the eastern section of the Deccan plateau and situated under Agro-climatic Zone V.

The climate of state is falling under tropical and sub-tropical. During the summer season temperatures varied from 18 to 40°C, while during the winter, temperatures ranged from 0 to 22°C. The lowest temperature was recorded in the months of December and January; in some areas of Kanke sometimes the temperature

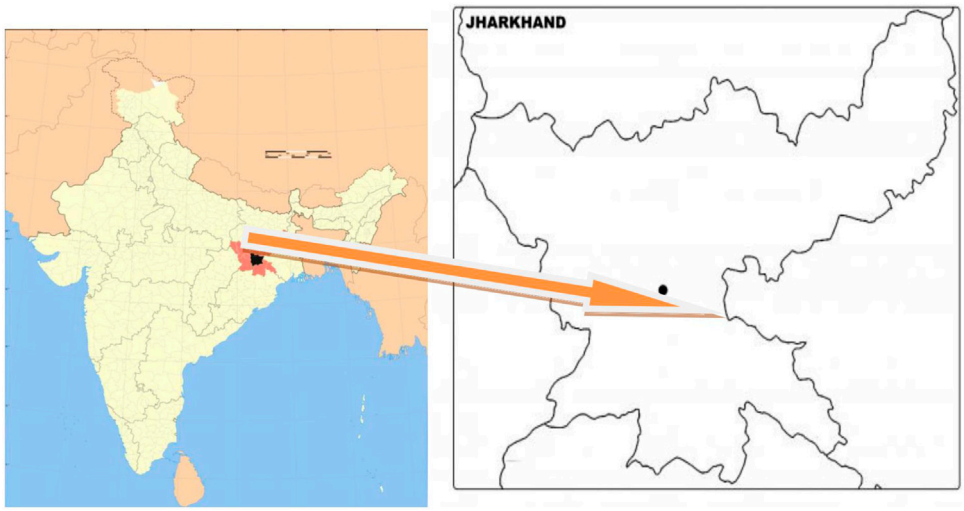

FIGURE 1 | Experimental site under study.

TABLE 1 | Treatments details of maize and wheat crop.

Treatments	Treatments details for maize/wheat	Application schedule for maize	Application schedule for wheat
N1	0/0 kg N	S1 (33/33/33 at basal, V4 and V10)	S1 (33/33/33 at basal, Crown root initiation) Stage (CRI), Panicle Initiation stage (PI)
N2	80/50 kg N (33-33-33)	S2 (33/33/33 (LCC)at basal, V4 and V10)	S2 (33/33/33 LCC) At basal, CRI and PI stage)
N3	160/100 kg N (33-33-33)	S3 (50-0-50 at basal and V10)	S3 (50-50 at basal and CR I stage)
N4	240/150 kg N (33-33-33)		
N5	0/0 kg N		
N6	80/50 kg N (33-33-33 LCC)		
N7	160/100 kg N (33-33-33 LCC)		
N8	240/150 kg N (33-33- 33LCC)		
N9	0/0 kg N		
N10	80/50 kg N (50-0-50)		
N11	160/100 kg N (50-0-50)		
N12	240/150 kg N (50-0-50)		

Note: LCC-Leaf Color Chart and CRI-Crown Root Initiation and PI-Panicle Initiation stage.

dipping down to the freezing point. The annual total rainfall received by the experimental areas is about 1,430 mm (56.34 inches) and 78–91% rainfall is received during the peak period of monsoon through South West Monsoon (from June to September). The rest is received in different seasonal spells like North East Monsoon (6.5% with amount 92.4 mm) from October to December. In the winter season, it received 3.74% with amount 52.4 mm (January to February) and summer 7.5% with the amount 104.7 mm with thunderstorm showers. During the maize growing season, total rainfall was about 528 mm, with average temperatures ranging from 20.3 to 30.80°C; however, rainfall was around 47 mm, with temperatures ranging from 3.10 to 39.50°C during the wheat cropping season. From the second week of February to the first week of March 2016, the highest average morning relative humidity was 87%, and the lowest average evening relative humidity was 31% in the third week of March.

Treatments and Cropping Systems

This experiment consisted four levels of nitrogen application (0, 80, 160, 240 kg Nha^{-1} for maize and 0, 50, 100, 150 kg Nha^{-1} for wheat) with three different modes of application. Methods of application of nitrogen were two splits (50-0–50 kg ha^{-1}) at basal and V10 stages, three splits (33-33-33 $kgha^{-1}$) at basal, V4, and V10 stage and (33-33-33 on the basis of LCC), in case of wheat apply as basal, and at CRI stage (50-0-50), basal, CRI, and PI stage (33-33-33). The phosphatic (single super phosphate) and potassic fertilizer (Murate of Potash) at the rate of 100 kgP2O5 and 100 kg K_2O^{-1}ha were applied as basal irrespective of treatments as shown in **Table 1**. The date of sowing of maize was 26/June 25, 2015/16 and date of harvesting was 05/October 6, 2015/16. However, the phosphatic and potassic fertilizer at 90 kgP2O5 and 80 kgK_2Oha^{-1} were applied as basal to all the treatment, and date of sowing were 10/December 11, 2015/16 and date of harvesting 12/April 13, 2016/17 respectively.

Methods Used for Calculating CO_2 Emission From Farm Operation

The emission of CO_2 from on farm and off farm through various activities like irrigation, tillage, fertilizer, and pesticide production are calculated from various published emission factors.

Irrigation

The emission of CO_2 after irrigation was calculated at 30% electric pump efficiency (Nelson et al., 2009; Gupta et al., 2015) and 19% electric power transmission and distribution losses in India (World Bank, 2014) by the following formula:

$$CO_2 - C\,(irrigation)\,(kgC/ha) = [amount\ of\ irrigation\ water\ applied\,(m^3/ha)] \times [2.724/1000] \times [Groung\ water\ depth\,(m)] \times [100/pump\ efficiency\,(\%)] \times [100/power\ loss\ in\ transmission\,(\%)]\ ^{*}0.4062 \quad (1)$$

where 2.724 is energy (kWh) needed to lift 1,000 m^3 of water from 1 m depth without any loss in pump efficiency and 0.4062 is carbon density (kgC per kWh) of coal-based electricity generation (Nelson et al., 2009).

Tillage and Sowing

Two tillage operations were conducted and CO_2 emission was calculated as per Gupta et al. (2015).

$$CO_2 - C\,(tillage)\,(kgc/ha) = duration\ of\ tractor\ operation\,(hour/ha) \times diesel\ consumption\ rate\ (liter/hour) \times 0.728 \quad (2)$$

where 0.728 is CO_2-C emissions (kg) from consumption of 1 L diesel (EPA 2005).

Pesticide Production and Transportation

The CO_2 emission from pesticide production and transportation was calculated from the following equation

$$CO_2 - C\,(kgC/ha) = Herbicide\,(kg/ha) \times 6.3 + Insecticide\,(kg/ha) \times 5.1 + fungicide\,(kg/ha) \times 3.9 \quad (3)$$

where 6.3, 5.1, and 3.9 is amount of CO_2-C emitted from production and transportation of 1 kg of herbicide, insecticide, and fungicide respectively (Lal, 2004).

Fertilizer Production and Transportation

The CO_2 emission from fertilizer production and transportation was calculated from the following equation

$$CO_2 - C\,(kg/ha) = Amount\ of\ N\ applied\ by\ urea\,(kg/ha) \times 2.02 + Amount\ of\ N\ applied\ by\ DAP\,(kg/ha) \times 1.84 + Amount\ of\ P_2O_5\ applied\ by\ SSP\,(kg/ha) \times 0.06 + Amount\ of\ K_2O\ applied\ by\ MOP\,(kg/ha) \times 0.25 \quad (4)$$

where 2.02, 1.84, 0.06, and 0.25 is CO_2-C emission (kg) from the production and transport of 1 kg of N (urea), N (DAP), P2O5(SSP), and K2O (MOP) adopted from Kool et al., 2012.

RESULTS AND DISCUSSION

Carbon Dioxide Emission

CO_2 emitted by maize grown during the wet season emission ranged from 331.4 to 1,088.1 kg ha^{-1}, while in wheat (winter season) it varied from 292.3 to 765.3 kg ha^{-1} depending on the application rates of nitrogen fertilizer (**Table 2**). The mean value of emitted CO_2 was 1,088.1 kgha^{-1}, when maize received 240 kg N ha^{-1}, while 836.0 kg CO_2 ha^{-1} was released at 160 kg N ha^{-1}. However, the emission of CO_2 was lowest at a level of 0 kg N (331.4 kg CO_2 ha^{-1}). During the winter season, the highest CO_2 emission (765.3 kg CO_2 ha^{-1}) was recorded at 150 kg N ha^{-1}, followed by 100 kg N ha^{-1} (613.7 kg CO_2ha^{-1}). At 50 kg level of N fertilizer application, the emission was 456.0 kg CO_2ha^{-1}, that was 35.9% higher than that of the emission noted at 0 kg level (292.3 kg CO_2ha^{-1}). Soil manipulation like tillage triggers CO_2 emission through biological decomposition of soil organic matter (SOM) acts as the primary source of CO_2 from agriculture field. Disintegration of soil aggregates through ploughing increases oxygen availability and facilitates organic matter (OM) decomposition of exposed organic material (Bhattacharyya et al., 2018). Other sources of CO_2 emissions include the fuel used for various agricultural activities and the burning of crop residues (Gupta et al., 2015). Carbon dioxide production at the time of manufacturing of fertilizers and pesticides is an off-site source (Pathak et al., 2010; Pathak et al., 2016).

Nitrous Oxide Emission

Emission of N_2O from the soil occurs as a result of additional nitrogenous fertilizer application to the soil (within a defined boundary of producer's field) referred as direct emissions (Sharma, 2020). N_2O gas emission emitted off-site (beyond the boundary) are referred as indirect emissions, which do not include N_2O gas produced through receiving runoff water and NO3 leaching in soil (Fagodiya et al., 2019). Nutrient management strategies had a significant impact on the amount of N_2O gas released per hectare and per ton of crop yield. Different rates of nitrogen application showed a major impact during the estimation of N_2O emission per hectare in both crops (maize and wheat). In maize, application of 160 kg N ha^{-1} estimated higher N_2O emission (4.3 kg N_2O ha^{-1}) compared to 80 kg N ha^{-1} (2.8 kg N_2O ha^{-1}). However, calculated N_2O emission was highest with N at 240 kg N ha^{-1} (6.5 kg N_2O ha^{-1}) and lowest value of 1.8 kg N_2O ha^{-1} at 0 kg N ha^{-1} (**Table 2**). The same pattern of emission was not followed in case of emissions per ton of maize yield than per hectare. That might be directly associated to the crop yield, while per hectare value is preferably reliant on yield, fertilizer doses, and other factors influencing crop production. The calculated value of nitrous oxide emission per ton of maize yield was lower (0.27 kg $tonne^{-1}$) at application of 160 kg N than that of 240 kg N ha^{-1} applied plot (0.37 kgton^{-1}). The highest value was observed with the produce recorded at N omitted plot (0.94 kg ton^{-1}). The calculated N_2O emission per tone was 0.28 kg ton^{-1} at 80 kg N ha^{-1} that was marginally higher than the 160 kg N ha^{-1} applied plot (0.27 kg $tonne^{-1}$) (**Table 2**). This has been found and reported that N inputs gradient in

TABLE 2 | Response of various doses of nitrogen treatments on GHG emission (maize–wheat cropping system).

Dose of nitrogen (kg ha^{-1})	Maize						Wheat					
	CO_2 (kg ha^{-1})	CH_4 (kg ha^{-1})	N_2O		Total emission		CO_2 (kg ha^{-1})	CH_4 (k gha^{-1})	N_2O		Total emission	
			(kg ha^{-1})	(kg ton^{-1})	(kg CO_2 eq ha^{-1})	(kg CO_2 eq ton^{-1})			(kg ha^{-1})	(kg ton^{-1})	(kg CO_2 eq ha^{-1})	(kg CO2 eq ton^{-1})
N1 (0/0 kg N)	331.4	0	1.8	0.94	859.5	450.0	292.3	0	1.8	0.63	820.4	287.5
N2 (80/50 kg N)	583.7	0	2.8	0.28	1,417.1	143.9	456.0	0	2.7	0.29	1,243.7	135.6
N3 (160/100 kg N)	836.0	0	4.3	0.27	2109.1	132.5	613.7	0	3.5	0.28	1,650.2	133.7
N4 (240/150 kg N)	1,088.3	0	6.5	0.37	3003.4	170.3	765.3	0	4.1	0.31	1974.1	148.0

row-crop agriculture directly dependent to the emissions of N_2O with different rate of nitrogenous fertilizer (Halvorson et al., 2008; Hoben et al., 2010; Millar et al., 2010). Application of increased nitrogen dose to the soil enhanced N_2O emissions in both of crops. The latest IPCC (2006) greenhouse gas inventory calculations are based on many factors, like heat, structure, water holding capacity, and organic matter content of the soil, and these are directly responsible for the rise in N_2O emissions. In general, management of crop residues and fertilizer application are major responsible factors for theN_2O pollution in agro-ecosystems (Rochette et al., 2008). The estimated value of N_2O emission per hectare in the case of wheat grown with 150 kg N ha^{-1} during winter season was maximum 4.1 kg ha^{-1}, followed by 100 kg N ha^{-1} (3.5 kg N_2O ha^{-1}). The lowest value (1.8 kg N_2O ha^{-1}) was recorded with the omission of nitrogenous fertilizer. On the other hand, in terms of N_2O emission per ton in wheat was highest (0.63 kg tonne^{-1}) under the N-omitted plot (0 kg N ha^{-1}), followed by the application of 150 kg N ha^{-1} (0.31 kg ton^{-1}), and the lowest value (0.28 kg tonne^{-1}) was recorded with the application of 100 kg N ha^{-1}. It may be concluded that the variation in NO2 emission per ton is due to the variation in yield and urea application. Jain et al. (2016) recorded that factor of N_2O emission varied from 0.48 to 0.58% and 0.40–0.46% in wheat and maize crops, respectively whereas, Bhatia et al. (2005) noted emission factor of 0.58–0.62% with the application of N fertilizers. Moreover, as per IPCC (2014) the default coefficient factor of nitrous oxide emission for N fertilizers was 1%.

Methane Emission

With removal of crop residues from the field at the time of tillage operation before sowing of maize and wheat, no methane gas emission was observed by using the CFT model. Soil CH_4 production is reliant on a limited supply of oxygen (anaerobic condition), which is regulated by moisture content of soil. Sowing of wheat in dry soil during winter (devoid of submerged condition) may be one of the key factors which suppressed the methane gas emission (Aryal et al., 2015).

Total Greenhouse Gas Emission

Maize

Global warming potential (GWP) per hectare for total GHG emission and CO_2-equivalent (CO_2-eq) per ton of crop yield positively varied at various level of nitrogen application (**Table 2**). The extent of total GHG emissions in maize contributed from 859.5 to 3,004 kg CO_2 eq ha^{-1}, depending on the doses of N fertilizers at 0 kg N ha^{-1}–240 kg N ha^{-1}. Emissions of gases increased with the escalating amount of nitrogen fertilizer. The application of 240 kg N ha^{-1} resulted in the highest GHG emission, followed by 160 kg N ha^{-1} (2,109.1 kg CO_2eq ha^{-1}) and at 0 kg N ha^{-1} resulted the lowest emission (859.5 kg CO_2eq ha^{-1}). While the emission of gases at the rate of 80 kg N ha^{-1} was 1,417.1 kg CO_2 eq ha^{-1}, it was marginally inferior to the use of 160 kg Nha^{-1}. The availability of mineral affected the enormity of N_2O emissions throughout the crop growth. Under the control scenario, the overall predictable GHG emission in terms of CO_2eqton^{-1} of product was considerably higher compared to the supplementary

TABLE 3 | Response of various level of nitrogen application on GHG emission (kg ha^{-1}) from various sources of farm (maize-wheat cropping system).

Dose of nitrogen (kg ha^{-1})	Fertilizer production (kg ha^{-1})	Direct and indirect N2 production (kg ha^{-1})	Pesticides production (kg ha^{-1})	Fertilizer production (kg ha^{-1})	Direct and indirect N2 production (kg ha^{-1})	Pesticides production (kg ha^{-1})
N1 (0/0 kg N)	1,392	528	21	1,253	850	20.5
N2 (80/50 kg N)	1,669	1,661	21	1,426	1720	20.5
N3 (160/100 kg N)	1946	3914	21	1,599	3083	20.5
N4 (240/150 kg N)	2223	8920	21	1772	5316	20.5

TABLE 4 | Correlation among yield, total GHG emission, and various soil properties (maize).

	Yield (qha^{-1})	GHG (kg CO_2 eqha^{-1})	pH	Org. C (g kg^{-1})	Av. N (kg ha^{-1})	Av. P (kg ha^{-1})	Av. K (kg ha^{-1})
GHG (kg CO2 eq ha^{-1})	0.832**	—	—	—	—	—	—
pH	–0.192^{NS}	–0.319^{NS}	—	—	—	—	—
Org. C (g kg^{-1})	0.052^{NS}	0.025^{NS}	0.506^{NS}	—	—	—	—
Av. N (kg ha^{-1})	–0.017^{NS}	–0.064^{NS}	–0.417^{NS}	–0.551^{NS}	—	—	
Av.P (kg ha^{-1})	–0.779**	–0.610*	–0.129^{NS}	–0.499^{NS}	0.234^{NS}	—	
Av.K (kg ha^{-1})	–0.940**	–0.749**	0.193^{NS}	–0.002^{NS}	–0.094^{NS}	0.739**	

TABLE 5 | Correlation among yield, total GHG emission, and various soil properties (wheat).

	Yield (q ha^{-1})	GHG (kg CO_2 eq ha^{-1})	pH	Org.C (g kg^{-1})	Av.N (kg ha^{-1})	Av.P (kg ha^{-1})	Av.K (kg ha^{-1})
GHG (kg CO2 eq ha^{-1})	0.889**	—	—	—	—	—	—
pH	–0.860**	–0.868**	—	—	—	—	—
Org. C (g kg^{-1})	0.262^{NS}	0.128^{NS}	–0.180^{NS}	—	—	—	—
Av. N (kg ha^{-1})	0.271^{NS}	0.197^{NS}	–0.207^{NS}	0.016^{NS}	—	—	—
Av. P (kg ha^{-1})	–0.739**	–0.730**	0.710*	–0.151^{NS}	–0.264^{NS}	—	—
Av. K (kg ha^{-1})	–0.649*	–0.770**	0.799**	0.038^{NS}	–0.395^{NS}	0.780**	—

TABLE 6 | Regression equation among different parameters (yield of maize and wheat with GHG emission, available P and K in soil, and various doses of nitrogen to GHG emission).

Crop	Parameters	Regression equation	R^2
Maize Grain yield	GHG emission	y = 104.79x + 505.71	0.7099**
	Available P	y = –0.611x + 115.73	0.609**
	Available K	y = –0.6536x + 154.82	0.8813**
Maize Nrate	GHG emission	y = 37.745x + 1054.1	0.9215**
	Grain Yield	y = 0.3032x + 12.072	0.9197**
Wheat Grain yield	GHG emission	y = 116.39x + 634.25	0.8053**
	Available P	y = –1.5956x + 178.3	0.5482**
	Available K	y = –1.0646x + 185.34	0.4243**
Wheat Nrate	GHG emission	y = = 32.677x + 1742.5	0.9319**
	Grain Yield	y = 0.2512x + 11.809	0.9267**

treatments. Application of different doses of nitrogen (0, 80, 160, and 240 kg N ha^{-1}) in maize emits 450.0, 143.9, 132.5, and 170.3 kg CO_2 eqton^{-1}, respectively.

Wheat

The amount of produced total GHG followed the same trend per ha and per tons maize, with a lower magnitude. The application of nitrogen at150 kg ha^{-1} had the highest GHG emission per ha (1974.1 kg CO_2 eq), subsequently with the addition of 100 kg N ha-1 released 1,650.2 kg CO_2 eq per hectare and omission of N fertilizer (0 kg N) showed 820.2 kg CO_2 eq per hectare (**Table 2**). Because of variation in wheat yield, the total anticipated GHG emission with respect to CO_2eq ton-1 of produce was lowest at the rate of 100 kg N ha-1 (133.7 kg CO_2 eq ton-1) and the highest value 287.5 kg CO_2 eq ton-1 was at 0 kg N ha^{-1}. Total GHG emission varied marginally between the application of nitrogen at the rate of 100 kg ha-1 (133.5 kg CO_2 eq ton-1) and at 50 kg N per hectare (135.6 kg CO_2 eq ton-1), while the higher value 1,545 kg CO_2 eq ton-1 was found at the rate of 150 kg N ha^{-1}. The yield, biological produce, and rate of N application all affected the value of total emission of GHGs by using CFT. The findings showed that when a greater amount of input was used, the total emission was higher than that at lesser amount of input. Among various emission sources, manufacture and use of synthetic fertilizers was found to be the most important source of pollution at the farm level. Pesticides account for just 0.50% of total on-farm emissions in maize, while synthesis of fertilizer and emissions of nitrous oxide account for 32 and 67% as whole farm emissions, respectively. Whereas, in case of wheat, fertilizer production and nitrous oxide emissions showed 35 and 64% of emissions, respectively, and pesticides account for only 0.6 percent. GHG emission by the use of nitrogenous fertilizer was split into two categories as intended towards N_2O emissions and GHG emission from fertilizer synthesizer unit. Nitrous oxide emissions

TABLE 7 | Response of various doses and time of nitrogen application on yield (q ha^{-1}) and harvest index.

Nitrogen rate (kg ha^{-1})	Maize			Wheat		
	Grain yield (q ha^{-1})	Straw yield (q ha^{-1})	Harvest index (%)	Grain yield (q ha^{-1})	Straw yield (q ha^{-1})	Harvest index (%)
N1(0 kg N)	5.80	13.37	31.90	9.04	19.50	31.53
N2(80/50 kg N)	40.20	58.26	40.68	28.18	63.55	30.85
N3(160/100 kg N)	71.69	87.39	45.20	41.97	81.44	34.01
N4 (240/150 kg N)	76.08	100.30	43.09	45.92	87.46	34.60
CD (0.05)	4.929	8.154	6.57	3.97	7.53	NS
Napplication Timing						
S1 (33/33/33)	48.30	63.10	40.48	31.70	61.09	33.60
S2 (33/33/33LCC)	49.09	67.16	39.47	31.61	68.21	31.45
S3 (50-0-50)	47.98	64.37	40.72	30.52	59.66	33.19
CD (0.05)	NS	NS	NS	NS	6.52	NS
CV%	10.35	12.78	16.61	12.91	12.14	9.75

could occur from microbial activities in soils too (**Table 3**). In agriculture, the mineralization process of nitrogen (ammonium to nitrates and the reduction of nitrate to gaseous form of nitrogen) plays an important role for N_2O production (Granli and Bockman 1994). N_2O emission is accounting for approximately 57% of total annual global GHG emission (IPCC, 2006). During synthesis of chemical fertilizers such as ammonia, phosphoric acid, and nitric acid, all emit greenhouse gases (Kongshaug, 1998). In maize and wheat, the regression analysis for yield and fertilizer doses indicated substantial variation in yield with respect to fertilizer doses (R2 value of 0.91 and 0.92, respectively).

Correlation Matrix

Maize

Correlation coefficient(r) among yield, total GHG emission, and various soil properties were presented in **Table 4**. Yield was positively correlated with GHG emission ($r = 0.832^{**}$) and negatively correlated with available P and K (-0.779^{**} and -0.940^{**}, respectively). Available P content in soil had negative relationship with GHG emission ($r = -0.610^{*}$) while positively correlated with yield ($r = 0.739^{**}$). Available K was significantly and negatively correlated with GHG emissions (-0.749^{**}) and yield (-0.940^{**}).

Wheat

Coefficient (r) values in wheat were illustrated in **Table 5**, with respect to produce and different variables. It was observed that yield had significant and positive association with GHG emission ($r = 0.889^{**}$). Available P and available K showed significant and negatively correlation with yield ($r = -0.739^{**}$ and -0.649^{*}) and GHG (-0.730^{**} and -0.770^{**}). The correlation coefficient among soil pH, yield ($r = -0.860^{**}$), and GHG emission ($r = -0.868^{**}$) was calculated and observed to be a significant and negative correlation, thus it could be stated that increased amounts of N application increases the amount of yield and GHG emission. Similarly, soil's available P registered a significant and negative correlation with GHG emission ($r = -0.730^{**}$), which had a positive "r" value with pH ($r = 0.710^{*}$). Soil available K was found to have a negative relation with GHG emission ($r = -0.770^{**}$), and positively correlated with available P ($r = 0.780^{**}$) and pH ($r = 0.799^{**}$).

The fertilizer recommendation and GHG emission mitigation for the entire cropping system may be given by using the prediction equation with soil test value estimated after harvesting of crops and GHG emission. In derived equations, the relationships are among GHG emission, soil properties after harvest, applied fertilizer quantity, and yield of maize and wheat (**Table 6**). These equations yielded R^2 values significant at 5% of important parameters. Such can be used for prediction of GHG emission, yield of crop, and status of available P and K after crop harvest can be predicted using regression equations and accordingly, optimum fertilizer recommendation can be made with the perspective of environment (Verma and Singh, 1991; Bera et al., 2006). **Table 7** stated that split application of N at 160 kg ha^{-1} to maize (basal, knee high, and tasseling stage) along with 100 kg P2O5 + 100 kg K2O ha^{-1} as basal and split application of N at 100 kg ha^{-1} to wheat (basal, crown root initiation, and panicle initiation stage) along with 90 kg P2O5 + 80 kg K2O ha^{-1} as basal could be the most effective in terms of yield (71.76 and 41.97 qha^{-1}, respectively, **Table 7**), GHG emission (2,109.1 and 1,650.2 $kgCO_2$ eq ha^{-1}, respectively), economic benefit, and available nutrient status of soil.

CONCLUSION

Direct measurement of the GHG is comparatively costlier. The GHG measurement through modeling provides not only the economic options, but variation of the key controlling factors can also be used to trap the minute changes in the GHG effluxes. Therefore, the present investigation is an attempt to utilize the Cool Farm Tool to optimize the N fertilizers and its subsequent effect on the GHG effluxes. In this study, greenhouse data (2015-16 and 2016-17) under maize-wheat cropping system was used to estimate CO_2 and N_2O emission from maize and wheat crops at four different levels of N fertilizer using cool farm tool model. Results stated that emissions of CO_2 per hectare varied from 331.4 to 1,088.3 kg in maize and 292.3–765.3 kg in wheat on application of different doses of N. The total GHG emission in maize crops ranged from 859.5 to 3,003.4 kg CO_2 eq per hectare with the application of nitrogen at varying levels (0–240 kg N per hectare). The highest N_2O efflux (0.368 kg per ton) was observed at 240 kg N per hectare under wheat crop. The total on-farm emissions, through fertilizer production, account for about

33.7%, and emission of N_2O contributes only 65.9%, whereas pesticides account for merely 0.4% under maize-wheat cropping. This study confirms that the direct emission of N_2O was totally dependent on N fertilizers application rate; however, the indirect emission was controlled by the fuels and energy consumption. This study establishes the efficacy of nutrient expert (N-management) rather make a prediction in implementing of site-specific nutrient management to smallholder production systems to enhance the crop yields and improve the increment of farmers' income considering to minimize GHG emission.

DATA AVAILABILITY STATEMENT

The original contributions presented in the study are included in the article/supplementary material, further inquiries can be directed to the corresponding author.

AUTHOR CONTRIBUTIONS

RK carried out the study and organized the field experiment wrote the first draft of the manuscript. SK performed statistical analysis in collaboration with AM and JS. RK compiled the raw data. AbK provided consultation on statistical analysis of N_2O emission data with consultation ArK. All authors are taken keen interest during the preparation of the manuscript.

ACKNOWLEDGMENTS

Authors are very much thankful to Director and Dy-Director IPNI (International Plant Nutrient Institute), South East Asia (India Programme), for providing financial assistance to BAU Ranchi, Jharkhand, India.

REFERENCES

Aryal, J. P., Sapkota, T. B., Jat, M. L., and Bishnoi, D. (2015). On-farmeconomicandenvironmental Impact of Zero Tillage Wheat: a Case of North-West India. *Exp. Agric.* 51, 1–16. doi:10.1017/S001447971400012X

Bera, R., Seal, A., Bhattacharyya, P., Das, T. H., Sarkar, D., and Kangjoo, K. (2006). Targeted Yield Concept and a Framework of Fertilizer Recommendation in Irrigated rice of Subtropical India. *J. Zhejiang Univ.* 7, 963–968. doi:10.1631/jzus.2006.B0963

Bhatia, A., Pathak, H., Jain, N., Singh, P. K., and Singh, A. K. (2005). Global Warming Potential of Manure Amended Soils under rice-wheat System in the Indo Gangetic plains. *Atmos. Environ.* 39, 76–84. doi:10.1016/j.atmosenv.2005.07.052

Bhattacharyya, R., Bhatia, A., Das, T. K., Lata, S., Kumar, A., Tomer, R., et al. (2018). Aggregate-associated N and Global Warming Potential of Conservation Agriculture-Based Cropping of maize-wheat System in the north-western Indo-Gangetic Plains. *Soil Tillage Res.* 182, 66–77. doi:10.1016/j.still.2018.05.002

Chai, R., Ye, Xinxin., Ma, Chao., Wang, Q., Tu, Renfeng., Zhang, L., et al. (2019). Greenhouse Gas Emissions from Synthetic Nitrogen Manufacture and Fertilization for Main upland Crops in China. *Carbon Balance Manage.* 14, 20. doi:10.1186/s13021-019-0133-9

EPA (2005). *Average Carbon Dioxide Emissions Resulting from Gasoline and Diesel Fuel.* EPA420-F-05-001February 2005.

Fagodiya, R. K., Pathak, H., Kumar, A., Bhatia, A., and Jain, N. (2017). Global Temperature Change Potential of Nitrogen Uses in Agriculture: a 50-year Assessment. *Sci. Rep.* 7, 1–8. doi:10.1038/srep44928

Fagodiya, R. K., Pathak, H., Bhatia, A., Jain, N., Gupta, D. K., Kumar, A., et al. (2019). Nitrous Oxide Emission and Mitigation from maize–wheat Rotation in the Upper Indo-Gangetic Plains. *Carbon Manag.* 10, 489–499. doi:10.1080/17583004.2019.1650579

Fagodiya, R. K., Pathak, H., Kumar, A., Bhatia, A., Jain, N., and Malyan, S. K. (2020a). Global Warming Impacts of Nitrogen Use in Agriculture: an Assessment for India since 1960. *Carbon Manag.* 11 (3), 291–301. doi:10.1080/17583004.2020.1752061

FAS (2014). *Reducing Emissions of Greenhouse Gases from Agriculture*. Technical Article. Feb2014.

Granli, T., and Bockman, O. C. (1994). Nitrous Oxide from Agriculture. *Norwegian J. Agric. Sci. Suppl.* 12, 128.

Gupta, D. K., Bhatia, A., Kumar, A., Chakrabarti, B., Jain, N., and Pathak, H. (2015). Global Warming Potential of rice (*Oryza Sativa*)-wheat (*Triticum aestivum*) Cropping System of the Indo-Gangetic Plains. *Indian J. Agric. Sci.* 85, 807–816.

Halvorson, A. D., DelGrosso, S. J., and Reule, C. A. (2008). Nitrogen, Tillage, and Crop Rotation Effects on Nitrous Oxide Emissions from Irrigated Cropping Systems. *J. Environ. Qual.* 37 (4), 1337–1344. doi:10.2134/jeq2007.0268

Hillier, J., Walter, C., Malin, D., Garcia-Suarez, T., Mila-i-Canals, L., and Smith, P. (2011). Afarm-focused Calculator for Emissions from Crop and Livestock Production. *Environ. Model Softw.* 26, 1070–1078. doi:10.1016/j.envsoft.2011.03.014

Hoben, J. P., Gehl, R. J., Robertson, G. P., Millar, N., and Grace, P. R. (2010). On-farm Nitrous Oxide Response to Nitrogen Fertilizer in Corn Cropping Systems. In review.

Holka, M., and Bienkowski, J. (2020). Carbon Footprint and Life-Cycle Costs of Maize Production in Conventional and Non-inversion Tillage Systems. *Agronomy* 10, 1877. doi:10.3390/agronomy10121877

IPCC (2006). *2006 IPCC Guidelines for National Greenhouse Gas Inventories, Prepared by the National Greenhouse Gas Inventories Programme*. Editors. Eggleston, L. Buendia, K. Miwa, T. Ngara, and K. Tanabe. Published: (Japan: IGES).

IPCC (2014). *Intergorvernmental Panel on Climate Change, Fifth Assessment Report Onclimatechange*. Cambridge: Cambridge University Press.

Jain, N., Arora, P., Tomer, R., Mishra, S. V., Bhatia, A., Pathak, H., et al. (2016). Greenhouse Gases Emission from Soils under Major Crops in North West India. *Sci. Total Environ.* 542, 551561. doi:10.1016/j.scitotenv.2015.10.073

Jat, M. L., Singh, B., and Gerard, B. (2014). Nutrient Management and Use Efficiency in Wheat Systems of South Asia. *Adv. Agron.* 129, 171–259. doi:10.1016/b978-0-12-800137-0.00005-4

Kongshaug, G. (1998). "Energy Consumption and Greenhouse Gas Emissions in Fertilizer Production," in IFATechnical Conference Marrakech Morocco.

Kool, A., Marinussen, M., and Blonk, H. (2012). "LCI Data for the Calculation Tool Feed Print for Greenhouse Gas Emissions of Feed Production and Utilization," in *GHG Emissions of N, P and K Fertilizer Production*. Editor B Consultants.

Kumar, A., and Kumar, M. (2020b). Estimation of Biomass and Soil Carbon Stock in the Hydroelectric Catchment of India and its Implementation to Climate Change. *J. Sustainable For.* 39 (6). doi:10.1080/10549811.2020.1794907

Kumar, A., and Sharma, M. P. (2017a). Estimation of Greenhouse Gas Emissions from Koteshwar Hydropower Reservoir, India. *Environ. Monit. Assess.* 189 (5), 240. doi:10.1007/s10661-017-5958-7

Kumar, A., and Sharma, M. P. (2017b). Estimation of Greenhouse Gas Emissions from Koteshwar Hydropower Reservoir, India. *Environ. Monit. Assess.* 189 (5), 240–261. doi:10.1007/s10661-017-5958-7

Kumar, A., Tomer, R., Bhatia, A., Jain, N., and Pathak, H. (2016a). "Greenhouse Gas Mitigation in Indian Agriculture," in *Climate Change and Agriculture Technologies for Enhancing Resilience*. Editors H. Pathak and B. Chakrabarti (New Delhi: ICAR-IARI), pp137–149.

Kumar, A., Sharma, M. P., and Kumar, A. (2016b). Greenhouse Gas Emissions from Hydropower Reservoirs: Policy and Challenges. *Int. J. Renew. Energ. Res.* 6 (2), 472–476.

Kumar, A., Sharma, M. P., and Yang, T. (2018). Estimation of Carbon Stock for Greenhouse Gas Emissions from Hydropower Reservoirs. *Stochastic Environ. Res. Risk Assess.* 32 (10), 3183–3319. doi:10.1007/s00477-018-1608-z

Kumar, A., Medhi, K., Fagodiya, R. K., Subrahmanyam, G., Mondal, R., Raja, P., et al. (2020a). Molecular and Ecological Perspectives of Nitrous Oxide Producing Microbial Communities in Agro-Ecosystems. *Rev. Environ. Sci. Biotechnol.* 19, 717–750. doi:10.1007/s11157-020-09554-w

Lal, R. (2004). Carbon Emission from Farm Operations. *Environ. Int.* 30, 981–990. doi:10.1016/j.envint.2004.03.005

Majumdar, K., Jat, M. L., Pampolino, M., Dutta, S., and Kumar, A. (2013). Nutrient Management in Wheat: Current Scenario, Improved Strategies and Future Research Needs in India. *J. Wheat Res.* 4, 1–10.

Malyan, S. K., Smita, S. K., Fagodiya, R. K., Ghosh, P., Kumar, A., Singh, R., et al. (2021). Biochar for Environmental Sustainability in the Energy-Water-Agroecosystem Nexus. *Renew. Sustainable Energ. Rev.* 149, 111379. doi:10.1016/j.rser.2021.111379

McCann, J. C. (2007). *Maize and Grace: Africa's Encounterwith a New World Crop*. Cambridge: Harvard University Press, 1500–2000.

Millar, N., Robertson, G. P., Grace, P. R., Gehl, R. J., and Rowlings, D. (2010). The Response of N_2O Emissions to Incremental Nitrogen Fertilizer Addition in winter Wheat. In review.

Nelson, G. C., Robertson, R., Msangi, S., Zhu, T., Liao, X., and Jawajar, P. (2009). Greenhouse Gas Mitigation Issues for Indian Agriculture. *IFPRID iscussion Paper00900*, 1–52.

Pampolino, M. F., Witt, C., Pasuquin, J. M., Johnston, A., and Fisher, M. J. (2012). Developmental Approach Ande Valuation of the Nutrient Experts Software for Nutrien T Management in Cereal Crops. *Comput. Electron. Agric.* 88, 103–110. doi:10.1016/j.compag.2012.07.007

Parihar, C. M., Jat, S. L., Singh, A. K., Hooda, K. S., Chikkappa, G. K., Singh, D. K., et al. (2011). *Maizeproductiontechnologiestechnicalbulletin2011/3*. NewDelhi: DirectorateofMaizeResearch, 36.

Pathak, H., Bhatia, A., Jain, N., and Aggarwal, P. K. (2010). "Greenhouse Gas Emission and Mitigation in Indian Agriculture– A Review," in *ING Bulletins on Regional Assessment of Reactive Nitrogen*. Bulletin No.19.

Pathak, H., Jain, N., Bhatia, A., Kumar, A., and Chatterjee, D. (2016). Improved Nitrogen Management: a Key to Climate Change Adaptation and Mitigation. *Indian J. Fertil.* 12 (11), 151–162.

Rochette, P., Worth, D. E., Lemke, R. L., McConkey, B. G., Pennock, D. J., Wagner-Riddle, C., et al. (2008). Estimation of N2O Emissions from Agricultural Soils in Canada. I. Development of a Country-specific Methodology. *Can. J. Soil Sci.* 88, 641–654. doi:10.4141/cjss07025

Sapkota, T. B., Jat, M. L., Rana, D. S., Khatri-Chhetri, A., Jat, H. S., Bijarniya, D., et al. (2021). Crop Nutrient Management Using Nutrient Expert Improves Yield, Increases Farmers' Income and Reduces Greenhouse Gas Emissions. *Sci. Rep.* 11, 1564. doi:10.1038/s41598-020-79883-x

Sharma, A., Kumar, S., Khan, S. A., Kumar, A., Mir, J. I., Sharma, O. C., et al. (2021). Plummeting Anthropogenic Environmental Degradation by Amending Nutrient- N Input Method in Saffron Growing Soils of north-west Himalayas. *Sci. Rep.* 11, 2488. doi:10.1038/s41598-021-81739-x

Sharma, U. C. (2020). Methane and Nitrous Oxide Emissions from Livestock in India: Impact of Land Use Change. *J. Agric. Aquacult.* 2 (1).

USDA (2018). India -Grain and Feed Annual. Available from:.

USDA (2019). *Crop Explorer*. Available from: https://ipad.fas.usda.gov/cropexplorer/util/new_get_psd_data.aspx?regionid=sasia.

Verma, D., and Singh, K. D. (1991). Changes in Nutrient Status of Soil Caused by Cropping and Fertilization inTypicUstrochrept. *Fertilizer Res.* 29, 267–274. doi:10.1007/bf01052395

World Bank (2014). Electric Power Transmission and Distribution Losses (% of Output). Available from: https://data.worldbank.org/indicator/EG.ELC.LOSS.ZS.

Conflict of Interest: The authors declare that the research was conducted in the absence of any commercial or financial relationships that could be construed as a potential conflict of interest.

Publisher's Note: All claims expressed in this article are solely those of the authors and do not necessarily represent those of their affiliated organizations, or those of the publisher, the editors and the reviewers. Any product that may be evaluated in this article, or claim that may be made by its manufacturer, is not guaranteed or endorsed by the publisher.

frontiers in Environmental Science

PERSPECTIVE
published: 22 October 2021
doi: 10.3389/fenvs.2021.740665

Achieving Chinese Carbon Neutrality Based on Water–Temperature–Radiation–Land Coupling Use

Yinglin Tian[1], Di Xie[1], Tiejian Li[1], Jiaye Li[2], Yu Zhang[1], Huan Jing[1], Deyu Zhong[1,3] and Guangqian Wang[1,3]*

[1]State Key Laboratory of Hydroscience and Engineering, Department of Hydraulic Engineering, Tsinghua University, Beijing, China, [2]School of Environment and Civil Engineering, Dongguan University of Technology, Dongguan, China, [3]Joint-Sponsored State Key Laboratory of Plateau Ecology and Agriculture, School of Water Resources and Electric Power, Qinghai University, Xining, China

Facing irreversible and catastrophic changes on the earth, China has committed to peak the net carbon emission by 2030 and to achieve carbon neutrality by 2060. The pledge requires significant mitigation immediately and sustainably. Considering this background, some perspectives are given in this article based on the comprehensive use of natural resources. First, utilizing the STIRPAT (stochastic impacts by regression on population, affluence, and technology) model and statistical data, net carbon emissions of provinces in China are anticipated, which lays a foundation for the further "three-step" carbon neutralization route. Second, a strategy of water–temperature–radiation–land coupling use is proposed, considering 1) the carbon emission cut, which relies on comparing the energy intensity and energy structure in China with those in developed countries; 2) the carbon sink increase, which depends on the evaluation of constraints of hydrometeorological factors on ecological productivity. Finally, the necessity and possibility of carbon trading and redistribution of the natural resources are discussed to ensure that China's national net carbon emission would be reduced to zero by 2060.

Keywords: carbon neutrality, carbon emission estimation, energy consumption, biological carbon sink, carbon trading

OPEN ACCESS

Edited by:
Munesh Kumar,
Hemwati Nandan Bahuguna Garhwal University, India

Reviewed by:
Poyyamoli Gopalsamy,
JSS Academy of Higher Education and Research, India
Uttam Kumar Sahoo,
Mizoram University, India

****Correspondence:***
Deyu Zhong
zhongdy@tsinghua.edu.cn

Specialty section:
This article was submitted to Interdisciplinary Climate Studies, a section of the journal Frontiers in Environmental Science

Received: *13 July 2021*
Accepted: *07 September 2021*
Published: *22 October 2021*

Citation:
Tian Y, Xie D, Li T, Li J, Zhang Y, Jing H, Zhong D and Wang G (2021) Achieving Chinese Carbon Neutrality Based on Water–Temperature–Radiation–Land Coupling Use. Front. Environ. Sci. 9:740665. doi: 10.3389/fenvs.2021.740665

INTRODUCTION

Greenhouse gas (GHG) emission is continuously increasing worldwide, which has received wide attention from researchers, governments, and the whole society. Since 2010, the GHG emission has been growing at a speed of 1.3%/a without land-use-change (LUC) emissions and reached a record high of 52.4 $GtCO_2e$ in 2019 (The UN Environment Programme 2020). Although 2020 has witnessed a dip in carbon emission due to COVID-19, it has a negligible impact on long-term climate change (Le et al., 2020). The global GHG emission is predicted to surge to around 59 $GtCO_2e$ in 2030 under current policies (The UN Environment Programme 2020).

The increasing GHG concentration in the atmosphere has led and will continue to lead to irreversible climate change on a global scale, bringing more unprecedented survival crises for human beings. As it has been reported by the Intergovernmental Panel on Climate Change Special Report on 1.5°C (IPCC 2018), human activities have induced the increase in the global mean surface temperature (GMST) of 0.87°C during the decade 2006–2015 relative to 1985–1900, resulting in multiple negative impacts on the natural and human system. The rising trends of frequency,

intensity, and duration of extreme weather (i.e., heat waves, floods, and droughts) have been detected worldwide (Landsea 2005; Trenberth et al., 2014; Fischer and Knutti 2015; Perkins–Kirkpatrick and Lewis 2020). In addition, other hazards also occur more frequently, such as earthquakes, landslides, volcanic activities, and wildfires. According to the analysis of the UN Office for Disaster Risk Reductions (2020), the number of natural disasters in the world doubled during the past 20 years compared with the period 1980–1999. Moreover, some other slow but hazardously evolving disasters are gradually appearing, such as the melting glaciers on the polar, rising sea levels, weakening Atlantic Meridional Overturning Circulation (AMOC), and intensified seabed methane release (Serreze et al., 2007; James et al., 2016; Sevellec et al., 2017; Kulp and Strauss 2019).

Threatened by these multiple and cascading risks, a comprehensive low-carbon transition for all countries is in urgent need. As the world's largest developing country, energy consumer, and carbon emitter, with the most frequent natural disasters (UN Office for Disaster Risk Reductions, 2020), China has made announcements to become carbon neutral by 2060, and to peak the CO_2 emission in the next decade (Central People's Government of the People's Republic of China 2021; The Guardian 2020; Chinadialogue 2020). Oriented at this target, China promised to lower its carbon dioxide emissions per unit of Gross Domestic Production (GDP) by 65% by 2030 compared with the 2005 levels, while boosting the forest stock volume by 6 billion m^3 from the 2005 levels. In addition, China also pledged a 25% share of nonfossil fuels in primary energy consumption and over 1.2 billion kilowatts of its total installed capacity of wind and solar power by 2030 (Reuters 2020).

Although the climate goal of China reignites the hope for controlling global warming and may even attract more countries to the track of carbon cut, the discrepancy between the ambitiousness and the status quo is still vast. On the one hand, despite a slowdown during 2010–2016 after the rapid growth during the 2000s, the GHG emission of China speeded up again in 2019 (3.1%/a), reaching a record high of 14 $GtCO_2e$ and accounting for more than 25 percent of the global GHG emission (The UN Environment Programme 2020). On the other hand, unlike developed countries, which have peaked carbon emission and therefore possess 50–70 years to rein in fossil fuel use and to offset the remaining emission (The UN Environment Programme 2020), the time from carbon emission peak to neutrality is only 30 years for China. China is bearing a heavier burden, but given a tighter time line. Therefore, China undoubtedly needs more investment in related researches and more vigorous measures and policies, especially during the 14th Five Year Plan (FYP for 2021–2025). And it is widely accepted that China should expand the generation and consumption of clean power while encouraging more capture, utilization, and storage for carbon (CCUS) both biophysically and chemically (Li et al., 2016; Zhou et al., 2016; Li et al., 2021).

However, the clear and quantitative roadmap for the Chinese carbon neutrality is still unclear, which is vital for implementing the commitments. Even if the carbon neutrality goal of China has been translated into several near-term breakdowns of energy and climate goals from the country's viewpoint, regional research remains to consider the uneven distribution of social and natural resources (Zhang and Hao 2015). Generally, China's population, urban regions, and carbon emissions are mainly concentrated in northeastern and eastern China (Chen et al., 2016; Chen et al. 2019; Chen et al. 2020), while China's main carbon sequestration is concentrated in southwestern and south China (Wang et al., 2020). In other words, there is a natural contradiction between the "carbon debt" (i.e., the positive amount of net carbon emission) and the "carbon credit" (i.e., the negative amount of net carbon emission) in various regions of China. Furthermore, the spatial distribution of water, soil, and heat resources is also not completely matched in China, leading to the inhomogeneous distribution of the carbon sequestration potential (Tao et al., 2005; Beer et al., 2010; Huang et al., 2019). As a result, the pathways for carbon neutrality in 2060 should vary with provinces, which nevertheless are currently unclear.

Furthermore, few strategies have been put forward from the perspective of hydrology and hydraulic engineering, which have played an important role in carbon removal for a long time. For the carbon cut, up to 2019, the hydropower of China has generated electricity more than 16 trillion kilowatt-hours, approximately equivalent to 15.4 billion tons of carbon dioxide emission reduction (China Society for Hydropower Engineering 2020). For carbon sequestration, water resources have become one of the key constraints for revegetation in relatively arid regions (Zhou et al., 2019), like China's Loess Plateau (Feng et al., 2016), thus limiting the opportunities for intensifying biological carbon sequestration. Furthermore, water resources play an important role in determining clean energy generation and ecological production not solely but coupled with other hydrometeorological factors like radiation, wind, and temperature. Therefore, long-term deep decarbonization in the context of hydrology, hydraulic engineering, and comprehensive natural resource use can give a worthy sight to achieving carbon neutrality.

Under this situation, this perspective paper is aimed to explore the solutions for the two issues mentioned above. In *The Roadmap for Chinese Carbon Neutrality Considering Differences Between Provinces*, the Chinese carbon neutrality goal is split into three steps considering the characteristics of carbon emission variation in different provinces. In *A Strategy of Water-temperature-radiation-land Coupling Use for Carbon Neutrality of China*, a strategy of carbon cut from the perspective of water–temperature–radiation–land coupling use is elaborated. In *Discussions*, the Chinese carbon cut is further discussed in the context of carbon trading and redistribution of natural resources in the foreseen future.

The Roadmap for Chinese Carbon Neutrality Considering Differences Between Provinces

The net carbon emission is estimated by extracting the carbon sink from the carbon emission. The data and methods used to assess the carbon emission and carbon sink are provided in Supplementary Text S1.1 and Text S1.2 in detail, respectively. **Supplementary Figure S1** (in Supplementary Material) presents the tendency of net carbon emission in the whole China and the three representative provinces under four different scenarios

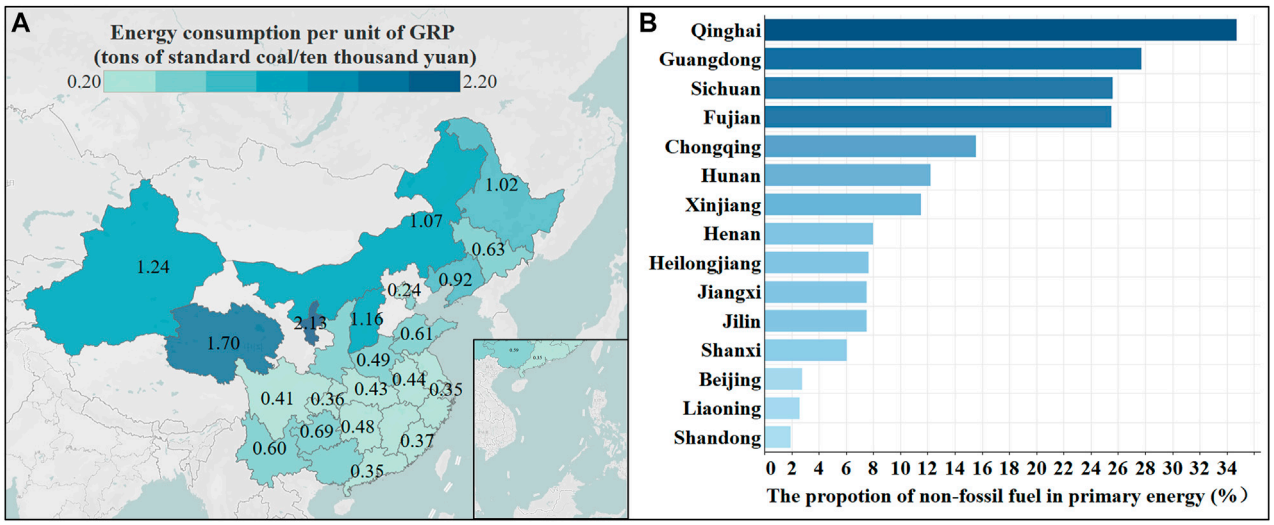

FIGURE 1 | (A) Energy consumption per unit of GRP and **(B)** the proportion of nonfossil fuel in primary energy of different provinces in China in 2017. Some provinces are not presented because of the data deficiency.

(including the scenario of total green development, S1; the scenario of strong energy conservation and emission reduction, S2; the scenario of energy conservation and emission reduction, S3; and the scenario of extensive development, S4), which are described in detail in **Supplementary Table S1** (in Supplementary Material). As shown by the blue solid line in **Supplementary Figure S1A**, only in the S1 scenario, carbon neutrality will be realized in China by 2060. However, it is still difficult to kick the coal habit quickly in a period as short as 1 or 2 decades, considering the inertia in energy consumption and the economic development of China. As a result, a gradual transition is more feasible. As presented by the red dashed line in **Supplementary Figure S1A**, the whole country is suggested to develop the S3 scenario before 2030. Thereafter, the transition is supposed to be made from the S3 to the S2 scenario by 2040. From then on, more efforts must be made to accomplish the total green development in all fields (the S1 scenario) and to finally cut the net carbon emission to zero by 2060.

After the national pathway is clear, the net carbon emission for different provinces is projected considering their economic structure, industrial development, and vegetational cover, to evaluate the challenge of meeting the regional targets. As shown in **Supplementary Figure S1B**, Qinghai has peaked carbon emission and has the potential to achieve carbon neutrality from 2037 to 2053 as long as Qinghai would not develop its economy by extensively using its fossil fuel (the S4 scenario). Comparatively, the possible carbon neutrality is much later for Hubei, which can approximately be achieved by 2052, and the total green development (the S1 scenario) is the only choice for Hubei. Furthermore, carbon neutrality is much harder for Guangdong, the earliest time for which to cut the carbon emission is 2060, which is only possible under the S1 scenario.

Under this situation, China's 2060 carbon neutrality target could be split into three steps based on the carbon emission estimation for more provinces. As shown in **Supplementary Table S3** (in Supplementary Material), in the first step, by 2045, the demonstrational areas of Chinese carbon neutrality should meet the standards, including the western provinces such as Qinghai and Xinjiang. In the second step, by 2055, the key areas of Chinese carbon neutrality should cut the carbon emission to zero, including Sichuan, Hubei, and Hunan etc. Finally, in the third step, by 2060, it is time for the difficult areas of Chinese carbon neutrality to reach the standard, including Henan, Shaanxi (105°E–111°E, 31°N–39°N), and Guangdong etc. It is worthy to note that some provinces, Liaoning, for instance, may be hard to realize carbon neutrality even in 2060. As a result, the demonstrational areas need to take their advantages and contribute to the carbon sink of the difficult areas after offsetting the carbon emission of their own, thus guaranteeing the achievement of national carbon neutrality.

A STRATEGY OF WATER–TEMPERATURE–RADIATION–LAND COUPLING USE FOR CARBON NEUTRALITY OF CHINA

After the general route of China's carbon neutrality is made clear, reformation should be performed in every field to reach the objectives, among which the natural resource regulation plays pivotal roles. In this context, a strategy of water–temperature–radiation–land coupling use is proposed, which is divided into two dimensions as the following:

Cutting the Carbon Emission

The carbon emission is largely determined by the efficiency and structure of the energy consumption, which can be represented by the energy consumption per unit of gross regional production (GRP), or carbon intensity, and the proportion of nonfossil fuel in primary energy. The data and methods used to assess the carbon intensity and the account of nonfossil fuel in primary energy are provided in **Supplementary Text S1.3** detail. The results of different provinces in China in 2017 are shown in **Figure 1**.

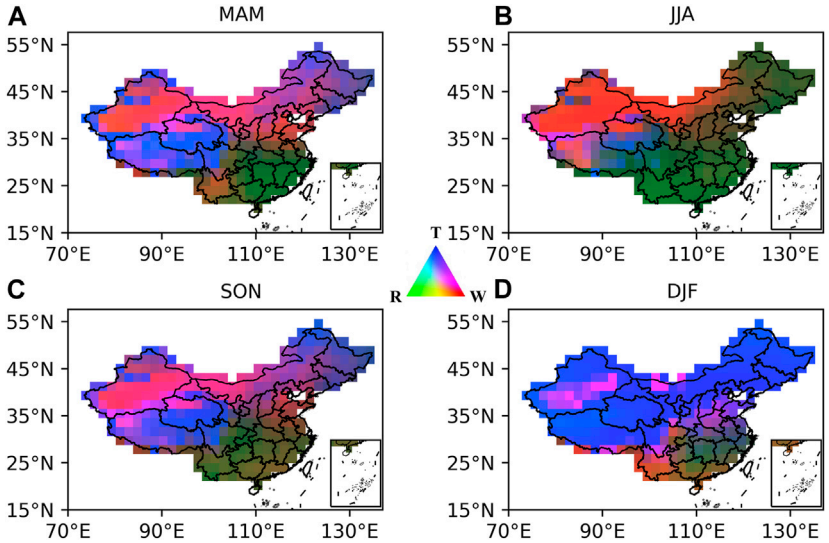

FIGURE 2 | Geographic distribution of potential climatic constraints to plant growth derived from long-term (2000–2019) climate statistics in **(A)** spring, **(B)** summer, **(C)** autumn, and **(D)** winter. R, T, and W represent radiation, temperature, and water resources, respectively. Deeper green indicates stronger constraints of radiation on GPP, deeper blue indicates stronger constraints of temperature on GPP, and deeper red indicates stronger constraints of water on GPP.

In 2017, the energy consumption per GDP of China, America, and Europe are approximately 0.4, 0.2, and 0.1 tons of standard coal per ten thousand yuan, respectively (National Bureau of Statistics of China 2000–2019). Moreover, as presented in **Figure 1A**, the carbon intensity in the majority of provinces in China exceeds the average value for America (0.2). Generally, southern, eastern, and southeastern China have relatively low energy consumption per unit of GRP, ranging from 0.35 (Jiangsu) to 0.69 (Guizhou) tons of standard coal per ten thousand yuan, although the net carbon emission is relatively high there (Chen et al., 2020). On the contrary, the northwestern, northern, and northeastern provinces have a lower efficiency of energy usage, with the energy consumption per unit of GRP varying from 1.02 (Heilongjiang) to 2.13 (Ningxia) tons of standard coal per ten thousand yuan. Notably, Ningxia, Qinghai, Xinjiang, and Inner Mongolia have especially high carbon intensity, asking for quick reformation of the energy utilization structure.

Apart from the use efficiency of the primary energy, the components of energy consumption also account for the final carbon emission. In other words, the fewer fossil fuel is consumed, the less GHGs would be generated. The average proportion of the nonfossil fuel of China is 15.6% in 2017, less than that of America (18%) and Europe (27%). Several provinces, such as Qinghai (34.7%), Guangdong (27.7%), Sichuan (25.6%), and Fujian (25.5%), have widely applied hydro, wind, and solar energies, thus gaining a higher proportion of nonfossil fuel than that of America. The ratio of the zero-emission resources is urgently needed to be increased in more provinces, especially in Shandong, Liaoning, Beijing, and Shanxi.

Enhancing the Biological Carbon Sequestration

Apart from cutting the carbon emission, the amount of carbon sequestration needs to be increased in the meanwhile, because even in the S1 scenario, about 1.6 billion tons of carbon emission (not the net one) would be emitted in total in 2050, which remains to be offset both naturally and artificially. In other words, increasing carbon sequestration capacity is not a risk compensation but a rigid demand for 2060 carbon neutrality. From 2010 to 2016, the whole terrestrial ecosystem in China absorbed approximately 1.11 billion tons of carbon annually, accounting for about 10% of the Chinese total carbon emissions in that period and 45% of the carbon released in total fossil fuel combustion and cement production (Wang et al., 2020). In the Chinese terrestrial ecosystem, the forest is of vital significance, with its vegetation carbon storage amounting to 5.49 PgC on average (Ni 2013). And the grassland also explains a lot for the carbon sink, accounting for about 40% of the country's land area (the NBS) and storing the carbon of approximately 1.41 PgC (Ni 2013). Therefore, growth in forest and grassland stock during the next 3 decades is the key to striving for carbon neutrality by 2060.

The carbon sequestration capacity of both forests and grasslands is affected by natural factors such as, among others, climate conditions, soil quality, and water resources, which all show obvious temporal and spatial heterogeneities (Bastin et al., 2019). To give some scientific supports for China's afforestation, the restrictions of temperature, water, and radiation on the gross primary production (GPP) in China during 2000–2019 are calculated based on the data and method provided in **Supplementary Text S1.4**, and the results are presented in **Figure 2**. It is found that the major factors determining the carbon capture of plants vary with the region and the season. Except for winter, the water resource is the most important factor in northwestern China, especially for Xinjiang, Inner Mongolia, and Qinghai, and its effect is more pronounced in the summer. Comparatively, radiation accounts for more in southeastern China, and its influences extend to the northeastern areas in

the summer. As for the temperature, it reasonably controls northern China in the winter and also explains the limited carbon sink over the large part of the Tibet Plateau nearly all over the year.

DISCUSSIONS

Carbon Trading

Based on the anticipation of the net carbon emission of provinces introduced in *The Roadmap for Chinese Carbon Neutrality Considering Differences Between Provinces*, the net carbon emissions of representative provinces in 2050 under the scenario of total green development (the S1 scenario) are provided in **Supplementary Table S4**, which quantifies the potential and the need of different provinces for the carbon trading in China. As it is presented in **Supplementary Table S4**, in 2050, Qinghai, Sichuan, and Hunan can additionally sequestrate 20.45 $GtCO_2e$, 14.08 $GtCO_2e$, and 9.52 $GtCO_2e$ in addition to local carbon emission, respectively, which can be regarded as the "carbon credit." On the contrary, the net carbon emissions of Liaoning, Chongqing, Guangdong, Henan, Shanxi, and Hubei in 2050 are still positive, ranging from 10.98 to 103.49 $GtCO_2e$, which can be regarded as the "carbon debt." In other words, provinces with a relatively low economic development level and high potential of carbon sequestration, like Qinghai, can swap the net carbon sinks for economic support and resource supply from those provinces having difficulties in carbon mitigation.

Moreover, embedded in distinctive political, economic, and institutional contexts, the emission trading systems (ETSs) can control carbon emission both effectively and economically. Comprehensive ETSs rely on the ex-ante investigation of carbon footprint, improvement of carbon tax policy, reasonable carbon pricing, fair allowance allocation among sectors and enterprises, unified carbon market construction, and ex-post impact assessments (Lu et al., 2010; Wang et al., 2015; Jiang et al., 2016; Zhang et al., 2020; Wei 2021).

Redistribution of Natural Resources

Figure 2 shows significantly different features of the climate constraints on plant growth in northwestern China and southeastern China. For further investigation, we present the multiyear-averaged distribution of minimum temperature, precipitable water, and cloud cover in **Supplementary Figures S2–S4** based on the data from NCEP-DOE Reanalysis 2 (Kanamitsu et al., 2002). Moreover, the distribution of elevation in China is drawn in **Supplementary Figure S5** based on the 90 m digital elevation model (Jarvis et al., 2008). The dividing line from southwest to northeast can be found in **Supplementary Figures S2–S4**, mainly due to the latitudes and spatial characteristics of the elevation in China (**Supplementary Figure S5**), which decreases from northwest to southeast. With higher elevation, northwestern China experiences lower temperature (**Supplementary Figure S2**) and thinner air overlying it, which together led to less precipitable water in the region (**Supplementary Figure S3**) and thus less cloud cover (**Supplementary Figure S4**). Since the reflection and absorption of radiation by the clouds are less, more radiation can arrive at the surface in northwestern China. Apart from that, southeastern China is close to the South China Sea, western North Pacific, and the East China Sea, thus having adequate moisture supply and experiences frequent moisture convergence due to the large-scale atmospheric circulation (Huang et al., 2018).

Further, **Figure 2** implies that rational redistribution of natural resources is conducive to the enhancement of the carbon fixation capacity. For example, land resources are adequate in western China, which nevertheless severely lacks the water and heat resources, and therefore has restricted the growth of grasslands. According to **Figure 2B**, the ecological productivity in the northwestern Qinghai (around the Chaidamu Basins) during the growing season (approximately in the summer season) can be added if more water resources were transferred there. The pronounced positive trend in natural precipitation has been observed around the Chaidamu Basins based on the Climate Forecast System Reanalysis (CFSR) product during 1980–2016, favoring the increases in ecological carbon capture (Ayantobo et al., 2016). If the artificial precipitation enhancements are performed at the places where the moisture converges and are followed by water resource regulation of surface water conservancy projects, the precipitation over the Chaidamu Basins can be increased by around 2.4 billion cubic meters per year during 2020–2060 (Meng and Wang 2019), which can largely boost the net ecological productivity there.

CONCLUSION

In this study, based on the statistical data and grid data, using the STIRPAT model (Pan et al., 2021) and Nemani's (Nemani et al., 2003) method, the roadmap is drawn for the Chinese commitment to peak emissions in 2030 and reach carbon neutrality in 2060. Further, a strategy of water–temperature–radiation–land coupling use for carbon neutrality of China is provided. Specifically, our major findings are as the following:

1) China's 2060 carbon neutrality target is supposed to be split into three steps based on the carbon emission estimation of provinces. The demonstrational areas (such as Qinghai and Xinjiang), the key areas (such as Sichuan, Hubei, and Hunan), and the difficult areas (such as Henan, Shaanxi, and Guangdong) should cut the net carbon emission to zero by 2045, 2055, and 2060, respectively. Also, carbon trading is a requisite considering the interprovincial dispatch of economic development levels, natural resource storage, and carbon emission.
2) The energy intensity of China is higher than that of Europe and America, while the account of nonfossil fuels in China is lower than those of Europe and America. Thereby, more efforts should be made to improve the efficacy of energy consumption in China.
3) In summer, the plant growth in northwestern and southeastern China is limited by water and radiation,

respectively. Rational redistribution of natural resources is conducive to the enhancement of the carbon fixation capacity.

DATA AVAILABILITY STATEMENT

The original contributions presented in the study are included in the article/**Supplementary Material**; further inquiries can be directed to the corresponding author.

AUTHOR CONTRIBUTIONS

YT analyzed the constraints of the natural sources on the GPP and wrote the manuscript. DX investigated the net carbon emission in the present and forecasted it based on the STIRPAT model. TL made suggestions on carbon trading. JL reviewed the reasons and effects of global warming. YZ generalized the difficulties for China to achieve carbon neutrality and compared the energy consumption of China with that of foreign countries. HJ reviewed the key technologies to lower carbon emission in sectors of industry, construction, transportation, and agriculture. DZ and GW put forward the framework of the strategy of water–temperature–radiation–land coupling use for the carbon neutrality of China and helped to improve the interpretation of the paper.

FUNDING

This research was supported by the Second Tibetan Plateau Scientific Expedition and Research Program (2019QZKK0208).

SUPPLEMENTARY MATERIAL

The Supplementary Material for this article can be found online at: https://www.frontiersin.org/articles/10.3389/fenvs.2021.740665/full#supplementary-material

REFERENCES

Ayantobo, O. O., Wei, J., Kang, B., Li, T., and Wang, G. (2021). Spatial and Temporal Characteristics of Atmospheric Water Vapour Content and its Relationship with Precipitation Conversion in China during 1980-2016. *Int. J. Climatol.* 41, 1747–1766. doi:10.1002/joc.6928

Bastin, J.-F., Finegold, Y., Garcia, C., Mollicone, D., Rezende, M., Routh, D., et al. (2019). The Global Tree Restoration Potential. *Science* 365 (6448), 76–79. doi:10.1126/science.aax0848

Beer, C., Reichstein, M., Tomelleri, E., Ciais, P., Jung, M., Carvalhais, N., et al. (2010). Terrestrial Gross Carbon Dioxide Uptake: Global Distribution and Covariation with Climate. *Science* 329 (5993), 834–838. doi:10.1126/science.1184984

Central People's Government of the People's Republic of China (2021). *How Can China Peak Emissions before 2030 and Reach Carbon Neutrality before 2060?* Beijing, China: Xinhuanet. (in Chinese) http://www.gov.cn/xinwen/2021-04/02/content_5597403.htm.

Chen, D., Zhang, Y., Yao, Y., Hong, Y., Guan, Q., and Tu, W. (2019). Exploring the Spatial Differentiation of Urbanization on Two Sides of the Hu Huanyong Line -- Based on Nighttime Light Data and Cellular Automata. *Appl. Geogr.* 112, 102081. doi:10.1016/j.apgeog.2019.102081

Chen, J., Gao, M., Cheng, S., Hou, W., Song, M., Liu, X., et al. (2020). County-level CO2 Emissions and Sequestration in China during 1997-2017. *Sci. Data* 7, 391. doi:10.1038/s41597-020-00736-3

Chen, M., Gong, Y., Li, Y., Lu, D., and Zhang, H. (2016). Population Distribution and Urbanization on Both Sides of the Hu Huanyong Line: Answering the Premier's Question. *J. Geogr. Sci.* 26, 1593–1610. doi:10.1007/s11442-016-1346-4

China Society for Hydropower Engineering (2020). *Annual Report for China Hydropower Information of 2019* Beijing, China: China Electric Power Press, 14–16. (in Chinese) http://www.hydropower.org.cn/showNewsDetail.asp?nsId=27366.

China dialogue (2020). *China's New Carbon Neutrality Pledge: What Next?* London, England: China Dialogue. https://www.thethirdpole.net/en/climate/chinas-new-carbon-neutrality-pledge-what-next/.

Feng, X., Fu, B., Piao, S., Wang, S., Ciais, P., Zeng, Z., et al. (2016). Revegetation in China's Loess Plateau Is Approaching Sustainable Water Resource Limits. *Nat. Clim Change* 6, 1019–1022. doi:10.1038/nclimate3092

Fischer, E. M., and Knutti, R. (2015). Anthropogenic Contribution to Global Occurrence of Heavy-Precipitation and High-Temperature Extremes. *Nat. Clim Change* 5, 560–564. doi:10.1038/nclimate2617

Huang, M., Piao, S., Ciais, P., Peñuelas, J., Wang, X., Keenan, T. F., et al. (2019). Air Temperature Optima of Vegetation Productivity across Global Biomes. *Nat. Ecol. Evol.* 3, 772–779. doi:10.1038/s41559-019-0838-x

Huang, W., He, X., Yang, Z., Qiu, T., Wright, J. S., Wang, B., et al. (2018). Moisture Sources for Wintertime Extreme Precipitation Events over South China during 1979-2013. *J. Geophys. Res. Atmos.* 123, 6690–6712. doi:10.1029/2018JD028485

IPCC (2006). *IPCC Guidelines for National Greenhouse Gas Inventories* Hayama, Japan: The Institute for Global Environmental Strategies (IGES). https://www.ipcc.ch/report/2006-ipcc-guidelines-for-national-greenhouse-gas-inventories/.

IPCC (2018). *IPCC Special Report on Global Warming of 1.5°C* Geneva, Switzerland: World Meteorological Organization. https://www.ipcc.ch/sr15/.

Jarvis, A., Reuter, H. I., Nelson, A., and Guevara, E. (2004). *Hole-Filled Seamless SRTM Data V4*. International Centre for Tropical Agriculture (CIAT).

James, R. H., Bousquet, P., Bussmann, I., Haeckel, M., Kipfer, R., Leifer, I., et al. (2016). Effects of Climate Change on Methane Emissions from Seafloor Sediments in the Arctic Ocean: A Review. *Limnol. Oceanogr.* 61 (1), S283–S299. doi:10.1002/lno.10307

Jiang, J., Xie, D., Ye, B., Shen, B., and Chen, Z. (2016). Research on China's Cap-And-Trade Carbon Emission Trading Scheme: Overview and Outlook. *Appl. Energ.* 178, 902–917. doi:10.1016/j.apenergy.2016.06.100

Kanamitsu, M., Ebisuzaki, W., Woollen, J., Yang, S.-K., Hnilo, J. J., Fiorino, M., et al. (2002). NCEP-DOE AMIP-II Reanalysis (R-2). *Bull. Am. Meteorol. Soc.* 83, 1631–1643. doi:10.1175/BAMS-83-11-163110.1175/bams-83-11-1631(2002)083<1631:nar>2.3.co;2

Kulp, S. A., and Strauss, B. H. (2019). New Elevation Data Triple Estimates of Global Vulnerability to Sea-Level Rise and Coastal Flooding. *Nat. Commun.* 10, 4844. doi:10.1038/s41467-019-12808-z

Landsea, C. W. (2005). Hurricanes and Global Warming. *Nature* 438, E11–E12. doi:10.1038/nature04477

Le Quéré, C., Jackson, R. B., Jones, M. W., Smith, A. J. P., Abernethy, S., Andrew, R. M., et al. (2020). Temporary Reduction in Daily Global CO2 Emissions during the COVID-19 Forced Confinement. *Nat. Clim. Chang.* 10, 647–653. doi:10.1038/s41558-020-0797-x

Li, Q., Chen, Z. A., Zhang, J.-T., Liu, L.-C., Li, X. C., and Jia, L. (2016). Positioning and Revision of CCUS Technology Development in China. *Int. J. Greenhouse Gas Control.* 46, 282–293. doi:10.1016/j.ijggc.2015.02.024

Li, Y., Lan, S., Ryberg, M., Pérez-Ramírez, J., and Wang, X. (2021). A Quantitative Roadmap for China towards Carbon Neutrality in 2060 Using Methanol and

Ammonia as Energy Carriers. *ISCIENCE* 24 (6), 102513. doi:10.1016/j.isci.2021.102513

Lu, C., Tong, Q., and Liu, X. (2010). The Impacts of Carbon Tax and Complementary Policies on Chinese Economy. *Energy Policy* 38 (11), 7278–7285. doi:10.1016/j.enpol.2010.07.055

Meng, C. Q., and Wang, G. Q. (2019). *Status Analysis and Development Potential Evaluation of Air Water Resources in the Northwest Inland in China. (Postdoctor Thesis, in Chinese)*. Beijing: Tsinghua University.

National Bureau of Statistics of China (2000–2019). *China Statistical Yearbook: Total Consumption of Energy and its Composition* Beijing, China: China Statistic Press. http://www.stats.gov.cn/tjsj/ndsj/.

Nemani, R. R., Keeling, C. D., Hashimoto, H., Jolly, W. M., Piper, S. C., Tucker, C. J., et al. (2003). Climate-driven Increases in Global Terrestrial Net Primary Production from 1982 to 1999. *Science* 300 (5625), 1560–1563. doi:10.1126/science.1082750

Ni, J. (2013). Carbon Storage in Chinese Terrestrial Ecosystems: Approaching a More Accurate Estimate. *Climatic Change* 119, 905–917. doi:10.1007/s10584-013-0767-7

Pan, D., Li, N., and Li, F. (2021). Mitigation Strategy of Eastern China Based on Energy-Source Carbon Emission Estimation. *Acta Scientiae Circumstantiae* 41 (3), 1142–1152. doi:10.13671/j.hjkxxb.2020.0325

Perkins-Kirkpatrick, S. E., and Lewis, S. C. (2020). Increasing Trends in Regional Heatwaves. *Nat. Commun.* 11, 3357. doi:10.1038/s41467-020-16970-7

Reuters (2020). *China's Xi Targets Steeper Cut in Carbon Intensity by 2030*. London, England: Thomson Reuters. https://www.reuters.com/world/china/chinas-xi-targets-steeper-cut-carbon-intensity-by-2030-2020-12-12/.

Serreze, M. C., Holland, M. M., and Stroeve, J. (2007). Perspectives on the Arctic's Shrinking Sea-Ice Cover. *Science* 315, 1533–1536. doi:10.1126/science.1139426

Sévellec, F., Fedorov, A. V., and Liu, W. (2017). Arctic Sea-Ice Decline Weakens the Atlantic Meridional Overturning Circulation. *Nat. Clim. Change* 7, 604–610. doi:10.1038/nclimate3353

Tao, F., Yokozawa, M., Hayashi, Y., and Lin, E. (2005). A Perspective on Water Resources in China: Interactions between Climate Change and Soil Degradation. *Climatic Change* 68, 169–197. doi:10.1007/s10584-005-6013-1

The Guardian (2020). *China Pledges to Become Carbon Neutral before 2060* London, England: Guardian News and Media. https://www.theguardian.com/environment/2020/sep/22/china-pledges-to-reach-carbon-neutrality-before-2060.

The UN Environment Programme (2020). *Emissions Gap Report 2020: 1.5°C Goal Requires Green Recovery*. Nairobi, Kenya: UN Environment Programme. https://wedocs.unep.org/bitstream/handle/20.500.11822/34438/EGR20ESE.pdf.

Trenberth, K. E., Dai, A., van der Schrier, G., Jones, P. D., Barichivich, J., Briffa, K. R., et al. (2014). Global Warming and Changes in Drought. *Nat. Clim. Change* 4, 17–22. doi:10.1038/nclimate2067

UN Office for Disaster Risk Reductions (2020). *Human Cost of Disaster. An Overview of the Last 20 Years 2000-2019*. Geneva, Switzerland: The United Nations Office for Disaster Risk Reduction (UNDRR). https://www.undrr.org/media/48008/download.

Wang, J., Feng, L., Palmer, P. I., Liu, Y., Fang, S., Bösch, H., et al. (2020). Large Chinese Land Carbon Sink Estimated from Atmospheric Carbon Dioxide Data. *Nature* 586, 720–723. doi:10.1038/s41586-020-2849-9

Wang, P., Dai, H.-c., Ren, S.-y., Zhao, D.-q., and Masui, T. (2015). Achieving Copenhagen Target through Carbon Emission Trading: Economic Impacts Assessment in Guangdong Province of China. *Energy* 79, 212–227. doi:10.1016/j.energy.2014.11.009

Wei, S. (2021). A Sequential Game Analysis on Carbon Tax Policy Choices in Open Economies: From the Perspective of Carbon Emission Responsibilities. *J. Clean. Prod.* 283, 124588. doi:10.1016/j.jclepro.2020.124588

Zhang, Y.-J., and Hao, J.-F. (2015). The Allocation of Carbon Emission Intensity Reduction Target by 2020 Among Provinces in China. *Nat. Hazards* 79, 921–937. doi:10.1007/s11069-015-1883-7

Zhang, Y., Li, S., Luo, T., and Gao, J. (2020). The Effect of Emission Trading Policy on Carbon Emission Reduction: Evidence from an Integrated Study of Pilot Regions in China. *J. Clean. Prod.* 265, 121843. doi:10.1016/j.jclepro.2020.121843

Zhou, B., Li, Z., Zhao, Y., Zhang, C., and Wei, Y. (2016). Rare Earth Elements Supply vs. Clean Energy Technologies: New Problems to Be Solve. *Gospodarka Surowcami Mineralnymi - Mineral. Resour. Management* 32 (4), 29–44. doi:10.1515/gospo-2016-0039

Zhou, S., Zhang, Y., Park Williams, A., and Gentine, P. (2019). Projected Increases in Intensity, Frequency, and Terrestrial Carbon Costs of Compound Drought and Aridity Events. *Sci. Adv.* 5 (1), eaau5740. doi:10.1126/sciadv.aau5740

Conflict of Interest: The authors declare that the research was conducted in the absence of any commercial or financial relationships that could be construed as a potential conflict of interest.

Publisher's Note: All claims expressed in this article are solely those of the authors and do not necessarily represent those of their affiliated organizations, or those of the publisher, the editors, and the reviewers. Any product that may be evaluated in this article, or claim that may be made by its manufacturer, is not guaranteed or endorsed by the publisher.

frontiers in Environmental Science

ORIGINAL RESEARCH
published: 26 October 2021
doi: 10.3389/fenvs.2021.764294

COVID-19 and Greenhouse Gas Emission Mitigation: Modeling the Impact on Environmental Sustainability and Policies

Muhammad Mohsin[1], *Sobia Naseem*[2], *Muddassar Sarfraz*[3]*, *Larisa Ivascu*[4] and *Gadah Albasher*[5]

[1]School of Business, Hunan University of Humanities, Science and Technology, Loudi, China, [2]School of Economics and Management, Shijiazhuang Tiedao University, Shijiazhuang, China, [3]College of International Students, Wuxi University, Wuxi, China, [4]Department of Management, Faculty of Management in Production and Transportation, Politehnica University of Timisoara, Timisoara, Romania, [5]Department of Zoology, College of Science, King Saud University, Riyadh, Saudi Arabia

The COVID-19 pandemic has compelled countries worldwide to enforce stringent measures to maintain social distancing, by locking down populations and restricting all kinds of transport. Besides their impact on the virus, these dramatic changes may also have positively contributed to a sustainable environment. The study aims to measure the effect of COVID-19 on environmental sustainability by employing the autoregressive distributed lag (ARDL) model. The study is based on the daily data of COVID-19 confirmed cases; confirmed deaths; manually generated lockdown data by the indexing method; and NO_2, NH_3, SO_2, and CO levels from March 3, 2020, to July 27, 2021. This research study investigates the long- and short-term relationship between COVID-19 and the aforementioned greenhouse gases. The findings suggest conclusively that NO_2, SO_2, and CO declined during the COVID-19 period in India because these gases are anthropologically emitted by transport, industries, and fossil fuel burning. On the other hand, the evolving NH_3 is not related to COVID-19 confirmed cases and deaths but is impacted by lockdown because ammonia emission is directly related to agricultural activities. Therefore, a decline in pollutants such as greenhouse gases during the COVID-19 period until July 2021 was observed. This means the prioritized control of human activities can be helpful to enhance the quality of the environment.

Keywords: greenhouse gas, COVID-19, ARDL, environmental sustainability, India

OPEN ACCESS

Edited by:
Munesh Kumar,
Hemwati Nandan Bahuguna Garhwal University, India

Reviewed by:
Mian Sajid Nazir,
Université de Montréal, Canada
Zeying Li,
Hanshan Normal University, China
Benedict Arulanandam,
Sunway College, Malaysia

****Correspondence:***
Muddassar Sarfraz
muddassar.sarfraz@gmail.com

Specialty section:
This article was submitted to Interdisciplinary Climate Studies, a section of the journal Frontiers in Environmental Science

Received: *25 August 2021*
Accepted: *21 September 2021*
Published: *26 October 2021*

Citation:
Mohsin M, Naseem S, Sarfraz M, Ivascu L and Albasher G (2021) COVID-19 and Greenhouse Gas Emission Mitigation: Modeling the Impact on Environmental Sustainability and Policies. Front. Environ. Sci. 9:764294. doi: 10.3389/fenvs.2021.764294

INTRODUCTION

Over the years, phenomenal advances in epidemiology have predicted the emergence of wide epidemics in the human population. The globalization of human communities has facilitated the transmission of infectious diseases, leading to a higher risk of global outbreaks. The distressing effects of the great pandemics of the past have potentially influenced human development, while the historical evolution of epidemics has drastically modified the living standards, affecting worldwide economies.

Similarly, the recent coronavirus pandemic (COVID-19) has strongly affected the global economy. The shift in the rhythm of people's livelihoods has transformed the world's socio-economic structure, developing an inextricable relationship between human development and

epidemics. In December 2019, the massive disruptions caused by COVID-19 imposed a new strain in many countries causing them to experience an extensive turmoil. The emergence of the causative virus was first reported from Wuhan, China (Huang et al., 2021). Its clinical manifestation has caused an extensive turbulence worldwide. The wide spread of this deadly disease has seen a high fatality rate, with vulnerable population particularly experiencing its severity. The latest statistics (August 1, 2021) report 210 million confirmed cases, with more than 4 million people dying because of COVID-19 (Ritchie et al., 2020). However, besides the unprecedented consequences of the pandemic, research has also revealed that the impact of COVID-19 has improved the environmental conditions, thereby limiting the greenhouse emissions (Kumar and Kumar, 2020; Mandal et al., 2020; Mishra and Kumar, 2021).

Air is an essential element needed for human survival. It plays a fundamental role in sustaining a healthy environment, thereby providing a safe and clean place to live. Improved air quality enhances individual well-being, making humans enjoy substantial health benefits.

In contrast, the historical reputations of air pollutants correctly make environmental containments the chief agent leading to the great tragedies of human civilization (Vulichi et al., 2021). The greenhouse emissions are crucial determinants of atmospheric quality. Environmental substances such as toxic gases produce a high concentration effect, thereby reducing the air quality. The greenhouse gases (GHSs) (i.e., CO_2, NO, NH_4, and SO_3) result in environmental degradation (Manisalidis et al., 2020). Research shows that among these GHGs, CO_2, SO_2, and NO_2 are the most harmful environmental contaminants affecting the global climate (Conibear et al., 2018). The emission of these gases deteriorates the air quality, resulting in environmental depletion (Gautam and Hens, 2020).

Subsequently, due to the increasing greenhouse emission, environmental unsustainability has become a global concern that hinders long-term social benefits. Unsustainable resources cause adverse effects such as atmospheric deterioration, air pollution, and global warming. The tremendous increase in pollution due to anthropogenic activities has made environmental sustainability the prime concern for meteorologists. Therefore, to maintain sustainable atmospheric conditions, unwanted greenhouse emissions should be restricted. Environmental sustainability should be ensured, mitigating the negative consequences of climate changes and thus achieving a clean atmosphere.

While the pandemic has undoubtedly had an adverse overall impact on human health, significant developments have been witnessed regarding the health of natural assets such as land, water, and air. It has been found that lockdown measures during COVID-19 reduced pollution levels, including air pollution, a crucial determinant of environmental quality during the COVID-19 period. According to a recent study, the decrease in human activities in China during the lockdown restrictions resulted in a significant decline in air containment (Wang et al., 2020). Furthermore, other findings illustrate that the global lockdown conditions remarkably reduced the atmospheric concentration, thereby positively modifying the air quality (Kumar et al., 2021; Sharma et al., 2020). This suggests that the precautionary policies during the lockdown period relieved the environment from some of the burden of human activities. Hence, the health-damaging impact of COVID-19 during the lockdown restriction significantly reduced the pollution level across the globe.

COVID-19 has disturbed the globalized economy, thereby throwing many countries into deep recessions. An immense increase in the death rate has had negative consequences for countries. To prevent the rapid transmission of the virus, governments enforced severe lockdown conditions worldwide. In the case of India, lockdown implications halted the nation's economy while the number of confirmed cases grew. As of August 1, 2021, the data record 31.70 million confirmed cases, causing 424,773 to lose their lives. This vulnerable situation in India provoked the government to implement strict lockdown measures. Indeed, to manage the outbreak during this global emergency, a public curfew was officially announced on March 24, 2020, whereby Indian citizens were encouraged to practice social distancing. Socio-economic activities were also suspended (MHA, 2020). All industrial and commercial establishments remained closed. This abrupt lifestyle changes in India forced people to follow lockdown guidance, leaving their homes only as the final resort for their survival.

However, the pandemic and the steps taken to mitigate it reduced air pollution across the Indian Territory. A significant reduction in air containments reveals a decrease of poisonous substances in most of the cities of India (i.e., New Delhi, Bangalore, and Mumbai). Given this statement, a notable decline in the greenhouse concentration (i.e., NO_2) was recorded across the Indian region (e.g., New Delhi, Ahmedabad, Bangalore, and Nagpur) (Vadrevu et al., 2020). Likewise, the recent finding demonstrates that during the lockdown situation in India, the decline in the concentration level of greenhouse emissions (e.g., NO_2, CO_2, and O_3) lead to an improvement in the national environment (Kumar ad Gupta, 2020; Sharma et al., 2020; Kumar et al., 2021). Perhaps, aside from curtailing COVID-19, the findings provide a clear justification for the Indian government to accelerate efforts to improve the national air quality (McDonald et al., 2020).

Over various geographical regions of India during COVID-19, a healthy correlation was witnessed between the pollution intensity and COVID-19 severity. The decline in socio-economic activities improved the pollution status, reducing the exhausting environmental emissions (Kumar and Kumar, 2020; Mishra and Kumar, 2021; Singh et al., 2020). As such, the viral outburst of COVID-19 has drastically enhanced air quality, contributing to the recovery of the global environment, albeit perhaps temporarily.

Altogether, the results show that the COVID-19 implications have enhanced the environment by widely improving the air quality. This temporary improvement in atmospheric conditions has demonstrated the importance of reducing greenhouse emissions, thereby gaining environmental sustainability. Primarily, therefore, this study aims to determine the air pollution level during the COVID-19 lockdown period. It investigates the fundamental relationship between the pollution status and COVID-19 susceptibility. As such, this study has great significance in the context of India during the lockdown period.

The reduction in air substances and improvement in public health conditions reflect the truth regarding the atmospheric quality. The deadly COVID-19 pandemic provides a broad scope to the meteorologists and policymakers studying and planning for the rejuvenation of environmental health. This study aims to provide

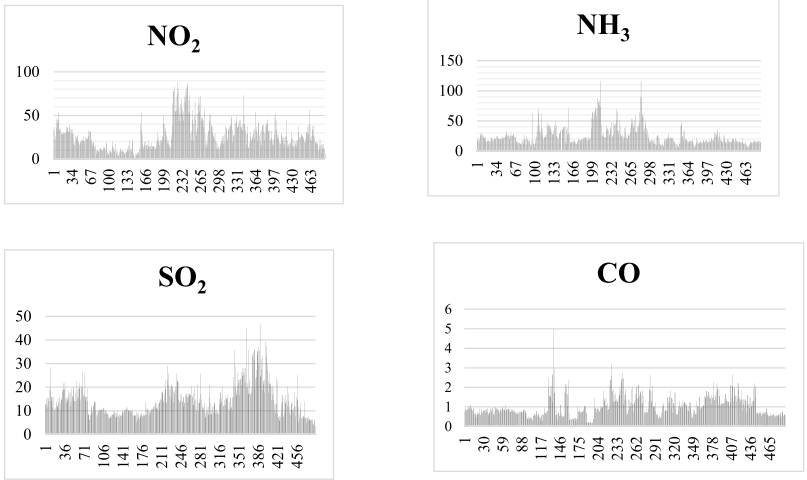

FIGURE 1 | Daily data series of greenhouse gases from March 3, 2020, to July 27, 2021.

a scientific research that articulates pollution parameters to achieve air quality standards. Perhaps, the sustainable environmental management unintentionally implemented during the COVID-19 escalation gives reason to express the optimism regarding the recovery of global meteorological conditions. However, the question remains as to whether nations will be able to maintain the same kind of pollution reduction in the future. This research is conducted to find the solution to this question. Overall, this study suggests that countries can control greenhouse emissions, thereby achieving long-term environmental sustainability.

MATERIALS AND METHODS

Data Description

This research aims to analyze the GHG emission data during the COVID-19 pandemic, in the period from March 3, 2020, to July 27, 2021. The fundamental reason behind the data selection period is that the first COVID-19 confirmed case in Delhi was recorded on March 3, 2020, and all data available at time of writing were included. The GHGs are considered as dependent variables, i.e., the nitrogen dioxide (NO_2), ammonia (NH_3), sulfur dioxide (SO_2), and carbon monoxide (CO) measured in $\mu g/m^3$, which shows the micrograms of gaseous pollutant per cubic meter of ambient air in India. The daily data series of GHGs are presented in **Figure 1**. The COVID-19 factors are used as the independent factors i.e., Lockdown (LD), Confirmed COVID-19 Cases (CC), and Confirmed COVID-19 Deaths (CD). The daily data series of GHGs are obtained from the Central Control Room for Air Quality Management—All India, and the COVID-19 data are obtained from the World Health Organization (WHO). The lockdown data are generated based on restrictions, with the proxies generated as 1 representing restriction and 0 showing no restraint in the specified areas.

Research Methodology

This research specifies the four log–log models with NO_2, NH_3, SO_2, and CO with COVID-19. The simplest form of models is presented below:

$$NO_2 = f\ (LD,\ CC, CD) \tag{1}$$

$$NH_3 = f\ (LD, CC, CD) \tag{2}$$

$$SO_2 = f\ (LD,\ CC, CD) \tag{3}$$

$$CO = f\ (LD, CC, CD) \tag{4}$$

The log–log form of models:

$$NO_{2t} = \delta LD_t + \delta CC_t + \delta CD_t + \varepsilon_t \tag{5}$$

$$NH_{3t} = \delta LD_t + \delta CC_t + \delta CD_t + \varepsilon_t \tag{6}$$

$$SO_{2t} = \delta LD_t + \delta CC_t + \delta CD_t + \varepsilon_t \tag{7}$$

$$CO_t = \delta LD_t + \delta CC_t + \delta CD_t + \varepsilon_t \tag{8}$$

Nitrogen dioxide (NO_2), ammonia (NH_3), sulfur dioxide (SO_2), and carbon monoxide (CO) are considered as dependent variables. The measurement scale of these selected greenhouse gases is micrograms of gaseous pollutant per cubic meter of ambient air. The COVID-19 parameters for structuring the models are lockdown, and confirmed cases and confirmed deaths of COVID-19. The last term of the equation $\boldsymbol{\varepsilon_t}$ is an indication of an error term that measures data disturbance (Dar et al., 2021; Naseem et al., 2021; Sarfraz et al., 2021).

After designing the fundamental research structure, first, the stationarity of time series data is checked for the accuracy of different results. Then, the unit-root presence is confirmed with the nonstationarity of the data series. Finally, the basic equation of the Augmented Dickey–Fuller test is given as follows:

$$ADF\ \Delta y_t = \alpha_0 + \alpha y_{t-1} + \sum\nolimits_{i=1}^{p} \beta_j \Delta y_{t-i} + \varepsilon_t \tag{9}$$

In the above equation, α_0 is a constant, $\Delta y_t = \alpha_0 + \mu_t$, and $y_t = y_0 + \sum_{i=1}^{t} \mu_i + \alpha_0 t$. The deterministic trend is coming from $\alpha_0 t$, and the stochastic intercept term is coming from $y_0 + \sum_{i=1}^{t} \mu_i$, resulting in what is referred to as a stochastic trend.

Autoregressive Distributed Lag Model

The long- and short-run relationship can be checked by implementing the ARDL model's cointegration approach on the selected data series. The ARDL model is the best model when the integration orders are a mixture of level I(0) and the first difference I(1) (Naseem et al., 2020; Mohsin et al., 2021). ARDL instantaneously acquires the dynamic, short- and long-run coefficients. Additionally, the OLS method is employed to check the cointegration relationship of NO_2, NH_3, SO_2, and CO with COVID-19. The conditional error-correction model is given as follows:

$$\begin{aligned}\Delta lnNO_2 &= \alpha_0 + \sum_{i=1}^{m}\varphi_i\Delta lnNO_{2t-i} + \sum_{i=0}^{m}\omega_i\Delta lnLD_{t-i} \\ &+ \sum_{i=0}^{m}\beta_i\Delta lnCC_{t-i} + \sum_{i=0}^{m}\omega_i\Delta lnCD_{t-i} + \lambda_1 lnNO_{2t-1} \\ &+ \lambda_2 lnLD_{t-1} + \lambda_3 lnCC_{t-1} + \lambda_4 CD_{t-1} + \varepsilon_t ,\end{aligned} \tag{10}$$

$$\begin{aligned}\Delta lnNH_3 &= \alpha_0 + \sum_{i=1}^{m}\varphi_i\Delta lnNH_{3t-i} + \sum_{i=0}^{m}\omega_i\Delta lnLD_{t-i} \\ &+ \sum_{i=0}^{m}\beta_i\Delta lnCC_{t-i} + \sum_{i=0}^{m}\omega_i\Delta lnCD_{t-i} + \lambda_1 lnNH_{3t-1} \\ &+ \lambda_2 lnLD_{t-1} + \lambda_3 lnCC_{t-1} + \lambda_4 CD_{t-1} + \varepsilon_t ,\end{aligned} \tag{11}$$

$$\begin{aligned}\Delta lnSO_2 &= \alpha_0 + \sum_{i=1}^{m}\varphi_i\Delta lnSO_{2t-i} + \sum_{i=0}^{m}\omega_i\Delta lnLD_{t-i} + \sum_{i=0}^{m}\beta_i\Delta lnCC_{t-i} \\ &+ \sum_{i=0}^{m}\omega_i\Delta lnCD_{t-i} + \lambda_1 lnSO_{2t-1} + \lambda_2 lnLD_{t-1} \\ &+ \lambda_3 lnCC_{t-1} + \lambda_4 CD_{t-1} + \varepsilon_t,\end{aligned} \tag{12}$$

$$\begin{aligned}\Delta lnCO &= \alpha_0 + \sum_{i=1}^{m}\varphi_i\Delta lnCO_{t-i} + \sum_{i=0}^{m}\omega_i\Delta lnLD_{t-i} + \sum_{i=0}^{m}\beta_i\Delta lnCC_{t-i} \\ &+ \sum_{i=0}^{m}\omega_i\Delta lnCD_{t-i} + \lambda_1 lnCO_{t-1} + \lambda_2 lnLD_{t-1} \\ &+ \lambda_3 lnCC_{t-1} + \lambda_4 CD_{t-1} + \varepsilon_t ,\end{aligned} \tag{13}$$

In the above equations, cointegration among the dependent and independent variables is checked individually, such as NO_2 $(\lambda_1 lnNO_{2t-1} + \lambda_2 lnLD_{t-1} + \lambda_3 lnCC_{t-1} + \lambda_4 CD_{t-1})$, NH_3 $(\lambda_1 lnNH_{3t-1} + \lambda_2 lnLD_{t-1} + \lambda_3 lnCC_{t-1} + \lambda_4 CD_{t-1})$, SO2 $(\lambda_1 lnSO_{2t-1} + \lambda_2 lnLD_{t-1} + \lambda_3 lnCC_{t-1} + \lambda_4 CD_{t-1})$, and CO $(\lambda_1 lnCO_{t-1} + \lambda_2 lnLD_{t-1} + \lambda_3 lnCC_{t-1} + \lambda_4 CD_{t-1})$. The null hypothesis of this method shows that no cointegration exists among variables, which can be presented as $H_0 = \lambda NO_2 = \lambda LD = \lambda CC = \lambda\ CD = 0$, $H_0 = \lambda NH_3 = \lambda LD = \lambda CC = \lambda C\quad D = 0$, $H_0 = \lambda SO_2 = \lambda LD = \lambda CC = \lambda CD = 0$, *and* $H_0 = \lambda CO = \lambda LD = \lambda CC = \lambda CD = 0$. The alternative hypothesis has shown the existence of cointegration by utilizing the equation as $H_1 = \lambda NO_2 \neq \lambda LD \neq \lambda CC \neq \lambda CD \neq 0$, $H_1 = \lambda NH_3 \neq \lambda LD \neq \lambda CC \neq \lambda CD \neq 0$, $H_1 = \lambda SO_2 \neq \lambda LD \neq \lambda CC \neq \lambda CD \neq 0$, *and* $H_1 = \lambda CO \neq \lambda LD \neq \lambda CC \neq \lambda CD \neq 0$. The third measuring scale of cointegration is inconclusive cointegration, which is checked based on the lower bound value and upper bound value with a comparison of the F-statistics value (Sulaiman and Abdul-Rahim, 2018). The confirmation of cointegration among variables is a clear indication to apply the short- and long-run ARDL models.

Short-run ARDL model:

$$\begin{aligned}\Delta lnNO_2 &= \alpha_0 + \sum_{i=1}^{m}\varphi_i\Delta lnNO_{2t-i} + \sum_{i=0}^{m}\omega_i\Delta lnLD_{t-i} \\ &+ \sum_{i=0}^{m}\beta_i\Delta lnCC_{t-i} + \sum_{i=0}^{m}\omega_i\Delta lnCD_{t-i} + \lambda ECT_{t-1} + \varepsilon_t,\end{aligned} \tag{14}$$

$$\begin{aligned}\Delta lnNH_3 &= \alpha_0 + \sum_{i=1}^{m}\varphi_i\Delta lnNH_{3t-i} + \sum_{i=0}^{m}\omega_i\Delta lnLD_{t-i} \\ &+ \sum_{i=0}^{m}\beta_i\Delta lnCC_{t-i} + \sum_{i=0}^{m}\omega_i\Delta lnCD_{t-i} + \lambda ECT_{t-1} + \varepsilon_t,\end{aligned} \tag{15}$$

$$\begin{aligned}\Delta lnSO_2 &= \alpha_0 + \sum_{i=1}^{m}\varphi_i\Delta lnSO_{2t-i} + \sum_{i=0}^{m}\omega_i\Delta lnLD_{t-i} + \sum_{i=0}^{m}\beta_i\Delta lnCC_{t-i} \\ &+ \sum_{i=0}^{m}\omega_i\Delta lnCD_{t-i} + \lambda ECT_{t-1} + \varepsilon_t,\end{aligned} \tag{16}$$

$$\begin{aligned}\Delta lnCO &= \alpha_0 + \sum_{i=1}^{m}\varphi_i\Delta lnNO_{2t-i} + \sum_{i=0}^{m}\omega_i\Delta lnLD_{t-i} \\ &+ \sum_{i=0}^{m}\beta_i\Delta lnCC_{t-i} + \sum_{i=0}^{m}\omega_i\Delta lnCD_{t-i} + \lambda ECT_{t-1} + \varepsilon_t.\end{aligned} \tag{17}$$

Long-run ARDL model:

$$\begin{aligned}\Delta lnNO_2 &= \alpha_0 + \sum_{i=1}^{m}\varphi_i\Delta lnNO_{2t-i} + \sum_{i=0}^{m}\omega_i\Delta lnLD_{t-i} \\ &+ \sum_{i=0}^{m}\beta_i\Delta lnCC_{t-i} + \sum_{i=0}^{m}\omega_i\Delta lnCD_{t-i} + \varepsilon_t,\end{aligned} \tag{18}$$

$$\begin{aligned}\Delta lnNH_3 &= \alpha_0 + \sum_{i=1}^{m}\varphi_i\Delta lnNH_{3t-i} + \sum_{i=0}^{m}\omega_i\Delta lnLD_{t-i} \\ &+ \sum_{i=0}^{m}\beta_i\Delta lnCC_{t-i} + \sum_{i=0}^{m}\omega_i\Delta lnCD_{t-i} + \varepsilon_t,\end{aligned} \tag{19}$$

$$\begin{aligned}\Delta lnSO_2 &= \alpha_0 + \sum_{i=1}^{m}\varphi_i\Delta lnSO_{2t-i} + \sum_{i=0}^{m}\omega_i\Delta lnLD_{t-i} + \sum_{i=0}^{m}\beta_i\Delta lnCC_{t-i} \\ &+ \sum_{i=0}^{m}\omega_i lnCD_{t-i} + \varepsilon_t,\end{aligned} \tag{20}$$

TABLE 1 | Descriptive statistics.

	NO_2	NH_3	SO_2	CO	CC	CD
Mean	27.489	25.698	14.599	1.040	524379	27.489
Maximum	88.870	116.150	46.900	4.960	1436207	88.870
Minimum	0.630	0.420	3.620	0.200	6	0.630
Std. Dev.	16.408	15.939	6.891	0.547	482055	16.408
Skewness	1.215	2.149	1.389	1.641	0.758	1.215
Kurtosis	4.594	9.054	5.469	8.697	2.380	4.594
Jarque–Bera	172.043	1123.102	281.429	880.735	54.665	172.043

TABLE 2 | Augmented Dickey–Fuller (ADF) test results.

Variables	Constant	
	Level	1st Diff
NO_2	−5.794*	−15.200*
	[0.000]	...
NH_3	−6.359*	−14.810*
	[0.000]	...
SO_2	−3.025*	−17.494*
	[0.033]	...
CO	−8.213*	−20.977*
	[0.000]	...
LD	−3.882*	−22.105*
	[0.002]	...
CC	0.529	−4.562*
	[0.987]	[0.000]
CD	−0.366	−2.889*
	[0.912]	[0.047]

*Note: "***, **, and * represent 1, 5, and 10% respectively".*

TABLE 3 | Bound test results.

Green house gases (GHG)	F-statistics	Level of significance	Bound test critical values (unrestricted intercept and no trend)	
			I(0)	I(1)
NO_2	13.916*	10%	2.72	3.77
Lag criteria	[3,3,1,0]	5%	3.23	4.35
		2.50%	3.69	4.89
		1%	4.29	5.61
NH_3	13.521*	10%	2.72	3.77
Lag criteria	[3,3,1,0]	5%	3.23	4.35
		2.50%	3.69	4.89
		1%	4.29	5.61
SO_2	7.424*	10%	2.72	3.77
Lag criteria	[3,3,1,0]	5%	3.23	4.35
		2.50%	3.69	4.89
		1%	4.29	5.61
CO	12.717*	10%	2.72	3.77
Lag criteria	[3,3,1,0]	5%	3.23	4.35
		2.50%	3.69	4.89
		1%	4.29	5.61

*Note: "***, **, and * represent 1, 5, and 10% respectively".*

$$\Delta lnCO = \alpha_0 + \sum_{i=1}^{m} \varphi_i \Delta lnCO_{t-i} + \sum_{i=0}^{m} \omega_i \Delta lnLD_{t-i} + \sum_{i=0}^{m} \beta_i \Delta lnCC_{t-i} + \sum_{i=0}^{m} \omega_i \Delta lnCD_{t-i} + \varepsilon_t. \quad (21)$$

The main models of short run and long run are presented above. The ECT term of the short-run model is to measure the speed of adjustment from the short to the long run. The sign of λ is used for the coefficient of ECT term. The ECT value must be between 0 and −1, while the lagged ECT value checks the error ratio in the previous period. Finally, the post-normality tests (serial correlation, heteroskedasticity, and functional form) are employed in the last method implication process to check the validity of the results.

EMPIRICAL RESULTS

Table 1 contains the summary of descriptive results of the data series. The mean values are NO_2 (27.489), NH_3 (25.698), SO_2 (14.599), and CO (1.040), confirmed COVID cases (524379), and confirmed deaths (27.489). The maximum range and minimum range of the data series are highly differentiated against each other, leading to instability. The content of the dependent variables is from 0.200 to 116.150, while the range of the independent variables is highly unpredictable and fluctuates between 0.630 and 1436207. Due to the unstructured data series with increasing trend, especially in COVID-19 cases and deaths, the standard deviation lies between 0.547 and 482,055. The confirmed cases of COVID-19 have shown a highly deviated series in the selected set of variables. The skewness confirms the positive skewness in all variables. The value of kurtosis is more than 3 in all series except the confirmed cases of COVID-19. The confirmed cases of COVID-19 show the normal distribution, and the remaining series are all leptokurtic. The range of Jarque–Bera is 54.665–1123.102, which is used to check the goodness-of-fit test.

The ADF results are presented in **Table 2**, which is employed to check the stationarity of the data series. The alternative hypothesis of ADF is checked on the stationary method, and the results indicate that some variables are stationary at the level and some at first difference. This mixture of results confirms the feasible ground to run the ARDL method (Sulaiman and Abdul-Rahim, 2018; Mishra and Kumar, 2021). All dependent variables are significant at the level, and the first difference is at 1% significance level. In comparison, the independent variables, i.e., confirmed cases and death via COVID-19, are significant at first, showing a 1% significance level.

TABLE 4 | The estimated short-run coefficients based on Akaike information criterion (AIC).

Variables	Coefficients	St. error	T-value
NO_2			
C	13.49468*	1.842284	7.324973
Δ [NO_2(−1)]	0.038881	0.045836	0.84827
Δ [NO_2(−2)]	−0.087259**	0.044565	−1.95803
Δ (CC)	0.000161	0.000284	0.567726
Δ [CC(−1)]	0.000884*	0.000332	2.658725
Δ [CC(−2)]	−0.001027*	0.000286	−3.58573
Δ (CD)	−0.021524*	0.007465	−2.88321
ECT(−1)	−0.257156*	0.03436	−7.48426
R^2: 0.169, DW-statistic: 2.00, AIC: 6.945, F-stat.: 13.94*** (0.000)			
NH_3			
C	8.773747*	1.246347	7.03957
Δ [NH_3(−1)]	−0.19944*	0.027165	−7.34174
Δ[CC)	−3.50E-06	6.57E-06	−0.53257
Δ(CD)	0.000152	0.000406	0.374799
Δ[LD(−1)]	−3.87178*	1.12675	−3.43623
Δ (LD)	−14.07442*	4.826,772	−2.915907
ECT(−1)	−0.199436*	0.027035	−7.377024
R^2: 0.1147, DW-statistic: 2.00, AIC: 7.09, F-stat.: 31.429*** (0.000)			
SO_2			
C	4.71924*	0.868681	5.432649
Δ [SO_2(−1)]	−0.230942*	0.054661	−4.225002
Δ [SO_2(−2)]	−0.091291***	0.052579	−1.736265
Δ [SO_2(−3)]	−0.102303*	0.046094	−2.219422
Δ (CC)	0.000402*	0.000151	2.656648
Δ [CC(−1)]	0.000185	0.000169	1.096123
Δ [CC(−2)]	−0.00055*	0.000147	−3.748432
Δ (CD)	−0.008534*	0.004104	−2.079368
ECT(−1)	−0.246466*	0.045085	−5.466659
R^2: 0.224958, DW-statistic: 2.04, AIC: 5.59, F-stat.: 17.27001*** (0.000)			
CO			
C	0.373074*	0.063509	−7.094238
Δ [CO(−1)]	−0.264676*	0.037309	2.367769
Δ [CO(−2)]	−0.109412*	0.045249	5.874318
Δ (CC)	6.92E-07*	2.92E-07	−2.226025
Δ (CD)	−3.99E-05*	1.79E-05	−2.732661
Δ (LD)	−0.122874*	0.044965	−1.054816
ECT(−1)	−0.264676*	0.036995	−7.154398
R^2: 0.1628, DW-statistic: 1.9971, AIC: 0.759735, F-stat.: 31.26532*** (0.000)			

*Note: "***, **, and * represent 1, 5, and 10% respectively".*

TABLE 5 | ARDL long-run form and bound test results.

Regressor	Coefficients	T-ratios
NO_2		
LD	−26.7437*	−7.25479
CC	0.000134*	3.739323
CD	−0.007706*	−3.554897
NH_3		
LD	−19.41362*	−3.818383
CC	−1.76E-05	−0.535349
CD	0.000763	0.376001
SO_2		
LD	−1.803963	−0.914273
CC	8.40E-05*	4.40155
CD	−0.005083*	−4.416934
CO		
LD	−0.464243*	−2.852327
CC	2.61E-06*	2.513787
CD	−0.000151*	−2.342845

*Note: "***, **, and * represent 1, 5, and 10% respectively".*

Table 3 contains the result of the bound test, which is generally used to check the binding of variables for long-term and short-term interactions. This test is based on the mixture of integrated results of ADF to avoid spurious results (Naseem et al., 2021; Sarfraz et al., 2021). The value of F-statistics is higher than tabulated, which confirms the significance of all variables at 1% significance level. The significance of all variables indicates that the long-run relationship among variables and the rejection of the null hypothesis of no cointegration exists.

The short-run ARDL model is employed, and the results are presented in **Table 4**. Before explaining the results, it is necessary to mention that the software automatically selected the lags and behavior of variables and delivered the final form (Sarfraz et al., 2020; Naseem et al., 2021; Sarfraz et al., 2021), which is presented in **Table 4** under consideration of a specific set of variables. The first and third interacted variables toward the independent variable are NO_2 and SO_2, which authorize the significance of confirmed cases and deaths of COVID-19 at a 1% level of significance. The values of the ECT coefficient are −0.257156 and −0.246966, which satisfy the basic assumption of negative significance. According to the value of the coefficient, long-run equilibrium speed from the short run is corrected about 25.7156 and 24.6966%, which is slow, taking approximately 3.89 and 4.05 periods, respectively. The second variable, NH_3, elucidated its relationship with lockdown only at 1% significance level, while the ECT term is negatively significant with the value of −0.199436. The value of the ECT coefficient demonstrates that the return to equilibrium from the short to long run required almost 5.01 periods. The last dependent variable, CO, shows a significant relationship with lockdown, confirmed cases, and deaths at 1% level. The error correction term is also negative and significant, with a value of −0.264676. The short-term return to the long-run equilibrium with 26.4676% speed will take approximately 3.78 periods. The values of R^2, Durban–Watson statistic, Akaike information criterion (AIC), and F-statistic are presented for individual variables to check the model fitness.

The long-run ARDL model is employed, and the extracted results of the long-run are presented in **Table 5**. The results reveal that lockdown and confirmed cases and deaths of COVID-19 have a long-run relationship with NO_2 and CO at a 1% level of significance. SO_2 emission shows a significant relationship with confirmed cases and confirmed deaths, while NH_3 is significantly related to lockdown only. The sign of negativity with coefficients of variables indicates emission reduction in specific gases under specific circumstances. Nitrogen dioxide (NO_2) and carbon monoxide (CO) are primarily emitted in air by fuel burning (Somani et al., 2020). Meanwhile, the primary source of nitrogen dioxide emissions is vehicles, i.e., trucks, cars, and buses; power plants; and offload equipment. The confirmed cases have a positive interaction with NO_2 because of people using vehicles to travel from home to hospitals. Still, the confirmed deaths and lockdown are negatively related because the lockdown reduces the percentage of traveling and established deaths are behind the lockdown (Beig et al., 2021; Mele and Magazzino, 2021). The sources of NH_3 emission are agriculture, animal husbandry, and

TABLE 6 | The results of the autoregressive distributed lag diagnostic tests.

Test statistics	LM-version	F-version
NO_2		
A: serial correlation	CHSQ(2) = 0.607282 (0.7381)	F(2,473) = 0.295889 (0.744)
B: heteroskedasticity	CHSQ(35) = 47.47963 (0.0776)	F(35,415) = 1.395153(0.0709)
C: functional form	CHSQ(474) = 0.293541(0.7692)	F(1,474) = 0.086166 (0.7692)
NH_3		
A: serial correlation	CHSQ(2) = 1.160904 (0.5596)	F (2,480) = 0.572298 (0.5646)
B: heteroskedasticity	CHSQ(1) = 75.90042(0.000)	F (1,485) = 89.54449 (0.000)
C: functional form	CHSQ(481) = 0.854845 (0.3931)	F (1,481) = 0.73076 (0.3931)
SO_2		
A: serial correlation	CHSQ(2) = 6.251483 (0.0439)	F(2,471) = 3.075152(0.0471)
B: heteroskedasticity	CHSQ(1) = 18.65458(0.000)	F(1,482) = 19.32223 (0.000)
C: functional form	CHSQ(472) = 3.044351(0.0025)	F(1,472) = 9.268,075(0.0025)
CO		
A: serial correlation	CHSQ(2) = 0.296043(0.8624)	F(2,477) = 0.145369 (0.8647)
B: heteroskedasticity	CHSQ(100) = 90.26277(0.7469)	F(100,285) = 0.869856 (0.7913)
C: functional form	CHSQ(478) = 3.100357 (0.002)	F(1, 478) = 9.612211 (0.002)

*"***, **, and * are significant at 1, 5, and 10% levels, respectively".*

Note: "The values in parentheses are probability values. LM, lagrange multiplier; A, Langrange multiplier test of residual serial correlation; B, based on the regression of squared residuals on squared fitted values; CHSQ, chi-square; and C, Ramsey's RESET test using the square of the fitted values".

NH_3-based fertilizer applications; hence, it does not show any relationship with confirmed cases and deaths. The lockdown restricted people in their homes, which strongly affected all human activities (Mohsin et al., 2021; Naseem et al., 2021). The SO_2 emission sources are related to burning of fossil fuels such as coal, oil, diesel, and materials containing a minor or significant quantity of sulfur. The main hubs of SO_2 emission are power plants and metal processing and smelting facilities, which are more relevant to labor than public lockdown. The threatening condition of the pandemic breakout restricted people from going to workplaces, and most workplaces were closed. Hence, a relationship was detected toward confirmed cases and deaths rather than lockdown.

The results of the ARDL diagnostic test are given in **Table 6**, which covers three main reliability tests, i.e., serial correlation, heteroskedasticity, and functional form. In our data series (NO_2, NH_3, and SO_2), the variance is unequal over a range of measured values or unequal scattered residuals of regression; this caused the issue of heteroskedasticity to be observed in the series. Furthermore, the data series used in this research for analysis are strongly related to each other, so diagnostic tests show significance due to the strong interaction of data series (Sulaiman and Abdul-Rahim, 2018). Finally, the serial correlation test strongly rejects the null hypothesis and confirms the reliability of the results.

DISCUSSION

The National Capital Territory (NCT) of Delhi is one of the world's oldest cities. New Delhi, the capital of India, is also in the Union Territory of Delhi. This 1,484 square kilometers (573 Sq mi) historical city is interlinked with Haryana and Uttar Pradesh. According to the United Nations (UN), with regional coverage of 28 million people, Delhi is the second-largest urban populated area in the world. The air quality of Delhi is hazardous (500+), which causes lung diseases, especially asthma and cancer. The GHG emissions and poor quality of air have reduced the winter temperature of Delhi since 1998, the fundamental reason for the quick spreading of COVID-19 in Delhi. Being the capital of India, an industrial hub, cultural core, and contributor of GDP, the GHG emissions are a significant problem for the city. As COVID-19 became a game-changer for the world, Delhi also went through some positive changes. On March 3, 2020, the first confirmed case was reported in Delhi and the notification of lockdown was circulated on March 24, 2020. This research has explored the analytical data from March 3, 2020, to July 27, 2021. The results of this research confirmed a negative and a long-term relationship among the dependent and independent variables. The COVID-19 pandemic and lockdown dramatically reduced the level of toxic GHG emissions and enhanced Delhi's air quality. A vibrant change is observed in NO_2, SO_2, and CO emissions due to the reduction in fuel burning, transport, material processing, and plant running activities. At the same time, NH_3 was not highly affected because it is directly related to agricultural activities. This research identified that the mismanagement of city policies and carelessness in terms of environmental sustainability in Delhi are the key reasons for over-toxic emissions. The collaborative efforts of the Government of India, city governance, policymakers, and environmentalists can reduce GHG emissions and improve the quality of the environment.

CONCLUSION

India was severely affected by COVID-19 due to its temperature range between 27°C and 32°C and humidity level from 25 to 45% (Sasikumar et al., 2020). These specific ranges of humidity and temperature are most ideal for the survival and growth of COVID-19. Rapidly increasing temperature ranges are undoubtedly related to global warming. The release of unnecessary GHGs into air is the cause of uncontrollable

global warming. As such, by leading to reductions in the GHG release, social distancing, SOPs, lockdown, and other precautions adopted positively contributed to the environmental sustainability in India.

This research work also explains the behavior of various GHGs during the COVID-19 period. In this research, we examined the daily data regarding GHG emissions in Delhi from March 3, 2020, to July 27, 2021. The data series were collected from official websites, i.e., the World Health Organization (WHO) and the Central Control Room for Air Quality Management—All India. Our findings revealed a short- and long-run relationship between NO_2, NH_3, SO_2, and CO and COVID-19.

Although the speed of adjustment from the short-run to long-run equilibrium was minor in all the variables, the error correction term's negative significance supported the existence of a long-run relationship among the exogenous and endogenous variables. NO_2, SO_2, and CO are anthropologically related to fossil fuel burning, transport, material processing, and plant running, which were closed under the lockdown, except for household fuel burning. These dramatic changes showed a declining trend in the emission of these GHGs. The results were also confirmed by the negative significance of variables for the short and long run. Meanwhile, NH_3 comes from agricultural activities, which were not highly affected in the long and short run. Undoubtedly, agricultural activities were also restricted during the pandemic breakout, but the fields were still able to grow as normal.

Recommendations, Limitations, and Future Direction

The main limitation of this research is the data variables. The data are collected during the COVID-19 period by considering specific variables, and the current study considers overall specific time period data. Therefore, future research can be divided into three parts, i.e., Delhi before COVID-19, Delhi under COVID-19, and Delhi under farmer protest. These topics can be individually discussed and compared with different situations concerning GHG emissions and the environmental quality. In the analytical implementation, divergent econometric methods such as the ARDL method, linear regression, and dynamic regression can be utilized.

Overall, the current research work can act as a guideline for the Government of India, policymakers, and environmentalists to design new policies and frameworks for a sustainable environment. The main reasons for the toxic gases emission are now recognized due to the unique situation caused by the COVID-19 pandemic. As such, it is apparent that there is a need for improvements in transport systems, industries, material processing plants, and environment-friendly technology in every field of life. As per the environmental performance index, if India is unable to maintain ecological sustainability and enhance the quality of the environment, more people will die than from COVID-19.

DATA AVAILABILITY STATEMENT

Publicly available datasets were analyzed in this study. These data can be found here: https://app.cpcbccr.com/ccr/#/login (Central Control Room for Air Quality Management Delhi-NCR).

AUTHOR CONTRIBUTIONS

All authors listed have made a substantial, direct, and intellectual contribution to the work and approved it for publication.

ACKNOWLEDGMENTS

Data contributions are acknowledged to Delhi Pollution Control Committee, Haryana Pollution Control Board, Rajasthan Pollution Control Board, and Uttar Pradesh Pollution Control Board. This research work was also supported by the construct program of the applied characteristic discipline "Applied Economics" in Hunan Province, China.

REFERENCES

Beig, G., Korhale, N., Rathod, A., Maji, S., Sahu, S. K., Dole, S., et al. (2021). On Modelling Growing Menace of Household Emissions under COVID-19 in Indian Metros. *Environ. Pollut.* 272, 115993. doi:10.1016/j.envpol.2020.115993

Conibear, L., Butt, E. W., Knote, C., Arnold, S. R., and Spracklen, D. V. (2018). Residential Energy Use Emissions Dominate Health Impacts from Exposure to Ambient Particulate Matter in India. *Nat. Commun.* 9 (1), 617–619. doi:10.1038/s41467-018-02986-7

Dar, A. A., Pan, B., Qin, J., Zhu, Q., Lichtfouse, E., Usman, M., et al. (2021). A Review on Sustainable Ferrate Oxidation: Reaction Chemistry, Mechanisms and Applications to Eliminate Micro Pollutant (Pharmaceuticals) in Wastewater. *Environ. Pollut.* 117957. doi:10.1016/j.envpol.2021.117957

Gautam, S., and Hens, L. (2020). SARS-CoV-2 Pandemic in India: What Might We Expect?. *Environ. Dev. Sustain.* 22, 3867–3869. doi:10.1007/s10668-020-00739-5

Huang, X., Ding, A., Gao, J., Zheng, B., Zhou, D., Qi, X., et al. (2021). Enhanced Secondary Pollution Offset Reduction of Primary Emissions during COVID-19 Lockdown in China. *Natl. Sci. Rev.* 8 (2), nwaa137. doi:10.1093/nsr/nwaa137

Kumar, A., and Kumar, M. (2020). *Assessment of Biomass and Soil Carbon Stock in the Hydroelectric Catchment of Uttarakhand Himalayas*. India: J. Sustan. Forest, 36.

Kumar, A., and Gupta, H. (2020). Activated Carbon from Sawdust for Naphthalene Removal from Contaminated Water. *Environ. Technol. Innovation* 20, 101080. doi:10.1016/j.eti.2020.101080

Kumar, A., Kumar, M., Pandey, R., ZhiGuo, Y., and Cabral-Pinto, M. (2021). Forest Soil Nutrient Stocks along Altitudinal Range of Uttarakhand Himalayas: An Aid to Nature Based Climate Solutions. *CATENA* 207, 105667. doi:10.1016/j.catena.2021.105667

Kumar, A., Pinto, M. C., Candeias, C., and Dinis, P. A. (2021). Baseline Maps of Potentially Toxic Elements in the Soils of Garhwal Himalayas, India: Assessment of Their Eco-environmental and Human Health Risks. *Land Degrad. Dev.* 32 (14), 3856–3869. doi:10.1002/ldr.3984

Mandal, A., Roy, R., Ghosh, D., Dhaliwal, S., Toor, A., Mukhopadhyay, S., et al. (2020). COVID-19 Pandemic: Sudden Restoration in Global Environmental Quality and its Impact on Climate Change. *EnerarXiv Preprint*.

Manisalidis, I., Stavropoulou, E., Stavropoulos, A., and Bezirtzoglou, E. (2020). Environmental and Health Impacts of Air Pollution: a Review. *Front. Public Health* 8, 14. doi:10.3389/fpubh.2020.00014

McDonald, A. J., Balwinder-Singh, M. L., Jat, M. L., Craufurd, P., Hellin, J., Hung, N. V., et al. (2020). Indian Agriculture, Air Pollution, and Public Health in the Age of COVID. *World Develop.* 135, 105064. doi:10.1016/j.worlddev.2020.105064

Mele, M., and Magazzino, C. (2021). Pollution, Economic Growth, and COVID-19 Deaths in India: a Machine Learning Evidence. *Environ. Sci. Pollut. Res.* 28 (3), 2669–2677. doi:10.1007/s11356-020-10689-0

Mishra, S., and Kumar, A. (2021). Estimation of Physicochemical Characteristics and Associated Metal Contamination Risk in the Narmada River, India. *Environ. Eng. Res.* 26 (1), 1–11. doi:10.4491/eer.2019.521

Mohsin, M., Zhu, Q., Naseem, S., Sarfraz, M., and Ivascu, L. (2021). Mining Industry Impact on Environmental Sustainability, Economic Growth, Social Interaction, and Public Health: An Application of Semi-quantitative Mathematical Approach. *Processes* 9 (6), 972. doi:10.3390/pr9060972

Naseem, S., Fu, G. L., Mohsin, M., Rehman, M. Z.-u., and Baig, S. A. (2020). Semi-Quantitative Environmental Impact Assessment of Khewra Salt Mine of Pakistan: an Application of Mathematical Approach of Environmental Sustainability. *Mining, Metall. Exploration* 37, 1185–1196. doi:10.1007/s42461-020-00214-9

Naseem, S., Mohsin, M., Hui, W., Liyan, G., and Penglai, K. (2021). The Investor Psychology and Stock Market Behavior during the Initial Era of COVID-19: a Study of China, Japan, and the United States. *Front. Psychol.* 12, 16. doi:10.3389/fpsyg.2021.626934

Sarfraz, M., Mohsin, M., Naseem, S., and Kumar, A. (2021). Modeling the Relationship between Carbon Emissions and Environmental Sustainability during COVID-19: a New Evidence from Asymmetric ARDL Cointegration Approach. *Environ. Develop. Sustainability*, 1–19. doi:10.1007/s10668-021-01324-0

Sarfraz, M., Shehzad, K., and Farid, A. (2020). Gauging the Air Quality of New York: a Non-linear Nexus between COVID-19 and Nitrogen Dioxide Emission. *Air Qual. Atmos. Health* 13 (9), 1135–1145. doi:10.1007/s11869-020-00870-2

Sasikumar, K., Nath, D., Nath, R., and Chen, W. (2020). Impact of Extreme Hot Climate on COVID-19 Outbreak in India. *GeoHealth* 4 (12), e2020GH000305. doi:10.1029/2020GH000305

Sharma, S., Zhang, M., Anshika, J., Gao, J., Zhang, H., and Kota, S. H. (2020). Effect of Restricted Emissions during COVID-19 on Air Quality in India. *Sci. Total Environ.* 728, 138878. doi:10.1016/j.scitotenv.2020.138878

Singh, V., Singh, S., Biswal, A., Kesarkar, A. P., Mor, S., and Ravindra, K. (2020). Diurnal and Temporal Changes in Air Pollution during COVID-19 Strict Lockdown over Different Regions of India. *Environ. Pollut.* 266, 115368. doi:10.1016/j.envpol.2020.115368

Somani, M., Srivastava, A. N., Gummadivalli, S. K., and Sharma, A. (2020). Indirect Implications of COVID-19 towards Sustainable Environment: an Investigation in Indian Context. *Bioresour. Technol. Rep.* 11, 100491. doi:10.1016/j.biteb.2020.100491

Sulaiman, C., and Abdul-Rahim, A. S. (2018). Population Growth and CO2 Emission in Nigeria: a Recursive ARDL Approach. *Sage Open* 8 (2), 2158244018765916. doi:10.1177/2158244018765916

Vadrevu, K. P., Eaturu, A., Biswas, S., Lasko, K., Sahu, S., Garg, J. K., et al. (2020). Spatial and Temporal Variations of Air Pollution over 41 Cities of India during the COVID-19 Lockdown Period. *Sci. Rep.* 10 (1), 16574–16615. doi:10.1038/s41598-020-72271-5

Vulichi, S. R., Kabra, A., Khalid, M., Kumar, R., and Cruz-Martins, N. (2021). Interlink between Pollution and COVID-19 in India: Compelling View and Key Attributes. *Environ. Sci. Pollut. Res.* 28 (16), 19539–19542. doi:10.1007/s11356-021-13451-2

Wang, P., Chen, K., Zhu, S., Wang, P., and Zhang, H. (2020). Severe Air Pollution Events Not Avoided by Reduced Anthropogenic Activities during COVID-19 Outbreak. *Resour. Conservation Recycling* 158, 104814. doi:10.1016/j.resconrec.2020.104814

Conflict of Interest: The authors declare that the research was conducted in the absence of any commercial or financial relationships that could be construed as a potential conflict of interest.

Publisher's Note: All claims expressed in this article are solely those of the authors and do not necessarily represent those of their affiliated organizations, or those of the publisher, the editors and the reviewers. Any product that may be evaluated in this article, or claim that may be made by its manufacturer, is not guaranteed or endorsed by the publisher.

frontiers in Environmental Science

ORIGINAL RESEARCH
published: 28 October 2021
doi: 10.3389/fenvs.2021.724950

Quantifying Tree Diversity, Carbon Stocks, and Sequestration Potential for Diverse Land Uses in Northeast India

Uttam Kumar Sahoo[1], Om Prakash Tripathi[2], Arun Jyoti Nath[3], Sourabh Deb[4], Dhruba Jyoti Das[5], Asha Gupta[6], N. Bijayalaxmi Devi[7], Shiva Shankar Charturvedi[8], Soibam Lanabir Singh[1,9], Amit Kumar[10]* and Brajesh Kumar Tiwari[8]*

[1]Department of Forestry, Mizoram University, Aizawl, India, [2]Department of Forestry, North Eastern Regional Institute of Science & Technology, Itanagar, India, [3]Department of Ecology and Environment Science, Assam University, Silchar, India, [4]Department of Forestry and Biodiversity, Tripura University, Agartala, India, [5]Rain Forest Research Institute, Jorhat, India, [6]Department of Life Science, Manipur University, Imphal, India, [7]Department of Botany, Sikkim University, Gangtok, India, [8]Department of Environment Studies, North-Eastern Hill University, Shillong, India, [9]Department of Forestry, Dr. Rajendra Prasad Central Agricultural University, Bihar, India, [10]School of Hydrology and Water Resources, Nanjing University of Information Science and Technology, Nanjing, China

OPEN ACCESS

Edited by:
Moritz Bigalke,
University of Bern, Switzerland

Reviewed by:
Sileshi Gudeta Weldesemayat,
University of KwaZulu-Natal, South Africa
Sangram Chavan,
Indian Council of Agricultural Research (ICAR), India

***Correspondence:**
Uttam Kumar Sahoo
uttams64@gmail.com
Amit Kumar
amitkdah@nuist.edu.cn

Specialty section:
This article was submitted to Biogeochemical Dynamics, a section of the journal Frontiers in Environmental Science

Received: *14 June 2021*
Accepted: *15 September 2021*
Published: *28 October 2021*

Citation:
Sahoo UK, Tripathi OP, Nath AJ, Deb S, Das DJ, Gupta A, Devi NB, Charturvedi SS, Singh SL, Kumar A and Tiwari BK (2021) Quantifying Tree Diversity, Carbon Stocks, and Sequestration Potential for Diverse Land Uses in Northeast India. Front. Environ. Sci. 9:724950. doi: 10.3389/fenvs.2021.724950

In the modern era, rapid anthropogenic activities in the vicinity of the Himalayas disturb the carbon sequestration potential resulting in climate change. For the first time, this study estimates the biomass and carbon storage potential of Northeast India's diverse land uses through a biomass estimation model developed for this region. The mean tree density in tropical, subtropical, and temperate forests was 539, 554, and 638 trees ha^{-1}, respectively. The mean vegetation carbon stock was the highest for temperate forests (122.09 Mg C ha^{-1}), followed by subtropical plantations (115.45 Mg C ha^{-1}), subtropical forests (106.01 Mg C ha^{-1}), tropical forests (105.33 Mg C ha^{-1}), tropical plantations (93.00 Mg C ha^{-1}), and temperate plantations (50.10 Mg C ha^{-1}). Among the forests, the mean soil organic carbon (SOC) stock up to 45 cm depth was the highest for tropical forests (72.54 Mg C ha^{-1}), followed by temperate forests (63.4 Mg C ha^{-1}) and subtropical forests (42.58 Mg C ha^{-1}). A strong relationship between the tree basal area and biomass carbon storage was found for all land-use types. The land-use transformation from agriculture to agroforestry, and grassland to plantations increased both vegetation carbon (VC) and SOC stocks. The corresponding increase in VC and SOC was 40.80 and 43.34 Mg C ha^{-1}, respectively, in the former, and 83.18 and 97.64 Mg C ha^{-1} in the latter. In general, the landscape-level estimates were drawn from site-level estimates in a given land-use type, and therefore, the corresponding values might be overestimated. Nevertheless, the results provide baseline information on carbon stock which may serve as a reference for devising appropriate land-use change policies in the region.

Keywords: biodiversity hotspots, carbon storage, forest types, land use, species richness

INTRODUCTION

Since the mid-1900s, many objectives of global climate change research have shifted to reducing terrestrial carbon sources and enhancing sinks as a means of combating future climate change under carbon dioxide (CO_2) enrichment (Kumar et al., 2017). In general, CO_2 is a predominant greenhouse gas (GHG) in the atmosphere and a major contributor (>50%) to global warming. Studies have reported that a rapid change in land-use alone contributes to nearly 10% of global anthropogenic CO_2 emissions (IPCC, 2007; Le Quere et al., 2016). The tropical zones have shown an increased accumulation of atmospheric CO_2 to >400 ppm in 2015 (Betts et al., 2016), and this accumulation is projected to exceed 500 ppm by 2050 (Cai et al., 2014). Furthermore, the rapid increase of atmospheric CO_2 concentration will increase earth's surface temperature and further cause negative impacts (e.g., sea level rise, flooding, and increase ecological and human health risk) (IPCC, 2007; IPCC, 2014; Kumar et al., 2021). To combat these effects of climate change, the United Nations Framework Convention on Climate Change (UNFCCC) formulated "Reduction of Emissions from Deforestation and Forest Degradation" (REDD) policy in 2007, which was further enacted as REDD+ in 2010 (UNFCCC, 2008) to conserve and manage 2015 Pg (1 Pg = 1 giga ton = 10^{15}g = 1 million metric ton) of global terrestrial C stock. As per an estimate, the carbon emission from land-use change was 0.9 Pg C yr^{-1} during 2005 to 2014 (Le Quere et al., 2016). The Paris Agreement (2015) further emphasized on limiting the global temperature increase to 2°C by 2,100 and pursuing efforts to generate more carbon *via* agricultural materials through both conventional mitigation efforts and alternative routes (Gupta and Kumar, 2020; Kumar and Gupta, 2020), so as to limit the global temperature increase to 1.5°C. Terrestrial carbon stocks, especially in northeast India, are hotspots of current research as it covers an area of 26.3 million hectares which is equivalent to 8% of the total geographical area, and represents ~25% of the country's total forest area. In this perspective, studies on carbon accumulation in various pools (e.g., soil, vegetation, litter, *etc.*) in the terrestrial ecosystem can advance our understanding of climate change adaptation and mitigation. The rapid land-use change in Northeast India is driving climate change and biodiversity loss (Brahma et al., 2018; Ahirwal et al., 2021a; Deb et al., 2021). Thus, the conservation and sustainable development of land-use systems are expected to stabilize CO_2 accumulation at the local, regional, and national levels. Moreover, the accurate estimation of biomass, soil carbon stocks, and their spatial distribution in various habitats will be crucial to understanding carbon storage potential and its dynamics (Weiskittel et al., 2015; Singh et al., 2018a).

Biomass estimation models are of immense importance for climate change studies. There is a continuous change of biomass density at individual forest stand and other woodlands due to land-use change, and anthropogenic activities triggered by climate change events (Ahirwal et al., 2021a). These changes are of paramount importance in influencing the global carbon cycle (Qiu et al., 2015; Pellikka et al., 2018). The measurement of biomass at plot levels especially on a mountainous hilly terrain is extremely labor intensive, and due to heterogeneity in landscape, it is practically impossible to cover vast landscape for carbon accounting without bias (Brahma et al., 2021). A precise estimation of carbon across different ecosystems will be desirable to increase our understanding of the location and magnitude of carbon density, and identify the carbon source and sink. The use of the locally developed robust biomass model would be critical in this direction for a more reliable and accurate biomass estimation, and reporting to national carbon stock enhanced knowledge on the carbon budget at both local and regional scales and in relation to the current climate change scenario (Thangjam et al., 2019).

Several factors such as land history, inherent climatic conditions, vegetation patterns and types, and land-use and its management practices play a vital role in influencing the carbon storage and sequestration rate in different carbon pools (Zhang et al., 2015). Over the last decades, environmentalists and policy-makers have become more aware of the vital role that tree diversity plays in combating climate change, and this has prompted them to be more conscious while designing any climate change mitigation and adaptation strategy (Con et al., 2013; Bhat et al., 2020; Sheikh et al., 2021). It has been established that plantation forestry (Brahma et al., 2017; Singh et al., 2018a; Nath et al., 2018; Kurmi et al., 2020), agroforestry (Tamang et al., 2021), and home gardens (Singh et al., 2015; Singh and Sahoo, 2021) have great potential for carbon sink in the Northeastern region of India. Similarly, secondary forests (accounting for variation in age) play an important role in carbon storage (Gogoi et al., 2020; Thong et al., 2020). One of the basic prerequisites for the accurate estimation of biomass stock at the regional and global scales is the use of appropriate models. Till today, only generic models, including those developed by Brown et al. (1989), Chambers et al. (2001) Chave et al. (2005), and Chave et al. (2014), have been used to estimate biomass and carbon stocks for diverse forests in the Northeastern region of India. However, the accuracy of biomass estimates using these models has rarely been tested. To overcome this uncertainty, there is an urgent need to develop a regional biomass estimation model to predict medium and long-term biomass and carbon stocks under different land uses, which could be highly useful for regional and/or global biodiversity conservation.

Computation of the landscape level and carbon storage facilitates the understanding of biogeochemical cycle, carbon dynamic (source/sink), and regional carbon cycle (Weiskittel et al., 2015). Geostatistics and remote sensing techniques have been frequently used for the purpose of extrapolation (Kumar et al., 2015). The use of active remote sensing images like the Moderate Resolution Imaging Spectroradiometer (MODIS), Light Detection and Ranging (LIDAR), Phased Array L-based Synthetic Aperture Radar (PULSAR), and indices such as the Normalized Difference Vegetation Index (NDVI), and the Leaf Area Index (LAI) coupled with field inventory are on the rise to estimate biomass in timely and cost-effective manners, especially on hilly terrains. In Northeast India, some efforts have been made to estimate forest biomass and carbon stock using remote sensing images for a particular state or a forest type in Tripura (Pandey

et al., 2019), Manipur (Sharma et al., 2020), Arunachal Pradesh (Kumar et al., 2019), and Assam (Hussain et al., 2019). The use of remote sensing techniques for estimating carbon stock from a variety of complex land uses is often more challenging due to the lack of accurate and consistent measurement methods (Issa et al., 2020). For example, using remote sensing to trace transitions from intact forests to degraded forests on the same landscape may yield the same closed canopy area, while the carbon stock may have plummeted to 75% (UNFCCC, 2006). Low-vegetation signal-to-noise ratios, high soil background reflectance in shifting cultivation areas, and high spatial heterogeneity from plot to state-level data hamper the calibration and evaluation of data (Issa et al., 2020). These constraints pose unique challenges specific to varying environmental conditions and result in high inaccuracies when applying biomass estimation techniques for other ecosystems/land uses. To overcome these challenges and in view of the fact that there are no efforts to estimate the biomass of different habitats at a regional level, innovative ground-level field inventories using the best-fit equations for tree and other woody vegetation were necessitated (Brahma et al., 2021). The present study is the first of its kind for accounting for carbon from different land-use sectors at a regional scale. Further lack of accurate data on carbon stock and sequestration potential under land-use sectors makes this study indispensable. Therefore, the objective of the present study was to develop a robust regional model to estimate tree diversity, biomass, carbon stock, and sequestration potential under different land uses in the Northeast region of India. It also aimed to develop a relationship between tree basal areas and density with the biomass carbon storage at different pools for various land uses so that effective mitigation and adaptation strategies could be developed in advance to combat future climate change.

MATERIALS AND METHODS

Study Area

Northeast India accounts for 8% of the geographical area and ~25% of the forest cover of India. The region is currently facing dual pressure of economic growth and environmental protection. The region is endowed with diverse land-use types. Besides various forest types, several other tree-based ecosystems such as traditional agroforestry, home gardens, plantations, and secondary forests that provide livelihood opportunities for rural populace are widely prevalent in the region. We selected seven major land uses *viz*., 1) forest: tropical, subtropical, and temperate; 2) bamboo forest; 3) plantation: tropical, subtropical, and temperate; 4) shifting cultivation fallows: <5 years, 5–10 years, and 11–20 years; 5) agricultural lands; 6) agroforestry; and 7) grasslands, in Northeast India. The agricultural land includes wet rice cultivation. The plantations include rubber (*Hevea brasiliensis*), areca nut (*Areca catechu*), oil palm (*Elaeis guineensis*), and orange (*Citrus sinensis*), while agroforestry involved traditional home gardens, coffee (*Coffea* sp.), piper (*Piper betel*), sugarcane (*Saccharum officinarum*), and mango-based systems (*Mangifera indica*) for the study. The area and proportion of each land use have been given in **Supplementary Table S1**. The estimated above ground biomass (AGB) data of each land use for different northeast Indian states was used to prepare the spatial distribution map. The classified Land Use and Land Cover (LULC) map of each state in the studied region was utilized to estimate the total area coverage under each land use (**Figure 1**). The LULC map was developed by integrating land image data of the concerned area over a particular time span (from November 2015 to February 2016) using freely available Landsat 8 Operational Land Imager (Landsat OLI) present on the data portal of the United States Geological Survey (USUG): "Earth Explorer"(https://earthexplorer.usug.gov). All the imageries were geo-referenced to Common Universal Traverse Mercator (UTM) projection UTM zone 46 and WSG 84 datum.

Field Inventory on Tree Composition, Biomass, and Soil Carbon Estimation

All the major land-use sectors were stratified, and sub-stratified/classified based on forest types, canopy cover, crop composition, and age of plantation/shifting cultivation, and representative eight permanent sites (250 m × 250 m) were established in each of the eight northeastern states following the ISRO–GBP/NCP–VCP protocol (Singh and Dadhwal, 2009). The field inventory on tree composition, biomass, soil, and carbon estimation from various pools was estimated from the sample quadrant plots of representative size: 0.1 ha (31.62 m × 31.62 m) following standard methods and other studies carried out during 2016–2019. For each site and each land use, four 0.1 ha permanent plots were fixed at the four corners of the site. The number of sampling sites in tropical, subtropical, temperate, and bamboo forests were 231, 40, 12, and 12, respectively. The number of sampling sites for tropical, subtropical, and temperate plantations were 87, 31, and 9, respectively, and for <5 years, 5–10 years, and 11–20 years shifting cultivation fallows, the number of sampling sites were 34, 17, and 7, respectively. The data for agroforestry, agriculture, and grasslands were drawn from 69, 89, and 23 sampling sites, respectively. All trees having ≥ 10 cm dbh (diameter at breast height, i.e., 1.37 m from the base) in each plot were measured for vegetation parameters such as species richness, density, and diversity following standard methods. Diversity indices including the Shannon–Wiener diversity index (Shannon and Weiner, 1963), species richness (Margalef, 1958), species evenness (Pielou, 1966) and species dominance (Simpson, 1949) were determined for all the major land uses. The basal area values of these trees were collected from the calculated mean of four plots at four corners of the site in a given sampling site and were further expanded to per hectare basis.

In Northeast India, the widely used generalized models for estimating biomass have rarely been validated by ground truthing. Besides this, different species-specific models have certain limitations in adhering to sufficient sample size, sampling strategy, validation, *etc*., resulting in large degrees of uncertainty in obtaining accurate biomass estimation from diverse forest ecosystems (Weiskittel et al., 2015). To

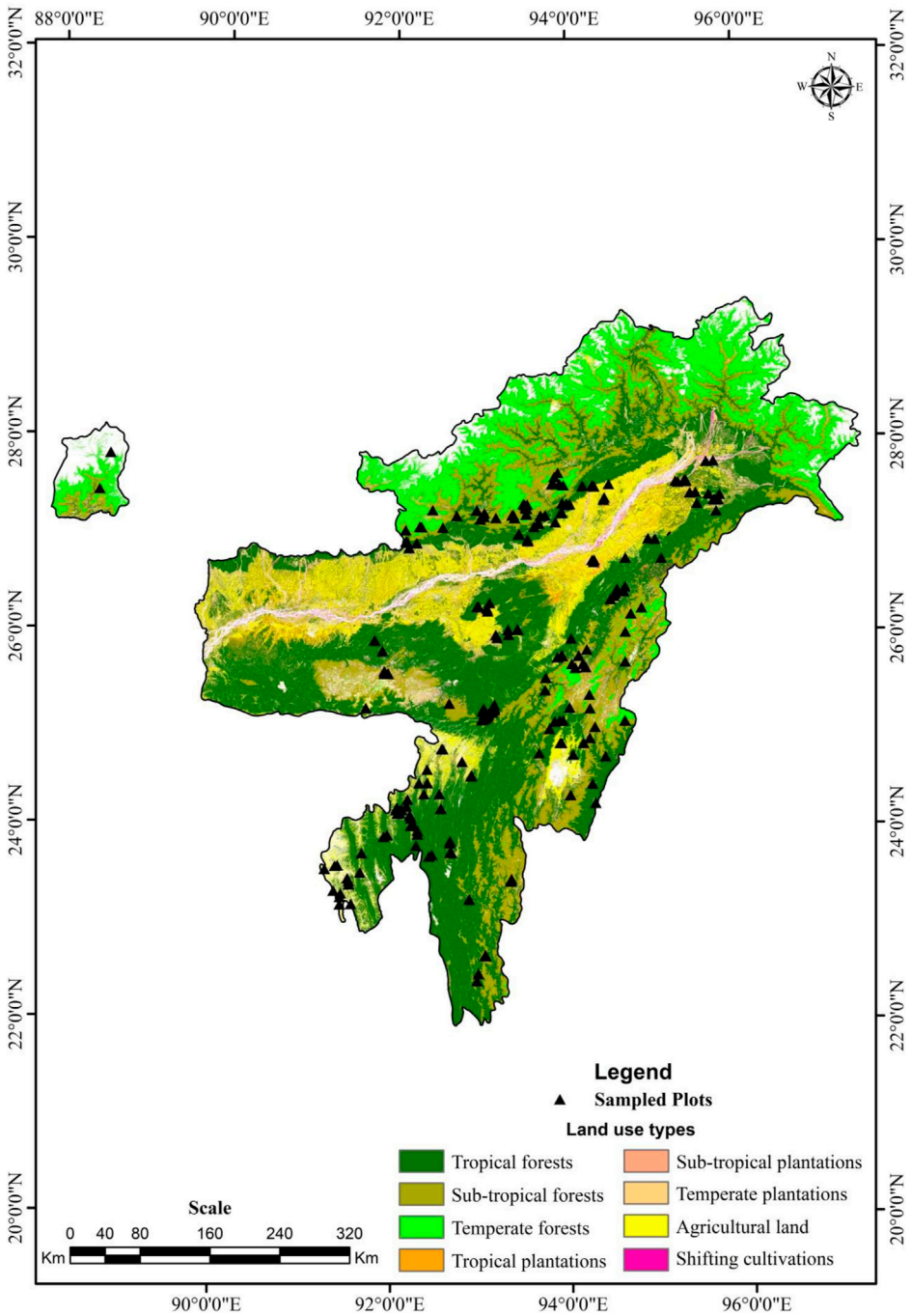

FIGURE 1 | Spatial distribution of major land uses showing sampling plots in northeast India.

overcome these issues, we used the biomass model developed by Nath et al. (2019) using 303 sample tree harvested data drawn from four major forest types of the region for calculation of AGB as

$$AGB_{est} = 0.18D^{2.16} \times 1.32 \quad (1)$$

where AGB_{est} = above ground biomass (Kg tree^{-1}), D = diameter at breast height, and 1.32 = correction factor.

Cross-validation is usually recommended to determine how accurately the biomass estimation model will perform when applied to an independent dataset. Usually, 5-fold or 10-fold cross-validation provides a good balance between bias and variance (Sileshi, 2014; Thangjam et al., 2019). However, a 10-fold cross-validation was employed to evaluate the predictive performance of the biomass estimation models developed by Nath et al. (2019). The goodness of fit criteria were calculated

for the validation dataset using the lava and forecast packages of the R package. It was found that with high R^2 and low AICc, RMSE, and MAPE values (Nath et al., 2019), the biomass model was best suited for tree biomass estimation in Northeast India over the generic model developed by Brown (1989) and the two pantropical models developed by, Chave et al. (2005), Chave et al. (2014). Details of the model development and validation procedure are available in the study by Nath et al. (2019).

We also used species-specific biomass estimation models for rubber and areca nut plantation developed for this region (Brahma et al., 2018). Belowground biomass (BGB) was calculated from the equation given by Mokany et al. (2006), and its carbon stock was calculated as BGB = 0.205 × AGB when AGB < 125 Mg ha^{-1} and BGB = 0.235 × AGB when AGB > 125 Mg ha^{-1}. Aboveground biomass carbon (AGBC) was estimated from the default value (47%) of total biomass (IPCC, 2003). Two soil profiles (1 m × 1 m × 1 m) were dug randomly within each 250 m × 250 m sized site, totaling eight profiles for a site, twice in 2016 and 2018. Soil samples in triplicates were collected from three depths (0–10, 10–20, and 20–45 cm) using a soil corer (5.6 cm dia). In addition to this, 72 bulk soil samples (8 profile × 3 depth × 3 replication) were obtained for each land use, air-dried, and sieved using 100 micron mesh for the assessment of SOC concentration following a widely used method called "wet oxidation method" (Walkley and Black, 1934). The SOC stock for each depth was computed following the method proposed by Blanco-Canqui and Lal (2008). Values for different soil depths were summed up to obtain SOC stock up to 0–45 cm. Soil bulk density (BD) was calculated following the procedure of Robertson et al. (1974). The carbon stock of major pools (AGB, BGB, and SOC stock) was summed up for particular land use to arrive at the total carbon stock (TCS). The rate of change (sequestration) in carbon stock was determined from the initial/baseline value (2016) to the final value (2018). The age of the land use was recorded by questioning the farmers during field survey. The carbon sequestration rate was estimated by dividing the change in the carbon stock values (between prior (C_{LU0}) and immediate (C_{LUn}) values) by the age of the land use/age interval (Dung et al., 2016), which is expressed as

$$R_{sequestation} = \frac{C_{LU0} - C_{LUn}}{Interval}. \quad (2)$$

Statistical Analysis

The variation in tree density, basal area, and carbon stock under different land use was determined using the analysis of variance and Tukey HSD tests at 5% level. The relationships among tree basal area, density, and carbon in different pools of all land-uses were computed using correlation and regression analyses with statistical package SPSS-21 (SPSS Inc., Chicago, IL, United States). All the basic analyses were done using Microsoft Office -2010.

RESULTS

Tree Species Richness, Diversity, Stand Density, and Biomass Stock

The mean value of species richness varied significantly ($p < 0.05$) among land uses and ranged from 1.0 (subtropical plantations) to 12.22 (tropical forest). Tree species richness differed significantly ($p < 0.05$) between forest types and shifting cultivation fallows (**Table 1**). The Shannon–Wiener diversity index (H) varied significantly ($p < 0.05$) among different land uses, showing maximum value (2.40) in 11–20 years shifting cultivation fallows followed by temperate forest (2.39), tropical forest (2.20), 5–10 years shifting cultivation fallow (1.99), and minimum (0.02) in subtropical plantation (**Table 1**). The Simpson dominance index ranged from 0.09 (11–20 years shifting cultivation fallow) to 0.83 (tropical forest) and Pileou's evenness index was maximum (0.99) in <5 years and 11–20 years shifting cultivation fallows and minimum (0.55) in bamboo forest (**Table 1**). Margalef's species richness index was maximum (3.21) in tropical forests followed by 11–20 years shifting cultivation fallow (2.81) and minimum (0.61) in tropical plantation. Tropical forests had a mean stand density of 539 trees ha^{-1}, and the corresponding values for subtropical and temperate forests were 554 trees ha^{-1} and 578 trees ha^{-1}, respectively (**Table 2**). Among the tree plantations, those located in subtropical climate showed the highest stand density (840 trees ha^{-1}), followed by tropical (598 trees ha^{-1}) and temperate (344 trees ha^{-1}). The culm density in bamboo forests was 6,550 culms ha^{-1}. The mean tree density in shifting cultivation fallows varied from 140 trees ha^{-1} (<5 years fallow) to 703 tree ha^{-1} (11–20 years fallow). In agroforestry systems, the stand density was 744 trees ha^{-1} with a mean basal area of 14.35 ± 4.02 m^2 ha^{-1}. The temperate forests had the highest average basal area (29.50 ± 2.63 m^2 ha^{-1}) followed by subtropical (26.71 ± 2.18 m^2 ha^{-1}) and tropical forests (25.07 ± 1.01 m^2 ha^{-1}). The basal area of tree plantations also varied significantly and was in the order of subtropical (30.63 ± 6.46 m^2 ha^{-1}) > tropical plantation (26.86 ± 1.83 m^2 ha^{-1}) > temperate plantation (11.43 ± 1.57 m^2 ha^{-1}). Biomass values varied significantly ($p < 0.05$) between different land uses and ranged from 2.53 ± 0.51 Mg ha^{-1} (in grassland) to 259.77 ± 15.43 Mg ha^{-1} (in temperate forest), and were in the order of natural forests > plantations > older shifting cultivation fallows (5–10 and 11–20 years) >agroforestry > bamboo forest > agriculture (**Table 2**). The details of the dominant species and their respective density, importance value index, basal area, and biomass stock are provided in **Supplementary Table S1**

Vegetation Carbon Stock

The mean value of AGBC stock was the highest (100.51 ± 11.33 Mg C ha^{-1}) in temperate forest and lowest (0.96 ± 0.31 Mg C ha^{-1}) in grassland. The mean vegetation carbon stock (ABG + BGB) was the highest (122.09 ± 13.59 Mg C ha^{-1}) in temperate forests followed by subtropical (106.01 ± 11.59 Mg C ha^{-1}) and tropical forests (105.33 ± 3.88 Mg C ha^{-1}). The AGBC and total vegetation carbon in bamboo forest were 17.79 ± 1.46 Mg C ha^{-1} and 21.98 ± 1.80 Mg C ha^{-1}, respectively (**Figure 2**). Vegetation carbon stock in the plantations were in the order of subtropical (115.45 ± 21.20 Mg C ha^{-1}, range 57.15–266.5 Mg C ha^{-1}) > tropical (93.00 ± 7.80 Mg C ha^{-1}, range

TABLE 1 | Species richness and diversity indices of the tree species across different land-use sectors of Northeast India.

Land uses	Species richness (plot-level)	Simpson's dominance index	Shannon–Weiner diversity index	Pielou's evenness index	Margalef's species richness index
Forest (tropical)	12.22 ± 0.51^{bcde}	0.83 ± 0.05	2.20 ± 0.07	0.73 ± 0.03	3.21 ± 0.82
Forest (subtropical)	11.49 ± 0.85^{bcde}	0.68 ± 0.02	1.88 ± 0.125	0.69 ± 0.01	1.91 ± 0.63
Forest (temperate)	11.61 ± 0.78^{bcde}	2.12 ± 0.07	2.39 ± 0.092	0.59 ± 0.01	1.21 ± 0.87
Forest (bamboo)	1.38 ± 0.03	0.18 ± 0.0	1.07 ± 0.32	0.55 ± 0.04	0.67 ± 0.03
Plantation (tropical)	2.92 ± 0.76^{ad}	0.21 ± 0.10	0.49 ± 0.22	0.59 ± 0.03	0.61 ± 0.03
Plantation (subtropical)	1.0 ± 0.0^{ad}	0.64 ± 0.03	0.02 ± 0.0	0.61 ± 0.03	1.06 ± 0.2
Plantation (temperate)	1.64 ± 0.23^{ae}	0.30 ± 0.41	0.17 ± 0.24	0.58 ± 0.55	2.10 ± 0.37
Shifting cultivation fallow (< 5 years)	1.8 ± 0.03^{ac}	0.21 ± 0.0	1.69 ± 0.03	0.99 ± 0.0	2.04 ± 0.06
Shifting cultivation fallow (5–10 years)	2.8 ± 0.02^{ac}	0.15 ± 0.0	1.99 ± 0.06	0.98 ± 0.0	2.22 ± 0.08
Shifting cultivation fallow (11–20 years)	3.6 ± 0.12^{ac}	0.09 ± 0.0	2.40 ± 0.16	0.99 ± 0.0	2.81 ± 0.17
Agroforestry systems	3.0 ± 0.0^{ac}	0.56 ± 0.06	1.24 ± 0.32	0.596 ± 0.0	1.70 ± 0.32

The value with the same letter between in species richness between the land uses is significantly different at $p < 0.05$.

TABLE 2 | Stand density, basal area, and biomass in major land-use sectors of Northeast India.

Land uses	Stand density (number of trees ha^{-1})	Basal area (m^2 ha^{-1})	Biomass (Mg ha^{-1})
Forest (tropical)	539 ± 17.61^{a}	25.07 ± 1.01^{a}	224.11 ± 8.26^{a}
Forest (subtropical)	554 ± 48.38^{b}	26.71 ± 2.18^{b}	225.55 ± 24.66^{b}
Forest (temperate)	578 ± 80.15^{c}	29.50 ± 2.63^{c}	259.77 ± 15.43^{c}
Forest (bamboo)	655 ± 46.8^{d}	7.68 ± 0.39^{acd}	46.77 ± 2.35^{abcd}
Plantation (tropical)	598 ± 41.31^{e}	26.86 ± 1.83^{de}	198.58 ± 16.55^{de}
Plantation (subtropical)	840 ± 174.15^{f}	30.63 ± 6.46^{df}	245.64 ± 45.10^{df}
Plantation (temperate)	344 ± 92.98^{f}	11.43 ± 1.57^{g}	106.60 ± 14.29^{g}
Shifting cultivation fallow (<5 years)	188 ± 31.72^{abdefg}	5.86 ± 1.58^{abcef}	23.09 ± 5.87^{abcef}
Shifting cultivation fallow (5–10 years)	431 ± 63.02^{f}	17.58 ± 4.36^{h}	85.12 ± 12.42^{abcf}
Shifting cultivation fallow (11–20 years)	703 ± 79.06^{g}	15.24 ± 0.65^{i}	167.60 ± 14.29^{h}
Agroforestry systems	744 ± 144.88^{g}	14.35 ± 4.02^{i}	92.58 ± 28.73^{abc}
Agriculture	-	-	6.48 ± 1.26^{abcef}
Grassland	-	-	2.53 ± 0.81^{abcef}

±Standard error of mean; Tukey's post hoc *test was used for pair-wise separations. The value with the same letter between the land uses is significantly different at* $p < 0.05$.

7.23–341.92 Mg C ha^{-1}) > temperate (50.10 ± 6.72 Mg ha^{-1}, range 18.75–75.05 Mg C ha^{-1}) zones. The agricultural land showed an average vegetation carbon stock of 2.71 ± 0.36 Mg C ha^{-1}. The cumulative aboveground carbon storage in four major land-use sectors in Northeast India amounts to 212,675,8462 Mg C (2.13 Pg C) to which tropical, subtropical, and temperate forests contributed 67.68, 10.44, and 13.77%, respectively (**Supplementary Table S2**).

Soil Organic Carbon Stock, Total Carbon Stock, and Carbon Sequestration

Among the forest types, the mean SOC stock was in the order of tropical forests (72.54 ± 2.02 Mg C ha^{-1}) > temperate forests (63.4 ± 6.94 Mg C ha^{-1}) > subtropical forests (42.58 ± 3.32 Mg C ha^{-1}). SOC values in tropical forests ranged from 10.13–119.65 Mg C ha^{-1}, and in temperate forests, its value varied between 22.32 and 114.59 Mg C ha^{-1}. The mean SOC stock was 29.83 ± 0.97 Mg C ha^{-1}, with variations from 25.28 to 34.67 Mg C ha^{-1} in bamboo forests (**Table 3**). The SOC stock in plantations was in the order of tropical > subtropical > temperate zones. On average, the SOC stock was the highest in 5–10 years fallows (84.56 ± 3.99 Mg C ha^{-1}) followed by 11–20 years fallows (78.19 ± 2.09 Mg C ha^{-1}) and <5 years fallows (75.76 ± 7.86 Mg C ha^{-1}), and the mean SOC stock in agriculture land-use was 40.13 ± 1.77 Mg C ha^{-1}. Total carbon stock (TCS) was maximum (185.5 ± 15.55 Mg C ha^{-1}) in tropical forests and minimum (40.55 ± 7.77 Mg C ha^{-1}) in grassland (**Figure 2**).

The mean annual increment (carbon sequestration) in vegetation pools varied between 1.80 Mg C ha^{-1} yr^{-1} (tropical plantations) and 5.51 Mg C ha^{-1} yr^{-1} (temperate forests). The carbon sequestration rate was significantly higher in forests (2.81–5.51 Mg C ha^{-1} yr^{-1}), followed by plantations (1.80–5.08 Mg C ha^{-1} yr^{-1}) and secondary forests (1.35–2.84 Mg C ha^{-1} yr^{-1}). The results revealed that tree-based land uses registered an increase in vegetation carbon by 2.68 ± 0.12 Mg C ha^{-1} yr^{-1}. SOC sequestration was the highest in temperate forests (1.85 ± 0.31 Mg C ha^{-1} yr^{-1}), followed by subtropical forests (1.78 ± 0.28 Mg C ha^{-1} yr^{-1}) and tropical forests (1.0 ± 0.18 Mg C ha^{-1} yr^{-1}). Agriculture land use and shifting cultivation fallows (<5-years) showed the lowest rate of SOC sequestration (**Table 3**). The carbon sequestration rate was found to be significantly ($p < 0.05$) higher in plant biomass than in soil.

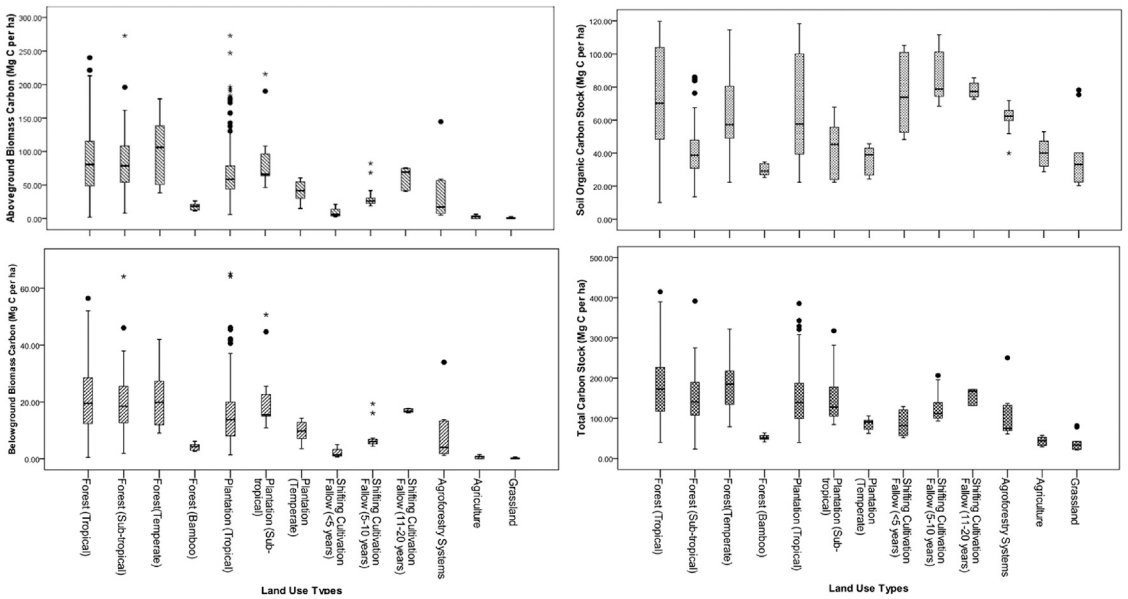

FIGURE 2 | Vegetation carbon and soil organic carbon stocks (0–45 cm soil depth) in major land uses in Northeast India.

TABLE 3 | Mean annual carbon increment (Mg C ha^{-1} yr^{-1}) in different carbon pools of major land uses in Northeast India.

Land uses	AGBC	BGBC	VC	SOC
All tree-based land uses	2.16 ± 0.09	0.51 ± 0.02	2.68 ± 0.12	1.05 ± 0.09
Forest (tropical)	2.27 ± 0.11	0.53 ± 0.03	2.81 ± 0.14	1.00 ± 0.18
Forest (subtropical)	3.32 ± 0.51	0.78 ± 0.12	4.10 ± 0.18	1.78 ± 0.28
Forest (temperate)	4.46 ± 0.80	1.05 ± 0.19	5.51 ± 0.99	1.85 ± 0.31
Forest (bamboo)	2.97 ± 0.49	0.70 ± 0.12	3.67 ± 0.61	0.60 ± 0.03
Plantation (tropical)	1.46 ± 0.28	0.34 ± 0.06	1.80 ± 0.34	1.68 ± 0.27
Plantation (subtropical)	4.11 ± 0.44	0.97 ± 0.10	5.08 ± 0.5	0.81 ± 0.06
Plantation (temperate)	2.02 ± 0.48	0.47 ± 0.11	2.49 ± 0.59	0.81 ± 0.06
Shifting cultivation fallow (< 5 years)	1.10 ± 0.42	0.26 ± 0.10	1.35 ± 0.52	0.51 ± 0.12
Shifting cultivation fallow (5–10 years)	1.64 ± 0.17	0.39 ± 0.04	2.03 ± 0.21	0.39 ± 0.07
Shifting cultivation fallow(11–20 years)	2.30 ± 0.12	0.54 ± 0.03	2.84 ± 0.15	0.67 ± 0.08
Agroforestry systems	0.55 ± 0.17	0.13 ± 0.04	0.69 ± 0.21	0.56 ± 0.09
Agriculture	-	-	-	0.32 ± 0.15
Grassland	-	-	-	0.49 ± 0.12

AGBC, above ground biomass carbon; BGBC, belowground biomass carbon; VC, vegetation carbon; SOC, soil organic carbon; ±SEM.

Relationship Among Tree Diversity, Basal Area, and Carbon Stock in Different Pools

Significant positive relationships were observed between the basal area and tree density for all land uses, except temperate forests. However, no relationship between the basal area and SOC stock was observed, except in the tropical forests. Similarly, there was no relationship between the basal area and BGB carbon stock in the old (11–20 years) shifting cultivation fallows (**Table 4**).

Carbon Dynamics and Land-Use Changes

Both progressive and retrogressive carbon change were noticed due to land-use change management. When the shifting cultivation fallows were vegetated with plantation/agroforestry, total biomass carbon stock increased, and it ranged from 21.58 to 97.34 Mg C ha^{-1} (**Figure 3**). This conversion, however, resulted in SOC loss from 3.87 to 17.66 Mg C ha^{-1}. The conversion of land use from both agriculture and grassland to plantation, on the other hand, resulted in an increase of carbon in all pools (SOC and vegetation carbon). The conversion of natural forest to grassland, current shifting cultivation fallow (<5 years), plantation, and agroforestry resulted in the total carbon stock (TCS) loss which ranged from 28.68 Mg C ha^{-1} (plantation) to 126.32 Mg C ha^{-1} (grassland). These conversions also resulted in the maximum loss of vegetation carbon (VC) in grasslands (106.33 Mg C ha^{-1}), followed by the current shifting cultivation fallow (101.80 Mg C ha^{-1}) and the least in plantations (23.15 Mg C ha^{-1}). The conversion of agroforestry to agriculture resulted in the loss of carbon from all pools. The increment in vegetation carbon was the highest (3.62 Mg C ha^{-1} yr^{-1}) when the grasslands were converted to

TABLE 4 | Relationships among density, aboveground biomass carbon (AGBC), belowground biomass carbon (BGBC), vegetation carbon (VC), soil organic carbon stock (SOCS), and total carbon stock (TCS) with basal area of the trees in different land-use sectors of Northeast India.

Land use	Variables	Model	R^2	R	N
Tropical forest	Density	y = 5.8863x + 402.23	0.1172	0.342**	239
	AGBC	y = 2.0618x + 31.08	0.4093	0.64**	239
	BGBC	y = 0.5967x + 5.7528	0.5448	0.738**	239
	VC	y = 3.1357x + 30.233	0.5448	0.738**	239
	SOCS	y = 1.1057x + 43.649	0.2935	0.542**	239
	TCS	y = 3.7642x + 80.481	0.5377	0.733**	239
Subtropical forest	Density	y = 11.973x + 234.53	0.2909	0.539**	35
	AGBC	y = 3.6584x – 11.892	0.7218	0.85**	35
	BGBC	y = 0.8597x – 2.7946	0.7218	0.85**	35
	VC	y = 4.5182x – 14.687	0.7218	0.85**	35
	SOCS	y = 0.4691x + 30.043	0.095	0.308^{NS}	35
	TCS	y = 4.9873x + 15.357	0.7232	0.85**	35
Temperate forest	Density	y = 9.2776x + 303.69	0.0926	0.304^{NS}	18
	AGBC	y = 3.4545x – 1.4143	0.642	0.801**	18
	BGBC	y = 0.7003x + 0.9199	0.5624	0.75**	18
	VC	y = 3.6805x + 4.8344	0.5624	0.75**	18
	SOCS	y = -0.1373x + 67.45	0.0027	0.052^{NS}	18
	TCS	y = 3.5432x + 72.285	0.3648	0.604**	18
Tropical plantation	Density	y = 13.308x + 221.27	0.4587	0.677**	37
	AGBC	y = 1.9378x + 7.36	0.5485	0.741**	37
	BGBC	y = 0.5097x - 0.2886	0.6181	0.786**	37
	VC	y = 2.6785x – 1.5167	0.6181	0.786**	37
	SOCS	y = 0.2245x + 47.567	0.0329	0.181^{NS}	37
	TCS	y = 2.903x + 46.051	0.5811	0.762**	37
Subtropical plantation	Density	y = 24.868x + 112.17	0.883	0.94**	16
	AGBC	y = 2.7103x + 6.9391	0.939	0.969**	16
	BGBC	y = 0.6369x + 1.6307	0.939	0.969**	16
	VC	y = 3.3472x + 8.5698	0.939	0.969**	16
	SOCS	y = 0.1381x + 38.226	0.0355	0.188^{NS}	16
	TCS	y = 3.4853x + 46.796	0.8894	0.943**	16
Temperate plantation	Density	y = 13.808x + 223.8	0.2746	0.524**	44
	AGBC	y = 2.3199x + 29.943	0.3184	0.564**	44
	BGBC	y = 0.5132x + 5.9818	0.28	0.529**	44
	VC	y = 2.6969x + 31.436	0.28	0.529**	44
	SOCS	y = 0.3911x + 60.498	0.0278	0.167^{NS}	44
	TCS	y = 3.088x + 91.934	0.2873	0.536**	44
Shifting cultivation fallows (<5 years)	Density	y = 16.49x + 91.427	0.6704	0.819**	10
	AGBC	y = 1.3793x + 0.708	0.9437	0.931**	10
	BGBC	y = 0.3241x + 0.1664	0.9437	0.931**	10
	VC	y = 1.7034x + 0.8744	0.9437	0.931**	10
	SOCS	y = 3.6985x + 54.1	0.5492	0.472^{NS}	10
	TCS	y = 5.4019x + 54.974	0.7231	0.904**	10
Shifting cultivation fallows (5–10 years)	Density	y = 6.8559x + 310.52	0.2258	0.475^{NS}	15
	AGBC	y = 0.5891x + 22.288	0.2927	0.541*	15
	BGBC	y = 0.1471x + 4.7719	0.3305	0.575*	15
	VC	y = 0.7731x + 25.078	0.3305	0.575*	15
	SOCS	y = 0.311x + 79.09	0.1159	0.34^{NS}	15
	TCS	y = 1.0841x + 104.17	0.2734	0.667*	15
Shifting cultivation fallows (11–20 years)	Density	y = 116.11x – 1067.2	0.8986	0.948**	6
	AGBC	y = 10.011x – 90.706	0.9525	0.976**	6
	BGBC	y = 0.2131x + 13.644	0.2796	0.529^{NS}	6
	VC	y = 1.1198x + 71.702	0.2796	0.529^{NS}	6
	SOCS	y = 1.6139x + 53.594	0.2488	0.499^{NS}	6
	TCS	y = 2.7337x + 125.3	0.8228	0.907*	6
Agroforestry	Density	y = 31.368x + 294.17	0.7578	0.871**	13
	AGBC	y = 2.4838x – 0.4093	0.8229	0.907**	13
	BGBC	y = 0.5837x – 0.0962	0.8229	0.907**	13
	VC	y = 3.0675x – 0.5055	0.8229	0.907**	13
	SOCS	y = 0.2758x + 56.869	0.2575	0.507^{NS}	13
	TCS	y = 3.3433x + 56.364	0.8272	0.909**	13

, Significant at* $p < 0.5$ *and* $p < 0.01$*, respectively (2-tailed); ns, non-significant; n = no of sites.*

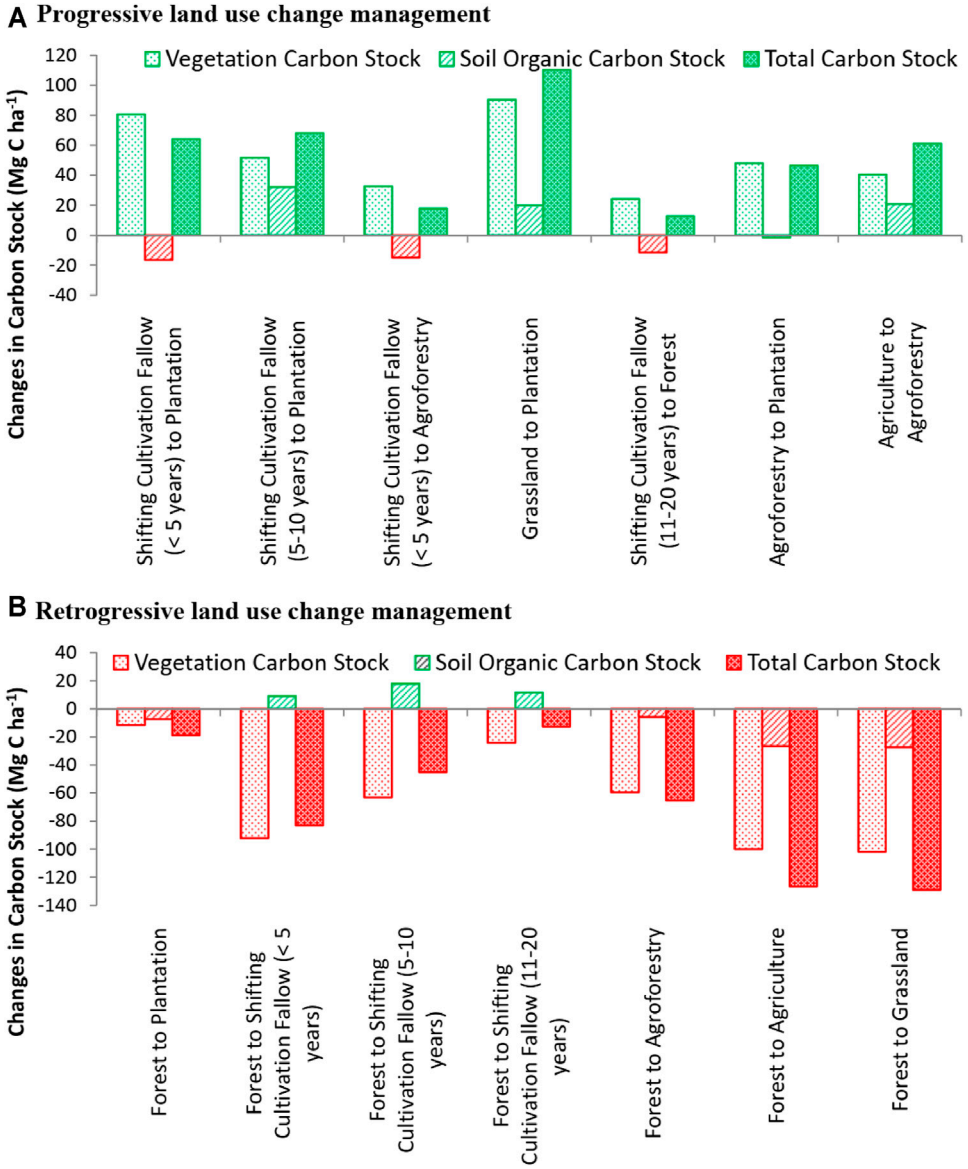

FIGURE 3 | Changes in soil organic carbon stock (SOCS) (Mg C ha^{-1}), vegetation carbon stock (VCS) (Mg C ha^{-1}), and total carbon stock (TCS) (Mg C ha^{-1}) with respect to **(A)** progressive and **(B)** retrogressive land-use change in Northeast India (the values of SOCS refers to 0–45 cm soil depth).

plantation forests. The SOC stock registered a 0.95 Mg C ha^{-1} yr^{-1} increase when less than 5 years shifting cultivation fallows were converted to tree plantations. Similarly, this land-use conversion (<5 years fallows to tree plantations) resulted in the highest (3.71 Mg C ha^{-1} yr^{-1}) increase in total carbon sequestration (**Table 5**).

DISCUSSION

Tree Diversity in Different Land Uses

Evidence from the existing literature advocates that climate change in the anthropogenic era has a direct effect on biodiversity, forcing tree species to adapt either through migrating, developing new physiological traits, or changing phenological cycles (Behera et al., 2019). Higher tree species richness indicates a more stable ecosystem and may demonstrate a better ecosystem/carbon service (Ives et al., 2001). Earlier reports from a similar geographical area suggest management practices and other human-induced disturbances such as small-scale mining, forest encroachment for agricultural expansion, fuelwood, and different non-timber forest product extraction influence tree richness and densities (Gogoi et al., 2018). Additionally, varying community structure, composition, topography, elevation, soil properties, and other microclimatic conditions also influence the tree-based ecosystems' structural

TABLE 5 | Vegetation carbon (VC), soil organic carbon (SOC), and total carbon (TC) sequestration after progressive land-use changes in Northeast India.

LU change managements	VC sequestration (Mg C ha^{-1} yr^{-1})	SOC sequestration (Mg C ha^{-1} yr^{-1})	TC sequestration (Mg C ha^{-1} yr^{-1})
<5 years shifting cultivation fallow to plantation	2.68	0.95	3.63
<5 years shifting cultivation fallow to agroforest	1.02	0.04	1.06
Agriculture to agroforest	0.69	0.44	1.13
Grassland to plantation	3.62	0.09	3.71
Grassland to agroforest	0.68	0.63	1.31
Agroforest to plantation	2.43	0.54	2.97

and functional attributes (Nath et al., 2018; Kurmi et al., 2020). Tree size and their growth pattern can influence the basal area and carbon stock (Borah et al., 2015). Many agroforests had lower diversity than the shifting cultivation fallows/secondary forests, and their total carbon stock was similar to the re-growing forests. The single-story vegetation in plantations favor homogenous growth environment, in contrast to the natural forests and shifting cultivation fallows. The forests, agroforests, and shifting cultivation fallows, as expected, had higher tree density and basal area than the plantation forests occupied by monoculture trees (Singh et al., 2018a). Relatively lower organic inputs and higher soil disturbance in the latter could have caused lower SOC stock than the former land uses (Singh et al., 2018b). Land uses may be non-randomly distributed based on the climatic conditions which subsequently influence tree biodiversity (Garcia-Vega et al., 2020). Natural forests had higher species richness, Shannon–Weiner diversity, and the species evenness index than other land uses. The presence of higher evenness or higher richness or both can result in increase in the Shannon–Wiener diversity (Magurran et al., 2004). Shannon diversity in different forests ranged from 1.21 to 2.66 in tropical, 0.28–2.65 in subtropical, and 1.93–2.56 in temperate forests. These values are well within the range reported by Nayak and Sahoo (2020), who found 1.59–2.56 in ten different tropical forest stands of the state of Odisha in India, while in Northeast India, the lowland rainforests showed tree diversity from 2.44 to 3.46 (Gogoi et al., 2018). In dry deciduous forests of central India, tree diversity values reported were 0.77–2.53 (Dar et al., 2019). Rapid urbanization and forest clearing deteriorate forest ecosystem adversely affect the microclimate, regeneration, and soil dynamics, and enhance the emission of greenhouse gases (Qiu et al., 2015; Pellikka et al., 2018). The scale of land-use transition in the region has significantly transformed the forest ecosystem processes, and this could mainly be responsible for poor diversity in all terrestrial ecosystems other than the temperate forests. In the temperate region, the physiography is mostly undulating, population density is thin, and accessibility is somewhat poor, and thus, anthropogenic activities are minimum in the temperate forest. These might have favored almost similar species richness and the Shannon diversity index as tropical forests in the region (**Table 1**). Furthermore, most tropical forests lie in moist to deciduous forest zone, leading to more homogeneity in species composition.

Species richness and diversity are two essential attributes in an ecosystem that may affect the total biomass and carbon stock (Solomon et al., 2017; Zuo et al., 2017). Habitat variability and other prevailing local factors also influence these indices (Jansen and Oksanen, 2013; Fischer et al., 2014). Higher tree diversity observed in the forests is well within the range reported by Saikia et al. (2017). Higher values of dominance in different forest types and temperate plantations than other land uses revealed an inequitable distribution of trees in these habitats. As there was a weak relationship between tree density and carbon storage, particular tree species having high DBH or basal area in these habitats could have also influenced the carbon storage as argued by Kirby and Potvin (2007).

Aboveground Biomass Carbon Stock

The aboveground biomass carbon storage in the present study was comparable with various studies reported by others in Northeast India, for example, 16.24–130.82 Mg C ha^{-1} in Assam (Borah et al., 2013), 60.09–121.43 Mg C ha^{-1} in forests of Manipur (Thokchom and Yadava, 2017), while being lower than the reported value of 460.5 Mg C ha^{-1} in an old-growth pine forest of Meghalaya (Baishya and Barik, 2011). The estimated total biomass and carbon pool of the Northeast India forest sites are within the range reported from other Indian forest systems (Ravindranath et al., 1997; Chhabra et al., 2002; Devi and Yadava, 2015; Wagner et al., 2015; Gandhi and Sundarpandian, 2017; Solomon et al., 2017; Gogoi et al., 2020; Tamang et al., 2021). Several factors such as the age of the forest stand (Kolh et al., 2017), tree density (Garcia-Vega et al., 2020), diversity, and basal area (Joshi and Dhyani, 2018) influence the biomass and total vegetation carbon. Among the land uses, forests store more biomass and biomass carbon, which implies that they must be prevented from deforestation and other anthropogenic activities to mitigate the elevated atmospheric CO_2 concentration in the region.

Soil Carbon Pools

SOC content is influenced by soil organic matter accumulation, which is governed by litter input and decomposition (Sahoo et al., 2019), quality of litter, rate of mineralization coupled with stand type, and age (Cao et al., 2018; Ahirwal et al., 2021b). A high lignin-containing litter with relatively lower soil moisture in plantation forests (rubber, areca nut, and oil palm) (Nath et al., 2018) might have been responsible for the reduced SOC stock in these systems. The average SOC stock for the different land-use sectors of the present study can be comparable with the findings reported in other regions of India. For example, Chhabra et al. (2002) reported the SOC stock of 37.5 Mg C ha^{-1} in dry tropical deciduous forests, while

Ramachandran et al. (2007) found SOC stock of 76.85 Mg C ha^{-1} in thorn forests to 175–369 Mg C ha^{-1} in forests of Kolli hills of Tamil Nadu (Mohanraj et al., 2011) in the same region.

Relationship Among Tree Basal Area, Density, and Carbon Stock

Basal area is a good predictor for biomass (Gebrewahid and Meressa, 2020) and is often used as a surrogate for biomass and carbon (Balderas Torres and Lovett, 2013). In the present study, basal area was strongly correlated with tree density and with vegetation (AGB + BGB) carbon in line with the findings of many others (Poorter et al., 2015; Salunkhe and Khare, 2016; Amara et al., 2019; Tamang et al., 2021). However, the tree basal area did not have any relationship with the SOC stock, except tropical forests. The variation in biomass and carbon pool in subtropical and temperate forest stands were due to the variation in vegetation composition, forest management practice, forest stand age, girth class, and altitude. The temperate forest has higher amount of biomass and carbon stock than tropical forest stands. It was also found that in the temperate forests, the five most dominant species *viz. Quercus* sp. (D-71.7, IVI-25), *Alnus* sp. (D-56.7,IVI-19), *Illicium griffithi* (D-47.8, IVI-18), *Rhododendron* sp. (D-44.4, IVI-15), and *Castanopsis hystrix* (D-38.3, IVI-14) together contributed more than half (154.2 Mg ha^{-1}) to total aboveground stand biomass (**Supplementary Table S1**).

Effect of Land-Use Change on Carbon Balance

Carbon sequestration is affected by several site factors such as tree age, diameter, and height of the tree; temperature, water, and nutrient (particularly carbon and nitrogen) requirements for the soil; and organic matter decomposition by microbes (Poorter et al., 2016). The annual precipitation and soil-water holding capacity of the land use also regulate net primary productivity. In infertile soil, trees allocate more biomass to the roots in order to increase nutrient uptake (Grower, 2003). The confounding effects from other soil characteristics and management regimes may affect carbon stock too (Newaj et al., 2016). The rate of carbon sequestration in a habitat is influenced by several factors such as age of the stand/ maturity index, management, and woody species composition (Singh et al., 2018a). The elevation, slope, and aspect could also influence the carbon sequestration rate (Gogoi et al., 2020; Thong et al., 2020). Significantly higher vegetation carbon sequestration in temperate forests (5.51 Mg C ha^{-1} yr^{-1}) and subtropical plantations (5.08 Mg C ha^{-1} yr^{-1}) in the present study could be due to favorable growth of certain species over others, resulting in high productivity in the habitats when one species is dominant. In our earlier studies, we found that a 10-year-old oil palm plantation can sequester 3.70 Mg C ha^{-1} yr^{-1} vegetation carbon (Singh et al., 2018b) and that shifting cultivation fallows can enhance the total carbon stock to 137.86–140.08 Mg C ha^{-1} within a span of 15 years of succession (Thong et al., 2020). Similarly, an increase of 33.47 Mg C ha^{-1} SOC stock and 26.55 Mg C ha^{-1} of vegetation carbon was reported when the shifting cultivation fallows were left to restore within a span of 15–20 years (Gogoi et al., 2020). Secondary forests show promising CO_2 uptake and their role in the recovery of vegetation carbon storage if kept undisturbed over time, though our results showed CO_2 uptake of secondary forests is slightly lower than the reported 3.05 Mg C ha^{-1} yr^{-1} carbon sequestration of neo-tropical secondary forests (Poorter et al., 2016).

Management Implications

Land-use change is nevertheless the most important factor in the alternation of carbon balance in the Indian Himalayas (Ahirwal et al., 2021a). Conversion of forests to oil palm and other agricultural land use is on the rise in the region to feed the growing population (Singh et al., 2018b). Conversion of forest to other land uses enhances decomposition and removal of carbon through harvest. On the other hand, SOC pools that are the most sensitive to land-use change were found to substantially improve when the shifting cultivation was converted to plantation. In addition to forests that store high amount of AGBC, agroforestry and plantation also show much promise in the region as key component land uses contributing to stronger mitigation and future climate solutions. So eco-restoration through plantation forestry could be the most effective strategy in the region (Gogoi et al., 2021). Furthermore, agroforestry systems were very effective in restoring soil carbon, besides adding to VC through trees. Under the current climate change, this study advocates converting much of the prevailing degraded shifting cultivation to agroforestry and plantation in order to enhance the C stock and abate GHG emissions. Carbon management through enhancing carbon uptake and storage by forests is now globally recognized as a vital strategy to mitigate climate change. Assessing carbon stocks of forest stands will help in prioritizing tree species-specific land-use practices to ensure sustainability. A combined approach of field-based inventory with geospatial techniques is highly recommended for improved carbon estimation at the national level. Such a study would provide more insight into climate change response to minimize the impact at a regional scale for better ecosystem structure and function. Besides, this will help the policy-makers take an appropriate decision for land-use change, reduce deforestation and land degradation, and maintain carbon balance in the global climate scenario.

CONCLUSION

Quantification of carbon stock at the regional/landscape level of Northeast India is crucial for sustainable management of various land uses that are undergoing various anthropogenic changes. The carbon stock at various terrestrial pools is affected by tree species richness, tree density, and diversity. For the various land uses in Northeast India, the relationship of tree species diversity with aboveground biomass carbon appears to be highly variable, indicating that tree diversity conservation and management may not necessarily assure higher biomass carbon storage. The findings

of this study suggest that the various land uses in Northeast India are important for storing carbon. However, the underlying mechanisms governing the complex relationship between tree species diversity and carbon stock are not elucidated yet and need further study. The total carbon stock showed positive gains following land-use conversion from agriculture to agroforestry and grassland to agroforestry, which suggests that the tree-based systems can enhance greater carbon storage and thus help in climate change mitigation and adaptation. This study provides baseline information to environmentalists and policy-makers, who are capable of devising strategies that can help in climate change mitigation and adaptation at the regional, national, and global scale.

DATA AVAILABILITY STATEMENT

The original contributions presented in the study are included in the article/**Supplementary Material**; further inquiries can be directed to the corresponding author.

AUTHORS' CONTRIBUTION

US, OT, AN, SD, DD, AG, BD, and SC led the research in their respective states and conceived the outline of the paper; BT supervised the entire work; SS helped in data analysis; US was responsible for most of the text; AK revised the manuscript; OT developed the LULC map. All authors were involved in the final preparation of the draft and have read and approved the manuscript.

FUNDING

The project was an All Indian Coordinated Carbon Project where all authors (barring SS, AK, and BT) have received separate funding from the Department of Science & Technology, Government of India, New Delhi, to carry out research work in their respective states. This research was funded by the Ministry of Science and Technology, Government of India (Grant No. DST/IS-STAC/CO2-SR-225/14(G)-AICP-AFOLU(I-VIII)).

ACKNOWLEDGMENTS

We thank the academic and administrative heads of various educational institutes/universities across Northeast India for providing all possible in-house laboratory facilities, and the Departments of Environment, Forests, and Climate Change, and Remote Sensing Application Centres of various states for help during field inventory and providing initial land-use and land-cover maps. We also profusely thank all the *Jhum* farmers and owners of other land uses for providing access to their land for the collection of need-based data and soil samples.

SUPPLEMENTARY MATERIAL

The Supplementary Material for this article can be found online at: https://www.frontiersin.org/articles/10.3389/fenvs.2021.724950/full#supplementary-material

REFERENCES

Ahirwal, J., Nath, A., Brahma, B., Deb, S., Sahoo, U. K., and Nath, A. J. (2021a). Patterns and Driving Factors of Biomass Carbon and Soil Organic Carbon Stock in the Indian Himalayan Region. *Sci. Total Environ.* 770, 145292. doi:10.1016/j.scitotenv.2021.145292

Ahirwal, J., Saha, P., Nath, A., Nath, A. J., Deb, S., and Sahoo, U. K. (2021b). Forests Litter Dynamics and Environmental Patterns in the Indian Himalayan Region. *For. Ecol. Manag.* 499, 119612. doi:10.1016/j.foreco.2021.119612

Amara, E., Heiskanen, J., Aynekulu, E., and Pellikka, P. K. (2019). Relationship between Carbon Stocks and Tree Species Diversity in a Humid Guinean savanna Landscape in Northern Sierra Leone. *South. Forests: a J. For. Sci.* 81 (3), 235–245. doi:10.2989/20702620.2018.1555947

Baishya, R., and Barik, S. K. (2011). Estimation of Tree Biomass, Carbon Pool and Net Primary Production of an Old-Growth Pinus Kesiya Royle Ex. Gordon forest in north-eastern India. *Ann. For. Sci.* 68, 727–736. doi:10.1007/s13595-011-0089-8

Balderas Torres, A., and Lovett, J. C. (2013). Using Basal Area to Estimate Aboveground Carbon Stocks in Forests: La Primavera Biosphere's Reserve, Mexico. *Forestry* 86 (2), 267–281. doi:10.1093/forestry/cps084

Behera, M. D., Behera, S. K., and Sharma, S. (2019). Recent Advances in Biodiversity and Climate Change Studies in India. *Biodivers Conserv* 28, 1943–1951. doi:10.1007/s10531-019-01781-0

Betts, R. A., Jones, C. D., Knight, J. R., Keeling, R. F., and Kennedy, J. J. (2016). El Niño and a Record CO2 Rise. *Nat. Clim Change* 6, 806–810. doi:10.1038/nclimate3063

Bhat, J. A., Kumar, M., Negi, A. K., Todaria, N. P., Malik, Z. A., Pala, N. A., et al. (2020). Species Diversity of Woody Vegetation along Altitudinal Gradient of the Western Himalayas. *Glob. Ecol. Conservation* 24 (e01302). doi:10.1016/j.gecco.2020.e01302

Blanco-Canqui, H., and Lal, R. (2008). No-tillage and Soil-Profile Carbon Sequestration: An On-Farm Assessment. *Soil Sci. Soc. Am. J.* 72, 693–701. doi:10.2136/sssaj2007.0233

Borah, M., Das, D., Kalita, J., Deka Boruah, H. P., Phukan, B., and Neog, B. (2015). Tree Species Composition, Biomass and Carbon Stocks in Two Tropical forest of Assam. *Biomass and Bioenergy* 78, 25–35. doi:10.1016/j.biombioe.2015.04.007

Borah, N., Nath, A. J., and Das, A. K. (2013). Aboveground Biomass and Carbon Stocks of Tree Species in Tropical Forests of Cachar District of Assam, Northeast India. *Int. J. Ecol. Environ. Sci.* 39 (2), 97–106.

Brahma, B., Nath, A. J., Deb, C., Sileshi, G. W., Sahoo, U. K., and Kumar Das, A. (2021). A Critical Review of forest Biomass Estimation Equations in India. *Trees, Forests and People* 5, 100098. doi:10.1016/j.tfp.2021.100098

Brahma, B., Pathak, K., Lal, R., Kurmi, B., Das, M., Nath, P. C., et al. (2018). Ecosystem Carbon Sequestration through Restoration of Degraded Lands in Northeast India. *Land Degrad. Dev.* 29, 15–25. doi:10.1002/ldr.2816

Brahma, B., Sileshi, G. W., Nath, A. J., and Das, A. K. (2017). Development and Evaluation of Robust Tree Biomass Equations for Rubber Tree (*Hevea Brasiliensis*) Plantations in India. *For. Ecosyst.* 4, 14. doi:10.1186/s40663-017-0101-3

Brown, S., Gillespie, A. J. R., and Lugo, A. E. (1989). Biomass Estimation Methods for Tropical Forests with Application to Forestry Inventory Data. *For. Sci.* 35, 881–902.

Cai, W., Borlace, S., Lengaigne, M., van Rensch, P., Collins, M., Vecchi, G., et al. (2014). Increasing Frequency of Extreme El Niño Events Due to Greenhouse Warming. *Nat. Clim Change* 4 (2), 111–116. doi:10.1038/nclimate2100

Cao, J., Zhang, X., Deo, R., Gong, Y., and Feng, Q. (2018). Influence of Stand Type and Stand Age on Soil Carbon Storage in China's Arid and Semi-arid Regions. *Land Use Policy* 78, 258–265. doi:10.1016/j.landusepol.2018.07.002

Chambers, J. Q., Santos, J. d., Ribeiro, R. J., and Higuchi, N. (2001). Tree Damage, Allometric Relationships, and Above-Ground Net Primary Production in central Amazon forest. *For. Ecol. Manag.* 152, 73–84. doi:10.1016/s0378-1127(00)00591-0

Chave, J., Andalo, C., Brown, S., Cairns, M. A., Chambers, J. Q., Eamus, D., et al. (2005). Tree Allometry and Improved Estimation of Carbon Stocks and Balance in Tropical Forests. *Oecologica* 145, 87–99. doi:10.1007/s00442-005-0100-x

Chave, J., Réjou-Méchain, M., Búrquez, A., Chidumayo, E., Colgan, M. S., Delitti, W. B. C., et al. (2014). Improved Allometric Models to Estimate the Aboveground Biomass of Tropical Trees. *Glob. Change Biol.* 20, 3177–3190. doi:10.1111/gcb.12629

Chhabra, A., Parila, S., and Dadhwal, V. K. (2002). Growing Stock-Based forest Biomass Estimate for India. *Biomass Bioenerg.* 22, 187–194. doi:10.1016/s0961-9534(01)00068-x

Con, T. V., Thang, N. T., Ha, D. T. T., Khiem, C. C., Quy, T. H., Lam, V. T., et al. (2013). Relationship between Aboveground Biomass and Measures of Structure and Species Diversity in Tropical Forests of Vietnam. *For. Ecol. Manag.* 310, 213–218. doi:10.1016/j.foreco.2013.08.034

Dar, J. A., Subashree, K., Raha, D., Kumar, A., Khare, P. K., and Khan, M. L. (2019). Tree Diversity, Biomass and Carbon Storage in Sacred groves of Central India. *Environ. Sci. Pollut. Res.* 26, 37212–37227. doi:10.1007/s11356-019-06854-9

Deb, D., Jamatia, M., Debbarma, J., Ahirwal, J., Deb, S., and Sahoo, U. K. (2021). Evaluating the Role of Community-Managed forest in Carbon Sequestration and Climate Change Mitigation of Tripura, India. *Water Air Soil Pollut.* 232, 166. doi:10.1007/s11270-021-05133-z

Devi, L. S., and Yadava, P. S. (2015). Carbon Stock and Rate of Carbon Sequestration in Dipterocarpus Forests of Manipur, Northeast India. *J. For. Res.* 26, 315–322. doi:10.1007/s11676-015-0070-8

Dung, L. V., Tue, N. T., Nhuan, M. T., and Omori, K. (2016). Carbon Storage in a Restored Mangrove forest in Can Gio Mangrove forest Park, Mekong Delta, Vietnam. *For. Ecol. Manag.* 380, 31–40. doi:10.1016/j.foreco.2016.08.032

Fischer, H. S., Michler, B., and Ewald, J. (2014). Environmental, Spatial and Structural Components in the Composition of Mountain forest in the Bavarian Alps. *Folia Geobot* 49, 361–384. doi:10.1007/s12224-013-9185-x

Gandhi, D. S., and Sundarapandian, S. (2017). Large-scale Carbon Stock Assessment of Woody Vegetation in Tropical Dry Deciduous forest of Sathanur reserve forest, Eastern Ghats, India. *Environ. Monit. Assess.* 189, 187. doi:10.1007/s10661-017-5899-1

García-Vega, D., and Newbold, T. (2020). Assessing the Effects of Land Use on Biodiversity in the World's Drylands and Mediterranean Environments. *Biodivers Conserv* 29, 393–408. doi:10.1007/s10531-019-01888-4

Gebrewahid, Y., and Meressa, E. (2020). Tree Species Diversity and its Relationship with Carbon Stock in the Parkland Agroforestry of Northern Ethiopia. *Cogent Biol.* 6 (1), 1728945. doi:10.1080/23312025.2020.1728945

Gogoi, A., Ahirwal, J., and Sahoo, U. K. (2021). Plant Biodiversity and Carbon Sequestration Potential of the Planted forest in Brahmaputra Flood plains. *J. Environ. Manage.* 280, 111671. doi:10.1016/j.jenvman.2020.111671

Gogoi, A., and Sahoo, U. K. (2018). Impact of Anthropogenic Disturbance on Species Diversity and Vegetation Structure of a lowland Tropical Rainforest of Eastern Himalaya, India. *J. Mt. Sci.* 15 (11), 2453–2465. doi:10.1007/s11629-017-4713-4

Gogoi, A., Sahoo, U. K., and Saikia, H. (2020). Vegetation and Ecosystem Carbon Recovery Following Shifting Cultivation in Mizoram-Manipur-Kachin Rainforest Eco-Region, Southern Asia. *Ecol. Process.* 9, 21. doi:10.1186/s13717-020-00225-w

Gower, S. T. (2003). Patterns Andmechanisms of Theforestcarboncycle. *Annu. Rev. Environ. Resour.* 28, 169–204. doi:10.1146/annurev.energy.28.050302.105515

Gupta, H., and Kumar, R. (2020). Distribution of Selected Polycyclic Aromatic Hydrocarbons in Urban Soils of Delhi, India. *Environ. Techn. Innovation* 17, 100500. doi:10.1016/j.eti.2019.100500

Hussain, T., Devi, H. S., and Sarma, K. K. (2019). Aboveground Biomass and Carbon Stock Mapping Using NDVI and Ecological Studies of Woody Trees of Jeypore Reserve forest, Assam, India. *Ind. For.* 145 (7), 614–618.

IPCC (2003). *Good Practices Guidelines for Land Use, Land-Use Change and Forestry*. Kanagawa Prefecture, Japan: Institute for Global Environmental Strategies.

IPCC (2007). *Good Practices Guidelines for Land Use, Land-Use Change and Forestry*. Kanagawa Prefecture, Japan: Institute for Global Environmental Strategies.

IPCC (2014). *Synthesis Report, Contributions of Working Groups I, II and III to the Fifth Assessment Report of the International Panel on Climate Change*. Geneva, Switzerland: IPCC, 151.

Issa, S., Dahy, B., Ksiksi, T., and Saleous, N. (2020). A Review of Terrestrial Carbon Assessment Methods Using Geo-Spatial Technologies with Emphasis on Arid Lands. *Remote Sens.* 12, 2008. doi:10.3390/rs212200810.3390/rs12122008

Ives, A. R., Klug, J. L., and Gross, K. (2000). Stability and Species Richness in Complex Communities. *Ecol. Lett.* 3 (5), 399–411. doi:10.1046/j.1461-0248.2000.00144.x

Jansen, F., and Oksanen, J. (2013). How to Model Species Responses along Ecological Gradients - Huisman-Olff-Fresco Models Revisited. *J. Veg. Sci.* 24, 1108–1117. doi:10.1111/jvs.12050

Joshi, R. K., and Dhyani, S. (2019). Biomass, Carbon Density and Diversity of Tree Species in Tropical Dry Deciduous Forests in Central India. *Acta Ecologica Sinica* 39, 289–299. doi:10.1016/j.chnaes.2018.09.009

Kirby, K. R., and Potvin, C. (2007). Variation in Carbon Storage Among Tree Species: Implications for the Management of a Small-Scale Carbon Sink Project. *For. Ecol. Manag.* 246 (2-3), 208–221. doi:10.1016/j.foreco.2007.03.072

Köhl, M., Neupane, P. R., and Lotfiomran, N. (2017). The Impact of Tree Age on Biomass Growth and Carbon Accumulation Capacity: a Retrospective Analysis Using Tree Ring Data of Three Tropical Tree Species Grown in Natural Forests of Suriname. *PLoS One* 12 (8), e0181187. doi:10.1371/journal.pone.0181187

Kumar, A., and Gupta, H. (2020). Activated Carbon from Sawdust for Naphthalene Removal from Contaminated Water. *Environ. Techn. Innovation* 20, 101080. doi:10.1016/j.eti.2020.101080

Kumar, A., Kishore, B. S. P. C., Saikia, P., Deka, J., Bharali, S., Singha, L. B., et al. (2019). Tree Diversity Assessment and above Ground Forests Biomass Estimation Using SAR Remote Sensing: A Case Study of Higher Altitude Vegetation of Northeast Himalayas, India. *Phys. Chem. Earth, Parts A/B/C* 111, 53–64. doi:10.1016/j.pce.2019.03.007

Kumar, A., Pinto, M. C., Candeias, C., and Dinis, P. A. (2021). Baseline Maps of Potentially Toxic Elements in the Soils of Garhwal Himalayas, India: Assessment of Their Eco-environmental and Human Health Risks. *Land Degrad. Dev.* 32 (8), 3856–3869. doi:10.1002/ldr.3984

Kumar, A., Sharma, M. P., and Taxak, A. K. (2017). Effect of Vegetation Communities and Altitudes on the Soil Organic Carbon Stock in Kotli Bhel-1A Catchment, India. *Clean. - Soil Air Water* 45 (8), 1600650. doi:10.1002/clen.201600650

Kumar, L., Sinha, P., Taylor, S., and Alqurashi, A. F. (2015). Review of the Use of Remote Sensing for Biomass Estimation to Support Renewable Energy Generation. *J. Appl. Remote Sens* 9 (1), 097696. doi:10.1117/1.JRS.9.097696

Kurmi, B., Nath, A. J., Lal, R., and Das, A. K. (2020). Water Stable Aggregates and the Associated Active and Recalcitrant Carbon in Soil under Rubber Plantation. *Sci. Total Environ.* 703, 135498. doi:10.1016/j.scitotenv.2019.135498

Le Quéré, C., Andrew, R. M., Canadell, J. G., Sitch, S., Korsbakken, J. I., Peters, G. P., et al. (2016). Global Carbon Budget 2016. *Earth Syst. Sci. Data* 8, 605–649. doi:10.5194/essd-8-605-2016

Magurran, A. E. (2004). *Measuring Biological Diversity*. Oxford, UK: Blackwell Publishing.

Margalef, R. (1958). Information Theory in Ecology. *Int. J. Gen. Syst.* 3, 36–71. doi:10.12691/ajss-2-5-1

Mohanraj, R., Saravanan, J., and Dhanakumar, S. (2011). Carbon Stock in Kolli Forests, Eastern Ghats (India) with Emphasis on Aboveground Biomass, Litter, Woody Debris and Soils. *IForest* 4, 61–65. doi:10.3832/ifor0568-004

Mokany, K., Raison, R. J., and Prokushkin, A. S. (2006). Critical Analysis of Root : Shoot Ratios in Terrestrial Biomes. *Glob. Chang. Biol.* 12, 84–96. doi:10.1111/j.1365-2486.2005.001043.x

Nath, A. J., Brahma, B., Sileshi, G. W., and Das, A. K. (2018). Impact of Land Use Changes on the Storage of Soil Organic Carbon in Active and Recalcitrant Pools in a Humid Tropical Region of India. *Sci. Total Environ.* 624, 908–917. doi:10.1016/j.scitotenv.2017.12.199

Nath, A. J., Tiwari, B. K., Sileshi, G. W., Sahoo, U. K., Brahma, B., Deb, S., et al. (2019). Allometric Models for Estimation of forest Biomass in Northeast India. *Forests* 10, 1–16. doi:10.3390/f10020103

Nayak, S., and Sahoo, U. K. (2020). Tree Diversity and Ecological Status of *Madhuca Latifolia* (Roxb.) J.F. Macbr in Forests of Odisha. *Ind. J. Ecol.* 47 (1), 138–149.

Newaj, R., Chaturvedi, O., and Handa, A. (2016). Recent Development in Agroforestry Research and its Role in Climate Change Adaptation and Mitigation. *Ind. J. Agrofor.* 18, 1–9.

Pandey, P. C., Srivastava, P. K., Chetri, T., Choudhary, B. K., and Kumar, P. (2019). Forest Biomass Estimation Using Remote Sensing and Field Inventory: a Case Study of Tripura, India. *Environ. Monit. Assess.* 191 (9), 593. doi:10.1007/s10661-019-7730-7

Pellikka, P. K. E., Heikinheimo, V., Hietanen, J., Schäfer, E., Siljander, M., and Heiskanen, J. (2018). Impact of Land Cover Change on Aboveground Carbon Stocks in Afromontane Landscape in Kenya. *Appl. Geogr.* 94, 178–189. doi:10.1016/j.apgeog.2018.03.017

Pielou, E. C. (1966). The Measurement of Diversity in Different Types of Biological Collections. *J. Theor. Biol.* 13, 131–144. doi:10.1016/0022-5193(66)90013-0

Poorter, L., Bongers, F., Aide, T. M., Almeyda Zambrano, A. M., Balvanera, P., Becknell, J. M., et al. (2016). Biomass Resilience of Neotropical Secondary Forests. *Nature* 530, 211–214. doi:10.1038/nature16512.Epub2016feb3

Poorter, L., vander Sande, M. J., Thompson, J., Aretes, E. J. M. M., Alarcon, A., Alvarez, Sanchez, J., et al. (2015). Diversity Enhances Carbon Storage in Tropical Forests. *Glob. Ecol. Biogeogr.* 24, 1314–1328. doi:10.1111/geb.12364

Qiu, L., Zhu, J., Wang, K., and Hu, W. (2015). Land Use Changes Induced County-Scale Carbon Consequences in Southeast China 1979-2020, Evidence from Fuyang, Zhejiang Province. *Sustainability* 8 (1), 38. doi:10.3390/su8010038

Ramachandran, A., Jayakumar, S., Haroon, R. M., Bhaskaran, A., and Arockiasamy, D. I. (2007). Carbon Sequestration: Estimation of Carbon Stock in Natural Forests Using Geospatial Technology in the Eastern Ghats of Tamil Nadu, India. *Curr. Sci.* 92 (3), 323–331.

Ravindranath, N. H., Somashekhar, B. S., and Gadgil, M. (1997). Carbon Flows in Indian Forests. *Clim. Chang.* 35, 297–320. doi:10.1023/a:1005303405404

Robertson, W. K., Pope, P. E., and Tomlinson, R. T. (1974). Sampling Tool for Taking Undisturbed Soil Cores. *Soil Sci. Soc. America J.* 38, 855–857. doi:10.2136/sssaj1974.03615995003800050045x

Sahoo, U. K., Singh, S. L., Gogoi, A., Kenye, A., and Sahoo, S. S. (2019). Active and Passive Soil Organic Carbon Pools as Affected by Different Land Use Types in Mizoram, Northeast India. *PLoS One* 14 (7), e0219969. doi:10.1371/journal.pone.0219969

Saikia, P., Deka, J., Bharali, S., Kumar, A., Tripathi, O. P., Singha, L. B., et al. (2017). Plant Diversity Patterns and Conservation Status of Eastern Himalayan Forests in Arunachal Pradesh, Northeast India. *For. Ecosyst.* 4, 28. doi:10.1186/s40663-017-0117-8

Salunkhe, O., and Khare, P. K. (2016). Aboveground Biomass and Carbon Stock of Tropical Deciduous forest Ecosystems of Madhya Pradesh, India. *Int. J. Ecol. Environ. Sci.* 42 (S), 75–81.

Shannon, C. E., and Wiener, W. (1963). *The Mathematical Theory of Communication*. Urbana: University of Illinois Press. Available at: https://pure.mpg.de/rest/items/item_2383164/component/file2383163/content.

Sharma, K., Saikia, A., Goswami, S., and Borthakur, M. (2020). Aboveground Biomass Estimation and Carbon Stock Assessment along a Topographical Gradient in the Forests of Manipur, Northeast India. *Arab. J. Geosci.* 13, 443. doi:10.1007/s12517-020-05398-4

Sheikh, M. A., Kumar, M., Todaria, N. P., Bhat, J. A., Kumar, A., and Pandey, R. (2021). Contribution of *Cedrus Deodara* Forests for Climate Mitigation along Altitudinal Gradient in Garhwal Himalaya, India. *Mitig. Adapt. Strateg. Glob. Change* 26, 5. doi:10.1007/s11027-021-09941-w

Sileshi, G. W. (2014). A Critical Review of forest Biomass Estimation Models, Common Mistakes and Corrective Measures. *For. Ecol. Manag.* 329, 237–254. doi:10.1016/j.foreco.2014.06.026

Simpson, E. H. (1949). Measurement of Diversity. *Nature* 163 (4148), 688. doi:10.1038/163688a0

Singh, S., and Dadhwal, V. K. (2009). *Manual on Spatial Assessment of Vegetation Carbon Pool of India*. Dehradun: Indian Institute of Remote Sensing (National Remote Sensing Centre), ISRO, Government of India, 32.

Singh, S. L., Sahoo, U. K., Gogoi, A., and Kenye, A. (2018a). Effect of Land Use Changes on Carbon Stock Dynamics in Major Land Use Sectors of Mizoram, Northeast India. *J. Environ.l Prot.* 9, 1962–1285. doi:10.4236/jep.2018.912079

Singh, S. L., Sahoo, U. K., Kenye, A., and Gogoi, A. (2018b). Assessment of Growth, Carbon Stock and Sequestration Potential of Oil palm Plantations in Mizoram, Northeast India. *Jep* 09, 912–931. doi:10.4236/jep.2018.99057

Singh, S. L., and Sahoo, U. K. (2015). Soil Carbon Sequestration in Homegardens of Different Age and Size in Aizawl District of Mizoram, Northeast India. *Nebios* 6, 12–17.

Singh, S. L., and Sahoo, U. K. (2021). Tree Species Composition, Diversity and Soil Organic Carbon Stock in Homegardens and Shifting Cultivation Fallows of Mizoram, Northeast India. *Vegetos* 34, 220–228. doi:10.1007/s42535-021-00194-1

Solomon, N., Birhane, E., Tadesse, T., Treydte, A. C., and Meles, K. (2017). Carbon Stocks and Sequestration Potential of Dry Forests under Community Management in Tigray, Ethiopia. *Ecol. Process.* 6, 20. doi:10.1186/s13717-017-0088-2

Tamang, M., Chettri, R., Vineeta, Shukla, G., Shukla, J. A., Kumar, A., Kumar, M., et al. (2021). Stand Structure, Biomass and Carbon Storage in *Gmelina Arborea* Plantation at Agricultural Landscape in Foothills of Eastern Himalayas. *Land* 10, 387. doi:10.3390/land10040387

Thangjam, U., Sahoo, U. K., Thong, P., and Sileshi, G. W. (2019). Developing Tree Volume Equation for Parkia Timoriana Grown in home Gardens and Shifting Cultivation Areas of Northeast India. *Forests, Trees and Livelihoods* 28, 227–239. doi:10.1080/14728028.2019.1624200

Thokchom, A., and Yadava, P. S. (2017). Biomass and Carbon Stock along an Altitudinal Gradient in forest of Manipur, Northeast India. *Trop. Ecol.* 58 (2), 389–396.

Thong, P., Sahoo, U. K., Thangjam, U., and Pebam, R. (2020). Pattern of forest Recovery and Carbon Stock Following Shifting Cultivation in Manipur, Northeast India. *PLoS One* 15 (10), e0239906. doi:10.1371/journal.pone.0239906

UNFCCC (2006). *Background Paper for the Workshop on Reducing Emissions from Deforestation in Developing Countries*. Rome, Italy: United Nations Framework Convention on Climate Change.

UNFCCC (2008). *United Nations Framework Convention on Climate Change Handbook*. Halesworth, United Kingdom: Technographic Design and Printers Ltd, 210.

WagnerLiang, B. E., Liang, E., Li, X., Dulamsuren, C., Leuschner, C., and Hauck, M. (2015). Carbon Pools of Semi-arid Picea Crassifolia Forests in the Qilian Mountains (north-eastern Tibetan Plateau). *For. Ecol. Manag.* 343, 136–143. doi:10.1016/j.foreco.2015.02.001

Walkley, A., and Black, I. A. (1934). An Examination of the Degtjareff Method for Determining Soil Organic Matter, and a Proposed Modification of the Chromic Acid Titration Method. *Soil Sci.* 37, 29–38. doi:10.1097/00010694-193401000-00003

Weiskittel, A. R., MacFarlane, D. W., Radtke, P. J., Affleck, D. L. R., Temesgen, H., Woodall, C. W., et al. (2015). A Call to Improve Methods for Estimating Tree Biomass for Regional and National Assessments. *J. For.* 113(4), 414–424. doi:10.5849/jof.14-091

Zhang, M., Huang, X., Chuai, X., Yang, H., Lai, L., and Tan, J. (2015). Impact of Land Use Type Conversion on Carbon Storage in Terrestrial Ecosystems of China: A Spatial-Temporal Perspective. *Sci. Rep.* 5, 10233. doi:10.1038/srep10233

Zuo, S., Ren, Y., Weng, X., Ding, H., Yun, G., and Chen, Q. (2017). Carbon Distribution and its Correlation with Floristic Diversity in Subtropical Broad-Leaved Forests during Natural Succession. *Jtfs* 29 (4), 493–503. doi:10.26525/jtfs2017.29.4.493503

Conflict of Interest: The authors declare that the research was conducted in the absence of any commercial or financial relationships that could be construed as a potential conflict of interest.

Publisher's Note: All claims expressed in this article are solely those of the authors and do not necessarily represent those of their affiliated organizations, or those of the publisher, the editors, and the reviewers. Any product that may be evaluated in this article, or claim that may be made by its manufacturer, is not guaranteed or endorsed by the publisher.

frontiers in Environmental Science

ORIGINAL RESEARCH
published: 29 October 2021
doi: 10.3389/fenvs.2021.757976

Biomass Production Assessment in a Protected Area of Dry Tropical forest Ecosystem of India: A Field to Satellite Observation Approach

*Tarun K. Thakur[1], Digvesh K. Patel[1], Anita Thakur[1], Anirudh Kumar[1], Arvind Bijalwan[2], Jahangeer A. Bhat[3], Amit Kumar[4], M. J. Dobriyal[3], Munesh Kumar[5] and Amit Kumar[6]**

[1]Indira Gandhi National Tribal University, Amarkantak, India, [2]College of Forestry, VCSG Uttarakhand University of Horticulture and Forestry, Tehri Garhwal, India, [3]College of Horticulture and Forestry, Rani Lakshmi Bai Central Agricultural University, Jhansi, India, [4]Central MugaEri Research and Training Institute, Central Silk Board, Jorhat, India, [5]Department of Forestry and Natural Resources, H.N.B. Garhwal University, Srinagar Garhwal, India, [6]Nanjing University of Information Science and Technology, School of Hydrology and Water Resources, Nanjing, China

OPEN ACCESS

Edited by:
Valdir Felipe Novello, University of São Paulo, Brazil

Reviewed by:
Dr. Manoj Kumar Jhariya, Sant Gahira Guru Vishwavidyalaya, India
Ravi Kant Chaturvedi, Xishuangbanna Tropical Botanical Garden (CAS), China

***Correspondence:**
Amit Kumar
amitkdah@nuist.edu.cn

Specialty section:
This article was submitted to Interdisciplinary Climate Studies, a section of the journal Frontiers in Environmental Science

Received: *13 August 2021*
Accepted: *14 September 2021*
Published: *29 October 2021*

Citation:
Thakur TK, Patel DK, Thakur A, Kumar A, Bijalwan A, Bhat JA, Kumar A, Dobriyal MJ, Kumar M and Kumar A (2021) Biomass Production Assessment in a Protected Area of Dry Tropical forest Ecosystem of India: A Field to Satellite Observation Approach. Front. Environ. Sci. 9:757976. doi: 10.3389/fenvs.2021.757976

In recent decades, degradation and loss of the world's forest ecosystems have been key contributors to biodiversity loss and future climate change. This article analyzes plant diversity, biomass, carbon sequestration potential (CSP), and the net primary productivity (NPP) of four vegetation types viz., Dense mixed forest (DMF); Open mixed forest (OMF); Teak plantation (TP), and Sal mixed forest (SMF) in the dry tropical forest ecosystem of central India through remote sensing techniques together with physical ground observations during 2013–2018. The total C storage in trees varied from 16.02 to 47.15 Mg ha^{-1} in studied vegetation types with the highest in DMF and lowest in OMF. The total C storage in stem wood, branches, and foliage falls in the range of 52.93–78.30%, 9.49–22.99%, and 3.31–12.89% respectively. The total standing biomass varied from 83.77 to 111.21 Mg ha^{-1} and these variations are due to different vegetation types, with the highest in DMF followed by TP, SMF while the lowest was estimated in OMF. The net primary productivity (NPP) [aboveground (AG) + belowground (BG)] varied from 7.61 to 9.94 Mg ha^{-1} yr^{-1} with mean values of 8.74 Mg ha^{-1} yr^{-1} where AG shares a maximum contribution of 77.66%. The total biomass production was distributed from 64.09 to 82.91% in AG and 17.08–35.91% in BG components. The present study outlines that the studied forest ecosystem has the substantial potential of carbon sequestration and a great possibility of mitigating local and global climate change.

Keywords: diversity index, C storage, litterfall, biomass production, remote sensing

INTRODUCTION

In recent decades, there is a growing concern among the scientific community, researchers, environmentalists, foresters, and policy developers around the globe regarding the sustainable management of natural resources (Kumar et al., 2021a,b). Overexploitation of natural resources is causing severe ecological deprivation and affecting the functioning of various natural ecosystems. Studies have shown that human activities changed carbon stocks in terrestrial pools through rapid land-use transformations (Pan et al., 2011; Thakur et al., 2014; Jones et al., 2019; Jhariya and Singh, 2021). Remote sensing techniques have immense potential in determining carbon and biomass

storage, net primary productivity, species diversity, and change in land use land cover (LULC) of the region (FSI, 2015, FSI, 2019; Thakur et al., 2019). In the mainland of Southeast Asia, almost 30% of dry forests are currently in existence, while 60% of Indian forests are considered tropical dry forests (Poffenberger, 2000; Waeber et al., 2012). The current study was designed to objectively assess biomass production along with land use pattern, plant diversity, structure and composition of plant communities, and carbon sequestration potential, in tropical dry forests (TDF) of the protected area of the Achanakmaar Amarkantak Biosphere Reserve (AABR) in central India, using remote sensing techniques assisted by ground-based direct measurements. Biomass production assessment is one of the major criteria for correlating ecosystem functioning and productivity in the forest ecosystem. To scale up the assessment at the landscape level, satellite data coupled with sampled ground verification gives more reliable information more economically and in less time. Furthermore, it helps the forest managers make suitable plans and design the required interventions as a management strategy for the improvement of protected habitats like biosphere reserves.

The flora and fauna of AABR are a key sign of the natural legacy of species diversity. Due to environmental implications, AABR was declared as the 14th biosphere reserve of India in 2005 and UNSECO tagged it as the world's greatest heritage site in 2012. Ecological degradation by anthropogenic activities like forest cutting, forest fire, overexploitation of overstorey and understorey vegetation, encroachment, mining, site development, and settlements are placing severe pressure on biological resources, leading to loss of biodiversity, the vegetational ecology, and carbon sequestration potential of the tropics of India were also studied and gave similar findings (Jhariya, 2017; Jhariya et al., 2019; Kumar and Kumar, 2020; Thakur et al., 2020; Thakur et al., 2021).

The structure and composition of vegetation play a strong role in controlling many important ecosystem processes like photosynthesis, evapotranspiration, and canopy light interception. The plant communities in any ecosystem largely determine the energy exchange, biomass accumulation, and gaseous exchange between plant canopies, thus regulating atmospheric concentrations of carbon dioxide (CO_2) which in turn is useful for understanding the carbon budgets of the vegetation type (Nelson et al., 1999; Houghton et al., 2015; Anderson-Teixeira et al., 2016; Chazdon et al., 2016; Kumar et al., 2017; Wang et al., 2019; Tripati et al., 2020; Chaturvedi et al., 2021). In the past, a few studies have indicated that the multispectral satellite images are useful and can assist in monitoring the structure, and composition of a forest type, its diversity, and spatial arrangements (Lepine et al., 2016; Shiklomanov et al., 2016; Ali et al., 2017; Middinti et al., 2017), before addressing any functional ecological and biophysical processes of an ecosystem (such as above-ground biomass (AGB), net primary production (NPP), evapotranspiration, energy exchange, and biomass allocation patterns). Tropical forests are considered as productive terrestrial environments with a maximum potential of carbon sink and NPP per unit area (Fearnside, 1996; Gaston et al., 1998; Chave et al., 2001; Clark et al., 2001; Malhi et al., 2004; Malhi et al., 2009; Beer et al., 2010; Bijalwan et al., 2010; Mohommad and Joshi, 2015; Anderson-Teixeira et al., 2016; Poorter et al., 2016; Moore et al., 2018; Wallis et al., 2019; Wang et al., 2019). The structure of vegetation helps to facilitate suitable management practices and obtain higher rates of biomass production with maximum economic returns. The structure of vegetation assists with facilitating suitable management practices to obtain higher rates of biomass production with maximum economic returns (Chaturvedi et al., 2011; Chaturvedi and Raghuwanshi, 2015). Therefore, the importance of structural inputs for ecosystem analysis at different spatial scales has been well recognized as hotspots for present research.

There is an increasing need to improve understanding of carbon pools and fluxes in dry tropical ecosystems particularly in the central part of India. The annual loss of forest cover in the tropics ranged between 15–17 million ha (FAO, 1995; Reich, 2012; Popkin, 2018). The biomass burning from forest areas of the world ranged between 12–13 million ha, of which 87% occurs in the tropics region (FAO, 1995). At present, the CO_2 levels in the atmosphere are increasing annually at 2 ppm per year triggering a major threat to the functioning of different ecosystems. Tropical forests have a great potential for atmospheric carbon sequestration and currently accumulate 55% of global terrestrial carbon (IPCC, 1996; Pan et al., 2011; Grace et al., 2014; Jones et al., 2019). Thus analysis of vegetation dynamics and LULC are urgently required for formulating constructive policies for biodiversity management, finding the best possible ways of augmenting carbon sequestration rates, and planning progressive management strategies for achieving sustainable development goals (SDGs). For evaluating and understanding the structural and functional processes of different land cover types, geospatial techniques have proved indispensable tools, which provide large spatial, multi-temporal, and synoptic data of dynamic land surface features and frequently monitor the carbon sequestration in space and time (Popkin, 2018). Earlier, several researchers demonstrated the potentials of geospatial technology for monitoring and creating an inventory of vegetation (Swamy, 1998; Mandal and Joshi, 2014). However, satellite remote sensing (RS) when combined with GIS techniques provides improved information and also helps in developing valuable strategies for natural resource management. Therefore, in the backdrop of reviews, we explored the potential of satellite images to forecast species diversity, carbon sequestration potential (CSP), AGB, and forest productivity in the TDF of AABR, India.

MATERIALS AND METHODS

Study Area

The AABR protected area is located in the central part of India with an area of 626.76 km^2 of dry tropical forest. The current study was conducted in the AABR area during 2013–2018 to assess species diversity, carbon sequestration potential, biomass, and NPP in four different vegetation types viz.; TP, SMF, DMF, and OMF. The geo-coordinates of the study area fall between

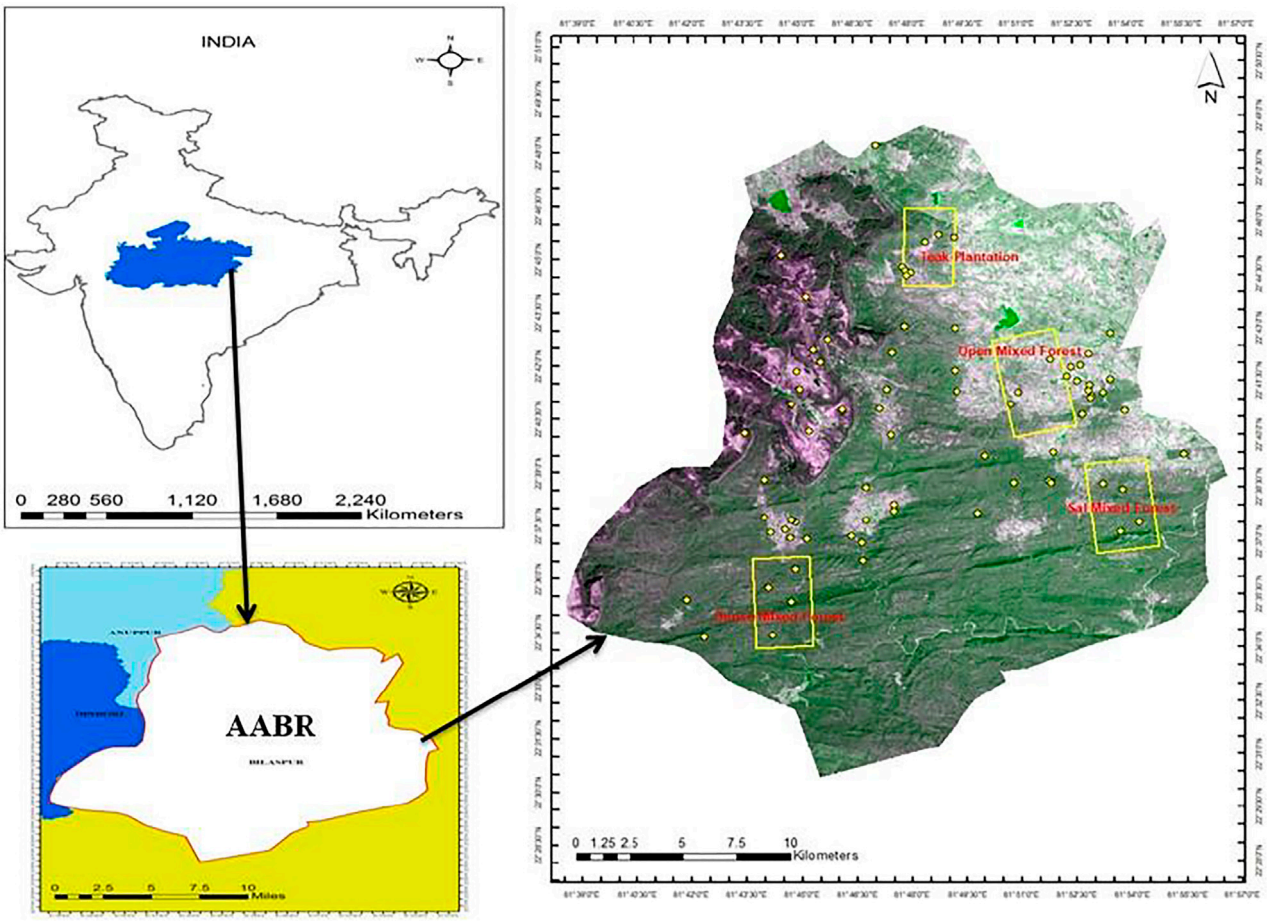

FIGURE 1 | Layout map along with identified sample plots, in yellow boxes at different locations in dry tropical forests of AABR.

21°15′ to 21°58′ N and 82°25′ to 82°5′ E. The map along with identified plots at selected sampling sites is presented in **Figure 1**. The climatic condition of the study area is moderate humid throughout the year, with a peak rainfall from July to September and a dry period from April to June. The rainfall varies from 1,050–1,500 mm yr^{-1} and the mean annual temperature is 25.8°C. The study area falls under the Biosphere Reserve where all harvesting or felling is banned. The methodologies adopted for various study parameters are described briefly in the sub-section given below.

Satellite Remote Sensing Data Predictors

Resourcesat-2A satellite data were procured from the National Remote Sensing Agency (NRSA), Hyderabad, India. All the electromagnetic wavelength/bands were stacked in Resourcesat-2A satellite data and pre-processed by ERDAS, including geometric and atmospheric corrections. The vegetation indices and climatic factors derived from different vegetation types were charted (Thakur et al., 2014; Wallis et al., 2019; Wang et al., 2019). The generation of spectral vegetation indices such as Advance Vegetation Index (AVI), Ratio Vegetation Index (RVI), Normalized Difference Moisture Index (NDMI), Normalized Difference Vegetation Index (NDVI), Enhanced Vegetation Index (EVI), and Very Dense Vegetation Index (VDVI) map was established using ERDAS Imagine (Version 9.3) software, as illustrated in **Table 1**.

Phytosociological, Diversity and Leaf Area Index Analysis

The systematic vegetation characterization was performed by quantifying the different parameters of vegetation composition, structure, and species richness. Phytosociological studies were conducted in two stages viz., in the first stage, different forest vegetation was characterized in terms of its spatial organization of plant communities. The stand or forest level community structural information is useful for local/patch scale simulation process models and also filtering information on structural attributes and variations for regional-scale process models. In the second stage, phyto-sociological studies were conducted on type-level to recognize the overall pattern and organization of plant communities in a given type in the region. The type-level community structural information is essential for regional ecosystem simulation models, primarily for the functional

TABLE 1 | Topographical, vegetation indices/spectral and diversity index.

	Metrics	Abbreviation	Expression
Topographical	Elevation	DEM	Digital Elevation Model
	Drainage	Drainage	Generate through DEM data (USGS)
	Slope	Slope	Gradient of DTM in degree
	ASPECT	Aspect	Compass Direction
Vegetation indices/Spectral	Normalized difference vegetation index	NDVI	$\frac{NIR-Red}{NIR+Red}$
	Enhanced vegetation index	EVI	$G^{*}\frac{NIR-Red}{NIR+C1^{*}Red-C2^{*}Blue+L}$ G (Gain factor) = 2.5, C1 = 6, C2 = 7.5, L = 1
	Normalized difference moisture index	NDMI	$\frac{NIR-SWIR}{NIR+SWIR}$
	Ratio vegetation index	RVI	RED /NIR
	Advance vegetation index	AVI	[NIR * (1-Red) * (NIR-Red)]
	Very dense vegetation index	VDVI	$\frac{2^{*}Green-Red-Blue}{2^{*}Green+Red+Blue}$
Diversity index	Shannon-Wiener index	H′	H' = - pi log 2 pi
	Simpson's concentration index	□ H′	H'□ = (Ni / N) ^{2}
	Margalef's index of species richness	D	D = S-1 / in N
	Pielou's evenness index	E	E = H' / ins
	Beta Diversity	B	B = Sc/s

process of an ecosystem. In the second stage, phyto-sociological studies on type-level to recognize the overall pattern and organisation of plant communities and groups in a given type in the region. The type-level community structural information is essential for regional ecosystem simulation models, primarily for the functional process of an ecosystem.

The phytosociological exploration was determined from different sampling plots of 20 m × 20 m for trees (TV; diameter above 20 cm), 5 m × 5 m for shrubs (SV; height up to 5 meter), and 1 m × 1 m size for herbaceous species (HV). In each sampling plot, TV, SV, and HV were enumerated for their diameter values. The diameter of trees measured at 1.37 m above ground level, shrubs 15 cm above ground level, and herbs at color zone. The TV and SV in forty quadrats were marked for periodic measurements of diameter at breast height (dbh) and height increment values for estimation of biomass and its production. The formula used for the analysis of density, abundance, frequency, and basal area were performed according to Curtis and Mc Intosh (1950). Moreover, analysis of the species diversity of various forests of AABR was determined by the formulas used in **Table 1**. The mortality in different stages of trees was also estimated by considering the deterioration status of the trees. The leaf area index (LAI) of the species was estimated by taking ten sample leaves randomly from respective plots for each tree, shrub, and herb with the help of a leaf area analyzer.

Estimation of Carbon Sequestration Potential

The Muffle furnace combustion methods were used for the determination of carbon concentration in the various components of TV, SV, and HV by adopting the methods of Negi et al. (2003) as follows:

$$Ty_{ni} = \sum_{i=1}^{n} Ty_{ai} \times (TV_{ci} + SV_{ci} + HV_{ci}) \quad (1)$$

Where; Ty_{ci} denotes Carbon content of i^{th} vegetation type; Ty_{ai} : Area of i^{th} vegetation type; Ty_{ci}: Carbon in Tree layer; SV_{ci} : Carbon in Shrub layer; HV_{ci} : Carbon in Herbaceous layer of i^{th} vegetation type

$$\begin{aligned} TV_{ci} &= (Sm_{ci} + Br_{ci} + Lf_{ci} + FRT_{ci}) \\ SV_{ci} &= (S_{ci} + Lf_{ci} + Rt_{ci}) \\ HV_{ci} &= (Lf_{ci} + Rt_{ci}) \end{aligned} \quad (2)$$

Where; Sm_{ci} denotes Stem Carbon; Br_{ci} : Branch Carbon; Lf_{ci} : Leaf Carbon; Rt_{ci}: Root Carbon; W_{ci} : Wood Carbon corresponding to i^{th} vegetation type

Estimation of Biomass

TV and SV biomass, Ty_{bi} (Mg ha^{-1}) in different vegetation types was estimated by using the allometric regression model established by Singh and Mishra (1979). Therefore, available biomass allometric equations (**Supplementary Tables S1, S2**) for dry tropical forests were used to estimate biomass precisely, only those regression equations were taken into consideration which were developed with similar climatic (temperature and rainfall) and edaphic conditions (soil type). The biomass was estimated by the non-harvest method by measuring dbh and height and applying biomass allometric equations. While using equations, dbh and height were used as independent variables while component biomass was used as a dependent variable. The different components of TV, SV, HV (i.e., stem, branch, foliage, and root) biomass, and fine roots were summed up to calculate total standing biomass (Mg ha^{-1}) in each sample plot for different vegetation types and the component-wise biomass was computed and extrapolated. The soil core method was used for the estimation of fine root biomass. The fine roots (<5 mm diameter) were sampled from four monoliths (15 cm × 15 cm x 15 cm) randomly drawn from each forest type at two different depths, i.e., 0–50 and 50–100 cm, during rainy, winter and summer seasons. In total 120 (2 soil depths x 20 samples x 3 seasons) soil cores were drawn for each forest type. The total fine root biomass was obtained by taking the mean fine root biomass of rainy, winter, and summer seasons. All these biomass values

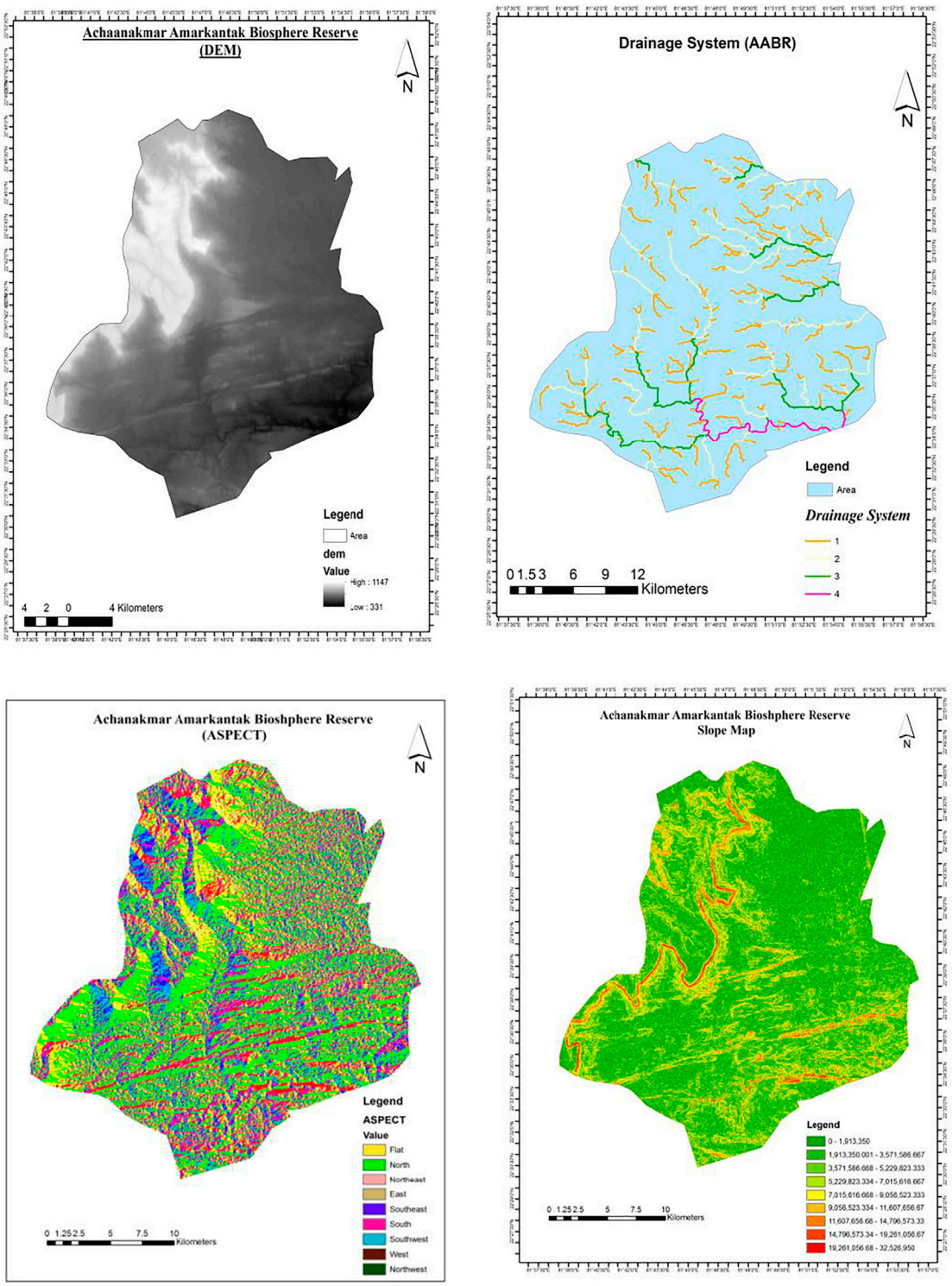

FIGURE 2 | Satellite map **(A)** Digital elevation model (DEM); **(B)** Drainage pattern; **(C)** Aspect map of the study area; **(D)** Slope map of AABR.

TABLE 2 | Species diversity indices in dry tropical forest of AABR.

Variable	TP	SMF	DMF	OMF
Tree Layer (TV)				
Tree Density (per Ha)	470	652.5	587.5	467.5
Number of Species	11	14	29	22
Basal area (m^2 ha^{-1})	28.81	34.12	29.05	9.26
Frequency	26.36	24.28	30	31.36
Total number of Species Censused (S)	11	14	29	22
Shannon-Wiener index (H′)	0.67	0.90	2.34	2.28
Simpson's concentration index (Cd)	0.75	0.65	0.09	0.14
Margalef's index of species richness (D)	5.79	5.31	12.54	9.45
Pielou's evenness index (E)	0.25	0.28	0.67	0.63
Beta Diversity (B)	1.27	1.58	1.20	1.72
Shrub Layer (SV)				
Shrub Density (per Ha)	3148.72	5870.59	6053.33	4579.31
Number of Species	13	15	23	14
Basal area (m^2 ha^{-1})	0.36	0.48	0.64	1.61
Frequency (%)	40.23	60	41.15	46.551
Total number of Species Censused (S)	13	17	28	24
Shannon-Wiener index (H′)	0.84	2.63	3.05	1.00
Simpson's concentration index (Cd)	0.63	0.08	0.05	0.39
Margalef's index of species richness (D)	0.19	2.72	3.49	0.32
Pielou's evenness index (E)	0.02	0.97	0.97	0.38
Beta Diversity (B)	2.00	1.71	1.13	1.86
Herbaceous Layer (HV)				
Herb Density (m^2)	137.2	141.6	328.40	233.60
Number of Species	24	33	29	31
Basal area (m^2 ha^{-1})	0.00297	0.0037	0.00296	0.00237
Frequency (%)	40	34.84	27.93	27
Total number of Species Censused (S)	24	33	29	31
Shannon-Wiener index (H′)	0.23	0.28	0.32	0.30
Simpson's concentration index (Cd)	3.25	3.64	3.16	2.86
Margalef's index of species richness (D)	0.05	1.45	0.05	0.04
Pielou's evenness index (E)	1.20	1.39	1.42	1.23
Beta Diversity (B)	2.22	1.94	1.89	2.95

were extrapolated on a Mg ha^{-1} basis. The mean of the biomass of twenty sample plots represents the standing biomass of a particular forest type. To obtain the total existing biomass of different vegetation types, the mean biomass values were multiplied with their respective areas of vegetation types derived from satellite data.

Estimation of Litterfall

The litterfall of dry tropical forests of AABR was measured in different seasons (i.e., rainy, winter, summer) by randomly laying five litter traps (each size of 50 cm × 50 cm x 50 cm) on the forest floor in every identified sample plot. Overall, litterfall was recorded in 50 sample plots (5 traps x 10 quadrats) and collected in each season i.e. rainy, winter and summer from the different vegetation types. The collected litterfall sealed in the polyethylene bags was brought to the laboratory, where the samples were separated into leaf, wood, fruits, flower, and bark components followed by oven-dried at 80°C for 24 h and weighted to determine oven-dry weights. The weights of dried components were added to derive the total litterfall of respective sample plots of a vegetation type. Furthermore, data of all three seasons were added to obtain the total annual litterfall (Mg ha^{-1}), and the mean of the litterfall of ten sample plots represented the litterfall of that vegetation type.

Estimation of Net Primary Productivity

To estimate the annual net primary productivity on a hectare basis, ΔB_i (Mg ha^{-1} yr^{-1}), the dbh of TV and SV were repeatedly measured for three successive years i.e., 2016, 2017, and 2018 in marked sample plots of different vegetation types. The biomass increment of TV and SV were estimated from the dbh values of respective periods using a regression equation. The biomass of herbs was estimated in respective years by harvest procedure using vegetation collection and measurement methods. The average biomass production of individual components (TV, SV) of the sample plots of each vegetation type were calculated using the expression = $\{(B_3 - B_2) + (B_2 - B_1)/2\}$. The total net production of a given sample plot of vegetation type was measured by adding the respective production of trees, shrubs, herbaceous layers, fine root (peak), and total litterfall of that vegetation type. In order to obtain the total NPP of different vegetation types, the mean NPP values were multiplied with their respective areas of vegetation types, which were derived from satellite data.

Expression used for computing NPP as follows:

$$Ty_{Ni} = \sum_{i=1}^{n} Ty_{ai} \times \Delta B_i + D_i + G \quad (3)$$

Where; ΔB_i denotes rate of biomass increment of tree, shrub and herb layer of i^{th} forest type;

ΔB_i : $\Delta(T_{bi} + S_{bi} + H_{bi})$; T_{bi}: Tree biomass increment; S_{bi}: Shrub biomass increment; H_{bi} : Herbaceous biomass increment corresponding to i^{th} forest type; :D_i Annual detritus production (litterfall and root hairs mortality) corresponding to i^{th} forest type; G: Annual grazing losses /burning/other removals (not accounted).

$$TNPP = Ty_{ni} + Ty_{nj} + Ty_{nk} \cdots Ty_{nn} \quad (4)$$

TNPP = Total net productivity, Ty_{ni} n = NPP of i^{th} , j^{th}, k . . . n^{th} vegetation types

Correlations Among Vegetation Indices, Shannon Index, Leaf Area Index, Carbon Sequestration Potential, Biomass, Litterfall, and NPP

The correlation relationship was carried out between spectral vegetation indices (NDVI, RVI, AVI, EVI, VDVI, and NDMI) with Shannon index, carbon storage, leaf area index (LAI), biomass, and NPP of all the vegetation types of AABR. The sample points used for the ground survey were overlaid on vegetation indice images to extract spectral vegetation indices data, which was performed in ARC-GIS (Version 10.3). Correlations were drawn between the spectral vegetation indices derived from satellite data and ground measurements. The results acquired from the two parameters were used to determine the strength of the relationship. The correlation between vegetation indices and species diversity was tested at $p < 0.01$.

Aspect and Slope Maps

Aspect and slope maps were generated by analyzing topographic data in a GIS environment. The map shows eight aspect classes and was merged to form only four major aspect classes (north (N), south (S), east (E), and west (W)). Among different aspects, northern and eastern aspects occupied a large area compared to southern and western aspects. The altitudinal range of the study area varied from 505.43 to 719.65 m in different forests and nine slope classes were delineated between 0–20% slope, which was merged to form a gentle slope class, from 21–40% slopes into a medium slope and slope categories >40% were merged to form steep slope class. The largest area was covered by gentle slope class, while only a relatively small area was occupied by steep slope class. Furthermore, slope, aspect, drainage, and Digital Elevation Model (DEM) were also generated using TIN data (**Figure 2**).

Statistical Analysis

Data on structure, composition, diversity, biomass, and carbon sequestration potential were analyzed using one-way analysis of variance. To understand the relationship between stand diversity and the functional parameters in the TDF ecosystem, correlation analysis was performed among diversity indices and functional attributes viz., carbon storage, and net productivity. Correlations were also drawn between spectral vegetation indices (viz. NDVI, AVI, RVI, EVI, VDVI, and NDMI) derived from satellite data and ground measured structural and functional variables. Attempts were also made to develop empirical models for directly estimating the diversity, carbon storage, and biomass production of TDF of AABR from satellite imagery. Towards this, a simple regression analysis was executed and multivariate analysis of the data by using MINITAB version 15.0 software.

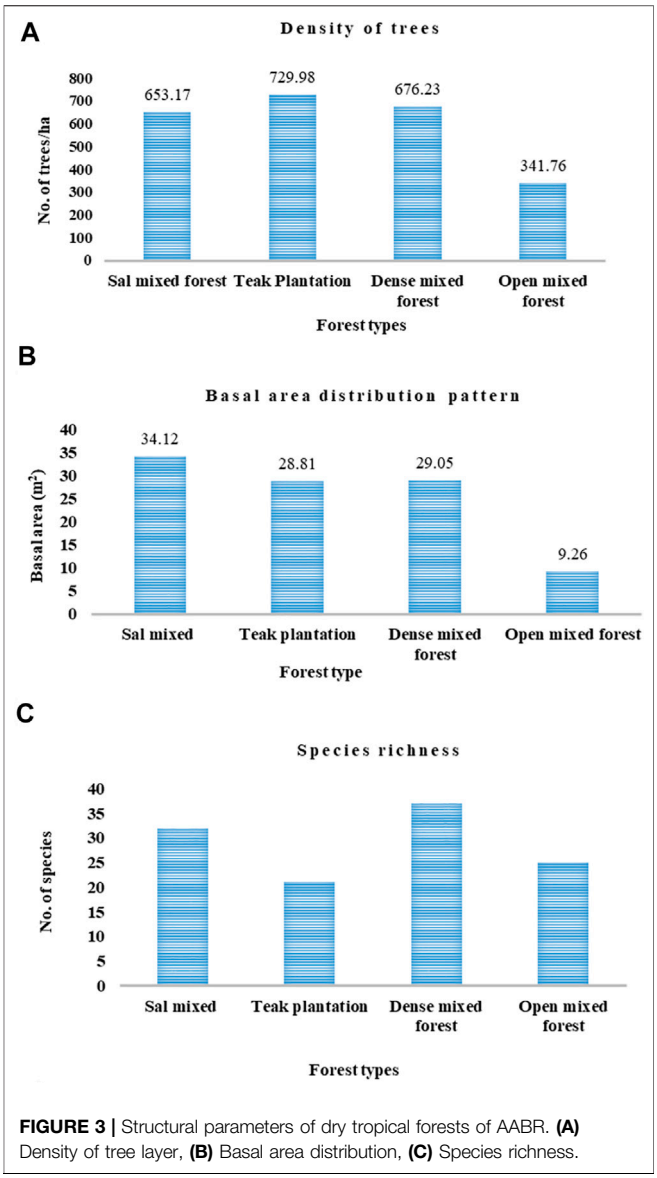

FIGURE 3 | Structural parameters of dry tropical forests of AABR. **(A)** Density of tree layer, **(B)** Basal area distribution, **(C)** Species richness.

RESULTS AND DISCUSSION

Structure, Composition, and Diversity

The composition of the flora of dry tropical forest ecosystems of AABR is very diverse. A variety of flora in these forests distributes species in three distinct canopy layers. Thirty-four species were

TABLE 3 | Pearson correlations among important spectral vegetation indices and structural attributes.

Parameter	NDVI	AVI	EVI	RVI	VDVI	NDMI	Density	Basal area	Shannon index	LAI	Carbon storage	Biomass	Litterfall	NPP
NDVI	1													
AVI	0.73[a]	1												
EVI	0.67[a]	0.93[a]	1											
RVI	0.49[b]	0.28 NS	0.20 NS	1										
VDVI	0.50[b]	0.22 NS	0.23 NS	0.43[b]	1									
NDMI	0.49[b]	0.37 NS	0.23 NS	0.32 NS	0.23 NS	1								
Density	0.67[a]	0.37 NS	0.31 NS	0.22 NS	0.19 NS	0.28 NS	1							
Basal Area	0.84[a]	0.61[a]	0.49[b]	0.43[b]	0.55[a]	0.37 NS	0.68[a]	1						
Shannon Index	0.548[a]	0.32 NS	0.25 NS	0.21 NS	0.19 NS	0.10 NS	0.098 NS	0.11 NS	1					
LAI	0.61[a]	0.45[b]	0.54[b]	0.51[b]	0.59[a]	0.43[b]	0.68[a]	0.57[a]	0.64[a]	1				
Carbon storage	0.74[a]	0.55[a]	0.48[b]	0.37 NS	0.43[b]	0.23 NS	0.53[b]	0.62[a]	0.59[a]	0.67[a]	1			
Biomass	0.79[a]	0.56[a]	0.58[a]	0.32 NS	0.52[b]	0.31 NS	0.62[a]	0.59[a]	0.67[a]	0.70[a]	0.74[a]	1		
Litterfall	0.55[a]	0.40[b]	0.43[b]	0.32 NS	0.44[b]	0.28 NS	0.52[b]	0.46[b]	0.39 NS	0.57[a]	0.61[a]	0.67[a]	1	
NPP	0.68[a]	0.35 NS	0.27 NS	0.31 NS	0.29 NS	0.24 NS	0.48[b]	0.51[b]	0.41[b]	0.54[b]	0.79[a]	0.87[a]	0.77[a]	1

[a]*Correlation is significant at the 0.01 level (2-tailed).*
[b]*Correlation is significant at the 0.05 level (2-tailed).*
NS denotes non-significant.

TABLE 4 | Consolidated statistics of forest biomass, productivity variables, and carbon storage.

	Response variable	Unit	Study site/Forest type	Minimum	Mean	Maximum
Tree vegetation						
Forest Biomass	Biomass (AGB + BGB)	Mg/ha	Teak forest	76.10	101.07	129.63
			Sal mixed	62.94	91.24	117.33
			Dense mixed	92.62	111.21	130.00
			Open mixed	64.13	83.74	102.57
Forest Productivity	Total Net production (AGNP + BGNP)	Mg/ha/yr	Teak forest	8.31	12.33	16.46
			Sal mixed	7.07	12.52	16.93
			Dense mixed	8.93	13.00	16.71
			Open mixed	6.95	10.53	13.81
Litterfall	FLP	Mg/ha	Teak forest	3.23	4.19	5.17
			Sal mixed	2.82	3.76	4.70
			Dense mixed	2.67	3.36	4.11
			Open mixed	2.54	3.93	5.31
Fine root biomass	FRB	Mg/ha	Teak forest	2.26	3.20	4.18
			Sal mixed	1.84	2.85	3.76
			Dense mixed	2.44	3.73	4.84
			Open mixed	1.86	2.79	3.49
Carbon storage	Carbon storage (AGCS + BGCS)	Kg/ha	Teak forest	29646.79	43674	56921.84
			Sal mixed	31914.34	39126	46199.88
			Dense mixed	27961.67	50640	67302.36
			Open mixed	15163.22	36489	50113.72

AGB, above ground biomass; BGB, Below ground biomass; AGNP, above ground net production; BGNP, below ground net production; FLP, fine litter production; TNNP, Total net primary production; AGCS, Above ground carbon storage; BGCS, Below ground carbon storage.

found in TV, thirty species in SV, and sixty-four species were found in HV (**Table 2**; **Supplementary Tables S3, S4, S5**). The secondary associated tree species were *Terminalia tomentosa* and *Buchanania lanzan* respectively contributing high density, frequency, relative basal area, and IVI in the SMF and TP. The dominant representative of tree species like Shorea robusta, *Diospyros* melanoxylon, and *Terminalia arjuna* was observed as predominant in DMF and OMF.

The results of density, BA distribution, and species richness of different forest types are illustrated in **Figures 3A–C**. The structural analysis shows that the density of various forests varied from 467.5 to 652.5 stems ha^{-1} and a maximum in SMF followed by DMF, TP, and a minimum in OMF. BA values lie between 9.26 and 34.12 $m^2\,ha^{-1}$ in each vegetation type and SMF exhibited maximum BA followed by DMF and TP while the minimum in OMF. The structural attributes significantly varied among each forest type in the current research. Bijalwan et al. (2010) also reported that the density of TDF ranged from 206 to 812 trees ha^{-1} and BA from 7.27 to 20.8 $m^2\,ha^{-1}$, and the number of tree species in each forest was reported as from 9 to 26. Interestingly, the structural analysis (number of tree species, density, and BA) of the TDF ecosystem has been attempted by several workers (Murphy and Lugo, 1986; Singh and Singh, 1991; Ravan, 1994; Sunderpandian and Swamy, 2000; Chaturvedi et al., 2011; Chaturvedi and Raghubanshi 2014; Kamruzzaman et al., 2017; Thakur, 2018; Darro et al., 2020). Singh and Singh, (1991) reported density 349 to 627 $treeha^{-1}$, 9.0–14.79 $m^2\,ha^{-1}$ BA, and 9 to 14 species in TDF of Uttar Pradesh, India. Murphy and Lugo (1986) also revealed a BA of 17–40 $m^2\,ha^{-1}$ in Puerto Rican subtropical dry forests.

Various diversity indices viz., species diversity (H′), the concentration of dominance (cd), species richness (d), equitability (e), and beta diversity (bd) were computed for different forest types to analyze the difference in species diversity among each vegetation type. Attempts were also made to compute the different components of the tree, shrub, and herbaceous vegetation. The results for species diversity of different vegetation types are illustrated in **Table 2**. Species diversity in various vegetation types lies from 0.67 to 2.34 for tree vegetation (TV) with a maximum in DMF and minimum in TP. Similarly, the concentration of dominance values varied from 0.09 to 0.75 in the vegetation of each forest type with a maximum in TP followed by SMF and minimum in DMF. The Margelef index values varied from 5.31 to 12.54 where DMF showed maximum values followed by OMF and SMF. Pielou's evenness index lies from 0.25 to 0.67 for TV. Beta diversity varied from 1.20 to 1.72 with OMF recorded maximum and DMF minimum. In the SV layer, Shannon-Weiner values varied between 0.84 and 3.05 where DMF recorded higher and TP as lower. Simpson index accounted for maximum values in TP followed by OMF and SMF, while, the Cd values were recorded as a minimum in DMF in shrub layer, where it varied from 0.05 to 0.63. The species richness value was higher in DMF followed by SMF, and OMF. Margalef's index values were reported in the range of 0.19–3.49 depending on vegetation types, where TP had a minimum value. Equitability accounted for 0.02 to 0.97 in all the vegetation types with the highest equitability in DMF and SMF, and minimum TP under the SV category. TP showed a maximum beta diversity index and the minimum was observed for DMF in SV, which varied from 1.13 to 2.0 in all the forest types in the AABR. For the herbaceous layer (HV), the Shannon-Weiner values were found maximum in DMF followed by OMF and SMF, while it was observed minimum for TP which is ranged from 0.23 to 0.32. On the contrary, Cd was recorded maximum in SMF and OMF, which ranged from 2.86 to 3.25 in different forest types. The species richness was recorded maximum in SMF followed by DMF and OMF and varied from 0.04 to 1.45. Similarly, equitability values in HV ranged from 1.20 to 1.42 in different forest types. DMF and SMF showed maximum values, while TP and OMF with minimum values. The beta diversity ranged from 1.89 to 2.95 with the maximum in OMF exhibited minimum in DMF. The species diversity values in various tropical forests are comparable with the present study as reported by various researchers (Ramprasad and Pandey 1992; Pandey, 2005; Thakur et al., 2019). Singh and Singh (1991) also revealed that the species diversity values range lies between 1.9 and 2.8, Simpson index values from 0.18 to 0.75, Margalef index values range between 0.21 and 0.93 in the U.P state of India. Ramprasad and Pandey (1992) analyzed the sal and teak forests of Madhya Pradesh state in India where Shannon

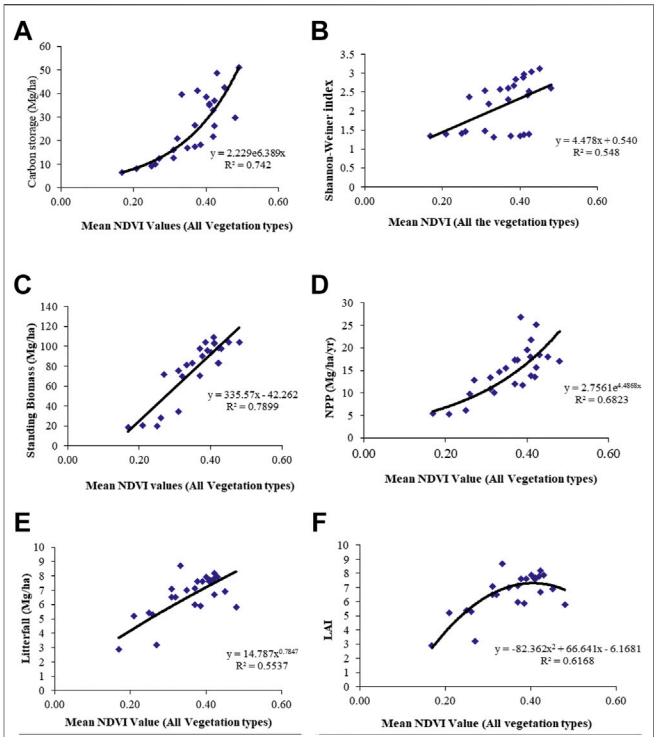

FIGURE 4 | (A) Exponential relationship among NDVI and Carbon storage; **(B)** Relationship between NDVI and Shannon- Weiner Index; **(C)** Relationship between NDVI and Biomass of dry tropical forests; **(D)** Exponential relationship between NDVI and Net primary productivity; **(E)** Relationship between NDVI and Litterfall; **(F)** Exponential relationship between NDVI and Leaf Area Index of dry tropical forests of AABR.

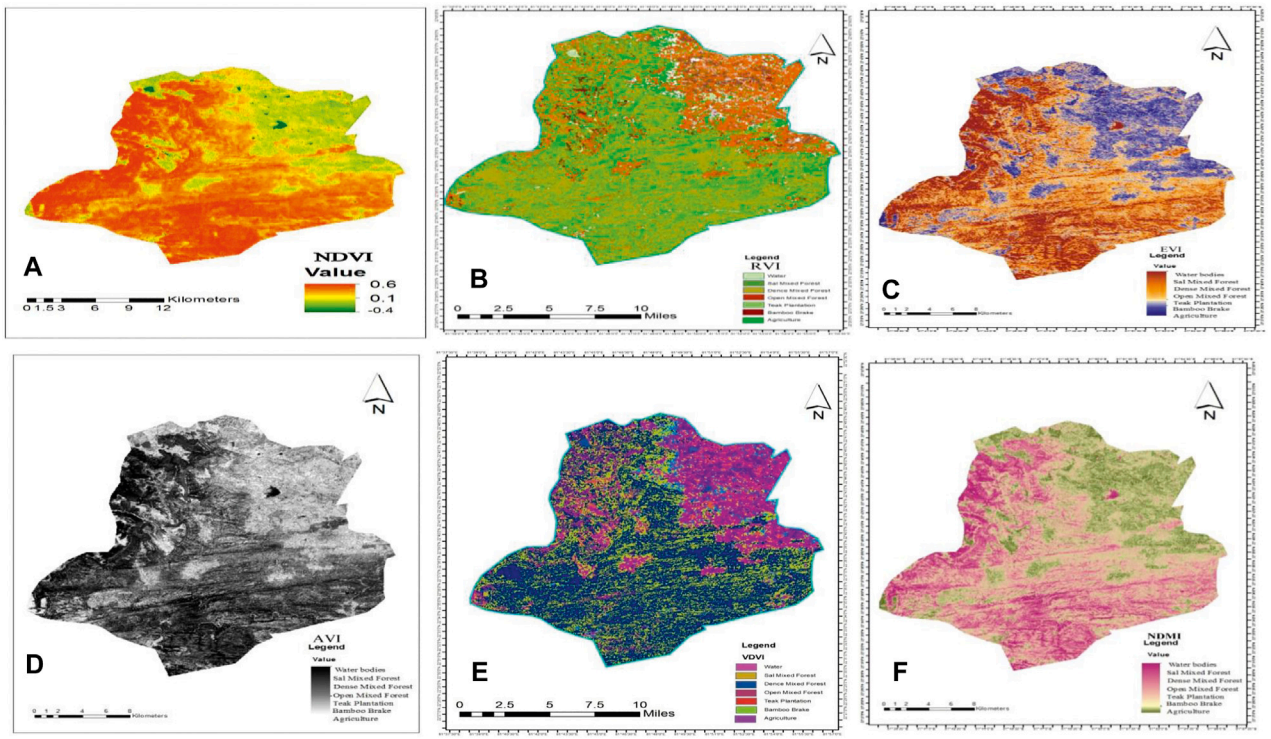

FIGURE 5 | Spectral vegetation indices **(A)** Normalized difference vegetation index (NDVI); **(B)** Ratio vegetation index (RVI); **(C)** Enhance vegetation index (EVI); **(D)** Advance vegetation index (AVI); **(E)** Very dense vegetation index (VDVI); **(F)** Normalized difference moisture index (NDMI).

diversity index ranged from 0.32 to 3.76 and Simpson index values from 0.07 to 0.63. However, many plant species are lost due to anthropogenic stress in this region (Thakur et al., 2021). Other workers (Ravan, 1994; Bijalwan et al., 2010; Thakur 2018) have also conducted studies on tropical forest ecosystems and reported similar observations. Swamy (1998), mentioned high precipitation (>2,500 mm), the number of rainy days, and better soil conditions, which resulted in rich diversity and complexity in tropical evergreen forests.

The NDVI values were positively performed with density, basal area, and species diversity (**Table 3**). The study indicated a positive correlation among the structural attributes and diversity with NDVI and other vegetation indices (**Figure 4** and **Figure 5**). Several researchers demonstrated similar research in TDF ecosystems (Franklin, 1986, Cohen and Spies, 1992 Spanner et al., 1990, Pandey, 2005, Jones et al., 2019, Wallis et al., 2019; Wang et al., 2019).

The slope and aspect in the current study showed a marked effect on structure, diversity, volume, and biomass of TDF of Central India (**Table 1** and **Figure 2**). Integration of slope and aspect along with forest types helped in improving the stratification and accounted for the physiographic variation in structure, diversity, volume, and biomass in a given forest type. Cook et al. (1989) reveal the importance of satellite data in the estimation of forest structure the NPP of North American forests. Ravan (1994) also demonstrated the topographical parameters, density, and TDF information in the GIS environment and derived homogenous vegetation strata, which were used for estimating the structural parameters of TDF ecosystems.

Total Carbon Sequestration Potential in Vegetation

Total carbon storage in the tree layer (TV) varied from16.02–47.15 Mg ha^{-1} where; DMF was recorded with the maximum amount of the C, while OMF had minimum. Total C storage was statistically alike in SMF and OMF. The DMF had 1.22, 1.54, 1.50, and 7.69 times higher C content than TP, SMF, and OMF, respectively. Total C storage ranges in stem wood accounted 52.93–78.30%, branches 9.49–22.99%, foliage 3.31–12.89%, coarse root 1.80–11.22% and fine roots 1.72–3.24% in different forest types. Similarly, in shrub vegetation (SV) the C ranged from 1.88 to 5.18 Mg ha^{-1} with a maximum in OMF followed by SMF, TP, and minimum in DMF. OMF had 1.67, 1.07, and 1.67 times higher C content than TP, SMF, and DMF, respectively. Further, C in total stem wood ranged between 56.27 and 67.79%, foliage 2.73–3.31%, and coarse root 29.45–41.12% in different forest types whereas in herb layer (HV) it ranged between 0.91–2.73 Mg ha^{-1}, with OMF registering highest C as compared to SMF, TP, and lowest in DMF.

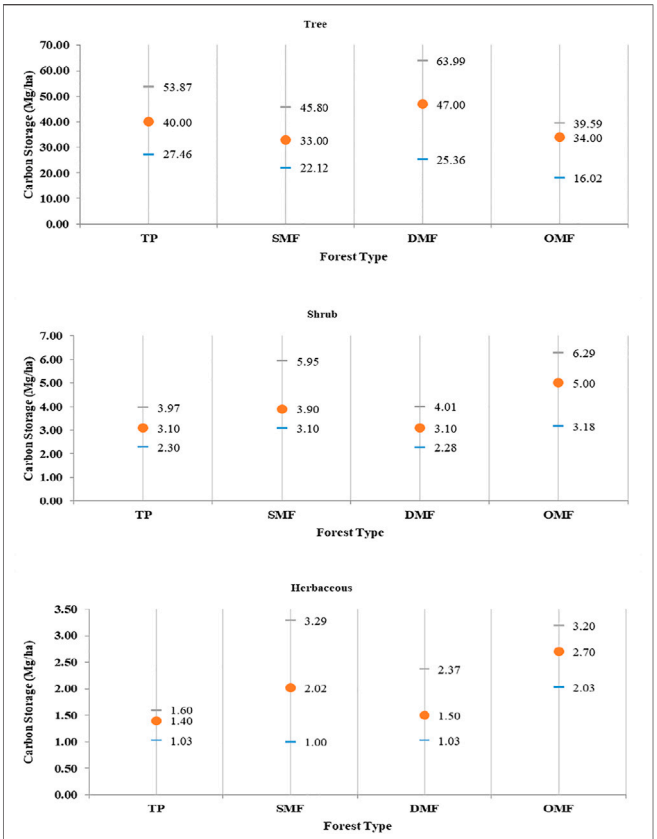

FIGURE 6 | Estimates of Carbon storage in tree/shrub/herb vegetation with 95% C.I. in dry tropical forest of AABR (Mg/ha).

In our study, total C storage accounted for 65.22–75.71% for shoots and 25.64–34.78% for roots in different forest types, while total carbon storage of forest vegetation (TV + SV + HV) i.e. standing biomass ranged between 18.0 – 50.40 Mg ha^{-1} in different forests. The maximum C storage is reported in DMF while the minimum was in OMF (**Table 4**; **Figure 6**). Similar results were also revealed by various researchers (Chaturvedi et al., 2011; Chaturvedi and Raghubanshi, 2015; Bahera et al., 2017; Thakur et al., 2014, Thakur et al., 2019). In the study of Srinivas and Sundarapandian (2019) the C content of trees varied from 44.51 to 218.84 Mg ha^{-1}.

Aboveground and Belowground Biomass

The biomass of different forest types for the components of trees, shrubs, and herbaceous flora results revealed that the total biomass (TV + SV + HV) varied from 83.77 to 111.21 Mg ha^{-1} (**Table 4**; **Figure 7**). It was highest in DMF followed by TP, SMF, and lowest in OMF. Total standing biomass (TV + SV + HV) varied significantly in each forest type. The total mean vegetation mass reported 95.85 Mg ha^{-1} of the total biomass of which 90.23% contributed for AGB and 9.77% for belowground biomass (BGB). TV, SV, and HV contributed 90.42, 8.74, and 0.71% respectively. These standards were more or less analogous to those assessed in other TDF, as Pandey (2005) reported total biomass ranging from 37.12 to 100.88 Mg ha^{-1} in TDF of Central India. Thakur et al. (2019) also reported biomass in the range of 20.25–103.43 Mg ha^{-1} in the TDF of Chhattisgarh. The estimated biomass in the current study was lower than other stated tropical dry deciduous forests worldwide. In their study, Murphy and Lugo (1986) reported 30–273 Mg ha^{-1} AGB for tropical dry forests, and similarly, the AGB varied from 58.04 to 368.39 Mg ha^{-1} according to Srinivas and Sundarpandian (2019) while Chave et al. (2008) reported 356–398 Mg ha^{-1} AGB in the rainforest of Eastern America. Likewise, Jaramillo et al. (2003) estimated 143.1 Mg ha^{-1} ABG and BGB for dry tropical forests in Mexico. Similar results were revealed by Malhi et al. (2004), Raich et al. (2006), Dube and Mutanga (2015), Kamruzzaman et al. (2017), and Wallis et al. (2019). Comparatively erratic rainfall patterns, a lower number of rainy days in a year, harsh hot weather conditions, and poor topsoil conditions might be reasons for lower biomass in the study area. Forest dwellers in these areas are consistently dependent on these forests for their subsistence livelihood, such as via the collection of NTFP'S, fuelwood, etc. Anthropogenic disturbances are moderate to severe in these forests e.g., forest surface fire, unlawful felling, and feeding of livestock are foremost to the squalor of these forests. Fine root biomass was estimated in different depths (0–20 cm, 20–40 cm) in three seasons under four forest types (**Figure 8**).

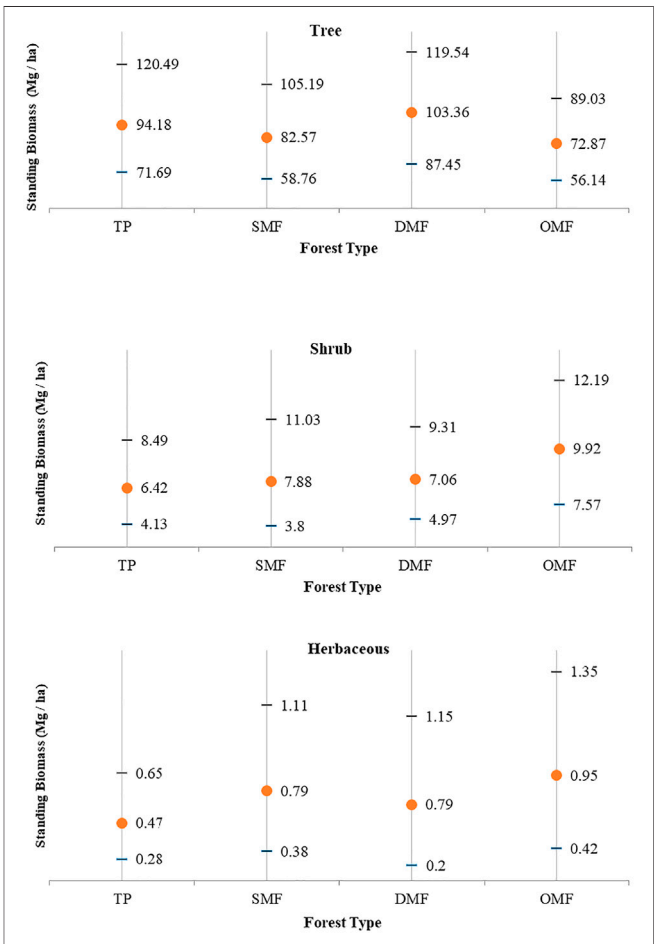

FIGURE 7 | Estimates of standing biomass with 95% C.I. of different components of tree, shrub and herb layers in tropical forests of AABR (Mg/ha).

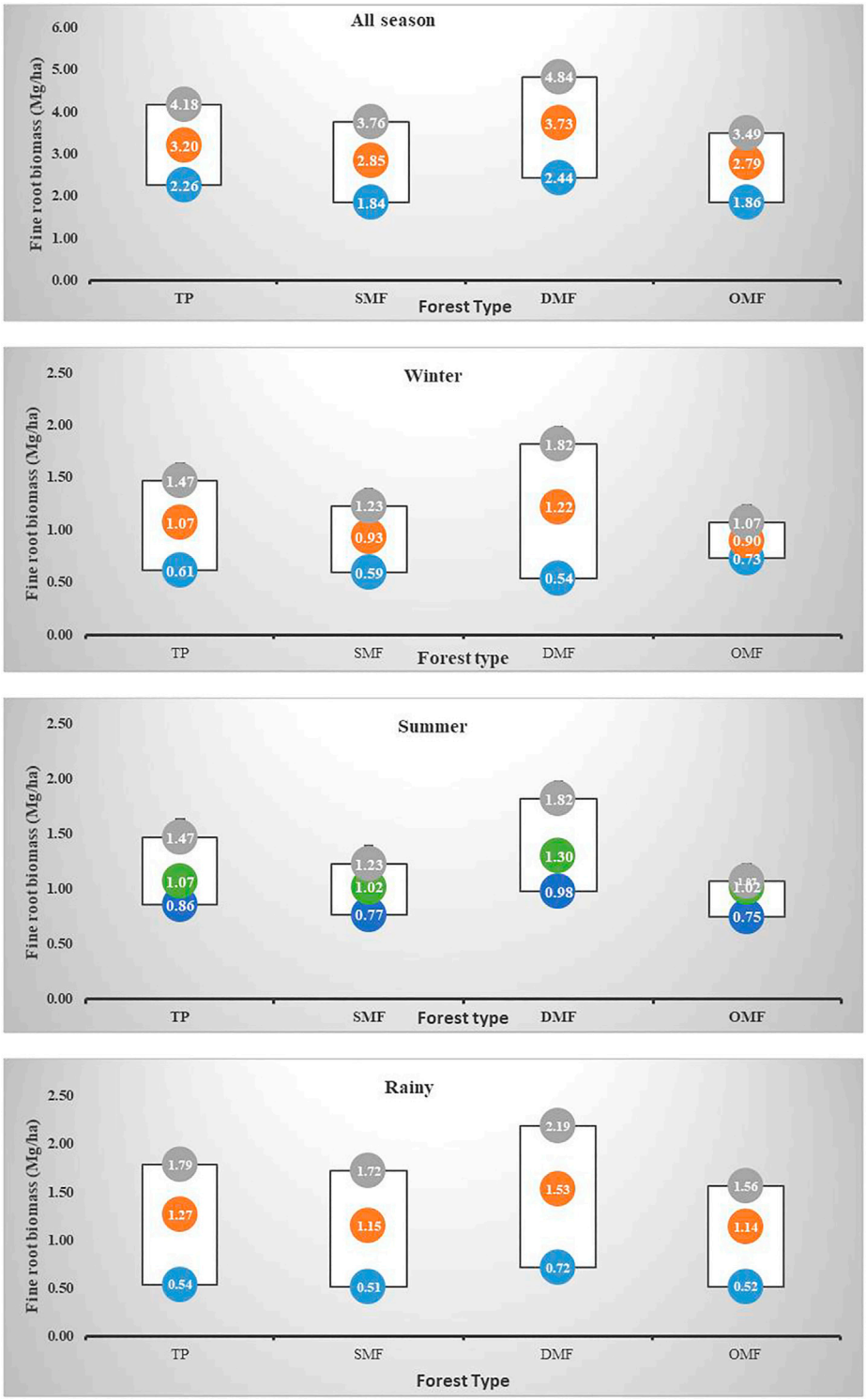

FIGURE 8 | Estimates of season wise fine root biomass (Mg/ha) for TP, SMF, DMF and OMF forest types during 2016–2018 with 95% C.I.

The results show annual root biomass was more in DMF than others. Similarly comparing the season, the rainy season produced more fine root biomass in all types of forests. The root biomass is an indicator of the growth and productivity of the forests. Ecologically it has a long-term effect, not on the improvement of the rhizosphere but also on the health of total forest biota.

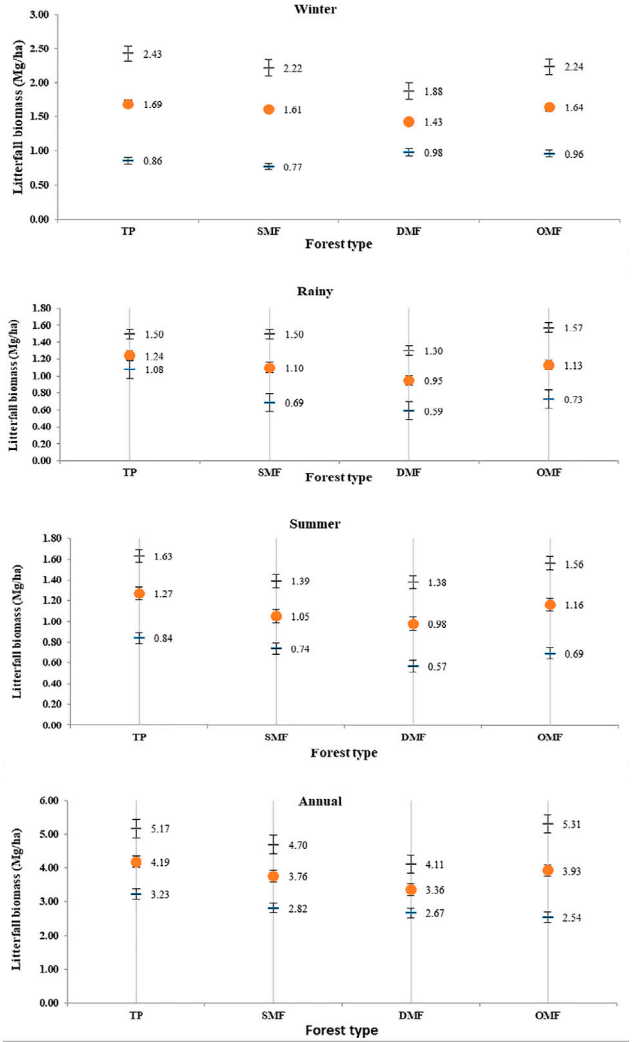

FIGURE 9 | Estimate annual litterfall biomass (Mg/ha) with 95% C.I. for TP, SMF, DMF and OMF forest types during 2016–18 for season.

Litterfall

The total mean annual litterfall fluxes 1.99–4.15 Mg ha^{-1} in various forests (**Table 4**; **Figure 9**). There was a significant difference in the quantity of litterfall due to seasons and components (wood, leaf, twig). The wood litterfall accounted for between 15.83–18.06% of the total litterfall of different forests. The leaf litterfall values varied from 1.52 to 3.05 Mg ha^{-1} in different forests. The highest litterfall values were recorded in TP followed by DMF, SMF, and the lowest in OMF. The percentage contribution of leaf fall to the total litterfall was 72.15–76.38% in different forest types. Similarly, the twig litterfall values varied from 0.16 to 0.38 Mg ha^{-1} which accounted for between 7.79–9.83% of the total litterfall of different forests. The total litterfall distributed in two annual cycles contributed between 39–42.61%, 28.48–29.12%, and 27.21–32.93% in winter, summer, and rainy seasons, respectively in different forest types. A similar finding was also reported by Thakur and Thakur (2014).

Net Primary Productivity

The total tree biomass production (AGB + BGB) varied from 7.61 to 9.94 Mg ha^{-1}yr^{-1} (**Table 4**; **Figure 10**). The highest tree biomass production was observed in TP followed by DMF, SMF, whereas the lowest was in OMF. The aboveground and belowground net production contributed between 64.09–82.91% and 17.08–35.91%, respectively of the total tree biomass production. The average net production of trees across all the forest types was 8.74 Mg ha^{-1}yr^{-1}, where AGB distributed maximum share as 77.66% and BGB share minimum as 22.34%. The total shrub biomass production (AGB + BGB) varied from 1.88 to 3.77 Mg ha^{-1}yr^{-1}. The highest shrub production was observed in SMF followed by DMF and OMF and it was lowest in TP. The aboveground and belowground net shrub biomass production contributed 56.31–80.08% and 19.91–43.69%, respectively. The average net production of shrubs in different forest types was 2.58 Mg ha^{-1}yr^{-}1fn1 of which 73.45% was contributed by aboveground and 26.54% by belowground biomass. The herbaceous species turnover of less than 1 year was considered equal to net production in these

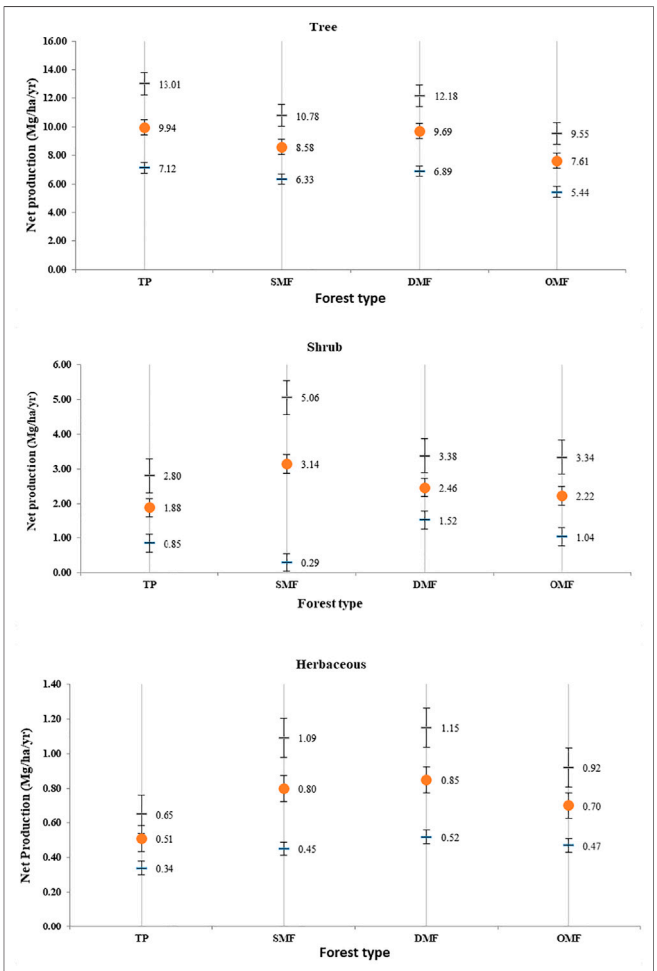

FIGURE 10 | Estimates of total production (Mg/ha/yr) with 95% confidence interval of trees, shrubs and herbs for different forest types in tropical forests of AABR.

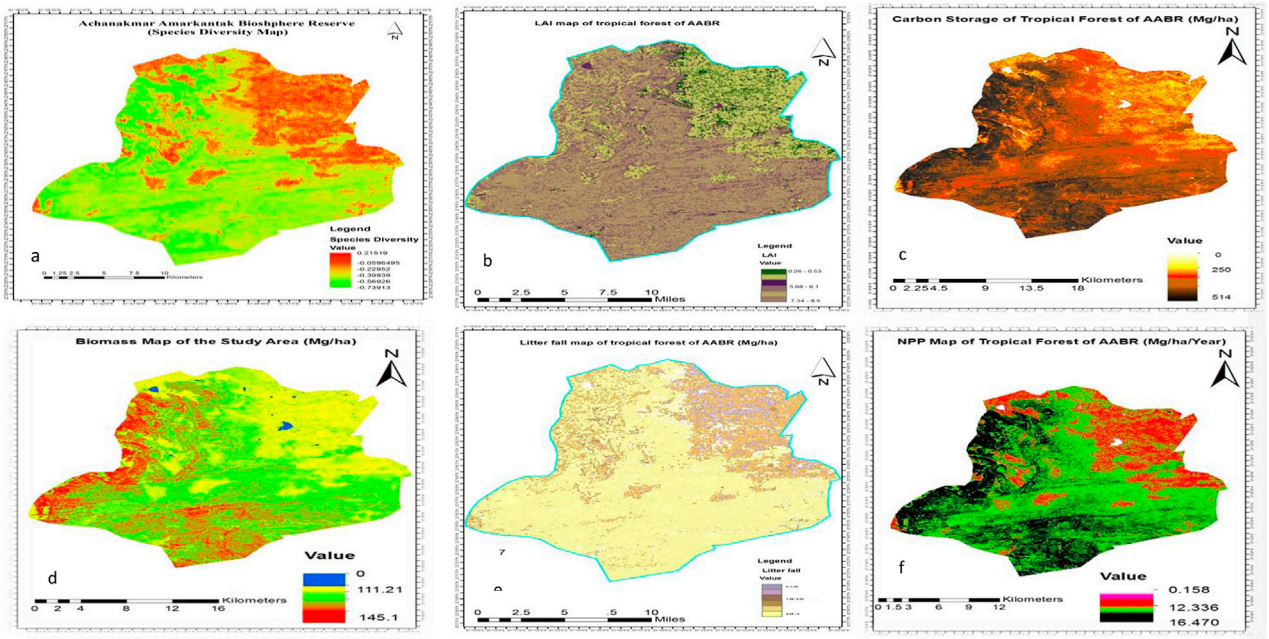

FIGURE 11 | (A) Species diversity map of AABR; **(B)** Leaf area index map of study site; **(C)** Carbon storage map (Mg/ha); **(D)** Biomass map (Mg/ha), **(E)** Litterfall production map (Mg/ha); **(F)** Net primary productivity map (Mg/ha/yr).

forests. The NPP for herbaceous biomass ranged from 0.51–0.80 Mg ha^{-1}yr^{-1}. The contribution of herbaceous production to the total stand NPP was ranged from 3.0–6.35%.

The total net production (tree, shrub, herb, and litterfall) varied from 10.53 to 13.15 Mg ha^{-1}yr^{-1} with a mean value of 12.02 Mg ha^{-1}yr^{-1}. It was highest was in SMF followed by TP and DMF while the lowest was in OMF. SMF had 1.06, 1.22, and 2.41 times higher net production than DMF, TP, and OMF. For all the forest type trees, shrub, herb, and litter accounted for 56.43–72.0%, 11.94–23.67%, 2.59–5.82%, and 12.93–14.58%, respectively. The species diversity (H), LAI, litterfall, carbon sequestration, biomass, and NPP generated from the satellite in tropical dry forests are illustrated in **Figure 11**. All these maps reflect that the coherence will field verified data.The illustrated maps for different layers of parameters are easy to understand at the landscape level and assist forest managers to design proper management plans. These types of satellite-generated maps are more in use globally for better forest ecosystem management.

Correlation Between Vegetation Indices, Diversity, Structural Attributes, Leaf Area Index, Carbon Storage, Biomass, and Net Production

Correlation analysis among the structural attributes, vegetation indices, LAI, Carbon sequestration, biomass, and NPP in tropical dry forests are illustrated in **Table 3**. The correlation relationship among NDVI with pooled data of species diversity, LAI, carbon storage, biomass, litterfall, and NPP is shown in **Figure 4**. Species diversity values were computed using stratified random sampling and a significant correlation was found between vegetation indices and diversity. It was evident from the result that density, basal area, and diversity were positively correlated with NDVI, whereas it was insignificant with AVI, EVI, NMDI, VDVI, RVI, and density. The present study showed that C storage, biomass, and NPP were positively correlated with NDVI, AVI, EVI, VDVI, NDMI, and RVI indices while NDVI was significantly correlated. The DMF recorded the highest values of NDVI, which is depicted in **Figure 5A**. The results demonstrated that NDVI from remotely sensed images could identify areas of high species richness, C storage, and biomass production values. In our study, we reported a positive relationship among spectral vegetation index (i.e., NDVI), carbon storage, species diversity, LAI, biomass, litterfall, and NPP (pooled data of TV + SV) for the entire vegetation types of AABR (**Figure 5A**). The RVI, EVI, AVI, VDVI, and NDMI images are represented in **Figures 5B–F**, respectively. The present study also indicated a positive and significant correlation between NDVI and Shannon index, C storage, biomass, and NPP for different vegetation types of the study area, which confirms the reports of earlier workers (Swamy, 1998; Thakur et al., 2019) who found NDVI as a key variable strongly correlated to vegetation analysis.

CONCLUSION

This study concluded that satellite remote sensing techniques are one of the most reliable tools for the assessment of vegetation structure, diversity, carbon storage, biomass, and NPP for the dry tropical forest ecosystems of AABR of India. Biomass and productivity studies contribute significantly to the global carbon pool and, being very young forests, AABR has the potential to mitigate a significant amount of carbon from the atmosphere. Forest degradation by anthropogenic activities (e.g., forest cutting, forest fire,

overexploitation of flora, encroachment, mining, human settlements) are placing severe pressure on forest ecosystems. Planting of multipurpose trees and shrubs in SMF could be explored for the enrichment of vegetation cover. These strategies will assist in reducing the biotic pressure and also restoring and conserving the fragile dry tropical forest ecosystems of Central India. The study also indicated that the Resourcesat-2A satellite data is likely to improve the retrieval of carbon values, leaf area index, biomass, and the NPP of the dry tropical forests of India due to their moderate spectral and spatial resolution as compared to IRS and Landsat satellite images. The empirical relationships drawn between structural aspects and spectral responses are important for predicting few important structural attributes of vegetation directly from multispectral satellite data. Therefore, there is a need to have an extensive forest management plan for AABR in India for optimum forest health.

DATA AVAILABILITY STATEMENT

The original contributions presented in the study are included in the article/**Supplementary Material**, further inquiries can be directed to the corresponding author.

AUTHOR CONTRIBUTIONS

TT, DP, AT, and ANK contributed to the conceptualization, data collection, and preparation of the first draft. TT, JB, DP, AK (7th author), ANK provided section contributions. AK (10th author), AB, MD, ANK, AK (7th author), and MK undertook editing and provided extra input to improve the quality. All the authors undertook editing and participated in proofreading the article.

ACKNOWLEDGMENTS

The authors are thankful to the authorities of Indira Gandhi National Tribal University, Amarkantak, MP, India for their support and encouragement in carrying out research work. All authors are highly thankful to the reviewers for their constructive comments to improve the article. The permission granted by the state forest department to conduct the study in AABR protected area and their support during the filed investigation is duly acknowledged. We acknowledge the financial support provided by the Ministry of Environment, Forests and Climate Change (MoEF&CC), Government of India, New Delhi (Sanction No. F.13/4/2013- NNRMS/RE)

SUPPLEMENTARY MATERIAL

The Supplementary Material for this article can be found online at: https://www.frontiersin.org/articles/10.3389/fenvs.2021.757976/full#supplementary-material

REFERENCES

Ali, A. M., Darvishzadeh, R., Skidmore, A. K., and van Duren, I. (2017). Specific Leaf Area Estimation from Leaf and Canopy Reflectance through Optimization and Validation of Vegetation Indices. *Agric. For. Meteorol.* 236, 162–174. doi:10.1016/j.agrformet.2017.01.015

Anderson-Teixeira, K. J., Wang, M. M. H., McGarvey, J. C., and LeBauer, D. S. (2016). Carbon Dynamics of Mature and Regrowth Tropical Forests Derived from a Pantropical Database (TropForC-Db). *Glob. Chang. Biol.* 22, 1690–1709. doi:10.1111/gcb.13226

Beer, C., Reichstein, M., Tomelleri, E., Ciais, P., Jung, M., Carvalhais, N., et al. (2010). Terrestrial Gross Carbon Dioxide Uptake: Global Distribution and Covariation with Climate. *Science* 329, 834–838. doi:10.1126/science.1184984

Bijalwan, A., Swamy, S. L., Sharma, C. M., Sharma, N. K., and Tiwari, A. K. (2010). Land Use, Biomass and Carbon Estimation of Chhattisgarh Region in India Using Satellite Remote Sensing and GIS Techniques. *J. For. Res.* 21 (2), 161–170. doi:10.1007/s11676-010-0026-y

Chaturvedi, R. K., Raghubanshi, A. S., and Singh, J. S. (2011). Effect of Small-Scale Variations in Environmental Factors on the Distribution of Woody Species in Tropical Deciduous Forests of Vindhyan Highlands, India. *J. Bot.* 297097. doi:10.1155/2011/297097

Chaturvedi, R. K., Tripathi, A., Raghubanshi, A. S., and Singh, A. S. (2021). Functional Traits Indicate a Continuum of Tree Drought Strategies across a Soil Water Availability Gradient in a Tropical Dry forest. *For. Ecol. Manag.* 118740. doi:10.1016/j.foreco.2020.118740

Chaturvedi, R. K., and Raghubanshi, A. S. (2015). Assessment of Carbon Density and Accumulation in Mono- and Multi-specific Stands in Teak and Sal Forests of a Tropical Dry Region in India. *For. Ecol. Manag.* 339, 11–21. doi:10.1016/j.foreco.2014.12.002

Chaturvedi, R. K., Raghubanshi, A. S., and Singh, J. S. (2011). Carbon Density and Accumulation in Woody Species of Tropical Dry forest in India. *For. Ecol. Manage.* 262, 1576–1588. doi:10.1016/j.foreco.2011.07.006

Chaturvedi, R. K., and Raghubanshi, A. S. (2014). Species Composition, Distribution, and Diversity of Woody Species in a Tropical Dry forest of India. *J. Sustain. For.* 33 (8), 729–756. doi:10.1080/10549811.2014.925402

Chave, J., Olivier, J., Bongers, F., Chatelet, P., Forget, P. M., van der Meer, P., et al. (2008). Above-ground Biomass and Productivity in a Rain forest of Eastern South America. *J. Trop. Ecol.* 24, 355–366. doi:10.1017/S0266467408005075

Chave, J., Riera, B., and Dubois, M. A. (2001). Estimation of Biomass in a Neotropical forest of French Guiana: Spatial and Temporal Variability. *J. Trop. Ecol.* 17, 79–96. doi:10.1017/S0266467401001055

Chazdon, R. L., Broadbent, E. N., Rozendaal, D. M. A., Bongers, F., Zambrano, A. M. A., Aide, T. M., et al. (2016). Carbon Sequestration Potential of Second-Growth forest Regenerationin the Latin American Tropics. *Sci. Adv.* 2 (5), 1–10. doi:10.1126/sciadv.1501639e1501639

Clark, D. A., Brown, S., Kicklighter, D. W., Chambers, J. Q., Thomlinson, J. R., and Ni, J. (2001). Measuring Net Primary Production in Forests: Concepts and Field Methods. *Ecol. Appl.* 11, 356–370. doi:10.1890/1051-0761(2001)011[0356:MNPPIF]2.0.CO;2

Curtis, J. T., and Mc Intosh, R. P. (1950). And the Interrelationship of Certain Analytic Synthetic Phytosociological Characters. *Ecology* 31, 434–455. doi:10.2307/1931497

Darro, H., Swamy, S. L., Thakur, T. K., and Mishra, A. (2020). Floristic Composition, Structure, Diversity and Conservation Strategies for Rehabilitation of Dry Tropical Forests in Buffer Zone of Achanakmaar Amarkantak Biosphere Reserve (AABR), India. *Int. J. Curr. Microbiol. App. Sci.* 9 (4), 650–663. doi:10.20546/ijcmas.2020.904.079

FAO (1995). *Climate Change forest and forest Management – an Overview Technical Report*. 126.

Fearnside, P. M. (1996). Amazonian Deforestation and Global Warming: Carbon Stocksin Vegetation Replacing Brazil's Amazon forest. *For. Ecol. Manag.* 80, 21–34. doi:10.1016/0378-1127(95)03647-4

FSI (2015). *State of Forest Report 2015*. Dehradun India –: Forest Survey of India (Ministry of Forests and Environment) Govt. of India Press.

FSI (2019). *State of Forest Report 2019*. Dehradun India: Forest Survey of India (Ministry of Forests and Environment) Govt. of India Press.

Gaston, G., Brown, S., Lorenzini, M., and Singh, K. D. (1998). State and Change in Carbon Pools in the Forests of Tropical Africa. *Glob. Change Biol* 4, 97–114.

Grace, J., Mitchard, E., and Gloor, E. (2014). Perturbations in the Carbon Budget of the Tropics. *Glob. Chang. Biol.* 20 (10), 3238–3255. doi:10.1111/gcb.12600

Houghton, R. A., Byers, B., and Nassikas, A. A. (2015). A Role for Tropical Forests in Stabilizing Atmospheric CO_2. *Nat. Clim. Chang.* 5 (12), 1022–1023. doi:10.1038/nclimate2869

IPCC (1996). *IPCC Guidelines for National Greenhouse Gas Inventories*. Reference Man. 3.

Jaramillo, V. J., Kaufmann, J. B., Rentarı´a-Rodrı´guez, L., Cummings, D. L., and Ellingson, L. J. (2003). Biomass, Carbon and Nitrogen Pools in Mexican Tropical forest Landscapes. *Ecosystems* 6, 609–629. doi:10.1017/S0266467408005075

Jhariya, M. K., Banerjee, A., Meena, R. S., and Yadav, D. K. (2019). *Sustainable Agriculture, Forest and Environmental Management*. Berlin, Germany:Springer. doi:10.1007/978-981-13-6830-1

Jhariya, M. K., and Singh, L. (2021). Herbaceous Diversity and Biomass under Different Fire Regimes in a Seasonally Dry forest Ecosystem. *Environ. Dev. Sustain.* 23 (5), 6800–6818. doi:10.1007/s10668-020-00892-x

Jhariya, M. K. (2017). Vegetation Ecology and Carbon Sequestration Potential of Shrubs in Tropics of Chhattisgarh, India. *Environ. Monit. Assess.* 189 (10), 518. doi:10.1007/s10661-017-6246-2

Jones, I. L., DeWalt, S. J., Lopez, O. R., Bunnefeld, L., Pattion, Z., and Dent, D. H. (2019). Above- and Belowground Carbon Stocks Are Decoupled in Secondary Tropical Forests and Are Positively Related to forest Age and Soil Nutrients Respectively. *Sci. Total Environ.* 697, 133987. doi:10.1016/j.scitotenv.2019.133987

Kumar, A., and Kumar, M. (2020). Estimation of Carbon Stock in the Hydroelectric Catchment of India and its Implementation to Climate Change. *J. Sustain. For.* 39 (6). doi:10.1080/10549811.2020.1794907

Kumar, A., Kumar, M., and Pandey, R. (2021a). Forest Soil Nutrient Stocks along Altitudinal Range of Uttarakhand Himalayas: An Aid to Nature Based Climate Solutions. *CATENA* 207, 105667. doi:10.1016/j.catena.2021.105667

Kumar, A., Pinto, M. C., Candeias, C., and Dinis, P. A. (2021b). Baseline Maps of Potentially Toxic Elements in the Soils of Garhwal Himalayas, India: Assessment of Their Eco-Environmental and Human Health Risks. *Land Degrad. Develop.* 32 (14), 3856–3869. doi:10.1002/ldr.3984

Kumar, Y., Thakur, T., Sahu, M. L., and Thakur, A. (2017). A Multifunctional Wonder Tree: Moringa oleiferaLam Open New Dimensions in Field of Agroforestry in India. *Int. J. Curr. Microbiol. App. Sci.* 6 (8), 229–235. doi:10.20546/ijcmas.2016.501.031

Lepine, L. C., Ollinger, S. V., Ouimette, A. P., and Martin, M. E. (2016). Examining Spectral Reflectance Features Related to Foliar Nitrogen in Forests: Implications for Broad-Scale Nitrogen Mapping. *Remote Sens. Environ.* 173, 174–186. doi:10.1016/j.rse.2015.11.028

Malhi, Y., Arag Ão, L. E. O. C., Metcalfe, D. B., Paiva, R., Quesada, C. A., Almeida, S., et al. (2009). Comprehensive Assessment of Carbon Productivity, Allocation and Storage in Three Amazonian Forests. *Glob. Chang. Biol.* 15, 1255–1274. doi:10.1111/j.1365-2486.2008.01780.x

Malhi, Y., Baker, T. R., Phillips, O. L., Almeid, S., Alvarej, E., Arroyo, L., et al. (2004). The Above-Ground Corse wood Productivity of 104 Neotropical forest Plots. *Glob. Change Biol* 10, 563–591. doi:10.1111/j.1529-8817.2003.00778.x

Mandal, G., and Joshi, S. P. (2014). Analysis of Vegetation Dynamics and Phytodiversity From Three Dry Deciduous Forests of Doon Valley, Western Himalaya, India. *J. Asia Pac. Biodivers* 30 (3), 292–304. doi:10.1016/j.japb.2014.07.006

Middinti, S., Thumaty, K. C., Gopalakrishnan, R., Jha, C. S., and Thatiparthi, B. R. (2017). Estimating the Leaf Area index in Indian Tropical Forests Using Landsat-8 OLI Data. *Int. J. Remote Sens.* 38, 6769–6789. doi:10.1080/01431161.2017.1363436

Mohommad, S., and Joshi, S. P. (2015). Biomass and Carbon Stock Assessment in Moistdeciduous Forests of Doon valley, Western Himalaya, India. *Taiwania* 60, 71–76. doi:10.6165/tai.2015.60.71

Moore, S., Adu-Bredu, S., Duah-Gyamfi, A., Addo-Danso, S. D., Ibrahim, F., Mbou, A. T., et al. (2018). Forest Biomass, Productivity and Carbon Cycling along a Rainfall Gradient in West Africa. *Glob. Chang. Biol.* 24, e496–e510. doi:10.1111/gcb.13907

Negi, J. D. S., Manhas, R. K., and Chauhan, P. S. (2003). Carbon Allocation in Different Components of Some Tree Species of India: a New Approach for Carbon Estimation. *Curr. Sci.* 85, 1528–1531.

Nelson, B. W., Mesquita, R. C. G., Pereira, J. L. G., De Souza, S. G. A., Batista, G. T., and Couto, L. B. (1999). Allometric Regressions for Improved Estimate of Secondary forest Biomass in central Amazon. *For. Ecol. Manag.* 117, 149–167. doi:10.1016/S0378-1127(98)00475-7

Pan, Y., Birdsey, R. A., Fang, J., Houghton, R., Kauppi, P. E., Kurz, W. A., et al. (2011). A Large and Persistent Carbon Sink in the World's Forests. *Science* 333, 988–993. doi:10.1126/science.1201609

Pandey, P. K. (2005). Biomass and Productivity in Some Disturbed Tropical Dry Deciduous Teak Forests of Satpura Plateau, Madhya Pradesh. *Trop. Ecol.* 46 (2), 229–239.

Poorter, L., Bongers, F., Aide, T. M., Almeyda Zambrano, A. M., Balvanera, P., Becknell, J. M., et al. (2016). Biomass Resilience of Neotropical Secondary Forests. *Nature*, 1–15. doi:10.1038/nature16512

Popkin, G. (2018). US Government Considers Charging for Popular Earth-Observing Data. *Nature* 556, 417–418. doi:10.1038/d41586-018-04874-y

Raich, J. W., Russell, A. E., Kitayama, K., Parton, W. J., and Vitousek, P. M. (2006). Temperature Influences Carbon Accumulation in Moist Tropical Forests. *Ecology* 87, 76–87. doi:10.1890/05-0023

Reich, P. B. (2012). Key Canopy Traits Drive forest Productivity. *Proc. R. Soc. B Biol. Sci.* 279, 2128–2134. doi:10.1098/rspb.2011.2270

Shiklomanov, A. N., Dietze, M. C., Viskari, T., Townsend, P. A., and Serbin, S. P. (2016). Quantifying the Influences of Spectral Resolution on Uncertainty in Leaf Trait Estimates through a Bayesian Approach to RTM Inversion. *Remote Sens. Environ.* 183, 226–238. doi:10.1016/j.rse.2016.05.023

Swamy, S. L. (1998). *Estimation of Net Primary Productivity (NPP) in an Indian Tropical evergreen forest Using Remote Sensing Data*. Hyderabad,India: Ph.D. Thesis, Jawaharlal Nehru Technology University.

Thakur, T. K., Patel, D. K., Dutta, J., Kumar, A., Kaushik, S., Bijalwan, A., et al. (2020). Assessment of Decadal Land Use Dynamics of Upper Catchment Area of Narmada River, the Lifeline of Central India. *J. King Saud University-Science*. doi:10.1016/j.jksus.2020.101322

Thakur, T. K., Swamy, S. L., and Nain, A. S. (2014). Composition, Structure & Diversity Characterization of Dry Tropical Forest of Chhattisgarh Using Satellite Data. *J. For. Res.* 25 (4), 819–825.

Thakur, T. K. (2018). Diversity, Composition and Structure of Understorey Vegetation in the Tropical forest of Achanakmaar Biosphere Reserve, India. *Environ. Sustainability* 1 (2), 279–293.

Thakur, T. K., Padwar, G. K., and Patel, D. K. (2019). Monitoring Land Use, Species Composition and Diversity of Dry Tropical Environ in Achanakmaar Amarkantak Biosphere Reserve, India Using Satellite Data. *Biodiversity Int. J.* 3 (4), 162–172. doi:10.15406/bij.2019.03.00141

Thakur, T., and Thakur, A. (2014). Litterfall Patterns of a Dry Tropical forest Ecosystem of Central India. *Eco. Env. Cons.* 20 (3), 1325–1328.

Thakur, U., Bisht, N. S., Kumar, M., and Kumar, A. (2021). Influence of Altitude on Diversity and Distribution Pattern of Trees in Himalayan Temperate Forests of Churdhar Wildlife Sanctuary, India. *Water Air Soil Pollut.* 232, 205. doi:10.1007/s11270-021-05162-8

Tripathi, S., Bhadouria, R., Srivastava, P., Devi, R. S., Chaturvedi, R., and Raghubanshi, A. S. (2020). Effects of Light Availability on Leaf Attributes and Seedling Growth of Four Tree Species in Tropical Dry forest. *Ecol. Process.* 9, 2. doi:10.1186/s13717-019-0206-4

Wallis, C. I. B., Homeier, J., Pena, J., Brandl, R., and Farwig, N. (2019). Modeling Tropical Montane forest Biomass, Productivity and Canopy Traits with Multispectral Remote Sensing Data. *Remote sensing Environ.* 225, 77–92. doi:10.1016/j.rse.2019.02.021

Wang, G., Guan, D., Xiao, L., and Peart, M. R. (2019). Forest Biomass-Carbon Variation Affected by the Climatic and Topographic Factors in Pearl River Delta, South China. *J. Environ. Manage.* 232, 781–788. doi:10.1016/j.jenvman.2018.11.130

Wulder, M. (1998). Optical Remote-Sensing Techniques for the Assessment of forest Inventory and Biophysical Parameters. *Prog. Phys. Geogr.* 22, 449–476. doi:10.1177/030913339802200402

Conflict of Interest: The authors declare that the research was conducted in the absence of any commercial or financial relationships that could be construed as a potential conflict of interest.

Publisher's Note: All claims expressed in this article are solely those of the authors and do not necessarily represent those of their affiliated organizations, or those of the publisher, the editors, and the reviewers. Any product that may be evaluated in this article, or claim that may be made by its manufacturer, is not guaranteed or endorsed by the publisher.

frontiers in Environmental Science

ORIGINAL RESEARCH
published: 22 November 2021
doi: 10.3389/fenvs.2021.785531

Root-To-Shoot Ratios of Flood-Tolerant Perennial Grasses Depend on Harvest and Fertilization Management: Implications for Quantification of Soil Carbon Input

Claudia Kalla Nielsen[1,2]*, *Uffe Jørgensen*[1,2] and *Poul Erik Lærke*[1,2]

[1]Department of Agroecology, Aarhus University, Tjele, Denmark, [2]Aarhus University Centre for Circular Bioeconomy, Aarhus university, Tjele, Denmark

Quantifying soil organic carbon stocks (SOC) is a critical task in decision support related to climate and land management. Carbon inputs in soils are affected by development of belowground (BGB) and aboveground (AGB) biomass. However, uncertain fixed values of root:shoot ratios (R/S) are widely used for calculating SOC inputs in agroecosystems. In this study, we 1) assessed the effect of harvest frequency (zero, one, two, and five times annually) on the root and shoot development of the perennial grasses *Phalaris arundinacea* (RCG), *Festuca arundinacea* (TF), and *Festulolium* (FL); 2) determined the effect of management on the carbon and nitrogen content in AGB and BGB; and 3) assessed the implications of R/S for SOC quantification. We found the highest yields of BGB in zero-cut treatments with 59% (FL)–70% (RCG) of total biomass. AGB yield was highest in the five-cut treatments with 54% (RCG)–60% (FL), resulting in a decreasing R/S with frequent management, ranging from 1.6–2.3 (zero cut) to 0.6–0.8 (five cuts). No differences in R/S between species were observed. Total carbon yield ranged between 5.5 (FL, one cut) and 18.9 t ha^{-1} year^{-1} (FL, zero cut), with a higher carbon content in AGB (45%) than BGB (40%). We showed that the input of total organic carbon into soil was highest in the zero-cut treatments, ranging between 6.6 and 7.6 t C ha^{-1} year^{-1}, although, in the context of agricultural management the two-cut treatments showed the highest potential for carbon input (3.4–5.4 t C ha^{-1} year^{-1}). Our results highlighted that using default values for R/S resulted in inaccurate modeling estimations of the soil carbon input, as compared to a management-specific application of R/S. We conclude that an increasing number of annual cuts significantly lowered the R/S for all grasses. Given the critical role of BGB carbon input, our study highlights the need for comprehensive long-term experiments regarding the development of perennial grass root systems under AGB manipulation by harvest. In conclusion, we indicated the importance of using more accurate R/S for perennial grasses depending on management to avoid over- and underestimation of the carbon sink functioning of grassland ecosystems.

Keywords: root:shoot ratio, perennial grass, peatland, soil organic carbon, paludiculture, wetland, carbon sink

OPEN ACCESS

Edited by:
Munesh Kumar,
Hemwati Nandan Bahuguna Garhwal University, India

Reviewed by:
Amit Kumar,
Nanjing University of Information Science and Technology, China
Calogero Schillaci,
Joint Research Centre, Italy

***Correspondence:**
Claudia Kalla Nielsen
claudia@agro.au.dk

Specialty section:
This article was submitted to Biogeochemical Dynamics, a section of the journal Frontiers in Environmental Science

Received: *30 September 2021*
Accepted: *27 October 2021*
Published: *22 November 2021*

Citation:
Nielsen CK, Jørgensen U and Lærke PE (2021) Root-To-Shoot Ratios of Flood-Tolerant Perennial Grasses Depend on Harvest and Fertilization Management: Implications for Quantification of Soil Carbon Input. Front. Environ. Sci. 9:785531. doi: 10.3389/fenvs.2021.785531

INTRODUCTION

Undisturbed mires are wetland biomes where peat accumulates, typically at rates of ~1 mm year^{-1} over centuries (Parish et al., 2008), making these ecosystems one of the largest global organic carbon (C) reserves with substantial impact on atmospheric carbon dioxide (CO_2) concentrations (Moomaw et al., 2018). In Denmark, wetlands with >6% organic C cover about 291,000 ha, of which 59% are used for agriculture (Greve et al., 2021). The massive losses of C from these agroecosystems are controlled by the balance between current net C inputs and peat mineralization, which is substantial and largely depends on the drainage conditions (Straková et al., 2012). National emission factors for drained organic agricultural soils in Denmark were established by empirical gas flux measurements in 2008–2009 and averaged 35 Mg CO_2 ha^{-1} year^{-1} across eight sites in crop rotation and with permanent grass (Elsgaard et al., 2012). Climate change mitigation by rewetting of agricultural soils with >6% organic C is currently supported by national governmental incentives. Following this, it is envisaged that an area of 88,500 ha potentially can be rewetted and converted to permanent natural grassland (Ministry of Food, Agriculture and Fisheries of Denmark, 2021). Whereas reductions in CO_2 emissions from slower peat mineralization are well documented in relation to increasing groundwater tables (Renou-Wilson et al., 2014), there is an unmet challenge in documenting the net C sequestration from new plant biomass on wet organic soils. This is in particular true for wetlands with >12% organic C and cultivated with perennial grasses, also known as paludiculture, which may contribute to greenhouse gas (GHG) mitigation (Tanneberger et al., 2020) and nutrient retention (Giannini et al., 2017; Vroom et al., 2018).

The input and cycling of organic C in soil ecosystems is highly affected by plant mechanisms regulating the development of aboveground (AGB) and belowground (BGB) biomass (i.e., shoots and roots, respectively) and consequently the quantity of litter input (Kumar et al., 2017), while decomposition of soil organic matter (SOM) is affected by soil nutrient stoichiometry (Kumar et al., 2021). Factors controlling AGB production of perennial grasses are well studied, but little is known about BGB, in particular for flood-tolerant perennial grasses. Roots play a significant role in the soil C cycle (Puget and Drinkwater, 2001; Moore et al., 2019; Dijkstra et al., 2020), indicate productivity (Thakur et al., 2021) and are crucial for the buildup of SOM on both mineral soils and peatlands (Klingenfuß et al., 2014; Leifeld et al., 2020). Not only root biomass but also in particular root exudates, secretions, lysates, cap cells, and mucilages (Carminati and Vetterlein, 2013; van Veelen et al., 2018) are important C inputs affecting the soil status of being either a source or a sink of C. For the estimation and modeling of changes in soil C stocks, a fixed default root:shoot ratio (R/S) is widely used to account for total biomass C. However, R/S is known to vary as a result of multiple environmental and climatic factors as well as management (Kibet et al., 2016; Sainju et al., 2017a; Hu et al., 2018). The optimal partitioning theory (OPT) of plant biomass allocation between AGB and BGB proposes that environmental factors will force plants to allocate new biomass to those parts needed to secure the most deficient resources for optimal plant growth (Fraser et al., 2015; Yang et al., 2018). In contrast, the isometric allocation hypothesis (IA) states that BGB scales linearly with AGB, independent of abiotic factors. Further, it has been stated that defoliation of AGB by harvest or grazing will decrease total BGB (Reid et al., 2015). However, due to the high on-site variability and the challenge of root extraction, in particular for perennial grasses, accurate estimations of R/S under different conditions are rare (Bolinder et al., 2002). Instead, and notably for grassland ecosystems, the allometric approach, using a fixed R/S (Bolinder et al., 2007), is used for modeling of BGB soil C inputs. Nevertheless, recent research highlighted the potential overestimation as well as uncertainty of this modeling approach (e.g., Mokany et al., 2006; Taghizadeh-Toosi et al., 2016; Keel et al., 2017).

While currently an effort is made to review R/S for different biomes and climate zones (e.g., Qi et al., 2019), an assessment of the R/S of grasses under different harvest frequencies is still lacking. This is particularly true for flood-tolerant grass species, which are increasingly introduced on both wetland and upland soils for both climate change mitigation and added-value products, such as grass protein as a substitute for soy (Nielsen et al., 2021). Hence, there is a need for consolidated estimates of R/S for commonly used paludiculture crops under different harvest frequencies (Karki et al., 2014). In the present study, we addressed this need in an annual trial and hypothesized that different R/S would be observed in flood-tolerant perennial grasses by manipulating the harvest frequency during the growth season under provision of adequate nutrient availability. The specific aims of the study were 1) to determine the effect of harvest frequency on the root and shoot development in the first year of cultivation of the perennial grasses reed canary grass (RCG; *Phalaris arundinacea* L.), tall fescue (TF; *Festuca arundinacea* Schreb.) and festulolium (FL; *Festuca* spp. × *Lolium* spp.), 2) to assess species-specific differences in R/S biomass ratios, 3) to determine the effect of harvest frequency on the C and nitrogen content in above- and belowground biomass, and 4) to assess the implications of R/S for soil C modeling.

MATERIALS AND METHODS

Site Description and Experimental Design

The experiment was performed at the outdoor semi-field facilities of Aarhus University Foulum, Denmark. The average air temperature in the 8-month study period from March to November 2019, representing the annual growth period of grasses, ranged between 5.0°C and 16.8°C, with August as the warmest month. Monthly average precipitation ranged between 12 and 122 mm, with April as the driest and October as the wettest month. Global and net radiation was highest in June, with 20 and 8 MJ m^{-2}, respectively (**Figure 1**).

The perennial grasses RCG (cultivar: Lipaula), TF (cultivar: Kora), and FL (cultivar: Hykor) were grown in polyvinyl carbonate (PVC) cylinders (diameter 15 cm, depth 50 cm) that were placed in three trenches at the semi-field facility. The PVC

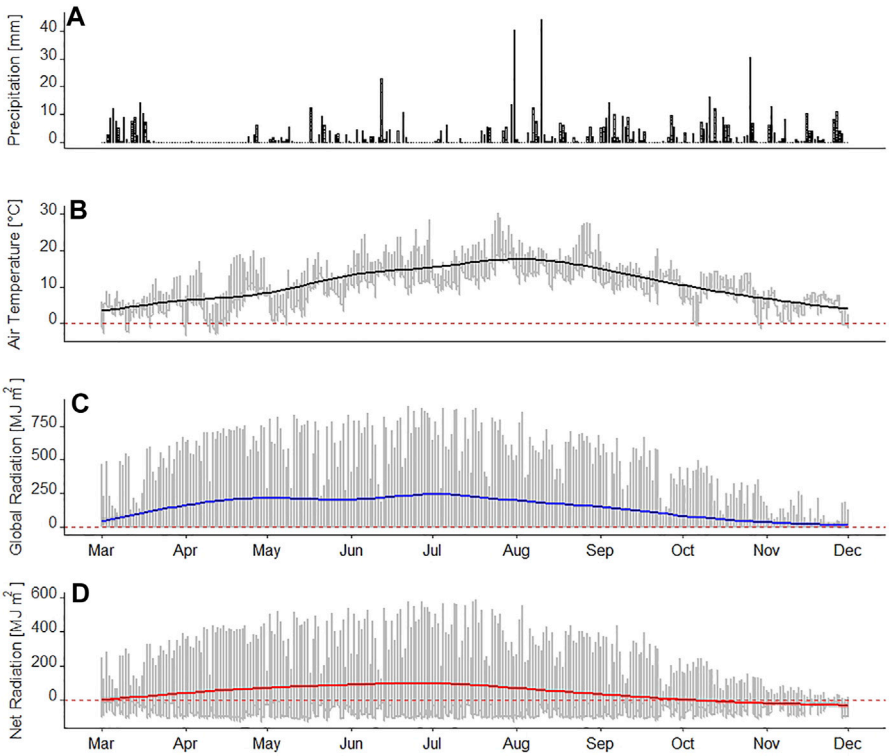

FIGURE 1 | Environmental data for the year 2019 showing **(A)** precipitation (in mm), **(B)** temperature in Celsius, **(C)** global radiation (MJ m^{-2}), and **(D)** net radiation (MJ m^{-2}). Bold lines for temperature and radiation indicate the daily means, while dashed red lines indicate zero.

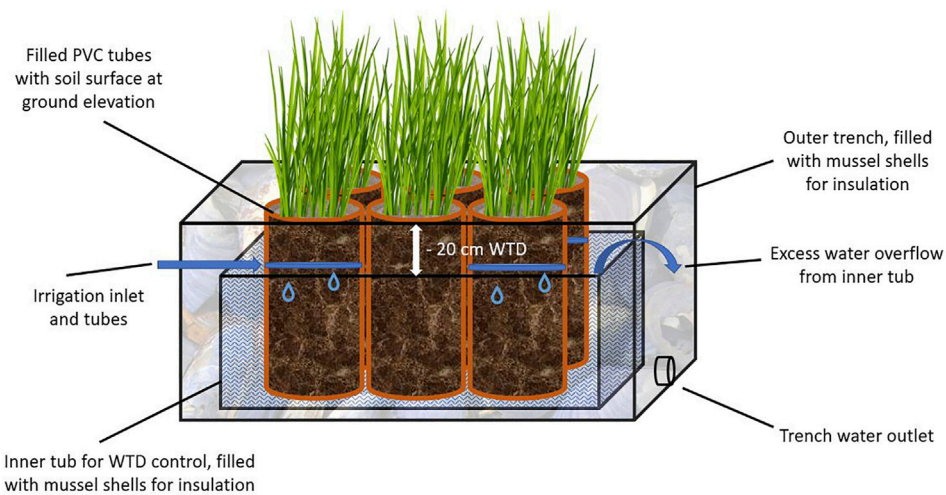

FIGURE 2 | Schematic sketch of the experimental setup representing water table depth (WTD) control of the polyvinyl carbonate (PVC) cylinders, filled with soil and cultivated with the various grass species.

cores were filled with coarse sandy soil (1.5% total organic C, 17.5 kg NH_4-N ha^{-1}, 35.0 kg NO_3-N ha^{-1}, pH 5.8) and maintained at a controlled water table depth (WTD) of -20 cm. This setup was chosen to simplify root washing as compared to peat soil where separation of new and old plant remains is unfeasible. The WTD control was ensured by placing the PVC tubes in tubs (78.5 cm × 48.5 cm × 30 cm) with the soil surface at ground elevation. The tubs allowed for overflow of excess

TABLE 1 | Dates and amounts of fertilizer application, calendar weeks of aboveground biomass harvest occurrences, and dates for root extraction following the final biomass harvest for the various treatments as indicated by number of cuts.

Number of cuts	Fertilizer application	Fertilizer date (week no.)	Biomass harvest (week no.)	Root extraction (week no.)
Zero	40 kg N and K ha^{-1} $year^{-1}$	12	45	45
One	1 × 100 kg N and K ha^{-1}	12	31	31
Two	2 × 100 kg N and K ha^{-1}	12, 26	25, 37	37
Five	5 × 40 kg N and K ha^{-1}	12, 22, 26, 31, 38	21, 25, 31, 37, 44	44

water and were automatically filled twice daily with demineralized water to maintain a stable WTD (**Figure 2**). Sowing of seeds (25 kg ha^{-1}) was performed by hand on March 14, 2019 (week 11). The cylinders (n = 20) in each cultivar group were randomly assigned to four harvest and fertilization treatments, including zero, one, two, and five annual cuts with five replicates each (**Table 1**). The treatment with one annual biomass harvest was chosen to determine BGB development in the first half of the growing period. Initial fertilization of all treatments was applied on March 19, 2019. The setup was exposed to natural changes in temperature and precipitation.

Above and Belowground Biomass and Net Primary Productivity

AGB was harvested at a stubble height of 5 cm in calendar weeks 21, 25, 31, 37, and 44, depending on treatment regarding harvest frequency (**Table 1**). Stubble and BGB were separated and determined following the last AGB harvest. Roots were extracted from the soil by fine washing: two rinsing cycles using a soft spray nozzle with demineralized water and a 20-cm-diameter soil sieve with 2-mm mesh size, followed by three rinsing cycles and a 250-µm mesh size sieve. Total biomass dry matter (DM) for each cut and plant fraction was determined after oven-drying at 60°C to constant weight. Following drying, all samples were milled (Retsch SM 200, Retsch GmbH, Haan, Germany) and analyzed for total nitrogen (TN) and total organic carbon (TC) concentrations using a vario MAX CN (Elementar Analysesysteme GmbH, Hanau, Germany). Recovered roots were considered as BGB, and harvested yields and stubble were considered as AGB. Root:shoot ratios and NPP were calculated as

$$Root{:}\ shoot\ ratio\ (R/S) = BGB/AGB \quad (1)$$

$$Net\ primary\ production\ (NPP) = BGB + AGB \quad (2)$$

The calculation of NPP has been chosen to be simplified, in our study excluding the, unquantified contribution of, e.g., root secretions and exudates to NPP. The amount of C in AGB and BGB plant parts was calculated by multiplying the biomass (t DM) and the TC concentration in biomass (Mg C t^{-1} DM).

Extrapolation of Results for Calculation of Soil Carbon Input

We calculated the soil carbon input from biomass for each treatment under the following observations and assumptions of 1) observed yields of AGB and BGB, 2) the determined R/S, and 3) the various individual concentrations of TC in AGB and BGB as well as the stubble fraction of AGB. The method has been adapted from Kätterer et al. (2011) and Poeplau (2016) under the modification to account for specific TC concentrations in the stubble fraction, and BGB. Hence, we calculated the TC input into soil using the following assumptions and equations: ANPP is the aboveground NPP, which was calculated by multiplying the AGB yield by the carbon concentration in AGB as derived by biomass analyses for the various treatments (**Eq. 3**).

$$ANPP = AGB\ Yield * C\ in\ AGB \quad (3)$$

BNPP is the belowground NPP, calculated as the harvested AGB yield multiplied with the derived R/S for the various treatments and multiplied with the carbon concentration in BGB as derived by biomass analyses for the various treatments (**Eq. 4**).

$$BNPP = (AGB\ Yield * R/S) * C\ in\ BGB \quad (4)$$

AC_{in} (t C ha^{-1} $year^{-1}$), the TC input into the soil from AGB, was calculated as the yield of the not harvested stubbles multiplied by the carbon concentration is those, divided by two. This was a conservative estimate, based on the assumption that only approximately 50% of the stubble biomass (S) fraction becomes available as structural soil carbon input according to Schneider et al. (2006) (**Eq. 5**).

$$AC_{in} = \frac{(Stubble\ Yield * C\ in\ Stubble\ biomass)}{2} \quad (5)$$

BC_{in}, the TC input into soil (t C ha^{-1} $year^{-1}$) for a depth of 50 cm, as equivalent to the length of the used PVC tubes, was calculated according to **Equation 6**. This is in detail described by Poeplau (2016), where d is the sampling depth (in cm), d_r is the assumed maximum rooting depth for a flooded soil, and d_{50} is the depth of 50% of BNPP distribution. In our calculations, d was set to 50 cm as the depth of the PVC tubes, d_r to 70 cm, since the maximum rooting depth under high WTDs is not likely to significantly exceed the sampling depth (Kohzu et al., 2003; Fan et al., 2017; D'Imperio et al., 2018), and d_{50} to 15 cm, according to average observations from this study across treatments. This was multiplied by 0.65 according to a conservative root turnover estimation for temperate wetlands with similar mean annual average temperature and precipitation values as our study site (Gill and Jackson, 2000; DuPont et al., 2014; Leifeld et al., 2015).

$$BC_{in} = \left(\frac{d*(d_{50}+d_r)}{d_r*(d_{50}+d)}*BNPP\right)*0.65 \quad (6)$$

This resulted in the final TC input into soil (t C ha^{-1} $year^{-1}$), which was calculated as the sum of AC_{in} and BC_{in} (**Eq. 7**).

$$TC_{in} = AC_{in} + BC_{in} \quad (7)$$

Scenarios of Soil Carbon Input Based on Default R/S

Two commonly used R/S were applied for default calculation of soil carbon input: first, an R/S of 0.8 as stated by Bolinder et al. (2007) for grass species in eastern and western Canada. This ratio is based on a literature review on 35 publications. Second, we used the R/S of 2.8, which is derived from semi-arid grassland data, but used as a default expansion factor by the IPCC (2006) and applied in Denmark's National Inventory Report (2020). These R/S values were applied to averaged total AGB yields and the commonly used average of 45% TC within biomass (Kätterer et al., 2011).

In addition, the carbon input into soil for RCG treatments was exemplarily calculated identical to the R/S scenarios, assuming identical biomass yields, for better comparability.

Statistical Analyses

Observations were averaged and summed up to yields over the entire growing period. Standard error was reported to present the distribution of data. Two-way analyses of variance were performed using linear mixed models with the function *lmer* of the package *lme4* (Bates et al. (2015), Version 1.1–23, 2020) in the statistical software R (R Core Team (2020) Version 4.0.2—"Taking Off Again"), in which the following model was used:

$$Y_{ijk} = \mu + s_i + t_j + st_{ij} + \epsilon_{ijk}$$

where Y_{ijk} is the observed dependent variable, μ is the overall mean, s_i is the fixed effect of species, t_j is the fixed effect of combined harvest frequency and fertilization treatment, st_{ij} is the species by treatment interaction, and ϵ_{ijk} is the experimental error. The model residuals were inspected for normality and homoscedasticity, and variables were log-transformed in order to stabilize the variance and normal distribution. A Tukey's HSD test at the 95% confidence level was used to test for significance of differences between treatment means. Correlation effects between the observed R/S and the various biomass treatments were determined by multiple linear regression using Pearson's correlation.

RESULTS

Root and Shoot Measurements

Cumulated Biomass Yield

Cumulated DM plant biomass at the end of the growing season ranged between 16.8 t ha^{-1} $year^{-1}$ (FL, five cuts) and 46.2 t ha^{-1} $year^{-1}$ (FL, zero cuts) across all treatments (**Table 2**) and were affected by the annual harvest strategy [$\chi2$ (3) = 110.4, $p < 0.001$]. Generally, and for all species, the highest yields were found in the zero-cut treatments, ranging between 39.4 (TF) and 46.2 (FL) t ha^{-1} $year^{-1}$. There was a consistent decrease of BGB and cumulative biomass yield with increasing number of annual cuts, with the one-cut treatment being an exception due to the different timing of harvest, presumably in combination with lesser N availability. However, while for RCG and TF there was no difference of total yields between the one-to five-cut treatments, there was, for FL, a significant ($p < 0.001$) increase of both AGB and BGB development, when comparing the one- and two-cut treatments. Species alone did not affect total biomass yield despite the observation of high overall yields for the FL two-cut treatment, close to three-fold as compared to the FL five-cut treatment. For all species, there was a significant difference ($p < 0.001$) between yields of the zero-cut treatment and all other treatments. Overall and across treatments, RCG and TF yields were near identical.

Root:shoot Ratio

The ratio between AGB and BGB (R/S) varied between 0.6 (FL, five cuts) to 2.3 (RCG, zero-cuts), significantly ($p < 0.001$) affected by the annual harvest strategy (**Table 2**). The smallest contribution of BGB to total biomass was observed for the five-cut treatments, ranging between 38% (FL) and 45% (RCG). In the zero-cut treatments, BGB contributed with 61% (FL) to 70% (RCG) of total biomass. For all species, the R/S of the zero-cut treatment was significantly ($p < 0.001$) higher than for the other treatments [$\chi2$ (2) = 46.8, $p < 0.001$], while no differences in R/S were observed for the one-to five-cut treatments. There was no significant ($p > 0.5$) difference of R/S in between species across the various treatments. The differences between one and two annual cuts and between two and five annual cuts were non-significant (**Figure 3**). However, the Pearson correlation identified strong positive correlations between AGB and BGB based on yield results combined for treatment but differentiated for species (minimum $R > 0.61$), combined for species but differentiated for treatment (minimum $R > 0.76$), and differentiated for both species and treatment (minimum $R > 0.71$) (**Figures 4A–C**).

Total Carbon

The mean content of TC across all species and treatments was 45% for aboveground grass biomass, 44% for stubble biomass, and 40% for belowground biomass. A decreasing trend of TC content within AGB was observed with increasing number of cuts for all species (**Table 3**). TC yield (t TC ha^{-1} $year^{-1}$) within biomass generally followed the pattern of total DM biomass yield, with an increasing aboveground TC yield with increasing number of annual cuts and an increasing belowground TC yield with fewer annual cuts. The highest total plant TC yeild was found in the FL zero-cut treatment (18.9 t ha^{-1} $year^{-1}$) and the lowest in FL one-cut (5.5 t ha^{-1} $year^{-1}$). There were no significant differences for TC yields between the zero- and five-cut treatments in AGB. Generally, TC yield was highly affected by management [$\chi2$ (15) = 80.9, $p < 0.001$].

TABLE 2 | Yields of dry matter (DM) of aboveground (AGB), belowground (BGB), and stubble (S) biomass for the various species and treatments. Total yields for above- and belowground plant fractions are indicated as sums. The root to shoot (R/S) ratio indicates the ratio of belowground to combined aboveground and stubble biomass. Letters indicate differences between treatments, where treatments with the same letters are not significantly different. Standard error is given in brackets (n = 5).

Treatment	DM (t ha^{-1} year^{-1})				R/S
	AGB	BGB	S	Sum	
Festulolium					
0 Cut	14.0 (±2.8)ab	28.1 (±4.3)a	4.2 (±0.7)a	46.2 (±7.7)a	1.6 (±0.1)a
1 Cut	5.6 (±0.8)c	6.3 (±1.6)c	1.3 (±0.3)b	13.2 (±2.7)b	0.9 (±0.1)b
2 Cuts	18.1 (±2.1)a	18.9 (±3.1)b	3.9 (±0.8)a	41.0 (±6.0)a	0.8 (±0.1) b
5 Cuts	9.6 (±1.5)bc	6.4 (±1.1)c	0.8 (±0.2)b	16.8 (±2.8)b	0.6 (±0.0)b
Reed canary grass					
0 Cut	11.2 (±1.5)a	28.0 (±3.7)a	1.1 (±0.1)b	40.3 (±5.3)a	2.3 (±0.1)a
1 Cut	6.7 (±0.9)b	9.5 (±0.9)b	1.3 (±0.2)ab	17.4 (±2.0)b	1.2 (±0.1)b
2 Cuts	9.4 (±1.7)ab	13.5 (±2.8)b	1.9 (±0.5)a	24.8 (±5.0)b	1.2 (±0.3)b
5 Cuts	11.2 (±1.4)a	10.0 (±0.7)b	0.8 (±0.1)b	22.0 (±2.2)b	0.8 (±0.0)b
Tall fescue					
0 cut	11.1 (±1.4)a	25.1 (±3.0)a	3.1 (±0.6)a	39.4 (±5.1)a	1.8 (±0.1)a
1 cut	6.4 (±0.7)b	9.9 (±1.4)b	2.2 (±0.5)ab	18.5 (±2.5)b	1.2 (±0.1)b
2 cuts	8.5 (±2.2)ab	10.5 (±2.0)b	2.9 (±0.5)a	21.9 (±4.7)b	1.0 (±0.1)b
5 cuts	11.0 (±2.0)a	9.5 (±1.0)b	1.2 (±0.2)b	21.7 (±3.2)b	0.8 (±0.1)b

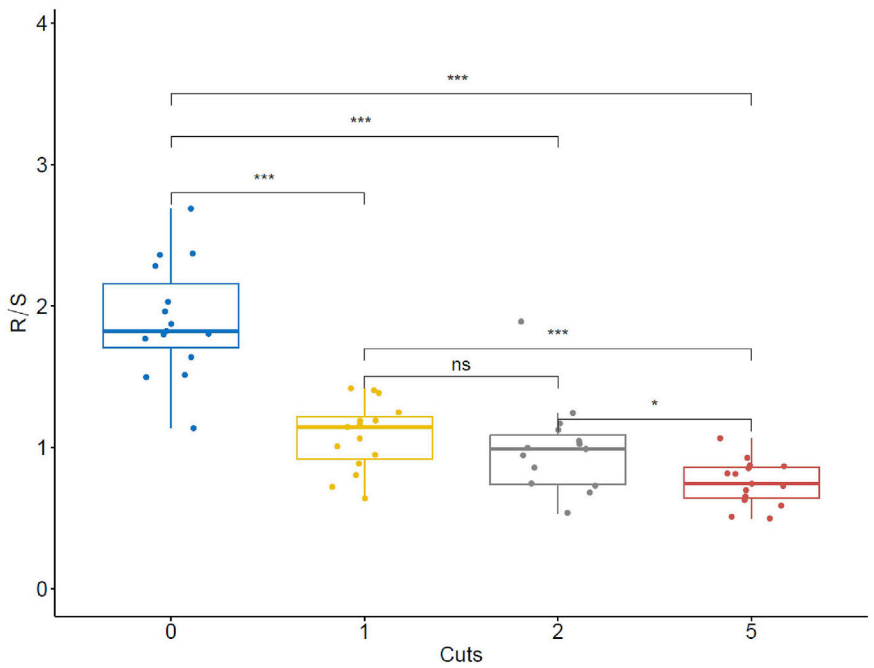

FIGURE 3 | Differences of root:shoot ratios (R/S) for the various treatments of zero, one, two, and five annual cuts across species. Stars denote statistical significances between treatments according to *p*-values with ns indicating non-significance.

Total Nitrogen

TN in biomass was significantly affected by treatment [$\chi 2$ (3) = 53.2, $p < 0.001$]. For all species and treatments, the content of TN was higher in AGB than in BGB and stubble biomass. Averaged across species, TN content in AGB increased from 1.4% in the zero-cut treatment to 4.0% in the five-cut treatments (**Table 3**). This is also depicted in TN yields, where more TN was harvested in the five-cut treatments (26.4–34.4 g N m^{-2} year^{-1}) as compared to the zero-cut treatments (13.6–17.8 g N m^{-2} year^{-1}), despite similar or lower AGB yields. In contrast to AGB, the TN content

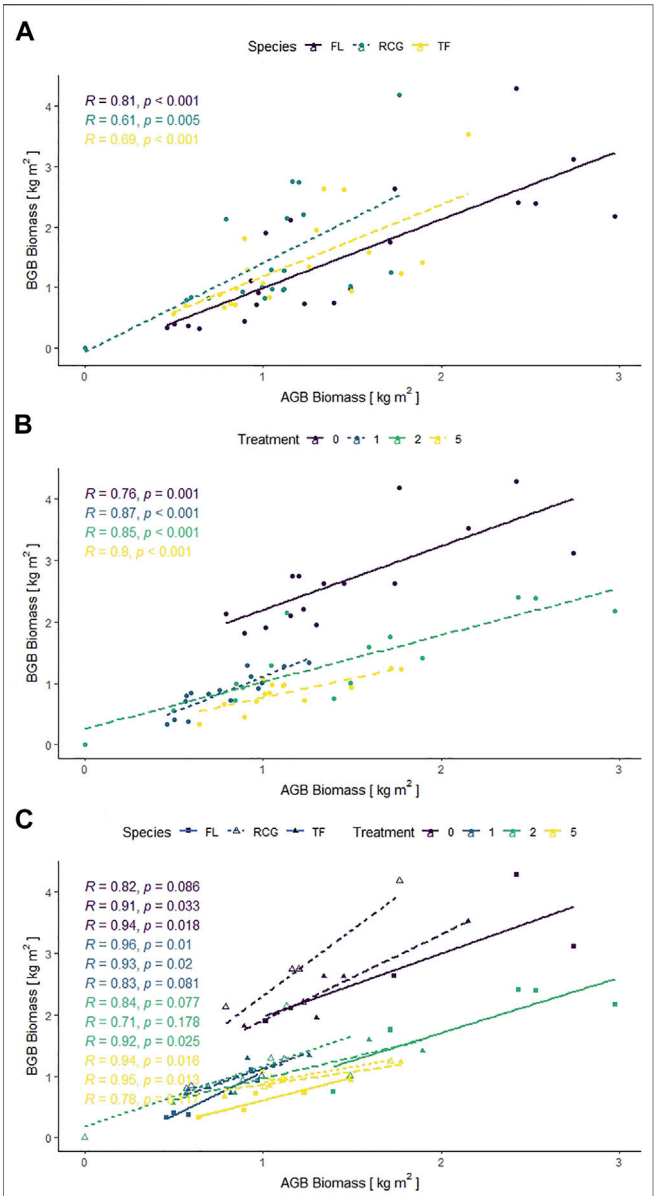

FIGURE 4 | Pearson correlation showing the relation between aboveground (AGB) biomass (kg m^{-2}) and belowground (BGB) biomass (kg m^{-2}) for **(A)** species and treatment, **(B)** treatment across species, and **(C)** species across treatments.

in BGB was not affected by increasing harvest and fertilization frequencies ($p < 0.5$). On a cumulative basis, the highest plant TN yield was found in the zero-cut treatment for RCG (51.1 g m^{-2} $year^{-1}$) and TF (41.6 g m^{-2} $year^{-1}$), while for FL, most TN (51.1 g m^{-2} $year^{-1}$) was found in the two-cut treatment.

Carbon-to-Nitrogen Ratio

We found that for all three grass species, the carbon-to-nitrogen (C/N) ratio within AGB, as well as in the combined AGB and S (AGB + S) biomass, decreased significantly ($p < 0.001$) with increasing number of annual cuts. For instance, in AGB + S, the C/N decreased from 32.1 (RCG)–39.3 (FL) for the zero-cut treatment to 15.4 (RCG)–19.0 (TF) for the treatment with five annual cuts (**Table 4**). Regarding S biomass, the C/N was for all treatments higher as compared to the C/N of AGB, with significant ($p < 0.001$) differences for the one-to five-cut treatments. For BGB, no significant difference of the C/N ratio between the various treatments was observed, except for FL. However, cumulative across all plant parts, the C/N ratio followed the pattern of the C/N in AGB + S, showing significant ($p < 0.001$) differences between the treatments with zero and five annual cuts, with one- and two-cut treatments ranging in between.

Scenarios of Soil Carbon Input

The input of TC into soil was for all species highest in the zero-cut treatments, ranging between 6.6 t C ha^{-1} $year^{-1}$ (TF) and 7.6 t C ha^{-1} $year^{-1}$ (FL). A gradient of lesser TC input with increasing number of cuts was observed for all species, with the five-cut treatment being significantly lower than the treatment with zero harvests (**Table 5**). The one-cut treatment, harvested in August, was not significantly different to the five-cut treatment. Generally, TC_{in} was significantly ($p < 0.001$) affected by the random effect of harvest and fertilization treatment. When theoretically assuming equal AGB yields for all treatments on the example of RCG and the two literature-derived R/S scenarios (**Table 6**), TC_{in} ranged between 2.8 t C ha^{-1} $year^{-1}$ (five cuts) and 7.3 t C ha^{-1} $year^{-1}$ (zero cuts) for RCG. TC_{in} using the R/S from Bolinder (2007) and the IPCC (2006) was 3.1 and 9.6 t C ha^{-1} $year^{-1}$, respectively. For all treatments and scenarios, TC_{in} was significantly affected by the R/S [X^2 (1) = 56.4, $p < 0.001$].

DISCUSSION

In this study, we highlight that AGB and BGB as well as R/S differed greatly among the various harvest frequencies, with frequent cuts resulting in reduced BGB yields and lower R/S for all assessed species. However, while the effects of water saturation and nutrient availability on biomass development and the R/S are relatively well known (e.g. Guo et al., 2016), there are only little comparable data available regarding R/S for RCG, TF, and FL under various annual cuts within the first year of establishment. Mander et al. (2012) reported an R/S of 0.91 (unfertilized) and 0.67 (fertilized) for RCG on an abandoned peat extraction site in Estonia without harvest, while Klimesová (1994) found a R/S of between 1.9 and 2.1 for RCG in a pot experiment under similar soil and water conditions and for the same timeframe as in this study. The latter values are similar to the R/S of 2.3 for the RCG treatment without harvest in our study. Bolinder et al. (2002) reported for RCG and TF in the second year after cultivation R/S values of 1.0 and 0.6 for a treatment with two annual cuts. These values, 0.2 and 0.4 lower than the corresponding R/S from RCG and TF under two annual cuts observed in our study, are within a similar range. However, the higher R/S observed in our study probably results from a younger sward age, indicating the plant's need for optimal biomass allocation under the establishing growth period. Cougnon

TABLE 3 | Yields of total carbon (TC) and total nitrogen (TN), as well as TC and TN content in percentages, of aboveground (AGB), belowground (BGB), and stubble (S) biomass for the various species and treatments. Total yields for above- and belowground plant fractions are indicated as sums. Letters indicate differences between treatments, where treatments with the same letters are not significantly different. Standard error is given in brackets (n = 5).

Treatment	TC (t ha^{-1} year^{-1})				TN (g m^{-2} year^{-1})				TC %			TN %		
	AGB	BGB	S	Sum	AGB	BGB	S	Sum	AGB	BGB	S	AGB	BGB	S
Festulolium														
0 cut	6.4 (±1.3) ab	10.7 (±1.8)a	1.9 (±0.3)a	18.9 (±3.5)a	16.1 (±2.5)b	27.2 (±3.4)a	4.5 (±0.6)a	47.8 (±6.6)ab	45.6 (±0.32)a	37.6 (±1.00)b	44.6 (±0.41)a	1.2 (±0.15)d	1.0 (±0.06)b	1.1 (±0.16) ab
1 cut	2.4 (±0.4)c	2.6 (±0.7)b	0.6 (±0.1)b	5.5 (±1.2)b	13.8 (±2.8)b	9.8 (±2.8)b	2.2 (±0.8) bc	25.8 (±6.5)c	42.3 (±0.66)c	41.4 (±0.97)a	43.1 (±0.61) ab	2.4 (±0.24)c	1.5 (±0.08)a	1.5 (±0.19)a
2 cuts	8.2 (±1.0)a	8.0 (±1.3)a	1.7 (±0.4)a	17.9 (±2.6)a	27.6 (±2.1)a	20.3 (±3.0)a	3.3 (±0.5) ab	51.1 (±5.6)a	44.3 (±0.12)b	42.3 (±0.54)a	43.9 (±0.14) ab	3.2 (±0.11)b	1.1 (±0.05)b	0.9 (±0.11)b
5 cuts	4.2 (±0.7) bc	2.4 (±0.4)b	0.3 (±0.1)b	7.0 (±1.1)b	26.4 (±3.4)a	7.2 (±0.8)b	1.1 (±0.2)c	34.6 (±4.4)bc	43.6 (±0.30)b	38.5 (±0.92)b	42.6 (±1.08)b	3.9 (±0.20)a	1.2 (±0.10) ab	1.4 (±0.21)a
Reed canary grass														
0 cut	5.3 (±0.7)a	11.6 (±1.6)a	0.5 (±0.1)b	17.4 (±2.4)a	17.8 (±4.0)a	32.0 (±7.0)a	1.3 (±0.2)a	51.1 (±11.2)a	47.1 (±0.11)a	41.3 (±0.46) ab	41.4 (±1.68)b	1.5 (±0.15)c	1.1 (±0.08)a	1.2 (±0.16)b
1 cut	3.1 (±0.4)b	3.7 (±0.2)b	0.6 (±0.1) ab	7.3 (±0.7)b	13.1 (±3.1)a	10.9 (±1.5)b	1.3 (±0.4)a	25.3 (±5.0)b	46.1 (±0.07)b	39.2 (±1.67)b	44.6 (±0.16)a	1.9 (±0.19)c	1.1 (±0.04)a	0.9 (±0.15)b
2 cuts	4.4 (±0.8) ab	5.8 (±1.2)b	0.9 (±0.2)a	11.1 (±2.2)b	20.7 (±5.0)a	17.1 (±6.3)b	2.2 (±0.8)a	40.1 (±12.1) ab	45.4 (±0.17)c	43.5 (±0.25)a	45.4 (±0.25)a	3.1 (±0.31)b	1.2 (±0.19)a	1.1 (±0.13)b
5 cuts	5.1 (±0.7)a	4.0 (±0.4)b	0.4 (±0.0)b	9.5 (±1.1)b	34.4 (±7.2)b	11.9 (±1.3)b	1.7 (±0.2)a	47.9 (±8.7)a	44.5 (±0.33)d	40.0 (±1.10)b	43.8 (±0.94) ab	4.7 (±0.30)a	1.2 (±0.05)a	2.1 (±0.23)a
Tall fescue														
0 cut	5.1 (±0.7)a	9.6 (±1.2)a	1.4 (±0.3)a	16.1 (±2.1)a	13.6 (±1.5)b	24.6 (±2.0)a	3.4 (±0.6)a	41.6 (±4.1)a	45.4 (±0.10)a	38.4 (±0.60) ab	44.1 (±0.48)a	1.3 (±0.16)c	1.0 (±0.12)a	1.2 (±0.24)a
1 cut	2.9 (±0.3)b	3.7 (±0.4)b	0.9 (±0.2) ab	7.5 (±0.9)b	15.9 (±4.2) ab	13.3 (±3.3)b	3.6 (±1.6)a	32.9 (±9.2)a	44.4 (±0.15)b	38.2 (±1.50) ab	42.9 (±0.08)b	2.4 (±0.35)b	1.3 (±0.17)a	1.4 (±0.31)a
2 cuts	3.8 (±1.0) ab	4.1 (±0.7)b	1.3 (±0.2)a	9.2 (±1.9)b	18.3 (±7.3)a	10.7 (±2.1)b	3.1 (±0.8)a	32.1 (±10.2)a	44.4 (±0.28)b	40.0 (±1.36)a	44.0 (±0.26)a	3.1 (±0.29)a	1.0 (±0.10)a	1.0 (±0.16)a
5 cuts	4.9 (±0.9)a	3.5 (±0.4)b	0.5 (±0.1)b	9.0 (±1.4)b	27.4 (±5.5) ab	9.3 (±1.3)b	1.4 (±0.1)b	38.2 (±7.0)a	44.1 (±0.19)b	37.1 (±0.67)b	42.9 (±0.40)b	3.6 (±0.19)a	1.0 (±0.11)a	1.3 (±0.18)a

et al. (2013) reported 1 kg DM m^{-2} more BGB for TF with five annual cuts than in our experiment for an already established sward, receiving 100 kg N ha^{-1} and 100 kg K ha^{-1} more than in this study, and 300 (FL)–700 (TF) g DM m^{-2} more BGB in 3-year-old swards with five annual cuts, receiving similar fertilization amounts as in our study (Cougnon et al., 2017). We also found such differences in R/S for treatments without any harvest. For instance, Xiong et al. (2009) determined an R/S of 6.5 for RCG after a full year of growth, which differs significantly to our observed value of 2.3 after 210 days. Since the water table has been permanently controlled to −20 cm, a depth indicated as optimal for AGB development of flooding-tolerant perennial grasses (Miller and Zedler, 2003; Ustak et al., 2019), and adequate nutrients were provided, we interpret the observed differences in R/S for all species regarding harvest frequencies as a response of the plant's biomass allocation. This is in accordance with the OPT (Kobe et al., 2010), where, as a consequence of more frequent harvest and removal of biomass involved in light energy capturing, more biomass is allocated to AGB organs in order to maximize photosynthesis. Further, the IA was supported by significant linear relationships between AGB and BGB, which is in line with other studies for temperate grasslands (e.g., Wang et al., 2010; Yang et al., 2018), indicating a coexistence of the OPT and IA theories. However,

TABLE 4 | Carbon-to-nitrogen (C/N) ratios in aboveground biomass (AGB), stubble biomass (S), combined aboveground and stubble biomass (AGB + S), and belowground biomass (BGB), as well as across all plant parts (cum) for the various treatments and species. Letters indicate differences between treatments, where treatments with the same letters are not significantly different.

Treatment	C/N AGB	C/N S	C/N AGB + S	C/N BGB	C/N Cum
Festulolium					
0 cut	38.8 (±4.3)a	42.0 (±5.5)ab	39.3 (±4.4)a	38.6 (±2.9)a	38.9 (±3.5)a
1 cut	18.0 (±1.6)b	30.3 (±2.9)b	19.4 (±1.6)b	27.0 (±1.0)b	22.2 (±1.3)b
2 cuts	29.5 (±2.3)a	52.5 (±5.7)a	31.9 (±2.7)a	39.2 (±1.7)a	34.6 (±2.0)a
5 cuts	15.9 (±1.1)b	32.6 (±4.6)b	16.6 (±1.2)b	33.0 (±2.5)ab	20.0 (±1.4)b
Reed canary grass					
0 cut	31.6 (±3.0)a	38.6 (±5.4)ab	32.1 (±3.1)a	38.0 (±2.4)a	35.7 (±2.6)a
1 cut	25.1 (±2.0)ab	54.5 (±7.3)a	27.4 (±2.3)a	34.8 (±2.4)a	30.7 (±2.4)ab
2 cuts	21.8 (±2.1)ab	43.4 (±5.1)ab	23.8 (±2.3)ab	39.6 (±6.0)a	29.6 (±3.5)ab
5 cuts	15.0 (±1.3)b	22.3 (±2.3)b	15.4 (±1.3)b	34.1 (±0.7)a	19.7 (±1.5)b
Tall fescue					
0 cut	38.0 (±4.6)a	42.9 (±7.6)a	39.0 (±5.2)a	39.6 (±4.3)a	39.4 (±4.6)a
1 cut	20.1 (±2.1)b	36.1 (±6.2)a	22.2 (±2.4)b	30.9 (±3.0)a	25.8 (±2.7)ab
2 cuts	24.9 (±3.8)ab	47.5 (±7.2)a	28.3 (±4.3)ab	41.0 (±3.9)a	32.5 (±4.0)ab
5 cuts	18.2 (±1.5)b	34.9 (±5.1)a	19.0 (±1.6)b	39.8 (±4.8)a	23.9 (±2.0)b

TABLE 5 | Total annual harvested biomass yields in t dry matter (DM) ha^{-1} $year^{-1}$ of the three perennial grasses under the various treatments, the content of total carbon (TC) in aboveground (AGB), stubble (S), and belowground (BGB) biomass and the determined root:shoot ratio (R/S), used for the calculation of aboveground net primary productivity (ANPP), stubble net primary productivity (SNPP), and belowground net primary productivity (BNPP), the input of carbon into soil from aboveground biomass residues (AC_{in}) and belowground biomass (BC_{in}), resulting in the total carbon input (TC_{in}) over a rooting depth of 50 cm. Letters indicate differences between treatments, where treatments with the same letters are not significantly different.

t DM ha^{-1} $year^{-1}$			%				t TC ha^{-1} $year^{-1}$					
AGB yield		S Yield	TC in AGB	TC in S	TC in BGB	R/S	ANPP	SNPP	BNPP	AC_{in}	BC_{in}	TC_{in}
Festulolium												
0 cut	14.0	4.2	46	45	38	1.6	6.4	1.9	11.0	0.9 a	6.7 a	7.6 a
1 cut	5.6	1.3	42	43	41	0.9	2.3	0.6	2.5	0.3 b	1.5 c	1.8 c
2 cuts	18.1	3.9	44	44	42	0.8	8.0	1.7	7.4	0.9 a	4.5 b	5.4 b
5 cuts	9.6	0.8	44	43	39	0.6	4.2	0.4	2.4	0.2 b	1.5 c	1.7 c
Reed canary grass												
0 cut	11.2	1.1	47	41	41	2.3	5.3	0.5	11.6	0.2 a	7.0 a	7.3 a
1 cut	6.7	1.3	46	45	39	1.2	3.1	0.6	3.7	0.3 a	2.3 b	2.5 b
2 cuts	9.4	1.9	45	45	44	1.2	4.3	0.9	6.0	0.4 a	3.6 b	4.1 b
5 cuts	11.2	0.8	45	44	40	0.8	5.0	0.4	3.8	0.2 a	2.3 b	2.5 b
Tall fescue												
0 cut	11.1	3.1	45	44	38	1.8	5.1	1.4	9.8	0.7 a	5.9 a	6.6 a
1 cut	6.4	2.2	44	43	38	1.2	2.9	0.9	3.9	0.5 b	2.4 b	2.9 b
2 cuts	8.5	2.9	44	44	40	1.0	3.8	1.3	4.5	0.6 a	2.8 b	3.4 b
5 cuts	11.0	1.2	44	43	37	0.8	4.9	0.5	3.6	0.2 c	2.2 b	2.4 b

even though we were able to confirm our hypothesis, that different ratios between AGB and BGB will be observed in flood-tolerant perennial grasses under different harvest frequencies during the growth season under provision of adequate nutrient availability, there might remain a limitation of our observation for wet organic soils: that the R/S analysis was not performed on samples grown on peat soil cores. However, since R/S is rather affected by nutrient availability than soil types (Lambert et al., 2014; Pinno et al., 2014; Lehtonen et al., 2016), we assume a reliable validity of the indicated R/S for similar growth conditions, including fertilizer management, also on peat soils. This is supported by other research, comparing differences in R/S for certain species and treatments between cultivation on mineral and organic soil types. Xiong et al. (2009) for example found similar R/S for RCG under different fertilization rates on both mineral and organic soils. Björk et al. (2007) reported similar

TABLE 6 | Calculation of the total carbon input into soil using averaged biomass yields on the example of reed canary grass and two literature-derived scenarios, applying different root to shoot (R/S) ratios. The contents of total carbon (TC) in aboveground (AGB), stubble (S), and belowground (BGB) biomass and the determined R/S were used for the calculation of aboveground net primary productivity (ANPP), stubble net primary productivity (SNPP), and belowground net primary productivity (BNPP), the input of carbon into soil from aboveground biomass residues (AC_{in}), and belowground biomass (BC_{in}), resulting in the total carbon input (TC_{in}) over a rooting depth of 50 cm. Yields are indicated in t dry matter (DM) ha^{-1} $year^{-1}$.

t DM ha^{-1} $year^{-1}$			%				t TC ha^{-1} $year^{-1}$					
AGB yield		**S yield**	**TC in AGB**	**TC in S**	**TC in BGB**	**R/S**	**ANPP**	**SNPP**	**BNPP**	**AC_{in}**	**BC_{in}**	**TC_{in}**
Reed canary grass scenario												
0 cut	10.0	2.0	47	41	41	2.3	4.7	0.8	11.3	0.4	6.9	7.3
1 cut	10.0	2.0	46	45	39	1.2	4.6	0.9	5.6	0.4	3.4	3.9
2 cuts	10.0	2.0	45	45	44	1.2	4.5	0.9	6.3	0.5	3.8	4.3
5 cuts	10.0	2.0	45	44	40	0.8	4.5	0.9	3.8	0.4	2.3	2.8
Scenarios												
Bolinder	10.0	2.0	45	45	45	0.8	4.5	0.9	4.3	0.5	2.6	3.1
IPCC	10.0	2.0	45	45	45	2.8	4.5	0.9	15.1	0.5	9.2	9.6

findings for root mass in Swedish heath and meadow tundra ecosystems, and Lambert et al. (2014) stated that R/S of *Arundo donax* was stable across soil types. Nonetheless, we propose that future research not only has to emphasize an assessment of cultivation treatments on R/S on mineral and organic soils but also needs to monitor TC and TN in AGB and BGB, as well as their development with increasing production years, due to expected variations (Sainju et al., 2017b). The C/N ratio can aid as an indicator for litter quality, with easier decomposable substrates having low C/N ratios (Rydin and Jeglum, 2013). Recalcitrant plant litter, indicated by high C/N ratios (Poirier et al., 2018), hence has the potential to increase soil C input-either directly to the pool of particulate organic matter (POM) or as microbial necromass following decomposition by microorganisms in the acrotelm (Worrall et al., 2017; Rossi et al., 2020). The potential for long-term C storage in the POM pool is in particular high for wet organic soils due to anoxic conditions in the catotelm, indicated by higher contents of lignin with increasing peat depth (Williams and Yavitt, 2003). Further, in soils with <12% SOC, additional C storage through the POM pool has the potential to overcome soil C saturation (Cotrufo et al., 2019). However, for drained soils where microbial activity is found in deeper layers, there is no consensus whether the C/N in BGB can be used as a predictor for the decomposability of root litter, and hence the C storage potential, as indicated by interspecific variation (Bonanomi et al., 2021). However, while R/S and C in biomass have been assessed for RCG on mineral and organic soils (Xiong et al., 2009; Xiong and Kätterer, 2010), this study was to our knowledge among the first to, besides R/S, also assess C/N in AGB and BGB parts.

The input of carbon into soil is a critical component of the global C cycle, thus significantly contributing to various aspects of ecosystem functioning. Modeling existing and changing soil organic carbon (SOC) stocks hence is a critical task in decision support related to optimal climate and land management (Taghizadeh-Toosi et al., 2016). However, while it is recognized that C allocation in belowground plant organs depends on vegetation type (Keller and Phillips, 2019), growing conditions (Whitehead, 2020), and plant development stages and management (Pausch and Kuzyakov, 2018), only few of these complex relationships (Cheng et al., 2014) are set into context with soil geochemistry and accounted for during SOC modeling (Finke et al., 2019). For instance, previously reported R/S for perennial grasses showed a broad distribution of median values, which has been shown in reviews by Bolinder et al. (2007) and Pausch and Kuzyakov (2018). Given the critical role of BGB carbon input, our study highlights the importance of acquiring more extensive knowledge regarding the development of perennial grass root systems depending on AGB manipulation by harvest. We only found marginally significant differences in R/S for the various treatments and species, apart for the, in agriculturally used grasslands, uncommon zero-cut strategy, which could indicate that a fixed R/S for perennial grasses might be reasonable to use if accurately defined.

However, our calculation of soil C input for perennial grasses under different harvest frequencies revealed significant differences for the various management options and applied R/S. This highlighted a potential risk for over- and underestimation of the C sink functioning of wetlands and grassland ecosystems. While, for instance, using the IPCC default R/S of 2.8 resulted in an estimated annual carbon input into soil of 9.6 t C ha^{-1} $year^{-1}$ for a RCG yield of 10 t DM ha^{-1} $year^{-1}$, our results ranged between 2.8 and 7.3 t C ha^{-1} $year^{-1}$ for the same AGB yield, depending on annual harvest frequencies. Since, for instance, the default IPCC (2006) estimate of R/S of 2.8 is applied in the Danish National Inventory Report (2020), the discrepancy of TC input from BGB resulting from varying R/S might have far-reaching consequences for policymaking. For instance, depending on whether management measures are extensive, e.g., designated nature areas without any biomass manipulation, or intensive, e.g., biomass harvest up to five times annually, the choice of R/S for the quantification of an organic soil C sink function must be made carefully and adapted to the ecosystem in question. This is in particular true for the designation of rewetting measures on wetland areas, including the choice of land use and land cover, for climate considerations. In the context of optimum grassland management for agricultural production, we showed that a strategy with two annual cuts has the highest potential to contribute to SOC

buildup. We hence advocate an inclusion of more accurate R/S for modeling, taking differences resulting from grass management, as well as site-specific climatic and biogeochemical conditions (Sahoo et al., 2021), into consideration to reduce uncertainties for policymaking on agroecosystems.

However, a limitation of this study is the assessment of harvest frequency on R/S during the establishment year only, which emphasizes the need for more long-term data on root growth of managed and unmanaged perennial grasses in wet environments. Hence, we suggest a future multi-annual study, with at least 2 years of trial, to increase the validity of results by accounting for the plants long-term response to management, taking interannual climatic variability into consideration. Previous studies demonstrated that R/S varies with ley age (Bolinder et al., 2002; Acharya et al., 2012; Huang et al., 2021), the associated interannual climatic variability (Poorter et al., 2012; Li et al., 2021), and nutrient availability (Cong et al., 2019); hence, further years of experimental analysis have to determine whether our findings regarding the effect of harvest frequency on R/S and the associated implications of management for SOC input are applicable on the long term. Further, it is yet unclear how the determined R/S for the assessed grasses can be applied in the evaluation of SOC input by plant biomass in wet or rewetted agricultural wetlands. For wet organic soils and in the context of paludiculture, we suggest that not only root growth but also rooting depth and specific root turnover rates have to be assessed. Only few studies assessed the maximum potential rooting depth by flood-tolerant perennial grasses in correlation with the WTD profile on organic soils, as compiled by Fan et al. (2017). Houde et al. (2020) highlighted the significance of turnover of perennial grass roots for the C storage potential, and Schwieger et al. (2020) emphasized the significance of roots as the main peat-forming component in grass-covered fen peatlands. However, while wetland ecosystems potentially have the second-highest root turnover rates of all ecosystems (Gill and Jackson, 2000), the complexity between rooting depth, WTD, C/N, and litter recalcitrance (Shurpali et al., 2010; Straková et al., 2012; Leifeld et al., 2015; D'Imperio et al., 2018) as well as AGB manipulation and root turnover rates for soil C input still needs to be defined.

With an increasing policy focus on wetland restoration, including paludiculture, for GHG mitigation and nutrient retention, as well as the concomitant need to point out sites with the highest mitigation potential, not only assessments of GHG emissions and optimum management (e.g., Geurts et al., 2019; Tanneberger et al., 2020; Nielsen et al., 2021) but also site- and plant community-specific BGB NPP should be taken into consideration for an accurate evaluation of the C sink potential.

CONCLUSION

While it is known that C inputs in soils are affected by development of AGB and BGB, as well as a variety of biotic and abiotic factors, little has been known so far on the effect of harvest frequency on the R/S of perennial grasses. In conclusion, this study found significant differences in the R/S for the flood-tolerant perennial grasses *Phalaris ar.*, *Festuca ar.*, and *Festuca* × *Lolium*, affected by annual harvest frequencies of AGB, with less biomass allocated to belowground parts with increasing number of cuts. No species-specific differences in the ratio were observed for any treatments. In addition, our results showed that both the OPT of plant biomass allocation and the IA hypothesis seemed to coexisted. Further, we demonstrated the importance to accurately define R/S for the calculation of carbon input into soils to avoid significant over- or underestimation. Our results showed that there are significant differences regarding the annual carbon input into soils, depending on the R/S applied. We found that using the IPCC default factor for R/S of 2.8, applied for both managed and unmanaged grasslands, resulted in 55%–71% higher carbon input rates as compared to our scenarios with two and five annual cuts, commonly applied in agricultural systems. This discrepancy indicates a significant inaccuracy for modeling and quantification of the C sink or source function of wet organic grassland areas, which might have far-reaching consequences for policymaking and carbon accounting. Further, we not only demonstrated how measurements of AGB and BGB provided a more accurate baseline for estimation of soil carbon input but also indicated the need for further assessment of R/S and C/N of perennial grasses, particularly for those cultivated on wet organic soils, to define the soil C sink capacity.

DATA AVAILABILITY STATEMENT

The raw data supporting the conclusions of this article will be made available by the authors, without undue reservation.

AUTHOR CONTRIBUTIONS

CN developed and performed the study design and experimental work, the analysis of the data, and the writing of the manuscript. All authors contributed to the study design and the writing and reading of the manuscript and approved the final manuscript.

FUNDING

This study was financially supported by the PEATWISE project (https://www.eragas.eu/en/eragas/Research-projects/PEATWISE.htm) in the frame of the ERA-NET FACCE ERA-GAS. FACCE ERA-GAS received funding from the European Union's Horizon 2020 research and innovation program under the grant agreement no. 696356. This publication further was funded by the Interreg project CANAPE under the North Sea Region Programme and the European Regional Development Fund. In addition, the study was partly supported by the Aarhus University Centre for Circular Bioeconomy (CBIO, https://cbio.au.dk/en/).

ACKNOWLEDGMENTS

The authors want to thank Lars Elsgaard for valuable and highly appreciated comments to the manuscript during the stage of writing.

REFERENCES

Acharya, B. S., Rasmussen, J., and Eriksen, J. (2012). Grassland Carbon Sequestration and Emissions Following Cultivation in a Mixed Crop Rotation. *Agric. Ecosyst. Environ.* 153, 33–39. doi:10.1016/j.agee.2012.03.001

Bates, D., Mächler, M., Bolker, B., and Walker, S. (2015). Fitting Linear Mixed-Effects Models Usinglme4. *J. Stat. Soft.* 67 (1), 1–48. doi:10.18637/jss.v067.i01

Björk, R. G., Majdi, H., Klemedtsson, L., Lewis-Jonsson, L., and Molau, U. (2007). Long-term Warming Effects on Root Morphology, Root Mass Distribution, and Microbial Activity in Two Dry Tundra Plant Communities in Northern Sweden. *New Phytol.* 176 (4), 862–873. doi:10.1111/j.1469-8137.2007.02231.x

Bolinder, M. A., Angers, D. A., Bélanger, G., Michaud, R., and Laverdière, M. R. (2002). Root Biomass and Shoot to Root Ratios of Perennial Forage Crops in Eastern Canada. *Can. J. Plant Sci.* 82 (4), 731–737. doi:10.4141/P01-139

Bolinder, M. A., Janzen, H. H., Gregorich, E. G., Angers, D. A., and VandenBygaart, A. J. (2007). An Approach for Estimating Net Primary Productivity and Annual Carbon Inputs to Soil for Common Agricultural Crops in Canada. *Agric. Ecosyst. Environ.* 118 (1), 29–42. doi:10.1016/j.agee.2006.05.013

Bonanomi, G., Idbella, M., Zotti, M., Santorufo, L., Motti, R., Maisto, G., et al. (2021). Decomposition and Temperature Sensitivity of fine Root and Leaf Litter of 43 Mediterranean Species. *Plant Soil* 464, 453–465. doi:10.1007/s11104-021-04974-1

Carminati, A., and Vetterlein, D. (2013). Plasticity of Rhizosphere Hydraulic Properties as a Key for Efficient Utilization of Scarce Resources. *Ann. Bot.* 112 (2), 277–290. doi:10.1093/aob/mcs262

Cheng, W., Parton, W. J., Gonzalez-Meler, M. A., Phillips, R., Asao, S., McNickle, G. G., et al. (2014). Synthesis and Modeling Perspectives of Rhizosphere Priming. *New Phytol.* 201 (1), 31–44. doi:10.1111/nph.12440

Cong, W.-F., Christensen, B. T., and Eriksen, J. (2019). Soil Nutrient Levels Define Herbage Yield but Not Root Biomass in a Multispecies Grass-Legume Ley. *Agric. Ecosyst. Environ.* 276, 47–54. doi:10.1016/j.agee.2019.02.014

Cotrufo, M. F., Ranalli, M. G., Haddix, M. L., Six, J., and Lugato, E. (2019). Soil Carbon Storage Informed by Particulate and mineral-associated Organic Matter. *Nat. Geosci.* 12 (12), 989–994. doi:10.1038/s41561-019-0484-6

Cougnon, M., De Swaef, T., Lootens, P., Baert, J., De Frenne, P., Shahidi, R., et al. (2017). *In Situ* quantification of Forage Grass Root Biomass, Distribution and Diameter Classes under Two N Fertilisation Rates. *Plant Soil* 411 (1), 409–422. doi:10.1007/s11104-016-3034-7

Cougnon, M., Deru, J., Eekeren, N. v., Baert, J., and Reheul, D. (2013). "Root Depth and Biomass of Tall Fescue vs. Perennial Ryegrass," in *Paper Presented at the the Role of Grasslands in a green Future: Threats and Perspectives in Less Favoured Areas* (Akureyri, Iceland: Proceedings of the 17th Symposium of the European Grassland Federation), 23–26.

Dijkstra, F. A., Zhu, B., and Cheng, W. (2020). Root Effects on Soil Organic Carbon: a Double-edged Sword. *New Phytol.* 230, 60–65. doi:10.1111/nph.17082

D'Imperio, L., Arndal, M. F., Nielsen, C. S., Elberling, B., and Schmidt, I. K. (2018). Fast Responses of Root Dynamics to Increased Snow Deposition and Summer Air Temperature in an Arctic Wetland. *Front. Plant Sci.* 9 (1258). doi:10.3389/fpls.2018.01258

Dupont, S. T., Beniston, J., Glover, J. D., Hodson, A., Culman, S. W., Lal, R., et al. (2014). Root Traits and Soil Properties in Harvested Perennial Grassland, Annual Wheat, and Never-Tilled Annual Wheat. *Plant Soil* 381 (1-2), 405–420. doi:10.1007/s11104-014-2145-2

Elsgaard, L., Görres, C.-M., Hoffmann, C. C., Blicher-Mathiesen, G., Schelde, K., and Petersen, S. O. (2012). Net Ecosystem Exchange of CO2 and Carbon Balance for Eight Temperate Organic Soils under Agricultural Management. *Agric. Ecosyst. Environ.* 162, 52–67. doi:10.1016/j.agee.2012.09.001

Fan, Y., Miguez-Macho, G., Jobbágy, E. G., Jackson, R. B., and Otero-Casal, C. (2017). Hydrologic Regulation of Plant Rooting Depth. *Proc. Natl. Acad. Sci. USA* 114 (40), 10572–10577. doi:10.1073/pnas.1712381114

Finke, P., Opolot, E., Balesdent, J., Berhe, A. A., Boeckx, P., Cornu, S., et al. (2019). Can SOC Modelling Be Improved by Accounting for Pedogenesis. *Geoderma* 338, 513–524. doi:10.1016/j.geoderma.2018.10.018

Fraser, L. H., Pither, J., Jentsch, A., Sternberg, M., Zobel, M., Askarizadeh, D., et al. (2015). Worldwide Evidence of a Unimodal Relationship between Productivity and Plant Species Richness. *Science* 349 (6245), 302–305. doi:10.1126/science.aab3916

Geurts, J. J., van Duinen, G.-J. A., van Belle, J., Wichmann, S., Wichtmann, W., and Fritz, C. (2019). Recognize the High Potential of Paludiculture on Rewetted Peat Soils to Mitigate Climate Change. *J. Sust. Org. Agric. Syst.*, 69(1), 5–8. doi:10.3220/LBF1576769203000

Giannini, V., Silvestri, N., Dragoni, F., Pistocchi, C., Sabbatini, T., and Bonari, E. (2017). Growth and Nutrient Uptake of Perennial Crops in a Paludicultural Approach in a Drained Mediterranean Peatland. *Ecol. Eng.* 103, 478–487. doi:10.1016/j.ecoleng.2015.11.049

Gill, R. A., and Jackson, R. B. (2000). Global Patterns of Root Turnover for Terrestrial Ecosystems. *New Phytol.* 147 (1), 13–31. doi:10.1046/j.1469-8137.2000.00681.x

Greve, M. H., Greve, M. B., Peng, Y., Pedersen, B. F., Møller, A. B., Lærke, P. E., et al. (2021). *Vidensyntese Om Kulstofrig Lavbundsjord*. Tjele, Denmark: Aarhus University, 137.

Guo, H., Xu, B., Wu, Y., Shi, F., Wu, C., and Wu, N. (2016). Allometric Partitioning Theory versus Optimal Partitioning Theory: The Adjustment of Biomass Allocation and Internal C-N Balance to Shading and Nitrogen Addition inFritillaria unibracteata(Liliaceae). *Polish J. Ecol.* 64 (2), 189–199. doi:10.3161/15052249pje2016.64.2.004

Houde, S., Thivierge, M.-N., Fort, F., Bélanger, G., Chantigny, M. H., Angers, D. A., et al. (2020). Root Growth and Turnover in Perennial Forages as Affected by Management Systems and Soil Depth. *Plant Soil* 451 (1), 371–387. doi:10.1007/s11104-020-04532-1

IPCC (2006). *IPCC Guidelines for National Greenhouse Gas Inventories, Prepared by the National Greenhouse Gas Inventories Programme*. Editors H. S. Eggleston, L. Buendia, K. Miwa, T. Ngara, and K. Tanabe. ISBN 4-88788-032-4.

Hu, T., Sørensen, P., Wahlström, E. M., Chirinda, N., Sharif, B., Li, X., et al. (2018). Root Biomass in Cereals, Catch Crops and Weeds Can Be Reliably Estimated without Considering Aboveground Biomass. *Agric. Ecosyst. Environ.* 251, 141–148. doi:10.1016/j.agee.2017.09.024

Huang, J., Liu, W., Yang, S., Yang, L., Peng, Z., Deng, M., et al. (2021). Plant Carbon Inputs through Shoot, Root, and Mycorrhizal Pathways Affect Soil Organic Carbon Turnover Differently. *Soil Biol. Biochem.* 160, 108322. doi:10.1016/j.soilbio.2021.108322

Karki, S., Elsgaard, L., Audet, J., Lærke, P. E., Audet, J., and Lærke, P. E. (2014). Mitigation of Greenhouse Gas Emissions from Reed Canary Grass in Paludiculture: Effect of Groundwater Level. *Plant Soil* 383 (1), 217–230. doi:10.1007/s11104-014-2164-z

Kätterer, T., Bolinder, M. A., Andrén, O., Kirchmann, H., and Menichetti, L. (2011). Roots Contribute More to Refractory Soil Organic Matter Than Above-Ground Crop Residues, as Revealed by a Long-Term Field experiment. *Agric. Ecosyst. Environ.* 141 (1-2), 184–192. doi:10.1016/j.agee.2011.02.029

Keel, S. G., Leifeld, J., Mayer, J., Taghizadeh-Toosi, A., and Olesen, J. E. (2017). Large Uncertainty in Soil Carbon Modelling Related to Method of Calculation of Plant Carbon Input in Agricultural Systems. *Eur. J. Soil Sci.* 68 (6), 953–963. doi:10.1111/ejss.12454

Keller, A. B., and Phillips, R. P. (2019). Relationship between Belowground Carbon Allocation and Nitrogen Uptake in Saplings Varies by Plant Mycorrhizal Type. *Front. For. Glob. Change* 2 (81), 81. doi:10.3389/ffgc.2019.00081

Kibet, L. C., Blanco-Canqui, H., Mitchell, R. B., and Schacht, W. H. (2016). Root Biomass and Soil Carbon Response to Growing Perennial Grasses for Bioenergy. *Energ Sustain. Soc.* 6 (1), 1. doi:10.1186/s13705-015-0065-5

Klimešová, J. (1994). The Effects of Timing and Duration of Floods on Growth of Young Plants of Phalaris Arundinacea L. And Urtica Dioica L.: an Experimental Study. *Aquat. Bot.* 48 (1), 21–29. doi:10.1016/0304-3770(94)90071-X

Klingenfuß, C., Roßkopf, N., Walter, J., Heller, C., and Zeitz, J. (2014). Soil Organic Matter to Soil Organic Carbon Ratios of Peatland Soil Substrates. *Geoderma* 235-236, 410–417. doi:10.1016/j.geoderma.2014.07.010

Kobe, R. K., Iyer, M., and Walters, M. B. (2010). Optimal Partitioning Theory Revisited: Nonstructural Carbohydrates Dominate Root Mass Responses to Nitrogen. *Ecology* 91 (1), 166–179. doi:10.1890/09-0027.1

Kohzu, A., Matsui, K., Yamada, T., Sugimoto, A., and Fujita, N. (2003). Significance of Rooting Depth in Mire Plants: Evidence from Natural 15 N Abundance. *Ecol. Res.* 18 (3), 257–266. doi:10.1046/j.1440-1703.2003.00552.x

Kumar, A., Kumar, M., Pandey, R., ZhiGuo, Y., and Cabral-Pinto, M. (2021). Forest Soil Nutrient Stocks along Altitudinal Range of Uttarakhand Himalayas: An

Aid to Nature Based Climate Solutions. *CATENA* 207, 105667. doi:10.1016/j.catena.2021.105667

Kumar, A., Sharma, M. P., and Taxak, A. K. (2017). Effect of Vegetation Communities and Altitudes on the Soil Organic Carbon Stock in Kotli Bhel-1A Catchment, India. *Clean. - Soil Air Water* 45 (8), 1600650. doi:10.1002/clen.201600650

Lambert, A. M., Dudley, T. L., and Robbins, J. (2014). Nutrient Enrichment and Soil Conditions Drive Productivity in the Large-Statured Invasive Grass Arundo donax. *Aquat. Bot.* 112, 16–22. doi:10.1016/j.aquabot.2013.07.004

Lehtonen, A., Palviainen, M., Ojanen, P., Kalliokoski, T., Nöjd, P., Kukkola, M., et al. (2016). Modelling fine Root Biomass of Boreal Tree Stands Using Site and Stand Variables. *For. Ecol. Manag.* 359, 361–369. doi:10.1016/j.foreco.2015.06.023

Leifeld, J., Klein, K., and Wüst-Galley, C. (2020). Soil Organic Matter Stoichiometry as Indicator for Peatland Degradation. *Sci. Rep.* 10 (1), 7634. doi:10.1038/s41598-020-64275-y

Leifeld, J., Meyer, S., Budge, K., Sebastia, M. T., Zimmermann, M., and Fuhrer, J. (2015). Turnover of Grassland Roots in Mountain Ecosystems Revealed by Their Radiocarbon Signature: Role of Temperature and Management. *PLOS ONE* 10 (3), e0119184. doi:10.1371/journal.pone.0119184

Li, J., Pan, P., Wang, C.-t., Hu, L., Chen, K.-y., and Yang, W.-g. (2021). Root Dynamics of Artificial Grassland for Swards of Differing Ages in the 'Three-River Source'region. *Acta Prataculturae Sinica* 30 (3), 28. doi:10.11686/cyxb2020161

Mander, Ü., Järveoja, J., Maddison, M., Soosaar, K., Aavola, R., Ostonen, I., et al. (2012). Reed Canary Grass Cultivation Mitigates Greenhouse Gas Emissions from Abandoned Peat Extraction Areas. *Glob. Change Biol. Bioenergy* 4 (4), 462–474. doi:10.1111/j.1757-1707.2011.01138.x

Miller, R. C., and Zedler, J. B. (2003). Responses of Native and Invasive Wetland Plants to Hydroperiod and Water Depth. *Plant Ecol.* 167 (1), 57–69. doi:10.1023/A:1023918619073

Ministry of Food, Agriculture and Fisheries of Denmark (2021). Overblik over arealkategorier vedr. udtagning af kulstofrige landbrugsjorder. MOF Alm. del Bilag 514. Available at: https://www.ft.dk/samling/20201/almdel/MOF/bilag/514/2382777.pdf (accessed 0707, , 2021).

Mokany, K., Raison, R. J., and Prokushkin, A. S. (2006). Critical Analysis of Root : Shoot Ratios in Terrestrial Biomes. *Glob. Change Biol.* 12 (1), 84–96. doi:10.1111/j.1365-2486.2005.001043.x

Moomaw, W. R., Chmura, G. L., Davies, G. T., Finlayson, C. M., Middleton, B. A., Natali, S. M., et al. (2018). Wetlands in a Changing Climate: Science, Policy and Management. *Wetlands* 38 (2), 183–205. doi:10.1007/s13157-018-1023-8

Moore, J. A. M., Sulman, B. N., Mayes, M. A., Patterson, C. M., and Classen, A. T. (2020). Plant Roots Stimulate the Decomposition of Complex, but Not Simple, Soil Carbon. *Funct. Ecol.* 34 (4), 899–910. doi:10.1111/1365-2435.13510

Nielsen, C. K., Stødkilde, L., Jørgensen, U., and Lærke, P. E. (2021). Effects of Harvest and Fertilization Frequency on Protein Yield and Extractability from Flood-Tolerant Perennial Grasses Cultivated on a Fen Peatland. *Front. Environ. Sci.* 9 (47), 258. doi:10.3389/fenvs.2021.619258

Denmark's National Inventory Report, Nielsen, O.-K., Plejdrup, M. S., Winther, M., Nielsen, M., Gyldenkærne, S., Mikkelsen, M. H., et al. (2020). Denmark's National Inventory Report 2020. Emission Inventories 1990-2018-Submitted under the United Nations Framework Convention on Climate Change and the Kyoto Protocol. Aarhus University, DCE –Danish Centre for Environment and Energy, 900pp. Scientific Report No. 372, available at: http://dce2.au.dk/pub/SR372.pdf (assessed 07 07, 2021).

Parish, F., Sirin, A., Charman, D., Joosten, H., Minaeva, T. Y., and Silvius, M. (2008). *Assessment on Peatlands, Biodiversity and Climate Change: Main Report*. Wageningen: Global Environment Centre, Kuala Lumpur and Wetlands International. ISBN 978-983-43751-0-2.

Pausch, J., and Kuzyakov, Y. (2018). Carbon Input by Roots into the Soil: Quantification of Rhizodeposition from Root to Ecosystem Scale. *Glob. Change Biol.* 24 (1), 1–12. doi:10.1111/gcb.13850

Pinno, B. D., Landhäusser, S. M., Chow, P. S., Quideau, S. A., and MacKenzie, M. D. (2014). Nutrient Uptake and Growth of Fireweed (Chamerion Angustifolium) on Reclamation Soils. *Can. J. For. Res.* 44 (1), 1–7. doi:10.1139/cjfr-2013-0091

Poeplau, C. (2016). Estimating Root: Shoot Ratio and Soil Carbon Inputs in Temperate Grasslands with the RothC Model. *Plant Soil* 407 (1), 293–305. doi:10.1007/s11104-016-3017-8

Poirier, V., Roumet, C., and Munson, A. D. (2018). The Root of the Matter: Linking Root Traits and Soil Organic Matter Stabilization Processes. *Soil Biol. Biochem.* 120, 246–259. doi:10.1016/j.soilbio.2018.02.016

Poorter, H., Niklas, K. J., Reich, P. B., Oleksyn, J., Poot, P., and Mommer, L. (2012). Biomass Allocation to Leaves, Stems and Roots: Meta-analyses of Interspecific Variation and Environmental Control. *New Phytol.* 193 (1), 30–50. doi:10.1111/j.1469-8137.2011.03952.x

Puget, P., and Drinkwater, L. E. (2001). Short-Term Dynamics of Root- and Shoot-Derived Carbon from a Leguminous Green Manure. *Soil Sci. Soc. Am. J.* 65 (3), 771–779. doi:10.2136/sssaj2001.653771x

Qi, Y., Wei, W., Chen, C., and Chen, L. (2019). Plant Root-Shoot Biomass Allocation over Diverse Biomes: A Global Synthesis. *Glob. Ecol. Conservation* 18, e00606. doi:10.1016/j.gecco.2019.e00606

R Core Team (2020). *R: A Language and Environment for Statistical Computing*. Vienna, Austria: R Foundation for Statistical Computing. Available at: https://www.R-project.org/.

Reid, J. B., Gray, R. A. J., Springett, J. A., and Crush, J. R. (2015). Root Turnover in Pasture Species: Chicory, lucerne, Perennial Ryegrass and white clover. *Ann. Appl. Biol.* 167 (3), 327–342. doi:10.1111/aab.12228

Renou-Wilson, F., Barry, C., Müller, C., and Wilson, D. (2014). The Impacts of Drainage, Nutrient Status and Management Practice on the Full Carbon Balance of Grasslands on Organic Soils in a Maritime Temperate Zone. *Biogeosciences* 11 (16), 4361–4379. doi:10.5194/bg-11-4361-2014

Rossi, L. M. W., Mao, Z., Merino-Martín, L., Roumet, C., Fort, F., Taugourdeau, O., et al. (2020). Pathways to Persistence: Plant Root Traits Alter Carbon Accumulation in Different Soil Carbon Pools. *Plant Soil* 452 (1-2), 457–478. doi:10.1007/s11104-020-04469-5

Rydin, H., Jeglum, J. K., and Bennett, K. D. (2013). *The Biology of Peatlands*. 2e. Oxford University Press. doi:10.1093/acprof:osobl/9780199602995.001.0001

Sahoo, U. K., Tripathi, O. P., Nath, A. J., Deb, S., Das, D. J., Gupta, A., et al. (2021). Quantifying Tree Diversity, Carbon Stocks, and Sequestration Potential for Diverse Land Uses in Northeast India. *Front. Environ. Sci.* 9, 724950. doi:10.3389/fenvs.2021.724950

Sainju, U. M., Allen, B. L., Lenssen, A. W., and Ghimire, R. P. (2017a). Root Biomass, Root/shoot Ratio, and Soil Water Content under Perennial Grasses with Different Nitrogen Rates. *Field Crops Res.* 210, 183–191. doi:10.1016/j.fcr.2017.05.029

Sainju, U. M., Allen, B. L., Lenssen, A. W., and Mikha, M. (2017b). Root and Soil Total Carbon and Nitrogen under Bioenergy Perennial Grasses with Various Nitrogen Rates. *Biomass and Bioenergy* 107, 326–334. doi:10.1016/j.biombioe.2017.10.021

Schneider, M. K., Lüscher, A., Frossard, E., and Nösberger, J. (2006). An Overlooked Carbon Source for Grassland Soils: Loss of Structural Carbon from Stubble in Response to Elevated pCO 2 and Nitrogen Supply. *New Phytol.* 172 (1), 117–126. doi:10.1111/j.1469-8137.2006.01796.x

Schwieger, S., Kreyling, J., Couwenberg, J., Smiljanić, M., Weigel, R., Wilmking, M., et al. (2020). Wetter Is Better: Rewetting of Minerotrophic Peatlands Increases Plant Production and Moves Them towards Carbon Sinks in a Dry Year. *Ecosystems* 24, 1093–1109. doi:10.1007/s10021-020-00570-z

Shurpali, N. J., Strandman, H., Kilpeläinen, A., Huttunen, J., Hyvönen, N., Biasi, C., et al. (2010). Atmospheric Impact of Bioenergy Based on Perennial Crop (Reed Canary Grass, Phalaris Arundinaceae, L.) Cultivation on a Drained Boreal Organic Soil. *Gcb Bioenergy* 2 (3), no. doi:10.1111/j.1757-1707.2010.01048.x

Straková, P., Penttilä, T., Laine, J., and Laiho, R. (2012). Disentangling Direct and Indirect Effects of Water Table Drawdown on above- and Belowground Plant Litter Decomposition: Consequences for Accumulation of Organic Matter in Boreal Peatlands. *Glob. Change Biol.* 18 (1), 322–335. doi:10.1111/j.1365-2486.2011.02503.x

Taghizadeh-Toosi, A., Christensen, B. T., Glendining, M., and Olesen, J. E. (2016). Consolidating Soil Carbon Turnover Models by Improved Estimates of Belowground Carbon Input. *Sci. Rep.* 6 (1), 32568. doi:10.1038/srep32568

Tanneberger, F., Schröder, C., Hohlbein, M., Lenschow, U., Permien, T., Wichmann, S., et al. (2020). Climate Change Mitigation through Land Use on Rewetted Peatlands - Cross-Sectoral Spatial Planning for Paludiculture in Northeast Germany. *Wetlands* 40 (6), 2309–2320. doi:10.1007/s13157-020-01310-8

Thakur, T. K., Patel, D. K., Thakur, A., Kumar, A., Bijalwan, A., Bhat, J. A., et al. (2021). Biomass Production Assessment in a Protected Area of Dry Tropical

forest Ecosystem of India: A Field to Satellite Observation Approach. *Front. Environ. Sci.* 9, 757976. doi:10.3389/fenvs.2021.757976

Usťak, S., Šinko, J., and Muňoz, J. (2019). Reed Canary Grass (Phalaris Arundinacea L.) as a Promising Energy Crop. *Jcea* 20 (4), 1143–1168. doi:10.5513/JCEA01/20.4.2267

van Veelen, A., Tourell, M. C., Koebernick, N., Pileio, G., and Roose, T. (2018). Correlative Visualization of Root Mucilage Degradation Using X-ray CT and MRI. *Front. Environ. Sci.* 6, 32. doi:10.3389/fenvs.2018.00032

Vroom, R. J. E., Xie, F., Geurts, J. J. M., Chojnowska, A., Smolders, A. J. P., Lamers, L. P. M., et al. (2018). Typha Latifolia Paludiculture Effectively Improves Water Quality and Reduces Greenhouse Gas Emissions in Rewetted Peatlands. *Ecol. Eng.* 124, 88–98. doi:10.1016/j.ecoleng.2018.09.008

Wang, L., Niu, K., Yang, Y., and Zhou, P. (2010). Patterns of above- and Belowground Biomass Allocation in China's Grasslands: Evidence from Individual-Level Observations. *Sci. China Life Sci.* 53 (7), 851–857. doi:10.1007/s11427-010-4027-z

Whitehead, D. (2020). Management of Grazed Landscapes to Increase Soil Carbon Stocks in Temperate, Dryland Grasslands. *Front. Sustain. Food Syst.* 4, 913. doi:10.3389/fsufs.2020.585913

Williams, C. J., and Yavitt, J. B. (2003). Botanical Composition of Peat and Degree of Peat Decomposition in Three Temperate Peatlands. *Écoscience* 10 (1), 85–95. doi:10.1080/11956860.2003.11682755

Worrall, F., Moody, C. S., Clay, G. D., Burt, T. P., and Rose, R. (2017). The Flux of Organic Matter through a Peatland Ecosystem: The Role of Cellulose, Lignin, and Their Control of the Ecosystem Oxidation State. *J. Geophys. Res. Biogeosci.* 122 (7), 1655–1671. doi:10.1002/2016JG003697

Xiong, S., and Kätterer, T. (2010). Carbon-allocation Dynamics in Reed Canary Grass as Affected by Soil Type and Fertilization Rates in Northern Sweden. *Acta Agriculturae Scand. Section B - Soil Plant Sci.* 60 (1), 24–32. doi:10.1080/09064710802558518

Xiong, S., Landström, S., and Olsson, R. (2009). Delayed Harvest of Reed Canary Grass Translocates More Nutrients in Rhizomes. *Acta Agriculturae Scand. Section B - Soil Plant Sci.* 59 (4), 306–316. doi:10.1080/09064710802154722

Yang, Y., Dou, Y., An, S., and Zhu, Z. (2018). Abiotic and Biotic Factors Modulate Plant Biomass and Root/shoot (R/S) Ratios in Grassland on the Loess Plateau, China. *Sci. Total Environ.* 636, 621–631. doi:10.1016/j.scitotenv.2018.04.260

Conflict of Interest: The authors declare that the research was conducted in the absence of any commercial or financial relationships that could be construed as a potential conflict of interest.

Publisher's Note: All claims expressed in this article are solely those of the authors and do not necessarily represent those of their affiliated organizations, or those of the publisher, the editors, and the reviewers. Any product that may be evaluated in this article, or claim that may be made by its manufacturer, is not guaranteed or endorsed by the publisher.

Advantages of publishing in Frontiers

OPEN ACCESS
Articles are free to read for greatest visibility and readership

FAST PUBLICATION
Around 90 days from submission to decision

HIGH QUALITY PEER-REVIEW
Rigorous, collaborative, and constructive peer-review

TRANSPARENT PEER-REVIEW
Editors and reviewers acknowledged by name on published articles

Frontiers
Avenue du Tribunal-Fédéral 34
1005 Lausanne | Switzerland

Visit us: www.frontiersin.org
Contact us: frontiersin.org/about/contact

REPRODUCIBILITY OF RESEARCH
Support open data and methods to enhance research reproducibility

DIGITAL PUBLISHING
Articles designed for optimal readership across devices

FOLLOW US
@frontiersin

IMPACT METRICS
Advanced article metrics track visibility across digital media

EXTENSIVE PROMOTION
Marketing and promotion of impactful research

LOOP RESEARCH NETWORK
Our network increases your article's readership